



**HAL**  
open science

# Electronic properties of carotenoids in natural and artificial photosynthesis

Denise Galzerano

► **To cite this version:**

Denise Galzerano. Electronic properties of carotenoids in natural and artificial photosynthesis. *Vegetal Biology*. Université Pierre et Marie Curie - Paris VI, 2014. English. NNT : 2014PA066153 . tel-01164978

**HAL Id: tel-01164978**

**<https://theses.hal.science/tel-01164978>**

Submitted on 18 Jun 2015

**HAL** is a multi-disciplinary open access archive for the deposit and dissemination of scientific research documents, whether they are published or not. The documents may come from teaching and research institutions in France or abroad, or from public or private research centers.

L'archive ouverte pluridisciplinaire **HAL**, est destinée au dépôt et à la diffusion de documents scientifiques de niveau recherche, publiés ou non, émanant des établissements d'enseignement et de recherche français ou étrangers, des laboratoires publics ou privés.

Université Pierre et Marie Curie

Ecole doctorale iViv- ED 387

**Étude des propriétés électroniques des caroténoïdes dans  
la photosynthèse naturelle et artificielle**

Par Denise Galzerano

Thèse de doctorat de Biologie

Dirigée par Dr. Bruno ROBERT

Présentée et soutenue publiquement le 12/05/2014

Devant un jury composé de :

ZITO Francesca	Rapporteur
OUCHANE Soufian	Rapporteur
RAPPAPORT Fabrice	Examineur
VAN GRONDELLE Rienk	Examineur
ROBERT Bruno	Directeur de thèse





## Sommaire

La photosynthèse est un processus à plusieurs étapes qui commence par la capture de la lumière par des structures moléculaires spécialisées incluses dans les organismes photosynthétiques. Les pigments présents dans les protéines de l'appareil photosynthétique jouent un rôle essentiel dans les premiers événements.

Ces pigments, des chlorophylles et des caroténoïdes, peuvent absorber la lumière et transférer l'énergie résultante en excitation aux molécules voisines, garantissant le respect de la succession des étapes photosynthétiques. En plus de l'absorption de la lumière, les caroténoïdes protègent l'appareil photosynthétique du stress photo-oxydatif survenant en condition de lumière intense. De cette manière, ce processus garantit l'équilibre entre l'absorption de l'énergie lumineuse, son utilisation et la protection à une exposition excessive. Les caroténoïdes possèdent une structure moléculaire composée d'une chaîne linéaire de polyène conjuguée. Cette structure confère à ces pigments des propriétés électroniques uniques grâce auxquelles ils réalisent leurs fonctions. La connaissance de ces propriétés est essentielle pour comprendre leurs mécanismes d'actions.

Malgré la simplicité apparente de leur structure, les calculs précis de leurs propriétés électroniques et vibrationnels ainsi que la prédiction de leur comportement selon l'environnement dans lequel le caroténoïde se trouve, s'effectuent difficilement et exigent des approches complexes. Ces travaux de recherche illustrent différentes approches pour être au plus près des mécanismes d'interactions entre les pigments et la lumière, avec un accent mis sur le rôle photo-protecteur joué par les caroténoïdes. Une série d'échantillons, à différents niveaux d'organisations structurelles des protéines collectrices de lumière contenant ces pigments, sera décrite et analysée.

Après une introduction générale, nous analysons deux cas où des molécules de caroténoïdes cycliques identiques sont attachés à la même protéine, mais exposent néanmoins des transitions d'absorption différentes. Le centre de réaction du photosystème II (PSII) contient deux  $\beta$ -carotènes, une qui absorbe à 489 nm et l'autre à 507 nm. Par contre, le complexe majeur du photosystème II (LHCII) contient deux molécules de lutéine, une qui absorbe à 495 nm et l'autre à 510 nm. Dans chaque cas, on remarque que l'espèce moléculaire identique dans la même protéine expose des propriétés électroniques différentes.

Nous démontrons que l'environnement du site de liaison à la protéine influence de façon différente les propriétés de ces caroténoïdes possédant un cycle à leur extrémité. Le carotène du PSII qui absorbe à 487 nm et la lutéine du LHCII qui absorbe à 495 nm sont principalement influencés par la *polarisabilité* locale de leur site de liaison. Inversement, le carotène qui absorbe à 507 nm et la lutéine qui absorbe à 510 nm sont influencés par la *structure* de leur site de liaison : des encombrements stériques locaux force les cycles à se retrouver sur le même plan que la chaîne polyène.

Dans le chapitre 3, nous analysons des mutants d'*Arabidopsis thaliana* qui présentent une modification de la voie de biosynthèse des caroténoïdes. Ces mutants expriment la phytoène désaturase bactérienne (CRTI) en plus de l'enzyme endogène impliqué dans les réactions de désaturation du phytoène (PDS). En conséquence ils présentent un changement de la composition des caroténoïdes, montrant une diminution de la quantité de lutéine et une augmentation des xanthophylles dérivées du  $\beta$ -carotène. Les mutants présentent une sensibilité majeure à la lumière intense. La cause de ce changement est l'altération de la chaîne de transport électronique photosynthétique plutôt que les changements de la composition de caroténoïde dans les protéines collectrices de lumière. Il s'avère que dans les lignes qui expriment CRTI, le niveau de protéine de l'oxydase terminale plastid (PTOX) augmente, tandis que le flux électronique cyclique est supprimé.

D'après les résultats, PTOX rivalise efficacement avec le flux électronique cyclique au niveau du plastoquinol dans les mutants et joue un rôle crucial dans le contrôle de l'état de réduction du plastoquinone « pool ». Ceci confirme l'hypothèse que PTOX est capable de moduler l'équilibre entre le flux d'électron linéaire et le flux cyclique autour du photosystème I (PSI).

Dans le chapitre 4, des antennes photosynthétiques artificielles (dyades), imitant l'interaction entre les chlorophylles et les caroténoïdes, sont analysées. Grâce à une ingénierie précise des interactions entre leurs composants (une molécule tétrapyrrolique et une molécule similaire au caroténoïde), ces molécules synthétiques peuvent imiter un certain nombre de caractéristiques et fonctions de leurs équivalentes naturelles. Ici nous nous concentrons sur le mécanisme de transfert d'énergie parmi les états excités de triplet (transfert T-T) entre le tétrapyrrole et le caroténoïde de deux différentes dyades artificielles. Nous étudions les caractéristiques spectroscopiques de leurs états de triplet et nous les comparons aux systèmes naturels, où le même mécanisme a lieu.

Les analyses spectroscopiques exécutées indiquent que dans la dyade carotenophthalocyanine (dyade 1) la structure électronique de l'état de triplet est partagée

entre le caroténoïde et le tétrapyrrole. Ce couplage permet un transfert d'énergie T-T extrêmement rapide. Des résultats similaires ont été trouvés dans des complexes de protéines collectrices de lumière des organismes qui réalisent une photosynthèse oxygénique.

Nous suggérons qu'une structure électronique partagée est essentielle pour la protection de la production de l'état singlet de l'oxygène dans des membranes photosynthétiques de ces organismes. Dans le carotenopurpurine (dyade 2) le lien tétrapyrrole-caroténoïde fournit un couplage électronique plus faible. En conséquence, le transfert d'énergie T-T est plus lent et montre moins de preuves spectroscopiques d'un état de triplet délocalisé. Cette dyade imite le comportement des pigments dans les complexes LH2 de bactéries photosynthétiques anaérobies dans lesquelles l'exposition à l'oxygène est intermittente et beaucoup plus basse.

Les deux cas analysés suggèrent qu'un transfert d'énergie T-T rapide, tant dans les protéines photosynthétiques naturelles que dans les dyades artificielles, exige un changement de la structure d'état de triplet du caroténoïde, probablement à travers le partage de triplet avec le tétrapyrrole. Les systèmes artificiels de cette étude décrivent l'avantage évolutif des organismes aérobies d'utiliser des chromophores bien couplés pour un transfert d'énergie rapide T-T. Cela permet de dissiper efficacement le triplet des chlorophylles pour empêcher la production de l'état singlet de l'oxygène. Au contraire, les organismes anaérobies ont une version plus faible et probablement plus archaïque de ce mécanisme de protection. Ce travail démontre que le mécanisme naturel de protection peut être pourvu dans des constructions photosynthétiques artificielles.

Dans le chapitre 5, des résultats préliminaires concernant l'effet des conditions de solubilisation sur LHCII, sont présentés. Nous décrivons le caractère dynamique de l'LHCII et de ses pigments en fonction des propriétés du détergent.

En conclusion, l'étude des fonctions des molécules de caroténoïde, impliquant l'interaction avec la lumière, exige un approche pluridisciplinaire et à plusieurs niveaux.

Cette thèse illustre qu'une combinaison de techniques spectroscopiques et biochimiques contribue à mettre en évidence et décrire les propriétés physico-chimiques des caroténoïdes leur conférant un rôle vaste et essentiel dans la photosynthèse.



This work was carried out at the  
*Laboratoire bioénergétique membranaire et stress (LBMS)*

Address

**iBiTec-S, Bâtiment 532**  
**CEA, UMR 8221 CNRS,**  
**CEA Saclay 91191 Gif sur Yvette, France**



## Acknowledgments

I would like to thank, first of all, my supervisor Prof. Bruno Robert for giving me the opportunity to work in his lab and for always encouraging and supporting me. When I started the PhD I had a limited background and no practical experience in the photosynthetic field, but Bruno trusted me and I will always be grateful for it.

I thank Cristian who introduced me to the world of spectroscopy and who was always around me to give good advices and to discuss about the experimental results. Many thanks to my colleagues Andrew, Andy, Maria, Luc and Ana for their constant help and thanks also to Dr. Ghada Ajlani, who was always “next door” to answer to any kind of questions. A special thanks to my colleague and good friend Liz; without her these years at the Cea wouldn't have been the same.

To Dr. Anja Krieger-Lizskay and Dr. Winfried Leibl, thanks for the fruitful collaborations we had and for giving me the opportunity of learning new experimental techniques.

I also express my gratitude to my collaborators Tom and Ana Moore and Katie Wong-Carter from Arizona State University and to people from the Free University of Amsterdam for sharing their advices on part of my work.

To all the people from the iBiTeC-S, thank you for your support all over the time course of my thesis.

Special thanks go to people from the Marie Curie ITN HARVEST Network: being part of this international, multidisciplinary and wonderful group was one of the most exciting experiences of my life from both the professional and human point of view. Huge thanks for the happy moments I had with the students and post-doc I met during the network meeting and courses all around Europe. Thanks to Luca and Julien: the best memories of these last three years are from the time I spent with you.

To Liz, Sané, Denise, Qian, Kathleen, Margaux, Mehdi, Stéphanie, Michal, Amin, Eiri, Hassina, Eduardo and Manolis, thanks for all the good moments we spent together inside and outside the Cea.

Finally special thanks to my family, my childhood friends and my dear Hugues for always encouraging me, especially during the bad moments and for being so understanding and patience.



## List of abbreviations

4-POBN= 4-pyridyl-1-oxide-N-tert-butyl nitron;  
Chl *a*= chlorophyll a  
Chl *b*= chlorophyll b  
Chl= chlorophyll  
CRTI= phytoene desaturase;  
DCMU= 3-(3,4-Dichlorophenyl)-1,1-dimethylurea;  
DNP-INT= 2'-iodo-6-isopropyl-3-methyl-2', 4-4'-trinitrodiphenylether;  
EADS= evolution associated difference spectra  
EET= electronic energy transfer  
FWHM=full width at half maximum  
ISC= intersystem crossing  
kDa= kilodalton  
LHCII= light harvesting complex II;  
LHCs= light harvesting complexes  
LT= low temperature  
Lut= lutein  
NDH= plastid NAD(P)H dehydrogenase;  
Neo= neoxanthin  
NPQ= non-photochemical quenching  
OG= octyl-gallate;  
P700= chlorophyll *a* molecule in association with photosystem I;  
PQ= plastoquinone;  
PSII= photosystem II;  
PTOX= plastid terminal oxidase;  
qE= rapidly relaxing , energy dependent quenching component of NPQ ;  
qI= very slowly relaxing, photoinhibitory quenching component of NPQ;  
qP= photochemical quenching  
qT= slowly relaxing quenching component of NPQ cause by state transitions  
RC= reaction centre;  
ROS= reactive oxygen species;  
RR= resonance Raman spectroscopy

RT= room temperature

TEMPD= 2,2,6,6-tetramethyl-4-piperidone hydrochloride

THF= tetrahydrofuran

Vio= violaxanthin

XC= xanthophyll cycle

Zea= zeaxanthin

$\alpha$ -DDM= *n*-dodecyl- $\alpha$ -D-maltoside

$\beta$ -DDM= *n*-dodecyl- $\beta$ -D-maltoside

$\beta$ -car =  $\beta$ -carotene

## Table of contents

Title page	i
Summary	iii
Acknowledgments	ix
List of abbreviations	xi
Contents	xiii
List of figures	xiv
List of tables	xvii

## CHAPTER 1 Introduction..... 1

<b>1.1</b>	<b>General introduction</b> .....	<b>3</b>
<b>1.2</b>	<b>Carotenoids</b> .....	<b>4</b>
<b>1.3</b>	<b>Chlorophylls</b> .....	<b>11</b>
<b>1.4</b>	<b>The proteins of the photosynthetic apparatus from higher plants</b> .....	<b>12</b>
1.4.1	<i>Peripheral Photosystem II Antenna Complexes</i> .....	12
1.4.2	<i>Photosystem II supercomplexes</i> .....	15
1.4.3	<i>Photosystem II</i> .....	16
1.4.4	<i>Cytochrome <i>b<sub>6</sub></i></i> .....	18
1.4.5	<i>Photosystem I</i> .....	18
1.4.6	<i>ATP-synthase complex</i> .....	20
1.4.7	<i>Linear electron transport</i> .....	20
1.4.8	<i>Cyclic electron transport</i> .....	20
<b>1.5</b>	<b>Photoprotective mechanisms in higher plants</b> .....	<b>21</b>
1.5.1	<i>Photoprotective role of carotenoids</i> .....	22
1.5.2	<i>Non-photochemical quenching (NPQ)</i> .....	23
<b>1.6</b>	<b>Photoinhibition</b> .....	<b>28</b>
<b>1.7</b>	<b>Realizing artificial photosynthesis</b> .....	<b>29</b>
<b>1.8</b>	<b>Experimental approach</b> .....	<b>31</b>
1.8.1	<i>Resonance Raman spectroscopy</i> .....	32
1.8.2	<i>Carotenoid molecules</i> .....	34
1.8.3	<i>Chlorophylls and derivatives</i> .....	35
1.8.4	<i>Step-scan Fourier transform infrared spectroscopy</i> .....	35
<b>1.9</b>	<b>Project outline</b> .....	<b>36</b>

## CHAPTER 2 Mechanisms underlying carotenoid absorption in oxygenic photosynthetic proteins.....51

<b>2.1</b>	<b>Introduction</b> .....	<b>54</b>
<b>2.2</b>	<b>Experimental procedure</b> .....	<b>56</b>
<b>2.3</b>	<b>Results and discussion</b> .....	<b>57</b>
2.3.1	<i>Isolated <math>\beta</math>-Carotene and Lutein</i> .....	57
2.3.2	<i><math>\beta</math>-Carotene in PSII Reaction Centres</i> .....	58

2.3.3	<i>Lutein Molecules in LHCII</i> .....	62
2.3.4	<i>Mechanisms tuning carotenoid absorption in PSII-RC and LHCII</i> .....	65
<b>CHAPTER 3 Effect of constitutive expression of bacterial phytoene desaturase CRTI on photosynthetic electron transport in <i>Arabidopsis thaliana</i></b> .....		
3.1	<b>Introduction</b> .....	78
3.2	<b>Materials and Methods</b> .....	80
3.3	<b>Results</b> .....	83
3.3.1	<i>Light sensitivity of CRTI expressing lines</i> .....	83
3.3.2	<i>Generation of H<sub>2</sub>O<sub>2</sub>-derived hydroxyl radicals in the CRTI-lines</i> .....	87
3.3.3	<i>Reduction state of the plastoquinone pool in CRTI-lines</i> .....	91
3.3.4	<i>Cyclic electron flow in the CRTI-lines</i> .....	92
3.4	<b>Discussion</b> .....	94
<b>CHAPTER 4 Carotenotetrapyrrole Dyads Mimic Photosynthetic Triplet-Triplet Energy Transfer</b> .....		
4.1	<b>Introduction</b> .....	109
4.2	<b>Methods</b> .....	110
4.3	<b>Results</b> .....	114
4.4	<b>Discussion</b> .....	121
<b>CHAPTER 5 Effect of the isomeric forms of dodecyl-maltoside detergent on LHCII spectroscopic properties</b> .....		
5.1	<b>Introduction</b> .....	134
5.2	<b>Material and methods</b> .....	136
5.3	<b>Results</b> .....	137
5.4	<b>Discussion</b> .....	143
<b>CHAPTER 6 General discussion and future perspective</b> .....		
6.1	<b>Introduction</b> .....	151
6.2	<b>Tuning of carotenoid absorption properties</b> .....	151
6.3	<b>Regulation of the photosynthetic electron flow in <i>Arabidopsis thaliana</i></b> .....	153
6.4	<b>Reengineering photosynthesis: artificial antenna system</b> .....	156
6.5	<b>Dynamic and flexibility of LHCII</b> .....	157
6.6	<b>Conclusions</b> .....	159
<b>Annexes</b> .....		164

## List of figures

<b>Figure 1.1</b> Zeaxanthin molecular structure.....	6
<b>Figure 1.2</b> Carotenoid biosynthesis pathway (Diretto et <i>al.</i> , 2006). .....	7
<b>Figure 1.3</b> General energy level scheme of carotenoids. ....	10
<b>Figure 1.4</b> Absorption spectrum of zeaxanthin in THF.....	10
<b>Figure 1.5</b> Molecular structure of chlorophylls derivatives. ....	11
<b>Figure 1.6</b> Pigment and absorption maxima of the most common chlorophylls .....	12
<b>Figure 1.7</b> Crystal structure of LHCII .....	13
<b>Figure 1.8</b> CP29 crystal structure .....	14
<b>Figure 1.9</b> Model of the PSII supercomplex C2S2M2 from higher plants. ....	16
<b>Figure 1.10</b> Overall structure of PSII dimer.....	18
<b>Figure 1.11</b> Overall structure of plant PSI, represented in surface and schematic.....	19
<b>Figure 1.12</b> Schematic representation or the behavior of photosynthetic organisms in presence of different light intensities. ....	21
<b>Figure 1.13</b> Mechanisms of photoprotection played by carotenoids in photosynthesis.....	23
<b>Figure 1.14</b> Structural model of an LHCII monomer showing the key pigments involved in the establishment of qE. ....	27
<b>Figure 1.15</b> Schematic representation of an artificial photosynthetic system for water splitting.....	29
<b>Figure 1.16</b> Biosynthetic scheme of a carotenoid ether dyad.....	31
<b>Figure 1.17</b> The Raman effect designates an exchange of energy between a molecule and a photon during scattering.....	32
<b>Figure 1.18</b> Resonance Raman spectrum of zeaxanthin in THF at 488nm excitation wavelength.....	34
<b>Figure 1.19</b> Resonance Raman spectrum of chlorophyll a in THF at 413 nm excitation wavelengt.....	35
<b>Figure 2.1</b> Molecular structures of $\beta$ -carotene and lutein .....	54
<b>Figure 2.2</b> Correlation between the $S_0 \rightarrow S_2$ electronic transition and the frequency of the $\nu_1$ Raman band for linear carotenoids with different conjugation length.....	58
<b>Figure 2.3</b> Absorption spectra of PSII-RC particles .....	59
<b>Figure 2.4</b> RR spectra of PSII-RC recorded with 488.0- and 514- nm excitation .....	60

<b>Figure 2.5</b> Correlation between the $S_0 \rightarrow S_2$ electronic transition and the frequency of the $\nu_1$ Raman band for the two $\beta$ -carotene molecules in PSII-RC .....	62
<b>Figure 2.6</b> Absorption spectra of LHCII trimers .....	63
<b>Figure 2.7</b> RR spectra of LHCII trimers recorded with 496.5- and 514.5-nm excitation .....	64
<b>Figure 2.8</b> Correlation between the $S_0 \rightarrow S_2$ electronic transition and the frequency of the $\nu_1$ Raman band for the two lutein molecules in LHCII trimers.....	65
<b>Figure 2.9</b> Structural details of the carotenoid end rings in PSII-RC and LHCII .....	69
<b>Figure 3.1</b> Phenotypes of <i>Arabidopsis thaliana</i> wild type (wt), CRTI-lines 11 and 14 after 7 weeks grown on soil.....	84
<b>Figure 3.2</b> Chlorophyll and carotenoid content of mature leaves from wt and CRTI-lines 11 and 14.....	85
<b>Figure 3.3</b> Non-photochemical (NPQ) and photochemical (qP) quenching in wt, CRTI-lines 11 and 14.....	86
<b>Figure 3.4</b> Generation of $^1O_2$ in isolated thylakoids from wild-type and CRTI-lines 11 and 14 .....	87
<b>Figure 3.5</b> Light-induced hydroxyl radical formation in thylakoids from wt and the CRTI-lines 11 and 14.....	88
<b>Figure 3.6</b> Light-induced hydroxyl radical formation in thylakoids from wt and line 14 in the presence and absence of 10 $\mu$ M octylgallate (OG). .....	89
<b>Figure 3.7</b> PTOX content in wt and the CRTI-lines 11 and 14.....	90
<b>Figure 3.8</b> $F_0'$ rise after illumination with actinic light in leaves from wt and the CRTI-lines 11 and 14.....	91
<b>Figure 3.9</b> Thermoluminescence measurements of dark-adapted leaves.....	92
<b>Figure 3.10</b> Dependence of PSI oxidation on the intensity of actinic light.....	94
<b>Figure 3.11</b> PSI oxidation probed by far-red illumination in wt and CRTI-lines 11 and 14..	94
<b>Figure S1</b> Protein complexes of PSII-enriched membrane fragments from wt, 11 and 14..	97
<b>Figure S2</b> 77K fluorescence emission spectra of thylakoids membranes from wt, and the CrtI insertion lines 11 and 14.....	98
<b>Figure S3</b> Pigment analysis from 7 days old <i>Arabidopsis</i> plantlets grown in the absence (control) or in the presence (NF) of 1 $\mu$ M norflurazon.....	98
<b>Figure 4.1</b> Molecular structure of carotenophthalocyanine dyad and model phthalocyanine, carotenopurpurin dyad and model purpurin .....	113
<b>Figure 4.2</b> Evolution-associated-difference spectra (EADS) for the carotenophthalocyanine, dyad 1 .....	115

<b>Figure 4.3 A:</b> Resonance Raman spectra of the carotenophthalocyanine, dyad <b>1</b> .....	116
<b>Figure 4.4</b> Time-resolved FTIR absorption measurements performed on the phthalocyanine model compared to the carotenophthalocyanine, dyad <b>1</b> .....	118
<b>Figure 4.5</b> Evolution-associated-difference spectra (EADS) for the carotenopurpurin, dyad <b>2</b> .....	119
<b>Figure 4.6</b> Resonance Raman spectra of carotenopurpurin, dyad <b>2</b> .....	120
<b>Figure 4.7</b> Time-resolved FTIR absorption measurements in THF performed on the purpurin model, compared to carotenopurpurin, dyad <b>2</b> .....	120
<b>Figure 4.8</b> Orbital diagrams of the carotenophthalocyanine, dyad <b>1</b> , and the carotenopurpurin, dyad <b>2</b> calculated using DFT (B3LYP/6-31G(d)).....	125
<b>Figure 5.1</b> Structural formula of <i>n</i> -dodecyl- $\alpha$ -D-maltoside ( $\alpha$ -DM) and <i>n</i> -dodecyl- $\beta$ -D-maltoside ( $\beta$ -DM) and chemical properties of the two isomers.....	135
<b>Figure 5.2</b> Absorption spectra of LHCII trimers in $\alpha$ -DM or $\beta$ -DM and difference between the two samples.....	137
<b>Figure 5.3</b> Resonance Raman spectra of LHCII trimers at 488 excitation wavelength.....	139
<b>Figure 5.4</b> $\nu_4$ band Raman band spectra of LHCII trimers in $\alpha$ -DM, $\beta$ -DM (from figure 5.3B) and of trimers in $\alpha$ -DM with the addition of $\beta$ -DM.....	140
<b>Figure 5.5</b> Resonance Raman spectra of LHCII trimers in $\alpha$ -DM from wild type (wt) and npq2 mutants (npq2) at 488 nm excitation wavelength.....	141
<b>Figure 5.6</b> Comparison of $\nu_4$ band between LHCII trimers and aggregates in $\alpha$ -DM at 488 nm excitation wavelength.....	142
<b>Figure 5.7</b> Resonance Raman spectra of LHCII trimers in $\alpha/\beta$ -DM or $\alpha$ -DM with the addition of $\beta$ -DM.....	143
<b>Figure 5.8</b> CD spectra of LHCII trimers in $\beta$ -DM compared to the trimers in $\alpha$ -DM with the addition of $\beta$ -DM.....	144
<b>Figure 6.1</b> Phytoene desaturation reactions.....	155

## List of tables

<b>Table 3.1</b> Photoinhibition of PSII in leaves from wild-type and the CRTI-lines 11 and 14.....	85
<b>Table 3.2</b> Hydroxyl radical production in isolated thylakoids from wild-type, line 11 and line 14.....	90



# CHAPTER 1 INTRODUCTION



## 1.1 General introduction

Photosynthesis is a multistep process occurring in green plants, algae and some species of bacteria. Its function is to convert sunlight into biologically useful energy such as electrochemical potential or proton motive force and store it in the form of chemical energy - (carbohydrate synthesis).

For higher plants, photosynthesis can be basically summarized by the following formula:



where light energy is used to oxidise water and reduce carbon dioxide in complex sugars, releasing  $\text{O}_2$  as a by-product.

In plants and algae, photosynthetic reactions occur in special organelles called chloroplasts. These organelles are surrounded by a chloroplast envelope, made up of a double membrane with two bilayers separated by an intermembrane space. The region inside the inner chloroplast envelope membrane is called stroma and it contains the enzymes necessary for the “dark” reactions, *i.e.* the synthesis of sugars. The inner membrane system forms the thylakoids, which accommodate all the light harvesting proteins and the electron transport system that carries out the first photosynthetic steps, also called ‘light’ reactions, which comprise all the necessary steps to transduce the energy of the light into chemical potential energy.

The first (and only endergonic) process in photosynthesis process is the absorption of solar photons by specialized molecules, most often carotenoids or chlorophyll molecules. This occurs in specialized proteins termed LHCs for light-harvesting complexes. After absorption, pigments are excited to a higher singlet state and the excitation energy is transferred, from pigment to pigment to the reaction centres of the two photosystems: photosystem I (PSI) and photosystem II (PSII). When the excitation reaches a special chlorophyll structure, a charge separation occurs, triggering a transmembrane cascade of electron transfers. The released electrons pass through a series of electron carriers till the reduction of  $\text{NADP}^+$  (nicotinamide adenine dinucleotide phosphate) to NADPH. At the same time, protons are transferred across the thylakoid membrane from the stroma to the lumen and used to drive the synthesis of ATP (adenosine triphosphate). NADPH and ATP are then used to assimilate  $\text{CO}_2$  into

carbohydrates through light-independent reactions (“dark” reactions). In the following, we will focus on the ‘light’ reaction of photosynthesis.

An essential role in the first photosynthetic events is played by the pigments embedded into the proteins of the photosynthetic apparatus. These pigments, namely chlorophylls and carotenoids, are able to absorb light, and transfer the resulting excitation energy to neighboring molecules, guaranteeing the correct sequence of the photosynthetic steps.

Many studies have been performed in order to highlight how this whole process works with a quantum efficiency close to unity, how it is regulated and eventually reproducing it in reengineered photosynthesis. Different advanced spectroscopic techniques can be used to follow the physics and the dynamic of the cascade of energy exchanges.

This research work exploits a series of approaches to investigate the precise mechanisms beyond the interaction between pigments, with a special focus on the photoprotective role played by carotenoids. A series of samples which represents different degree of organization and structuration of pigment-binding proteins will be described and analyzed.

## 1.2 Carotenoids

A large part of this work has been devoted to specific photosynthetic pigments, carotenoid molecules. Carotenoid molecules are natural organic molecules built from the assembly of isoprenoid units (figure 1.1). I will here first address the role and properties of these molecules.

In the last decades the study of carotenoids underwent a significant increase in basically all the research fields. The main interest in this class of pigments is basically due to their ubiquity and versatility. They are indeed present all over the kingdoms of life, from prokaryotes like photosynthetic bacteria to humans, where they assume numerous physiological and biological functions which can involve or not the interaction with light (Britton *et al.*, 2008). For instance the variety of colours, mainly red, orange or yellow, we find in fruits, vegetables marine organisms and birds is often due to the presence of one or a combination of carotenoid molecules, unique for a specific living organism. Highlighting the way they are arranged and combined and the significance and role of a specific colour in different species represents a wide area of research.

Some carotenoids such as  $\alpha$ - and  $\beta$ -carotene and  $\beta$ -cryptoxanthin are provitamin A molecules, *i.e.* they are converted into vitamin A, an essential component of the human diet.

Humans absorb carotenoids from their food at the level of the intestine. Human serum contains  $\beta$ -carotene,  $\alpha$ -carotene, cryptoxanthin, lycopene, and lutein as major components, with smaller concentrations of zeaxanthin, other xanthophylls, and polyenes such as phytofluene and phytoene (see Rao and Rao 2007 for a review). Epidemiological studies revealed a positive association between higher dietary intake and tissue concentrations of carotenoids and lower risk of human diseases including cardiovascular diseases, cancer and other chronic diseases. Even though a causal relation has not been established yet, the antioxidant properties of carotenoids have been suggested as being the main mechanism by which they afford their beneficial effects, together with their ability of enhancing animal and human immune system.

In animal and human photoactive tissues, like the retina in the eye, carotenoids also involved in different ways in the visual process (Snodderly, 1995). It has been recently discovered, though not yet fully understood, that the carotenoids present in the human retina, namely zeaxanthin and lutein, provide protection against the age-related macular degeneration (AMD), a multifactorial degenerative disease of the retina. Results showed a significantly lower risk of developing the eye disease in people with high amounts of lutein+zeaxanthin in their blood (Bone *et al.*, 2000). The first major function of carotenoids in photosynthesis is to act as accessory pigments, absorbing light in region of the electromagnetic spectrum where the chlorophylls do not absorb or poorly absorb (Cogdell *et al.*, 1994). Additionally they are able to protect the photosynthetic apparatus from photo-oxidative stress and thus to balance between the beneficial uses of light energy and protection against energy damage (Foote, 1976).

In photosynthesis, both carotenoids and chlorophylls are generally bound in a non-covalent way to peptides, to form pigment-protein complexes in the thylakoid membrane. The close proximity and the specific orientations between the pigments guaranteed by the binding to proteins maximize the interactions between them, facilitating the chlorophyll-chlorophyll and the carotenoid-chlorophyll fast energy exchange, a prerequisite of a highly efficient photosynthetic process. At the same time the binding of carotenoids to the photosynthetic proteins is essential for their correct folding, assembly and stabilization (Humbeck *et al.*, 1989; Paulsen, 1997) underlying that the role of carotenoids is also structural and not only functional.

### 1.2.1 Molecular structure of carotenoids

Carotenoids are lipophilic pigment molecules with a structure consisting of conjoined units of the hydrocarbon isoprene, with alternating single and double bonds that form a conjugated  $\pi$ -electron system. All carotenoids are tetraterpenoids, meaning that they are produced from 8 isoprene molecules and contain 40 carbon atoms. The resulting assembly is a linear polyene hydrocarbon chain which is sometimes terminated by rings at one or both extremities (as *e.g.* in  $\beta$ -carotene) and which may contain several functional groups which may or may not be conjugated with the isoprenoid chain, such as carbonyl groups in the case of fucoxanthin and spheroidenone. Other possible modifications involve the degree of unsaturation, *cis-trans* isomerization, double-bond rearrangements including allenic and actylenic units, and glycosylation/acylation of the substituent groups.

So far over then 800 different carotenoids have been identified and divided into two main classes: *xanthophylls*, which contain oxygen, and *carotenes*, which are purely hydrocarbons and contain no oxygen.

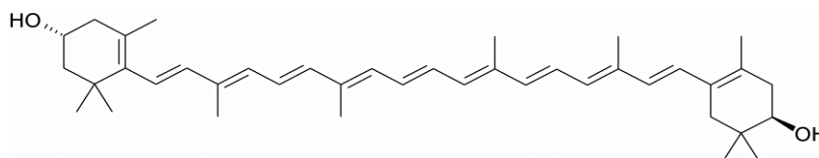


**Figure 1.1** Zeaxanthin molecular structure

### 1.2.2 Synthetic pathway

Animals and humans cannot synthesize carotenoids and they can only assume them by dietary intake, while plants and some bacteria and algae synthesize and accumulate them in plastids.

The core carotenoid pathway is conserved in most plant species although some plants accumulate special and rare carotenoids via unique biosynthetic routes.

The first committed step in carotenoid biosynthesis is the condensation of two molecules of geranyl-geranyl diphosphate (GGPP) by phytoene synthase (PSY) to form phytoene, the first  $C_{40}$  compound (figure 1.2). GGPP is also the precursor for several other groups of metabolites, including chlorophylls, ubiquinones and tocopherols. Phytoene then undergoes four sequential reactions to form lycopene.

In bacteria, only one phytoene desaturase, *crtI*, catalyzes the conversion of phytoene to lycopene; while in plants, at least four enzymes are required for this step. These enzymes are phytoene desaturase (PDS) and zeta-carotene desaturase (ZDS) which produce respective poly-*cis*-compounds, which are then isomerized to *trans* form by zeta carotene isomerase (ZISO) and carotenoid isomerase (CRTISO) to produce lycopene.

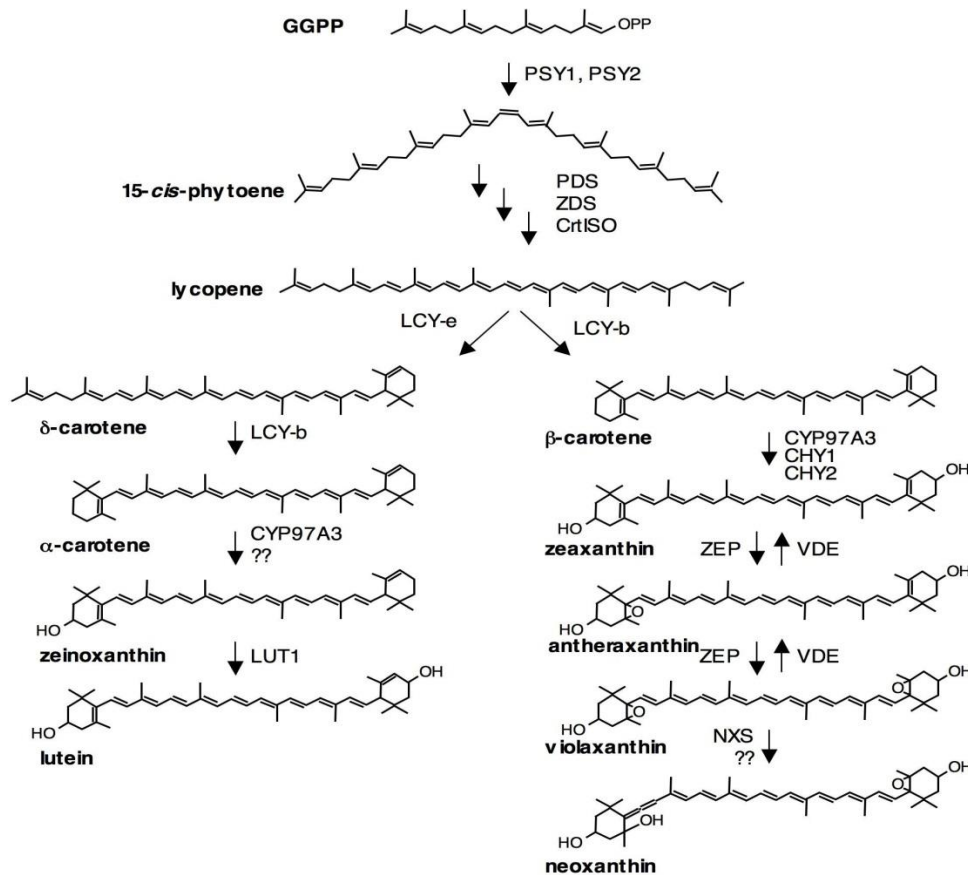


**Figure 1.2** Carotenoid biosynthesis pathway (Diretto et al., 2006).

In higher plants, the cyclization of lycopene by lycopene  $\epsilon$ - and  $\beta$ -cyclases is a critical branch-point in carotenoid biosynthesis (figure 1.2) (Cazzonelli and Pogson, 2010). In one branch, a single enzyme, lycopene  $\beta$ -cyclase ( $\beta$ -CYC), introduces a  $\beta$ -ring at both ends of lycopene to form  $\beta$ -carotene in a sequential two-step reaction. The first dedicated reaction in the other branch, leading to lutein, requires both  $\epsilon$ -CYC and lycopene  $\beta$ -cyclase ( $\beta$ -CYC) to introduce one  $\beta$ - and one  $\epsilon$ -ring into lycopene to form  $\alpha$ -carotene (Cunningham et al., 1996).  $\alpha$ -carotene is acted upon by a  $\beta$ -ring hydroxylase to form zeinoxanthin, which is then

hydroxylated by an  $\epsilon$ -ring hydroxylase to produce lutein, the most abundant carotenoid in green plant tissues.

$\beta$ -carotene can be hydroxylated in a two-step reaction to zeaxanthin, with  $\beta$ -cryptoxanthin as an intermediate product. In green tissues, zeaxanthin can be epoxidized to violaxanthin, and a set of light- and dark-controlled reactions known as the *xanthophyll cycle* rapidly optimize the concentration of violaxanthin and zeaxanthin in the cell (Demmig-Adams and Adams, 1996).

The knowledge of the key enzymes involved in carotenoid biosynthesis and regulation (Cunningham and Gantt, 1998; Farré et al., 2010; Walter and Strack, 2011) has led to a series of attempts at metabolic engineering of carotenoids in economically important crops. Considering the importance of carotenoids for industry, human health and plant development, emphasis has been given to targeted manipulation of carotenoid biosynthesis to modify their production and accumulation *in vivo*. In recent years, the carotenoid biosynthetic pathway in higher plants including Arabidopsis, maize, rice, potato, tomato and canola has successfully been engineered through transgenic approaches. An important example is the *Golden Rice*. In this project two genes have been inserted into the rice genome by genetic engineering, to restart the carotenoid biosynthetic pathway leading to the production and accumulation of  $\beta$ -carotene in the grains (the edible part), where normally it's not present (Beyer et al., 2002).

### 1.2.3 Photophysics properties

Carotenoids achieve all their roles through their electronic properties, which arise from their linear conjugated polyene chain, and more precisely through the energies, structures and dynamics of their low-energy excited electronic states. Despite of the apparent simplicity of their structure, the electronic states of carotenoid molecules is quite complex to predict through modern molecular physics. Although considerable progress has been achieved in this field, precise calculations of their electronic and vibrational properties are still difficult to perform (Wirtz et al., 2007).

Carotenoids absorb in the visible range of light from 450-550 nm, a spectral range in which the sun irradiation is maximal. Figure 1.3 shows a general carotenoid excited state diagram (Papagiannakis et al., 2002; Wang et al., 2005).

The transition from the ground state to the second excited singlet state, the  $S_0$ - $S_2$  transition, is the lowest-energy allowed (Tavan and Schulten, 1987) and is responsible for the intense yellow-orange coloration characteristic of all polyenes and carotenoids. Its energy decreases with the molecular conjugation length (Dale, 1954; Hemley and Kohler, 1977; Christensen et

*al.*, 2004) and it also depends on the refractive index and, consequently, on the polarizability of the solvent (Lerosen and Reid, 1952; Hirayama, 1955; Andersson *et al.*, 1991; Kuki *et al.*, 1994; Chen *et al.*, 2006; Renge and Sild, 2011). The presence of additional conjugated chemical group in the carotenoid molecule influences the position of this absorption transition, as well as distortions and isomerisations of the linear conjugated chain. Usually, this transition displays a clear vibrational sub-structure (see for instance figure 1.4), however, the presence of conjugated carbonyl groups tends to smear this substructure (Frank *et al.*, 2000).

The  $S_2$  excited state has a very short lifetime (200 fs; Truscott, 1990) and because of that the quantum yield fluorescence emission for carotenoids from this state is very low ( $<10^{-4}$ ). However this state plays an important role in transferring excitation energy to chlorophyll molecules in photosynthesis (Andersson *et al.*, 1996; Ricci *et al.*, 1996).

At lower energies than the  $S_2$  level, there are a number of excited states termed as dark, since they are not visible in conventional absorption spectroscopy. The lowest excited singlet state  $S_1$  has the same symmetry as the ground state. Consequently the transition from the ground state to the lowest excited singlet state of carotenoids,  $S_1$ , is optically forbidden, it is populated by internal conversion of  $S_2$  and decays almost totally via internal conversion. Its lifetime is in the order of 10-40 ps (Wasielowski and Kispert, 1986) making the fluorescence from  $S_1$  very weak. It has been shown that  $S_1$  excited state is involved in energy transfer in light-harvesting systems (Gradinaru *et al.*, 2000; Zhang *et al.* 2000; Polivka and Sundström 2004, Berera *et al.* 2007) and in protecting the photosynthetic apparatus in condition of high light stress (Berera *et al.*, 2006; Ruban *et al.*, 2007). The energy level of  $S_1$  also depends on the length of the conjugated chain as  $S_2$ .

Besides  $S_1$ , a number of low energy lying state have been postulated, generally termed  $S^*$ , although it is not always clear that this denomination always describes the same states. The clearest of these  $S^*$  states was shown to act as intermediate in the  $S_2$  to  $S_1$  internal conversion (Berera *et al.*, 2007) and it also plays a role in generation of triplet states in bacterial light harvesting complexes or in the energy transfer to bacteriochlorophyll (Papagiannakis *et al.*, 2002).

Underneath the  $S_1$  state lays the lowest triplet state of carotenoids,  $T_1$  (Foote *et al.*, 1970). The production of the lowest energy triplet state of a carotenoid by direct absorption of light into that state ( $S_0$ - $T_1$ ) is forbidden and therefore quite difficult to populate directly. Instead, this state is usually populated by energy transfer from another excited species, *e.g.*

triplet chlorophyll or singlet oxygen. The capacity of carotenoids to deactivate singlet oxygen confers them their (photo)protective functions (see paragraph 1.5.1). Carotenoid triplet states have absorption maxima between 500 and 560 nm and a lifetime between 5-10  $\mu$ s. Their precise energy is not known, but it is below that of singlet oxygen at around 1.0 eV, allowing energy transfer from the latter. The  $T_1$ - $S_0$  transition is radiationless and thus provides a safe way to dissipate excitation energy as heat.

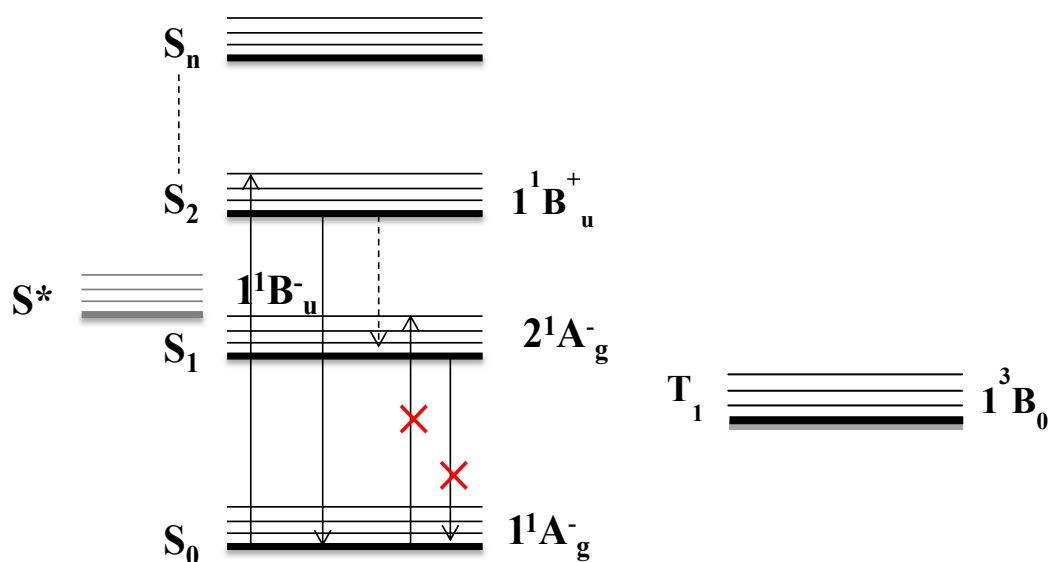


**Figure 1.3** General energy level scheme of carotenoids.  $S_0$  ( $1^1A_g^-$ ) ground state,  $S_1$  ( $2^1A_g^-$ ),  $S_2$  ( $1^1B_u^+$ ) and  $S_n$  excited electronic states;  $S^*$  ( $1^1B_u^-$ ) intermediate excited state;  $T_1$  ( $1^3B_0$ ) triplet state.

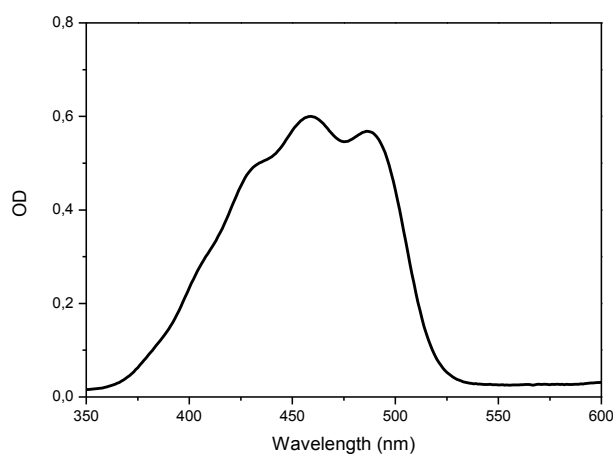


**Figure 1.4** Absorption spectrum of zeaxanthin in THF.

### 1.3 Chlorophylls

Apart from carotenoids, photosynthetic organisms possess two other classes of pigments: (bacterio)chlorophylls and phycobilins. The latter are light-harvesting pigments present only in cyanobacteria and some groups of algae, and they will not be further described in this chapter. Chlorophylls are molecule central to photosynthesis, as they perform not only light absorption in photosynthetic organisms, but are also responsible of the conversion of the absorbed light into chemical potential energy.

Chlorophylls are cyclic tetrapyrroles with a characteristic isocyclic five-membered ring, which are biosynthetically derived from a common precursor, protoporphyrin IX. They usually contain Mg as the central metal ligand. Physically, they are characterized by long-lived excited states and by intense absorption transitions in the blue (around 430 nm) and in the red (640-680 nm).

From a chemical point of view, the different kind of chlorophylls can be divided according to the degree of unsaturation of the macrocycle (figure 1.5):

- 1) the fully unsaturated porphyrin system present in the *c*-type chlorophylls of chromophyte algae and some prokaryotes;
- 2) the 17,18-dyhydroporphyrin system (chlorin) present in chlorophyll *a*, *b* and *d* of photoxygenic organisms and in the BChls *c*, *d* and *e* of green anoxygenic bacteria;
- 3) the 7,8,17,18-tetrahydroporphyrin system (bacteriochlorin) present in the bacteriochlorophyll *a*, *b* and *g* of anoxygenic bacteria.

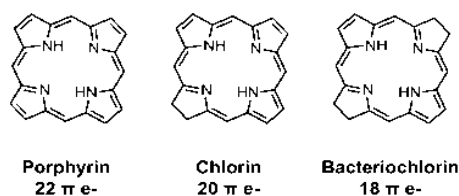


**Figure 1.5** Molecular structure of chlorophylls derivatives.

The two absorption bands in the blue or near UV and in the red or near IR spectral region are called the B (or Soret) and  $Q_y$  bands respectively. They arise from the  $\pi - \pi^*$  transitions, involving the electrons in the conjugated  $\pi$  system of the chlorin macrocycle (Weiss, 1978). Because of the variation in symmetry of the conjugated  $\pi$ -system of macrocycle, the relative intensities and positions of these bands depends on the precise chemical structure of the the pigments, as shown in figure 1.6.

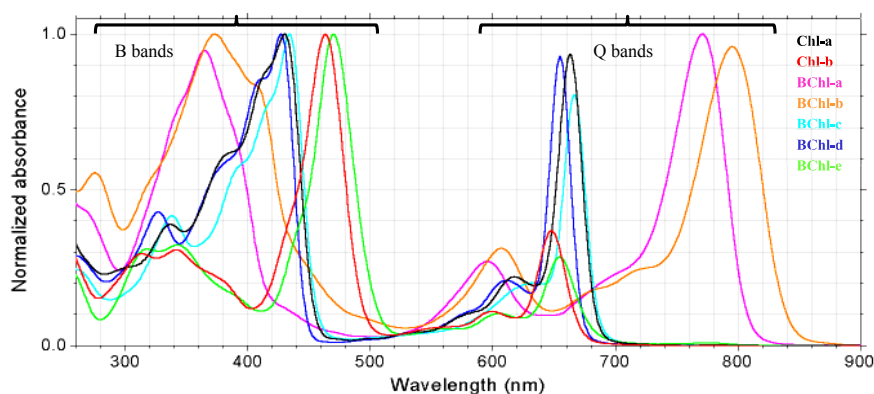


**Figure 1.6** Pigment and absorption maxima of the most common chlorophylls (with the exception of chlorophyll *g*). Adapted from Frigaard *et al.*, 1996.

The introduction of substituent groups or additional ring which alters this system can indeed strongly influence the spectroscopic properties of the pigment, including light absorption and redox potential, and nowadays tetrapyrroles are used in many industrial applications (Senge and Sergeeva, 2006). There has been an immense surge in the preparation of structural homologues, isomers and derivatives with different arrangements/distortion of the macrocycle atoms of these systems, different substituent groups and/or coordination with metals in order to improve their photophysical and biological activities. This surge was accompanied by significant progress in the synthetic methodology for their preparation as well as for the development of novel conformationally designed systems. Few examples are: 1) artificial porphyrins used as artificial light harvesting systems and in opto-electronic devices (Holten *et al.*, 2002; Moore *et al.*, 2007); 2) metallo-substituted chlorins for the structural analysis of chlorophylls and chlorin-containing proteins (Strachan *et al.*, 2000, Taniguchi *et al.*, 2010); 3) synthetic chlorins used as photosensitizers (PS) for Photodynamic Therapy (PTD) (Detty *et al.*, 2004; Josefsen and Boyle, 2008).

## 1.4 The proteins of the photosynthetic apparatus from higher plants

### 1.4.1 Peripheral Photosystem II Antenna Complexes

PSII receives the light energy from an ensemble of peripheral light-harvesting complexes, which belong to the Lhc gene family (Jansson, 1994). The antennas surrounding PSII can be divided in two groups: the major antenna complex LHCIIB and the three minor antenna complexes CP29, CP26 and CP24, all binding chlorophyll *a* and *b* and xanthophylls.

The two groups share large homology sequence thus suggesting a similar structure, going from the transmembrane helices arrangement to most of the pigment-binding sites (Green and Kuhlbrandt, 1995).

#### 1.4.1.1 LHCII

The major light-harvesting antenna, LHCII is the product of the gene *Lhcb1-2-3* (Jansson, 1994) which assembles in a trimeric structure (figure.1.7). Recently, the structure of LHCII at 2.5-2.7 Å resolution has been obtained (Liu *et al.*, 2004; Standfuss *et al.*, 2005). Each monomer is composed of three transmembrane helices and two amphipathic helices and binds 14 chlorophyll molecules (8 Chl *a* and 6 Chl *b*) and 4 xanthophylls (1 neoxanthin, 1 violaxanthin, 2 luteins). The two lutein molecules are situated in two binding sites, L1 and L2, at the centre of the molecule forming a cross-brace, while neoxanthin and violaxanthin are located at the periphery of the trimer, in site N1 and V1, respectively.

LHCII, as the main protein constituent of the thylakoid membrane, has also a structural role in the thylakoid membrane (Garab and Mustárdy, 1999). Thanks to its flexibility it also plays an important function in regulatory processes such as non-photochemical quenching (Horton *et al.*, 1996) and the regulation of phosphorylation by light (Allen *et al.*, 1981; Zer *et al.*, 1999).

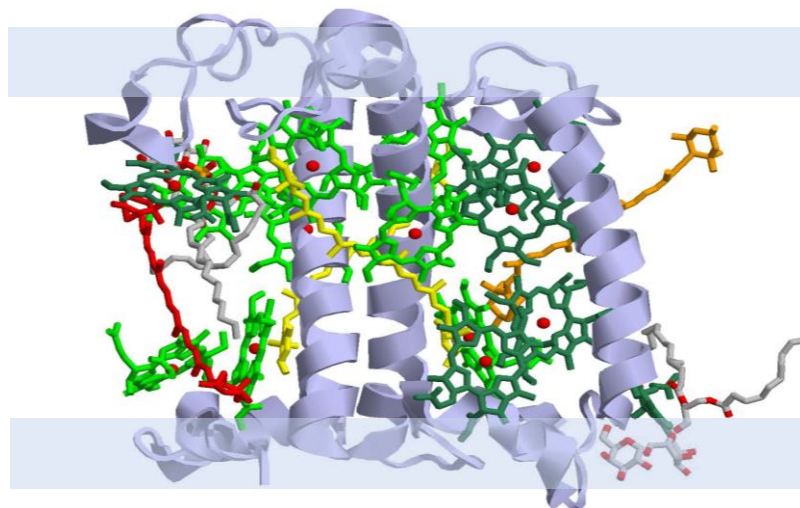


**Figure 1.7** Crystal structure of LHCII (1RWT from PDB databank). In grey the polypeptide backbone; in green chlorophyll *a*, olive green for chlorophyll *b*, yellow for luteins and orange and red for neoxanthin and violaxanthin, respectively. Adapted from Liu *et al.*, 2004.

#### 1.4.1.2 CP29

CP29, encoded by the *Lhcb4* gene (Jansson, 1994), is the largest of the minor light-harvesting proteins. It is located between the outermost antenna LHCII and the inner antenna CP47 in the core complex (Caffarri *et al.*, 2009) and is always present in monomeric form. The crystal structure of CP29 from *Spinacia oleracea* at 2.8 Å resolution has been recently obtained (Pan *et al.*, 2011; figure 1.8). The crystal revealed a different ratio between chlorophylls and carotenoids bound to the molecule compared to previous biochemical and spectroscopic analysis performed on it (Bassi *et al.*, 1999; Ruban *et al.*, 1999). The crystallized protein contains 13 chlorophyll and 3 carotenoid molecules. The 13 chlorophyll-binding sites are assigned as eight chlorophyll *a* sites, four chlorophyll *b* sites and one putative mixed site occupied by both chlorophylls *a* and *b*. The carotenoids identified correspond to one molecule of neoxanthin, lutein and violaxanthin bound in sites N1, L1 and V1 respectively.

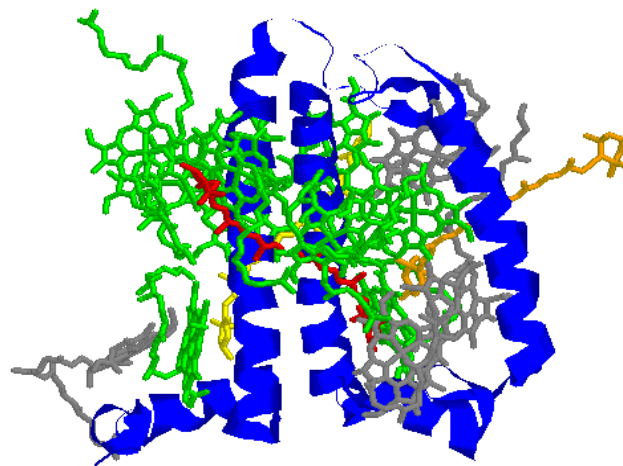


**Figure 1.8** CP29 crystal structure (3PL9 from PDB databank); blue: backbone; green: chlorophyll *a*; grey: chlorophyll *b*; orange: neoxanthin; red: xanthophyll; yellow: lutein.

In addition to its role as light harvesting and transfer, CP29 is proposed to have a role in the non-photochemical quenching. In the work of Pan and coworkers (2011), two special clusters of pigment molecules, namely *a615–a611–a612–Lutein* and *Vio(Zea)–a603–a609*, have been identified and suggested to function as potential energy-quenching centres and as the exit or entrance in energy-transfer pathways. CP29 is also necessary for PSII organization and a key component for the stability of the PSII–LHCII supercomplex (Van Oort. *et al.*, 2010).

#### 1.4.1.3 CP26

CP26 is encoded by *Lhcb5* gene and it's also present as a monomer. The structural data from this protein are not currently available and studies performed so far are quite contrasting between them concerning the precise number of chlorophylls (comprised between 8 and 9) and carotenoids (from 2 to 3 sites) binding this protein (Peter and Thornber, 1991, Sandona et al., 1998; Ruban et al., 1999).

#### 1.4.1.4 CP24

CP24 is encoded by *Lhcb6* gene and is the smallest of the Lhcb proteins. Biochemical and spectroscopic studies showed that the molecule binds 5 chlorophylls *b* and 5 chlorophylls *a*, together with two-three xanthophyll binding sites (Peter and Thornber, 1991; Pagano et al., 1998). As for CP29, CP24 is also believed to have a structural role in the assembly of the PSII-LHCII supercomplex and its correct functioning (Kovács et al., 2006)

### 1.4.2 *Photosystem II supercomplexes*

Heterogeneous preparations of PSII supercomplexes have been obtained directly from mildly solubilized thylakoid membranes or after a fast purification step, which allows enrichment of the PSII-enriched particles, *BBYs* (Boekema et al., 1999; Yakushevskaya et al., 2001). Cross-linking experiments first (Harrer et al., 1998) and electron microscopy (EM) and single particle analysis later, have been used in order to investigate how the different molecules were positioned and interconnected in these macrocomplexes (Yakushevskaya et al., 2003). The biggest complex identified so far is called  $C_2S_2M_2$  (Dekker and Boekema, 2005; figure 1.9). It contains a dimeric core (C2), two LHCII trimers (trimer S) strongly bound to the complex on the side of CP43 and CP26, and two more trimers, moderately bound (trimer M) in contact with CP29 and CP24.

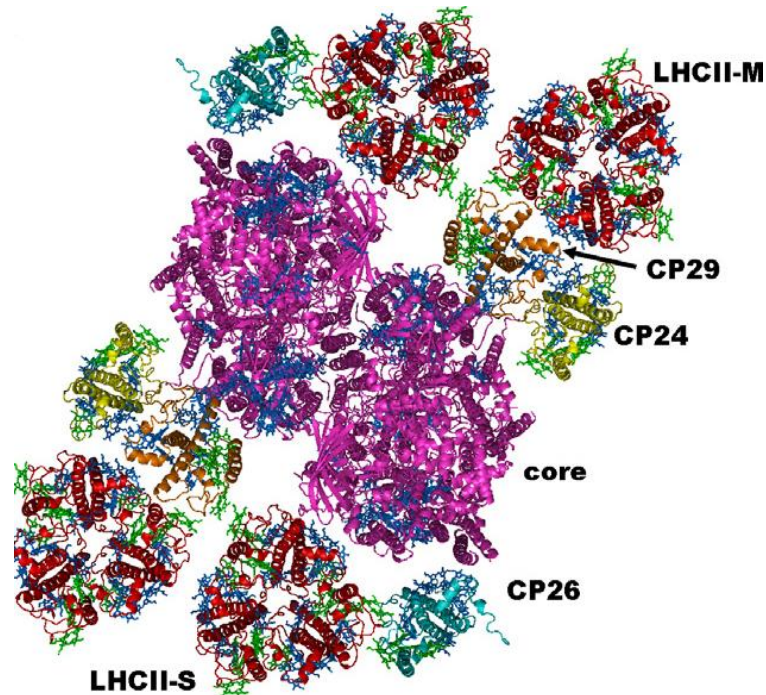


**Figure 1.9** Model of the PSII supercomplex C2S2M2 from higher plants. From Croce and Van Hamerongen, 2011.

In the work of Caffarri and coworkers (2009) more homogeneous and stable preparations of the various types of PSII–LHCII supercomplexes with different antenna sizes have been obtained. The comparison of their protein composition to that one of mutants lacking some of the supercomplex components gives the possibility to relate the supercomplex organization to the protein content and thus to determine the role of the individual subunits in the overall organization.

An additional smaller complex it has also been isolated and characterized after mild detergent solubilisation of PSII membranes (Bassi and Dainese, 1992). It contains CP24, CP29 and LHCII. Phosphorylation of the membranes induces dissociation of the LHCII moiety from the CP29-CP24 moiety and changes in the aggregation state of LHCII components of the CP29-CP24-LHCII complex, showing that this complex is involved in the mechanism of regulation of excitation-energy distribution between the photosystems (Bassi and Dainese, 1992).

### ***1.4.3 Photosystem II***

Photosystem II (PSII) is a large supramolecular pigment-protein complex, which works in series with PSI during the first steps of photosynthesis. It collects light energy and uses it for the reduction of plastoquinone; it oxidizes water and contributes to the formation of a proton gradient across the thylakoid membrane. The most recent PSII structure (Umena et

*al.*, 2011, figure 1.10) from the cyanobacterium *T. vulcanus* has been obtained at 1.9 Å resolution allowing the detailed characterization of the water oxidation  $\text{Mn}_4\text{CaO}_5$ -cluster. Its structure is supposed to be very similar to that of higher plants.

Each PSII monomer contains a core complex constituted by the reaction centre (RC) and the inner antenna proteins CP43 and CP47, the oxygen-evolving complex (OEC) and peripheral light-harvesting antenna.

The inner antenna proteins, CP43 and CP47, bound to D1 and D2 are involved in both light harvesting and energy transfer from the peripheral antennas to the RC (Ferreira *et al.*, 2004).

Several other small subunits are included in the PSII dimer and others are located at its luminal side. They might mainly have a role in stabilizing and guiding the assembly of the macrocomplex, respectively (Zouni *et al.*, 2001; Ferreira *et al.*, 2004). The RC is made of the cytochrome b559 who is thought to have a role in the protection of RC against photodamage (Stewart and Brudvig, 1998), and of the two proteins D1 and D2 which carry out the charge separation and the electron transport. They bind the cofactors involved in these events, including the primary electron donor of PSII, known as P680 and two  $\beta$ -carotene molecules. After light excitation, an electron is transferred from P680 to a pheophytin (Ph), resulting in a charge separation ( $\text{P680}^+ \text{-Ph}^-$ ). From pheophytin the electron goes to the quinone  $\text{Q}_A$ , then to the quinone  $\text{Q}_B$ .  $\text{P680}^+$  is reduced by the water oxidation carried out by D1 protein and the  $\text{Mn}_4\text{CaO}_5$ -cluster. After two charge separations and after proton uptake a reduced plastoquinone  $\text{PQH}_2$  is produced, which leaves PSII and is re-oxidised at the level of cyt  $\text{b}_6\text{f}$ .

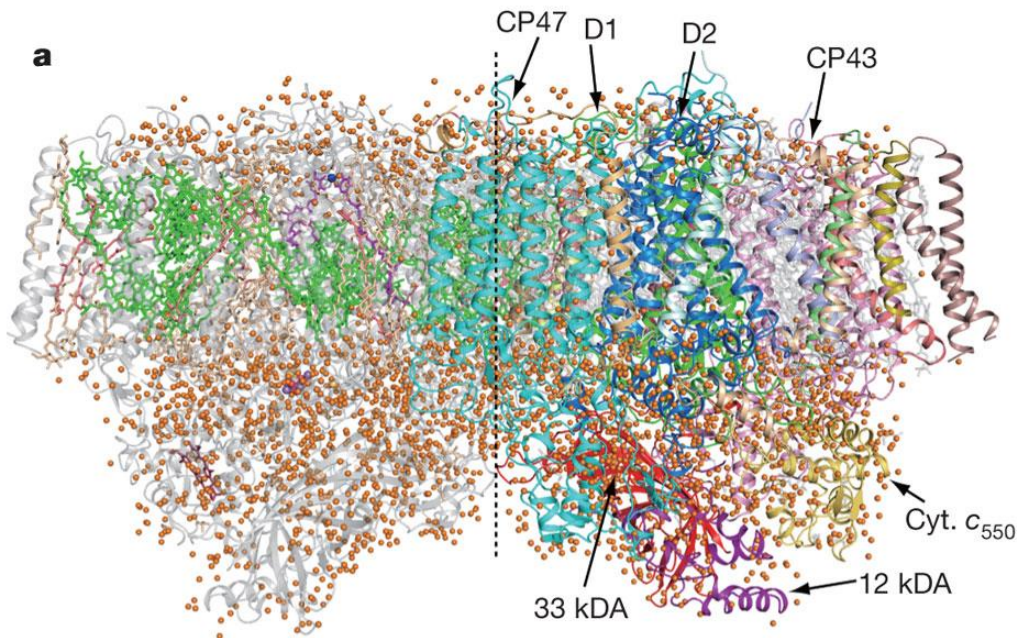


**Figure 1.10** Overall structure of PSII dimer. View from the direction perpendicular to the membrane normal. The protein subunits are colored individually in the right-side monomer and in light gray in the left-side monomer, and the cofactors are colored in the left-side monomer and in light gray in the right-side monomer. Orange balls represent water molecules.

#### 1.4.4 Cytochrome *b<sub>6</sub>f*

The cytochrome *b<sub>6</sub>f* complex (cyt *b<sub>6</sub>f*) provides the electronic connection between the photosystem I and photosystem II reaction centres of oxygenic photosynthesis. It acts by oxidizing lipophilic plastoquinol and reducing plastocyanin and simultaneously, by translocating protons into the thylakoid lumen, generates a trans-membrane electrochemical proton gradient for ATP synthesis. Its crystal structure revealed 4 large (cytochrome *b<sub>6</sub>*, cytochrome *f*, Rieske iron-sulfur, and subunit IV) and 4 smaller (PetG, PetM, PetL and PetN) subunits (Kurisu et al., 2003; for a review see Baniulis et al., 2008). The monomeric form contains four heme molecules, one chlorophyll *a* and one  $\beta$ -carotene.

#### 1.4.5 Photosystem I

Photosystem I is a large membrane protein complex which together with PSII catalyse the light-induced charge separation across the photosynthetic membrane. Solar energy absorbed by PSI antennas is transferred to reaction centre of the complex, which mediates the electron-transfer from plastocyanin at the luminal side to ferredoxin at the stromal side of the thylakoid membrane (Jensen et al., 2002).

A first crystal structure of PSI at 4.4 Å shows 12 core subunits, 4 different light-harvesting membrane proteins (the antenna complex LHCI) assembled into dimers in a half-moon shape on one side of the core, 45 transmembrane helices, 167 chlorophylls, 3 Fe–S clusters and 2 phylloquinones as highlighted by its crystal structure (Ben-Shem *et al.*, 2003a). LHCI proteins are unique among the chlorophyll-a/b binding proteins in their red-shifted absorbance and in the formation of dimers (Croce *et al.*, 2002).

Plant PSI is present in a monomeric structure both *in vitro* and *in vivo* (Ben-Shem *et al.*, 2003b). A more recent crystal structure (Amunts *et al.*, 2010, figure 1.11) obtained at 3.3-Å resolution includes an additional protein subunit, and a total number of 173 chlorophylls and 15  $\beta$ -carotenoids. The two large core complex subunits, PsaA and PsaB, form a symmetry-related dimer, which binds the majority of pigments, including the P700 special pair which forms the primary electron donor in the photosynthetic pathway.

PSI represents also the binding site for phosphorylated LHCII following the state 1 to state 2 transition phenomenon (Lunde *et al.*, 2000).

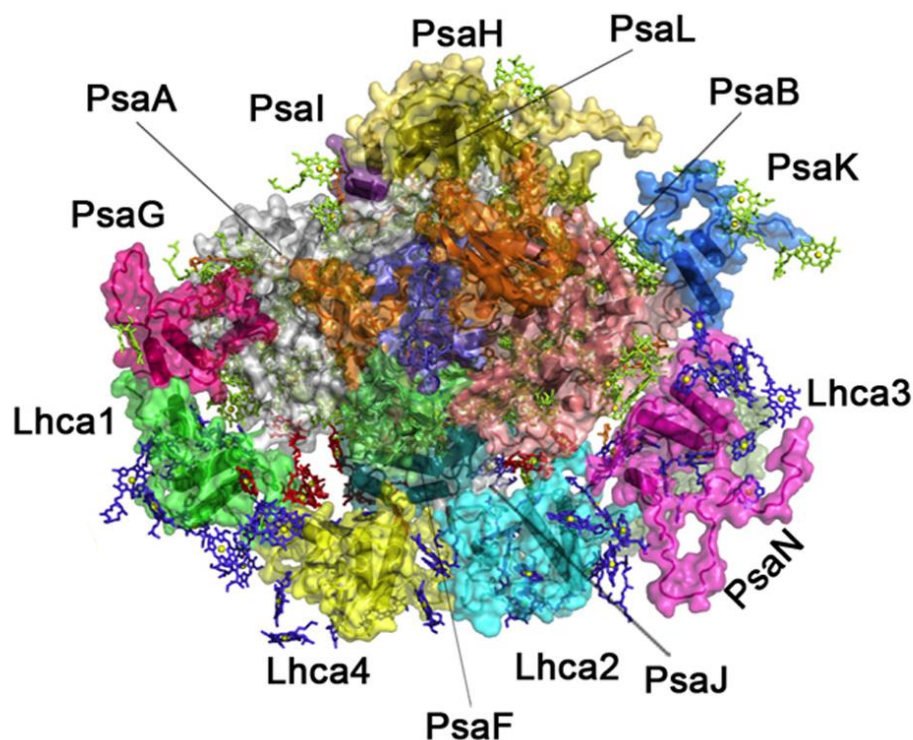


**Figure 1.11** Overall structure of plant PSI, represented in surface and schematic. View from the stroma. The 17 individual protein subunits are indicated with different colours (Amunts *et al.*, 2010).

#### **1.4.6 ATP-synthase complex**

In light reactions, the proton gradient formed by the photosynthetic process is ultimately converted into ATP by the plant ATP-synthase complex, a large multisubunit macromolecular enzyme of about 600 kDa. This complex is responsible for the generation of ATP, from adenosine diphosphate (ADP) and inorganic phosphate (Pi), utilising the proton gradient created by electron transport. In chloroplasts, ATP synthase is called the CF<sub>0</sub>CF<sub>1</sub> complex (Groth and Pohl, 2001). The CF<sub>0</sub> unit is a hydrophobic transmembrane multiprotein complex which contains a water-filled proton conducting channel. The CF<sub>1</sub> unit is a hydrophilic peripheral membrane protein complex that protrudes into the stroma (McCarty *et al.*, 2000). It contains a reversible ATPase and a gate which controls proton movement between CF<sub>0</sub> and CF<sub>1</sub>, a key step of the ATP synthase mechanism (Noji *et al.*, 1997). Entire CF<sub>0</sub>CF<sub>1</sub> complexes are restricted to non-appressed portions of thylakoid membranes due to their bulky CF<sub>1</sub> unit.

#### **1.4.7 Linear electron transport**

The electron transport generated by the photo-induced water oxidation catalyzed by PSII is defined as “linear” (LEF). The stoichiometry of the reactions is indicated for 4 photons absorbed by PSII and 4 photons absorbed by PSI. Electrons are transferred from PSII through the PQ pool to cytb<sub>6</sub>f, which acts as proton pump through the Q cycle. Electrons are then transferred from cytb<sub>6</sub>f to the soluble electron carrier plastocyanin (PC) and then to PSI, which acts as light-driven plastocyanin ferredoxin oxidoreductase. Ultimately FNR reduces NADP<sup>+</sup> to NADPH at the expense of reduced ferredoxin.

#### **1.4.8 Cyclic electron transport**

In addition to LEF, cyclic electron transfer reactions (CEF) can also occur (Joliot and Johnson, 2011). CEF operates via two different routes, one involving a plastoquinone reductase which is homologous to the mitochondrial complex I, the so-called NDH complex, and the other via a putative ferredoxin-quinone reductase, feeding electrons directly into the cytochrome b<sub>6</sub>f complex, the so-called PGRL1/PGR5-dependent pathway (Hertle *et al.*, 2013). CEF involves PSI only and generates ATP without NADPH accumulation (for a review see Johnson, 2011).

When electrons from PS I pass through their primary electron acceptor (ferredoxin), they do not then proceed to form NADPH and O<sub>2</sub>. Rather, they cycle back to plastoquinone

and then to the cytochrome b6/f system, where the energy released by each electron causes two protons (H<sup>+</sup>) to be pumped into the interior of the thylakoid membrane. The protons produce a concentration gradient, or a flow of current, that is used to power chemiosmosis and the production of ATP. The process is cyclic because no outside source of electrons is required. Functioning of either CEF is thought to achieve the appropriate ATP/NADPH balance required for the biochemical needs of the plant, especially under specific environmental conditions. In addition to maintaining the proper balance of ATP and NADPH for the Calvin cycle, it may also serve as a photoprotective device in stress conditions (Rumeau *et al.*, 2007). The regulation of CEF especially in regard to the possible competition with LEF is still under investigation.

### 1.5 Photoprotective mechanisms in higher plants

During the day photosynthetic organisms are exposed to different light intensities. The photosynthetic apparatus has evolved for both maximizing light capture in case of low light conditions and to guarantee protection during exposure to high light.

In low light conditions the amount of light energy absorbed matches the amount utilized in photosynthesis. In high light conditions, the rate of incoming photons is higher than the rate of electron transfer through the photosynthetic apparatus, and the reaction centers become progressively saturated (closed) (figure 1.12; Ruban *et al.*, 2012).

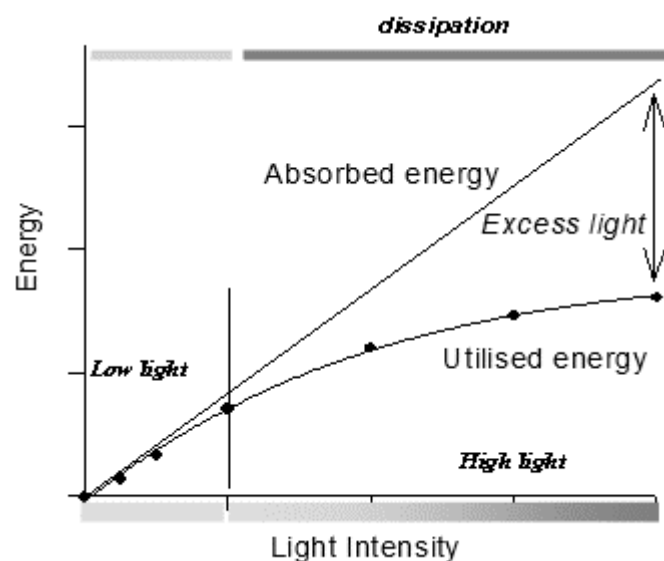


**Figure 1.12** Schematic representation of the behavior of photosynthetic organisms in presence of different light intensities.

Plants are able to respond to strong light (and thus to avoid photodamage) on different level of organization: at the whole organism level via leaf movements and leaf deposit, at the cellular level via chloroplast number and at the molecular level by the control of the number of pigments within the antenna (Bjorkman and Powles, 1987; Chow *et al.*, 1988; Koller, 1990). Molecular adaptations can be long-term (acclimation) based on genetic regulation and short term (regulatory mechanisms).

### ***1.5.1 Photoprotective role of carotenoids***

The communication between carotenoids and (Bacterio)chlorophyll molecules at level of the light harvesting complexes is bidirectional. Carotenoids not only are able to capture the light and transfer the excitation energy to chlorophylls, but they can also interfere with excited singlet and triplet states of chlorophyll to avoid photodamage. This action takes place in the nanosecond/microsecond timescale thus guaranteeing an extremely fast response. In high light conditions, the energy reaching the photosynthetic apparatus can exceed the normal level used for photosynthesis. The excess of energy can then provoke the persistence of excited states of chlorophylls. Triplet-excited chlorophylls can react with molecular oxygen to produce singlet O<sub>2</sub>, which is a powerful oxidizing agent and rapidly kills those cells exposed to it (Foote, 1976). Carotenoids are able to overcome this effect in one of two ways: 1) they can quench singlet oxygen directly through energy transfer or chemical reaction, or 2) they can quench the chlorophyll triplet itself *via* a rapid triplet-triplet energy transfer, preventing the production of singlet oxygen (Krinsky *et al.*, 1971).

*In vivo*, the latter process is dominant. For this reaction to occur efficiently, the energy level of the carotenoid's triplet state must be lower than that of chlorophyll and lower than that of singlet oxygen *i.e.*  $< 1\text{eV}$  ( $1274\text{ nm}-7849\text{ cm}^{-1}$ - or  $94\text{ kJ/mole}$ ; Foote *et al.*, 1970) in order to prevent the triplet-excited carotenoid from reacting with molecular oxygen itself. In practice, this means that only those carotenoids with 9 or more conjugated double bonds ( $n \geq 9$ ) have the ability to photoprotect (Foote *et al.*, 1970). This property could thus be one of the reasons why nature has selected only carotenoids of this length in the photosynthetic proteins. Moreover, because the carotenoid triplet state is lower in energy than singlet oxygen, it returns harmlessly to the ground state with the liberation of heat (Cogdell and Frank, 1987). Carotenoids can also quenching the singlet excited state of chlorophyll, which could also represent a source of singlet oxygen, through a not yet clarified mechanism which plays an essential role in the non-photochemical quenching or NPQ (Truscott *et al.*, 1973; Palozza and

Krinsky, 1992; Niyogi et al., 1997; Pascal et al., 2005; Ruban et al., 2007; Britton et al., 2008). This function will be better described in paragraph 1.5.2.

The different mechanisms of photoprotection guaranteed by carotenoids are schematized in figure 1.13.

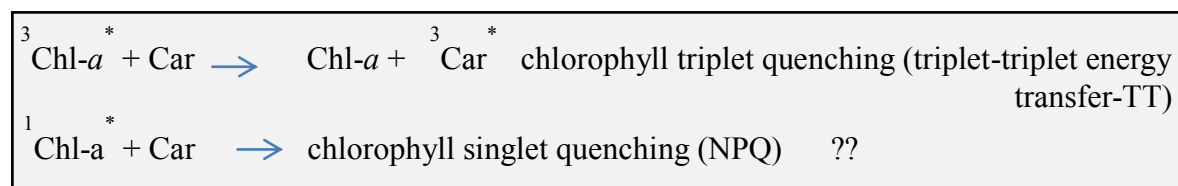


**Figure 1.13** Mechanisms of photoprotection played by carotenoids in photosynthesis

### 1.5.2 Non-photochemical quenching (NPQ)

As already anticipated, photosynthetic organisms possess short-term regulatory mechanisms which serve to reduce the flow of electrons to the acceptor side of PSII, thereby preventing the production of reactive oxygen and thus the irreversible damage of the photosystem in conditions of strong light.

Non-photochemical quenching (NPQ) is based on the reduction of PSII antenna chlorophyll fluorescence yield in order to dissipate the excess energy before it reaches the PSII reaction centers (Muller et al., 2001; Ruban et al., 2012). NPQ is a heterogeneous process and can be divided in three components (Walters and Horton, 1991). qI (photoinhibitory) is the slowest forming and relaxing component. It's partially related to the photodamage of PSII and partially to the antenna quenching associated with the photoprotective downregulation of PSII (Ruban and Horton, 1995; Horton et al., 1996). The second component, qT or state transition, is mainly observed in low light conditions (Walters and Horton, 1991). It forms and relaxes in tens of minutes and is related to the balance of excitation energy between PSII and PSI (Horton and Hague, 1988; Ruban and Johnson, 2009). qE, or energy dependent quenching, is the major component of NPQ in high light and it forms and relaxes within seconds to minutes (Horton and Hague, 1988). This component is dependent on the formation of an intrathylakoid proton gradient during the illumination (Briantais et al., 1979), the xanthophyll cycle (the reversible de-epoxidation of violaxanthin to neoxanthin through an intermediate called antheraxanthin; Yamamoto et al., 1962; 1999) and particularly on the amount of zeaxanthin present (Demmig et al., 1987, Demmig-Adams et al., 1989) and on PsbS which is a PSII-related protein (Funk et al., 1995; Li et al., 2002).

### 1.5.2.1 Site of qE

Most of evidences indicate that the qE component of NPQ occurs within the antenna.

Some of these evidences are as follow:

- quenching of excitation energy within the antenna complexes has been mainly studied by the analysis of PSII fluorescence at 77K (Ruban and Horton, 1995): following the induction of qE, the PSII emission spectrum of PSII resembled that of partially aggregated LHCII, with an enhancement band at 700 nm;

- the xanthophyll cycle carotenoids are associated with the light-harvesting antennae;

- *in vitro* quenching of isolated antenna complexes reproduces many features of *in vivo* qE, such as the kinetics of fluorescence change, the enhancement by zeaxanthin and the absorbance changes accompanying the *in vivo* quenching process (Ruban and Horton, 1992; Wentworth et al., 2000; 2001)

Nowadays is widely accepted the site of qE is within LHCII antenna (Horton and Ruban, 1992; Ruban and Horton, 1995; Wentworth et al., 2000) but there is no agreement on whether this is the only quenching site, and on which part or parts of the antenna is located the qE quencher(s). It seems that no individual LHCII complex acts as the sole site of qE and that potentially the quenching could happen in both the major and minor complexes (Horton et al., 1996; Horton et al., 2005; Kovacs et al., 2006). Important insights into this question were found by investigating various *Lhc* mutants (Yakushevskaya et al., 2003, Andersson et al., 2003; Ruban et al., 2003; Kovacs et al., 2006), which also demonstrated the importance of retaining a correct macro-structure organization of the LHCII antenna system in order to reach maxima levels of NPQ.

### 1.5.2.2 Mechanism(s) of qE

Most of the experiments on qE have been focused on the investigation of the precise role of zeaxanthin in this NPQ component. At first it was suggested a direct role of the xanthophyll cycle zeaxanthin in the quenching mechanism, in the so called “molecular gearshift” (Demmig-Adams, 1990). According to this model, as the energy of the S<sub>1</sub> state of zeaxanthin should lay below that of chlorophyll *a*, a possible energy transfer between the two pigments could happen, allowing to dissipation of the excess energy as heat. Anyway a weak point of this model is that the assignment of the energy levels mentioned above is not straightforward.

It is currently proposed that zeaxanthin acts as an allosteric modulator of the quenching rather than being the direct quencher (Horton et al., 2000). Horton et al. (1991; 2005) proposed the “LHCII aggregation model”, where 4 LHCII states are described,

depending on the epoxidation state of the XC and the luminal pH. The variation in the pH and the conversion of violaxanthin to zeaxanthin promote the aggregation of LHCII trimers, allowing the quenching mechanism to occur. Indeed in isolated LHCII, quenching occurs when protein is in the aggregated form induced by removal of detergent (Ruban *et al.*, 1991) or alternatively in its crystalline form as it has been recently highlighted (Pascal *et al.*, 2005).

#### 1.5.2.3 The *qE* switch and the quencher(s)

Spectroscopic analysis of quenched LHCII gives suggestions about the mechanism of *qE*. Quenched state *in vivo* and *in vitro* is characterized by the appearance of red-shift in Chl *a* absorption at 685 nm, decrease in Chl *a* absorption at 435 nm, Chl *b* at 472 nm and xanthophyll absorption at 488 and 495 nm, corresponding to neoxanthin and lutein1 respectively. Zeaxanthin was found to promote the formation of the 77K 700 nm fluorescence band *in vivo*, characteristic of the LHCII aggregated state *in vitro* (Ruban and Horton, 1992). Resonance Raman spectroscopy was applied to investigate the changes occurring when the LHCII are in aggregated state compared to the isolated trimeric form. It was found that aggregation induces the formation of a hydrogen bond to a formyl group of a chlorophyll *b* molecule and a distortion in the neoxanthin carotenoid molecule (Ruban *et al.*, 1995). Application of the same technique to study isolated chloroplasts and whole leaves showed that the same change in neoxanthin conformation occurs *in vivo*, to an extent consistent with the amount of energy dissipation (Ruban *et al.*, 2007). It's worthy to underline that the *twisting* of neoxanthin during *qE* is only a fingerprint of the quenching mechanism and it doesn't have a direct role, since it also manifests in plants lacking neoxanthin (Niyogi *et al.*, 1998).

Subsequently, similarities were evidenced between the Raman spectra of LHCII aggregates and LHCII crystals (Pascal *et al.*, 2005). Fluorescence analysis showed that the crystals are in a quenched state and Resonance Raman spectra indicated that the structure of the LHCII crystals is similar to the one present when the protein forms aggregate, while it differs from the unquenched, solubilised protein (Pascal *et al.*, 2005). In particular, crystals show a neoxanthin distortion even more pronounced compared to the aggregates and the formation of a hydrogen bond involving a chlorophyll *b* molecule; both features are absent in the not crystallized form. It has been recently shown that the lutein1 molecule attached to LHCII also undergoes to a distortion during the transition of LHCII into the quenched state (Ilioaia *et al.*, 2011).

It was then concluded that LHCII may exist in different conformational states, each having different capacities for energy dissipation. By the interconversion between these states, this dynamic protein is able to switch from a light-collecting form to a dissipative one, through only small structural changes.

In the proposed scenario, the conformational changes occurring in LHCII trimeric unit would somehow favour the formation of a quenching site, allowing thus the dissipation of the energy in excess as heat (Pascal *et al.*, 2005; van Grondelle *et al.*, 2010). Anyway this model doesn't exclude that other process may contribute to qE, such as the participation of the minor antenna complexes CP24, CP26 and CP29 (Bassi and Caffarri, 2000; Morosinotto *et al.*, 2002) or the quenching via formation of carotenoid radicals (Holt *et al.*, 2005).

#### 1.5.2.4 Role of xanthophylls as qE quenchers

An important question to solve for qE researchers was: what is the physical cause of the reduction in fluorescence emission during the quenching phenomenon?

During NPQ, chlorophyll excitation energy is mainly dissipated by internal conversion from to the ground state (loss as heat) or by energy transfer to another pigment. In LHC proteins chlorophylls are relatively close to each other and to the xanthophylls, thus allowing an efficient interaction and energy exchange potentially between all the pigments. The observation of the formation of singlet excited state ( $S_1$ ) of xanthophylls upon chlorophyll excitation in the NPQ state, support the idea that excitonic interactions between chlorophylls and xanthophylls are involved in quenching (Polivka *et al.*, 2002, Ma *et al.*, 2003; Ruban *et al.*, 2007; Bode *et al.*, 2009; Liao *et al.*, 2010 a and b). Indeed the short lifetime and the close proximity of the  $S_1$  state energy to that of the lowest excited state of chlorophyll in the Qy band could account for this physical mechanism of quenching. The existence of energy transfer from a porphyrin ring to the  $S_1$  state of a carotenoid in an artificial conjugated dyad model system (see also chapter 4) further strengthens this hypothesis (Berera *et al.*, 2006).

#### 1.5.2.5 Possible quenching site(s) within LHCII

By observing the LHCII crystal structure (Liu *et al.*, 2004; Standfuss *et al.*, 2005), Pascal and coworkers (2005) proposed several possible quenching sites: terminal emitter domain consisting in chlorophylls Chl *a*611, Chl *a*612, Chl *b*608 and lutein 1; neoxanthin domain: neoxanthin, lutein 2, Chl *b*606, Chl *b*607; xanthophyll cycle binding domain: violaxanthin, Chl *a*611 and Chl *a*601.

Time-resolved absorption spectroscopy applied to LHCII in different quenching states also showed the formation of a carotenoid excited state concomitant with the decay of the

chlorophyll excited state and identified this carotenoid as lutein1 (Ruban *et al.*, 2007). The authors proposed that the conformational change occurring in LHCII during NPQ gives rise to an increase in the rate of energy transfer to lutein 1 and, consequently, to energy dissipation (figure 1.14). Moreover, from a comparison of lutein 1 and lutein 2 in the crystal structure, it has been speculated how a change in the configuration of lutein 1 would bring it closer to chlorophyll *a* 612 (Yan *et al.*, 2007), providing the key step in the switching on of quenching. This idea provides an explanation of the link between the observed changes in protein conformation and fluorescence quenching.

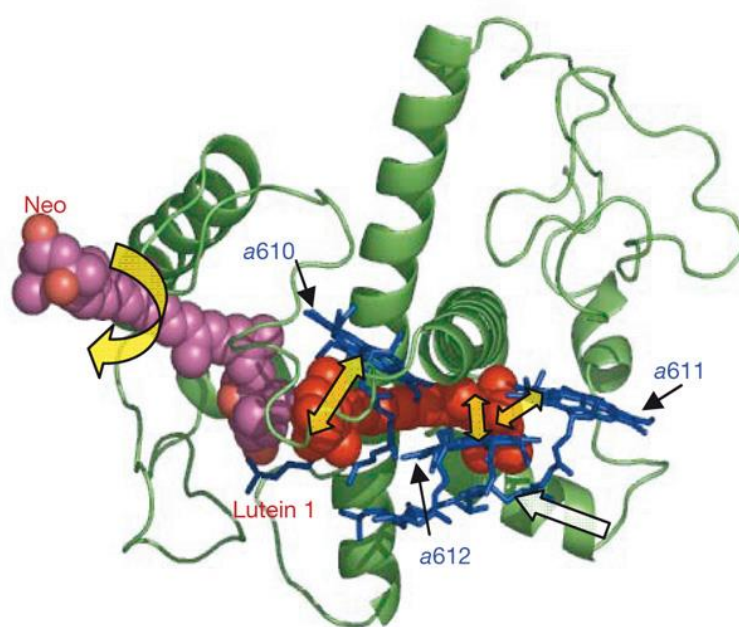


**Figure 1.14** Structural model of an LHCII monomer showing the key pigments involved in the establishment of qE. Lutein 1 (red) is closely associated with chlorin rings of chlorophyll *a* 610, 611 and 612 (blue, small black arrows). Curved broad yellow arrow: the twist of the neoxanthin (Neo) molecule (pink); white broad arrow: the putative movement of lutein 1 towards the chlorophyll cluster (broad yellow arrows).

#### 1.5.2.6 Quenching site(s): alternative hypothesis

A xanthophyll-chlorophyll charge transfer mechanism has also been considered having a role in quenching (Dreuw *et al.*, 2005). A xanthophyll radical cation, attributed to zeaxanthin, was indeed detected in thylakoid in the qE state (Holt *et al.*, 2005), in the minor antenna complex CP29 (Avenson *et al.*, 2008; Ahn *et al.*, 2008) and, in specific conditions, in LHCII trimers (Amarie *et al.*, 2007). Recently, lutein cations have also been detected in the PSII minor antenna complexes and they could play a role in quenching, particularly when zeaxanthin is absent (Avenson *et al.*, 2009; Li *et al.*, 2009).

Charge transfer could also occur between two chlorophyll molecules, excluding thus any involvement of carotenoids in qE (Muller *et al.*, 2010).

It is thus evident that the discussion about the exact photo-physical origins of the quencher thus still remains a subject of great debate in the NPQ field and it requires additional studies to be fully clarified.

## 1.6 Photoinhibition

Even though, plants have various protective mechanisms against light stress, photodamage to PSII can still occur. The energy in excess indeed can potentially cause the damage of the photosynthetic membrane, with photosystem II being the most sensitive component. Disequilibrium between the reduction/oxidation events of its special pair of chlorophylls, P680, can lead to degradation of the D1 protein or create P680 triplet state, leading to formation of the dangerous singlet oxygen (Telfer *et al.*, 1990; Barber, 1995; Melis, 1999). Damage to PSII will bring to a reduction of the photosynthetic efficiency, a phenomenon called photoinhibition (Powles, 1984). However, PSI can also be damaged by light, especially under conditions when electron transport from PSII becomes limited (Sheller and Haldrup, 2005; Kudoh and Sonoike, 2002).

Although significant efforts have been devoted to clarify the mechanisms of photoinhibition no consensus has been reached yet. Indeed photodamage of PSII seems to be a complex process in which different mechanisms participate.

An important role is played by the D1 protein turnover. During this repair cycle new D1 protein is co-translationally inserted into the partially disassembled Photosystem II complex (Ohad *et al.*, 1984; Aro *et al.*, 1993), to substitute the damaged ones, providing a new functional apparatus.

Two key points have been recently highlighted (for a review see Vass, 2012):

- 1) Primary photodamage to PSII is associated with light absorbed by the manganese cluster in the oxygen evolving complex of PSII (Hakala *et al.* 2005; Ohnishi *et al.*, 2005);
- 2) Excess of light absorbed by light-harvesting complexes acts to cause photoinhibition of PSII repair process through the generation of reactive oxygen species, meaning that these species affects only the repair process without damaging the structure and function of PSII (Nishiyama *et al.*, 2001; Murata *et al.*, 2007; Inoue *et al.*, 2011).

## 1.7 Realizing artificial photosynthesis

The importance of photosynthesis has driven many researchers to look for ways to duplicate the fundamental features of photosynthesis in simplified artificial systems (Gust et al., 2001; Barber, 2009). These biomimetic constructs reduce the complicated natural mechanisms to its basic elements, allow a better understanding of photosynthesis and represent artificial power sources for biological processes.

Solar fuel production through artificial photosynthesis may be a key to generating abundant and clean energy, thus addressing the high energy needs of the world's expanding population. As the crucial components of photosynthesis, the artificial photosynthetic system should be composed of a light harvesting antenna (e.g., semiconductor or molecular dye), a reduction co-catalyst (e.g., hydrogenase mimic, noble metal), and an oxidation co-catalyst (e.g., photosystem II mimic for oxygen evolution from water oxidation).

Solar fuel production catalyzed by an artificial photosynthetic system starts from the absorption of sunlight by the light harvester, followed by excitation energy transfer to a reaction centre (RC) which generates a charge separated state by photoinduced electron transfer. Electrons from the reaction centre enable reduction of hydrogen ions to hydrogen gas at the proton reduction catalyst. The oxidized reaction centre is regenerated by electrons from the water oxidation catalyst, which splits the water into oxygen gas and hydrogen ions. This series of events are schematized in figure 1.15 (Gust et al., 2012).

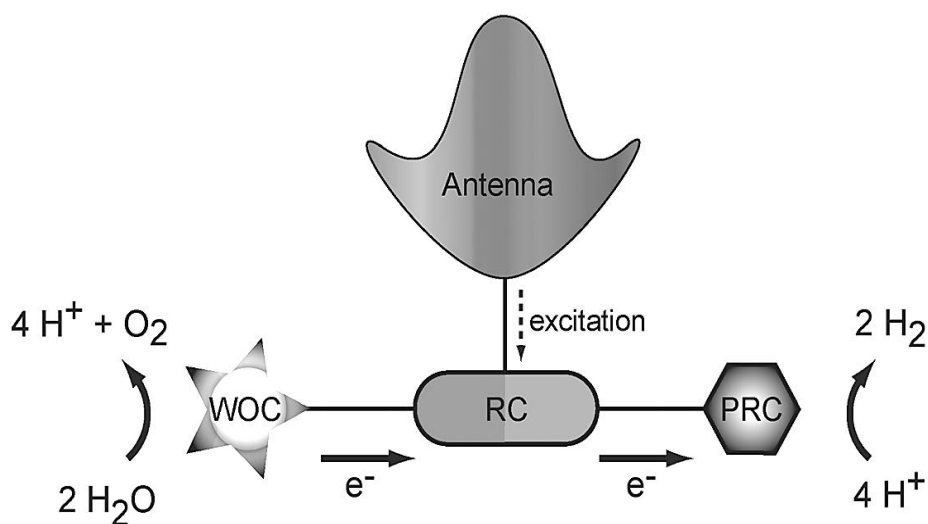


**Figure 1.15** Schematic representation of an artificial photosynthetic system for water splitting. WOC= water oxidation catalyst; RC=reaction centre; PRC= proton reduction catalyst.

A second catalytic system finally uses the reducing equivalents from the reaction center to make fuels such as carbohydrates, lipids, or hydrogen gas.

Every single step requires the realization of artificial systems able to perform the same functions as their natural counterparts. The following description is mainly focused on the realization of artificial antenna systems.

A number of researchers started to synthesize and modify artificial antennas with specific chemical-physical properties that are equal or could potentially exceed those of their natural progenitors (Bensasson. *et al.*, 1981; Gust *et al.*, 2001; Aratani *et al.*, 2009; Harriman and Sauvage, 1996). In these constructs the chromophores are linked by covalent bonds rather than being held in position by the protein scaffold.

The most basic constructs are represented by covalently attached donor/acceptor pairs (dyads) in which one component mimics the structure of chlorophyll and the second one has a carotenoid-like structure. An example of how this kind of compounds can be synthesized is shown in figure 1.16. Chlorophyll-like structure compounds can be represented by various tetrapyrrole rings such as porphyrin, phthalocyanine or purpurin. Carotenoid polyenes of different length can be covalently attached to the tetrapyrrole. The length and the nature of both the bond between the two components and the type of carotenoids, together with the nature of the tetrapyrrole influence the mechanism and dynamics of the energy transfer in the dyads (Gust *et al.*, 1992).

Concerning this last point many studies have shown that the carotenoid moiety of these dyads is effectively able to reproduce the light harvesting and the photoprotective mechanisms of the naturally occurring carotenoids (see *e.g.* Berera *et al.*, 2006; 2007). An example will be illustrated in chapter 4.

The study of such artificial antennas is thus interesting on the one hand because they allow the investigation of the fundamental mechanisms of natural light-harvesting offering the advantage of working on simpler and more controlled systems. On the other hand, they can be considered as the main building blocks of future bioinspired artificial systems that can be used to convert light into stored chemical energy. Indeed these synthetic compounds can be potentially used not only as light harvesters but also as molecular sensors, fluorescent labels and sensitizers for solar cells (Gust *et al.*, 2009).

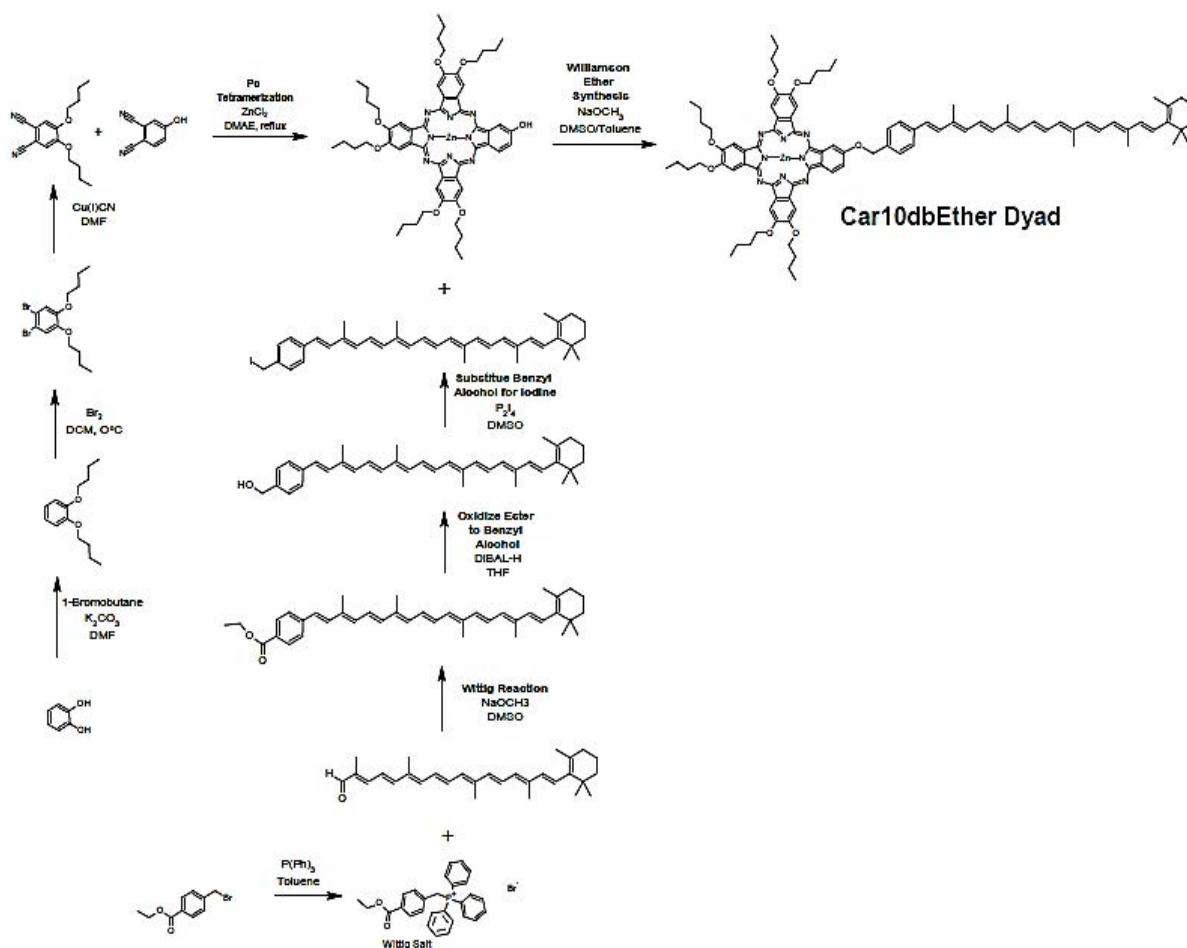


**Figure 1.16** Biosynthetic scheme of a carotenoid ether dyad (Car10EtherDyad) in which a carotenoid of 10 double bonds conjugated system has been covalently linked to a phthalocyanine moiety through an ether bond.

## 1.8 Experimental approach

Vibrational spectroscopy represents a valuable tool for the investigation and characterization of vibrational energy levels of a molecule. An analysis of the resulting spectra can provide information on the structure and on the intermolecular and intramolecular interactions. Generally the structure cannot be directly obtained by the spectrum but vibrational modes of specific chemical groups are transferable between molecules. These specific frequencies can thus be related to the structure of the analyzed molecule and variation in these frequencies can give information about the variation occurred in the molecule structure.

Here a description of Resonance Raman and Infrared spectroscopy will be given. Both techniques can provide detailed information on molecular vibrations, and have been

successfully employed in many areas of investigation. Examples of their application to the study of pigment/pigment-binding proteins will be described in the following paragraphs.

### 1.8.1 Resonance Raman spectroscopy

Raman Spectroscopy is a molecular spectroscopy based on the Raman effect. The Raman effect corresponds to the change in frequency of scattered light by polyatomic molecules (figure 1.17). Shortly, most photons are elastically scattered by molecules and so the molecule returns to its ground state after the collision (Rayleigh Raman scattering; green arrow). With a low probability, some of them are inelastically scattered. The molecule then can be moved to a higher vibrational energy level after the collision and the emitted photon will be of correspondingly lower energy (*i.e.* at a longer wavelength, towards the red end of the spectrum; red arrow). This is the case for ‘Stokes’ Raman, but ‘anti-Stokes’ Raman is also possible, where the molecule starts in a higher vibrational level than the one it is in after the collision. Here the emitted photon is of higher energy (shorter wavelength, towards the blue end of the spectrum; blue arrow).

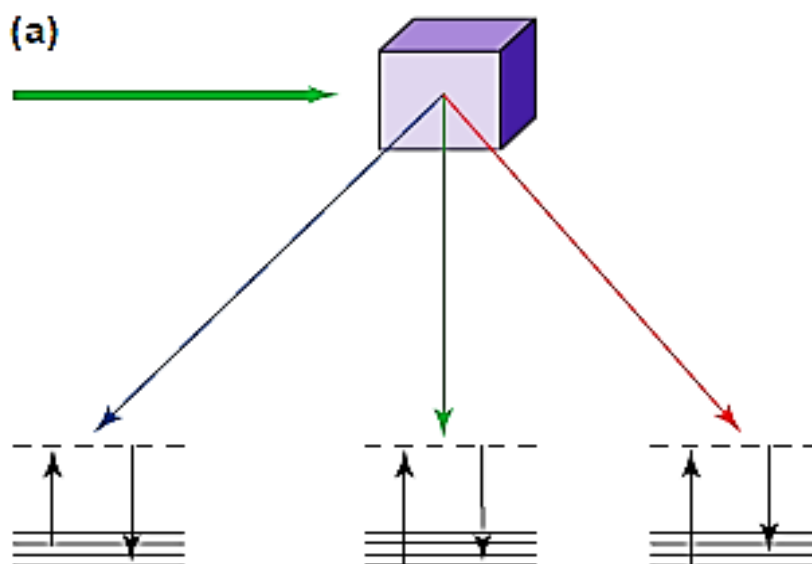


**Figure 1.17** The Raman effect designates an exchange of energy between a molecule and a photon during scattering

The scattered radiation gives information about the energies of vibrational levels of a given electronic state, most often the ground states, of the molecule. These depend on the molecule structure, the bonds between its constituent atoms, and its molecular symmetry. Raman spectroscopy is thus a powerful research tool for the investigation of the chemical

structure and conformation of the molecules as well as the intermolecular interactions they are involved in, even if they are included in a complex biological medium at very low concentration.

In Resonance Raman (RR) Spectroscopy, the frequency of the light used for inducing the Raman effect matches an electronic transition of the irradiated molecule. This allows the signal to be enhanced of about six orders of magnitude. It is thus possible, by this method, to selectively observe a molecule in a complex medium, provided that it possesses an absorption transition, the energy of which matches the energy of the incoming photons. The nature and the position of the bands give information on conformation and configuration of the chromophores and on their interactions, electronic properties (correlation with their structure and/or the physical properties of their environment), subtle changes in their conformation (association with regulatory processes), energy transfer dynamics in their electronic excited states.

Raman bands position will yield information about the vibrational structure of the low-energy electronic states involved in the transition used for inducing the resonance, whilst the intensity of these bands will yield information about the coupling of these modes with the electronic transition.

Under resonance conditions, only a fraction of the vibrational modes of the scattering molecule are enhanced. More precisely, in the simplest case when only one electronic state is involved in resonance, the signal arises from the vibrational modes involving nuclear motions corresponding to distortions experienced by the molecule during transition between the ground- and the excited state used for inducing the resonance (Albrecht, 1961). This intramode selection may apparently constitute a limitation. If a chemical group of the molecule is not directly involved in the electronic transition (for instance, a non-conjugated carbonyl group), resonance Raman will not yield any information about it. However, the functional part of most biological chromophores consists of those atoms that are conjugated with the electronic transition. Resonance Raman will therefore yield selective information on the 'biologically relevant' part of these molecules. Some examples are hemes, Iron-sulfur clusters, chlorins and derivatives, and carotenoid molecules with the latter being very suitable for studies in RR. More recently, it was shown that resonance Raman spectroscopy could be used on biological samples as integrated as chloroplasts or whole leaves, to follow the changes of conformation of specific chromophores (carotenoid molecules in this case), upon

the build-up of a regulatory process (Ruban *et al.*, 2007). In this case, resonance Raman allows a direct probing of the molecular events, which underlie a metabolic process *in vivo*.

### 1.8.2 Carotenoid molecules

Raman spectra of carotenoid molecules present four main groups of bands (figure 1.18; for a review see Robert, 1999). The very strong band near  $1520\text{ cm}^{-1}$  ( $\nu_1$ ) is assigned to the C=C stretching vibration. The  $\nu_1$  line can be used to monitor the degree of conjugation through the  $\pi$  electron system along the conjugated chain so its position is sensitive to the length of this system as well as to the molecular conformation.

A mixture of C=C and C-C stretching mode is usually attributed to the intense band near  $1157\text{ cm}^{-1}$  ( $\nu_2$ ). A strong mixing with C-H in plane bending modes can also perturb this vibration. Both  $\nu_1$  and  $\nu_2$  bands are important to determine the carotenoid configuration (Koyama *et al.*, 1988). The  $\nu_3$  band (around  $1050\text{ cm}^{-1}$ ) gives information on the stretching mode of C-CH<sub>3</sub> bonds, while the out-of-plane wagging motions of the C-H groups originate the  $\nu_4$  (near  $960\text{ cm}^{-1}$ ). This band is sensitive to the molecular conformation of the carotenoid and it increases when the molecule is distorted (Lutz *et al.*, 1987; Pascal *et al.*, 1998).

The application of RR to various photosynthetic pigment-proteins offers a tool to correlate the structural information with the spectroscopic properties of carotenoids to understand the molecular mechanism(s) of their function in photosynthetic systems.

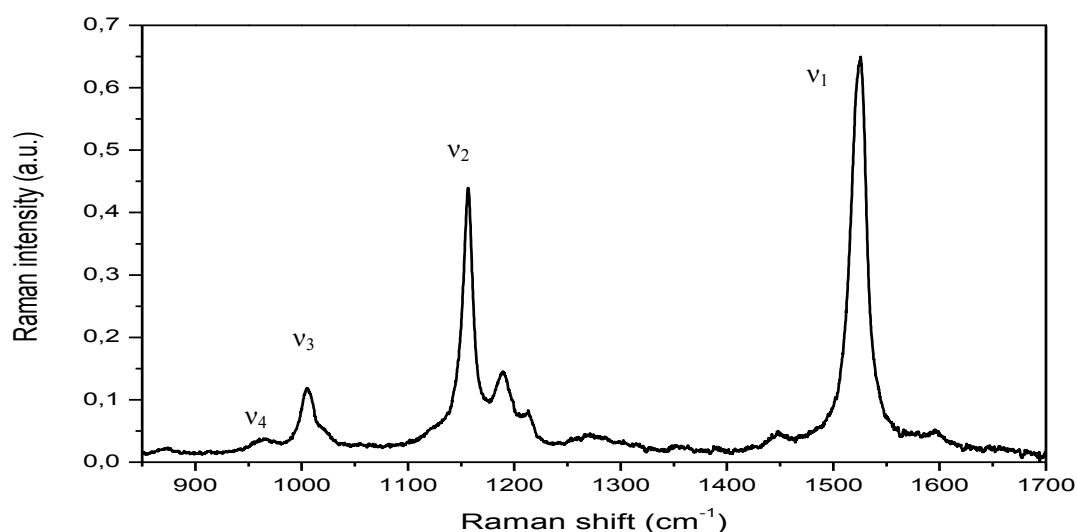


**Figure 1.18** Resonance Raman spectrum of zeaxanthin in THF at 488nm excitation wavelength. The four main groups of bands are indicated. Note that for carotenoid in solution,  $\nu_4$  is almost flat indicating that conjugated system of the carotenoid is symmetrical and the molecule is planar.

### 1.8.3 Chlorophylls and derivatives

The RR spectra of chlorophylls (figure 1.19) and chlorophyll-like molecules is a bit more complicated compared to the carotenoid one and present additional bands, the assignments of which to specific vibrational modes present some difficulties. All the bands can be divided in three main groups: 1) band modes between 200-500  $\text{cm}^{-1}$  which gives information about the central metal ligand (Mg in natural chlorophylls); because of their low intensities these bands are poorly use in the analysis of the RR spectra (Lutz and Robert, 1988); 2) bands between 900-1600  $\text{cm}^{-1}$ , sensitive to the conformation of the conjugated macrocycle (Fujiwara and Tasumi, 1986, Nèveke *et al.*, 1997); 3) region between 1600-1710  $\text{cm}^{-1}$  which contains contributions from the conjugated vinyl and carbonyl group of (B)Chls molecules (Lutz and Robert, 1988).

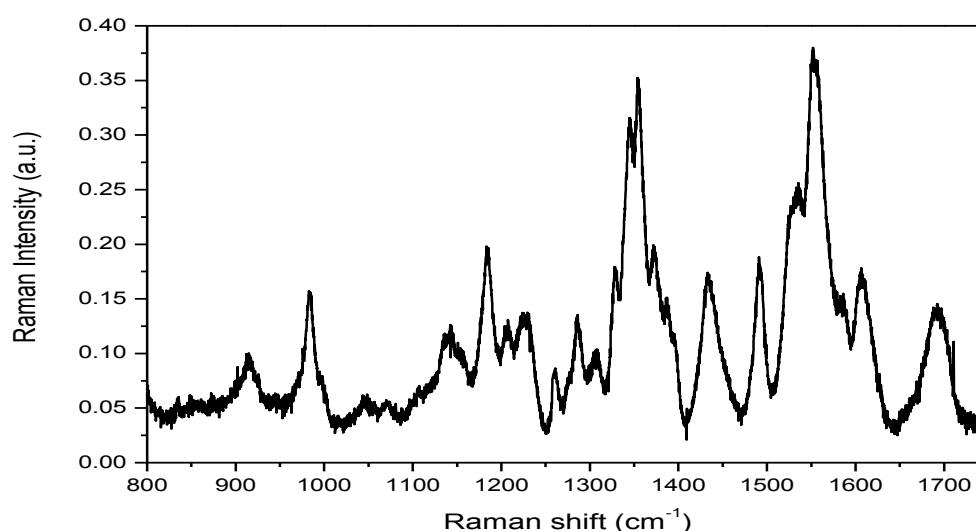


**Figure 1.19** Resonance Raman spectrum of chlorophyll *a* in THF at 413 nm excitation wavelength.

### 1.8.4 Step-scan Fourier transform infrared spectroscopy

Step scan-time resolved FTIR is a technique able to investigate the structure and the environment of unstable and short lived excited states (*e.g.* the triplet states) of molecules. Vibrational modes of functional groups as the carbonyl or alcohol and many others can be used as efficient probes of the molecular states of a selected pigment in the infrared. Thanks to these groups we can specifically identify which molecular species are predominant in the

observed excited states at a specific moment. The high time resolution ( $\mu\text{s}$ ) of this technique allows monitoring the structure and dynamic of the excited states in a short lifetime

It is then of interest the use time-resolved FTIR spectroscopy to measure triplet formation in pigment-binding molecular structures by monitoring excitation-induced variations in the vibrational modes of the chromophores.

Ideally suited to time-resolved study are the light-induced reactions in photobiological systems like the light-driven proton pump bacteriorhodopsin and rhodopsin, the photosynthetic reaction centers (Siebert *et al.*, 1983; Kottling and Gerwert 2005), PCP (Alexandre *et al.*, 2007), and LHCII (Gall *et al.*, 2011). All these samples carry intrinsic chromophores that can be directed activated by a laser flash.

#### 1.8.4.1 Principles

After taking a reference spectrum of the sample in its ground state, a photochemical reaction is triggered by a laser source and a series of infrared light intensity spectra are recorded at equi-spaced time intervals (for example microseconds). Time varying intensities are recorded and automatically digitized and averaged. The time resolved data are then analysed using a global and target analysis procedure which allows identification of the dynamic and the spectral properties of short lived intermediates such as triplet states.

Usually a large number of bands can be seen in the difference spectra. In order to draw more detailed conclusions from the spectra, the bands have to be assigned to individual and specific groups. Chapter 4 will give an example of application of this technique.

## 1.9 Project outline

The overall aim of the work presented here is to investigate which are the mechanisms underlying the photophysical and photochemical properties of carotenoids.

The following chapters will describe how, by using a combination of different spectroscopic and biochemical approaches, these characteristics can be assessed in different kind of samples having the carotenoid molecules as common denominator.

Chapter 2 offers an example of how the absorption properties of carotenoid molecules bound to proteins can be influenced by different factors like the local environment associated with the protein or by specific interactions with the carotenoid binding sites. In particular, the absorption shifts of the two  $\beta$ -carotenes molecules in PSII-RC and those of the two luteins in LHCII will be investigated.

In chapter 3, the photosynthetic and photoprotective activities of *Arabidopsis thaliana* mutants containing an alteration in the enzymatic pathway of the carotenoid biosynthesis will be analysed. In particular the mutant lines show an increased susceptibility of leaves to light-induced damage. We demonstrate here that changes in the photosynthetic electron transport chain rather than alterations of the carotenoid composition in the antenna are responsible for the increased photoinhibition.

In chapter 4, two artificial photosynthetic dyads mimicking the interaction between chlorophyll and carotenoid molecules in photosynthetic proteins will be studied. In particular the triplet-triplet energy transfer rates between the chromophores and the spectroscopic features of their triplet states will be elucidated and compared to those of natural systems.

Chapter 5 describes the preliminary results obtained in the very last period of my PhD. In this work, the effect of the detergent on the isolated LHCII will be investigated and associated to the intrinsic flexibility and dynamic of this protein.

## References

- AHN, T.K., AVENSON, T.J., BALLOTTARI, M., CHENG, Y.C., NIYOGI, K.K., BASSI, R., and FLEMING, G.R. Architecture of a charge-transfer state regulating light-harvesting in a plant antenna protein. *Science*, 2008, 320, p. 794-797.
- ALBRECHT, A.C. On the theory of Raman intensities. *J Chem Phys*, 1961, 34, p.1476-1484.
- ALEXANDRE, M T. A., LÜHRS, D C, VAN STOKKUM, I H. M., HILLER, R, GROOT, M-L, J T. M. KENNIS and VAN GRONDELLE, R.. Triplet State Dynamics in Peridinin-Chlorophyll-a-Protein: A New Pathway of Photoprotection in LHCs? *Biophysical Journal*, 2007, 93, p. 2118-2128.
- ALLEN, J.F., BENNETT, J., STEINBACK, K.E., and ARNTZEN, C.J. Chloroplast protein phosphorylation couples plastoquinone redox state to distribution of excitation energy between photosystems. *Nature*, 1981, 291, p. 25-29.
- AMARIE, S., STANDFUSS, J., BARROS, T., KÜHLBRANDT, W., DREUW, A., and WACHTVEITL, J. Carotenoid radical cations as a probe for the molecular mechanism of non-photochemical quenching in oxygenic photosynthesis. *J. Phys. Chem. B*, 2007, 111, p. 3481-3487.
- AMUNTS, A., TOPORIK, H., BOROVIKOVA, A. and NELSON, N. Structure Determination and Improved Model of Plant Photosystem I. *J Biol Chem.*, 2010, 285, p. 3478-3486.
- ANDERSSON, P.O., GILLBRO, T., FERGUSSON, L., and COGDELL, R.J. Absorption Spectral Shifts of Carotenoids Related to Medium Polarizability. *Photochem. Photobiol.*, 1991, 54, p. 353–360.
- ANDERSSON, P.O., COGDELL, R.J. and T. GILLBRO. Femtosecond dynamics of carotenoid-to-bacteriochlorophyll *a* energy transfer in the light-harvesting antenna complexes from the purple bacterium *Chromatium purpuratum*. *Chem. Phys.*, 1996, 210 p. 196-217.
- ANDERSSON, J., WENTWORTH, M., WALTERS, R.G., HOWARD C.A., RUBAN, A.V., HORTON, P., and JANSSON, S. Absence of the Lhcb1 and Lhcb2 proteins of the light harvesting complex of photosystem II-effects on photosynthesis, grana stacking and fitness. *Plant J.*, 2003, 35, p. 350-361.
- ARATANI, N., KIM, D., and OSUKA, A. Discrete cyclic porphyrin arrays as artificial light-harvesting antenna. *Acc. Chem. Res.*, 2009, 42, p. 1922-1934.
- ARO, E.M., VIRGIN, I., and ANDERSSON, B. Photoinhibition of Photosystem II. Inactivation, protein damage and turnover, *Biochim. Biophys. Acta*, 1993, 1143, p.113-134.
- AVENSON, T.J., AHN, T.K., ZIGMANTAS, D., NIYOGI, K.K., LI, Z., BALLOTTARI, M., BASSI, R., and FLEMING, G.R. Zeaxanthin radical cation formation in minor light-harvesting complexes of higher plant antenna. *J. Biol. Chem.*, 2008, 283, p. 3550-3558.

AVENSON, T.J., AHN, T.K., NIYOGI, K.K., BALLOTTARI, M., BASSI, R., and FLEMING, G. Lutein can act as a switchable charge transfer quencher in the CP26 light-harvesting complex. *J. Biol. Chem.*, 2009, 284, p. 2830-2835.

BANIULIS, D., YAMASHITA, E., ZHANG, H., HASAN S.S. and CRAMER, W.A. Structure–Function of the Cytochrome b<sub>6</sub>f Complex. *Photochem. and Photobiol.*, 2008, 84, p. 1349-1358.

BARBER, J. Molecular basis of the vulnerability of photosystem II to damage by light. *Aust. J. Plant Physiol.*, 1995, 22, p. 201-208.

BARBER, J. Photosynthetic energy conversion: natural and artificial. *Chem. Soc.Rev.*, 2009, 38, p. 185-196.

BASSI, R., and DAINESE, P. A supramolecular light-harvesting complex from chloroplast photosystem-II membranes. *European Journal of Biochemistry*, 1992, 204, p. 317-326.

BASSI, R., CROCE, R., CUGINI, D., and SANDONA, D. Mutational analysis of a higher plant antenna protein provides identification of chromophores bound into multiple sites. *PNAS*, 1999, 96, p. 10056-10061.

BASSI, R., and CAFFARRI, S. Lhc proteins and the regulation of photosynthetic light-harvesting function by xanthophylls. *Photos. Res.*, 2000, 64, p. 243-256.

BENSASSON, R.V., LAND, A.J., MOORE, A.L., CROUCH, R.L., DIRKS, G., MOORE, T.A. and GUST, D. Mimicry of antenna and photo-protective carotenoid functions by a synthetic carotenoporphyrin. *Nature*, 1981, 290, p. 329-332.

BEN-SHEM, A., FROLOW, F., and NELSON N. Crystal structure of plant photosystem I. *Nature*, 2003a, 426, p. 630-635.

BEN-SHEM, A., NELSON, N. and FROLOW, F. Crystallization and initial X-ray diffraction studies of higher plant photosystem I. *Acta Crystallogr.*, 2003b, 59, p. 1824-1827.

BERERA, R., HERRERO, C., STOKKUM, I. H. M. V., VENGRIS, M., KODIS, G., PALACIOS, R. E., AMERONGEN, H. V., GRONDELLE, R. V., GUST, D., MOORE, T. A.; MOORE, A. L., and KENNIS, J. T. M. A simple artificial light-harvesting dyad as a model for excess energy dissipation in oxygenic photosynthesis. *Proc. Natl. Acad. Sci. USA*, 2006, 103, p. 5343–5348.

BERERA, R., VAN STOKKUM, I.H.M., KODIS, G., KEIRSTEAD, A.E., PILLAI, S., HERRERO, C., PALACIOS, R.E., VENGRIS, M., VAN GRONDELLE, R., GUST, D., MOORE, T.A., MOORE, A.L. and KENNIS, J.T.M. Energy Transfer, Excited-State Deactivation, and Exciplex Formation in Artificial Caroteno-Phthalocyanine Light-Harvesting Antennas. *J. Phys. Chem. B*, 2007, 111, p. 6868-6877.

BEYER, P., AL-BABILI, S., YE, X., LUCCA, P., SCHAUB, P., WELSCH, R., and POTRYKUS, I. *J. Nutr.*, 2002, 132, p. 506S-510S.

BJÖRKMAN, O., and POWLES, S.B. Leaf movement in the shade species *Oxalis oregana* L. I. Response to light level and light quality. *Year B Carnegie Inst. Wash.*, 1987, 80, p. 59-62.

BODE, S., QUENTMEIER, C.C., LIAO, P.N., HAFI, N., BARROS, L., WILK, L., BITTNER, F. and WALLA, P.J. On the regulation of photosynthesis by excitonic interactions between carotenoids and chlorophylls. *Proc. Natl. Acad. Sci. USA*, 2009, 106, p. 12311-12316.

BOEKEMA, E.J., VAN ROON, H., VAN BREEMEN, J.F.L., and DEKKER, J.P. Supramolecular organization of photosystem II and its light-harvesting antenna in partially solubilized photosystem II membranes. *European Journal of Biochemistry*, 1999, 266, p. 444-452.

BONE, R.A., LANDRUM, J.T., DIXON, Z., CHEN, Y. and LLERENA, C.M. Lutein and Zeaxanthin in the Eyes, Serum and Diet of Human Subjects. *Experimental Eye Research*, 2000, 71, p. 239-245.

BRIANTAIS, J.M., VERNOTTE, C., PICAUD, M., and KRAUSE, G.H. A quantitative study of the slow decline in chlorophyll a fluorescence in isolated chloroplasts. *Biochim. Biophys. Acta*, 1979, 895, p. 128-138.

BRITTON, G., LIAAEN-JENSEN, S., and PFANDER, H. *Carotenoids: natural functions*, vol. 4; Birkhauser: Basel-Boston-Berlin, 2008.

CAFFARRI, S., KOURIL, R., KEREICHE, S., BOEKEMA, E.J. and CROCE, R. Functional architecture of higher plant photosystem II supercomplexes. *EMBO J.*, 2009, 28, p. 3052-3063.

CAZZONELLI, C.I. and POGSON, B.J. Source to sink: regulation of carotenoid biosynthesis in plants. *Trends in Plant Science*, 2010, 15, p. 266-274.

CHEN, Z., LEE, C., LENZER, T., and OUM, K.J. Solvent effects on the S-0(1(1) Ag(-)) -> S- 2(1(1)B(u(+)) transition of beta-carotene, echinenone, canthaxanthin, and astaxanthin in supercritical CO<sub>2</sub> and CF<sub>3</sub>H. *J. Phys. Chem. A*, 2006, 110, p. 11291-11297.

CHOW, W.S., ANDERSON, J.M., and HOPE, A.B. Variable stoichiometries of photosystem-II to photosystem-I reaction centers. *Photosynth. Res.*, 1988, 17, p. 277-281.

CHRISTENSEN, R.L., BARNEY, A.E., BROENE, R.D., GALINATO, M., GAND I., and FRANK, A.H. Linear polyenes: models for the spectroscopy and photophysics of carotenoids. *Archives of Biochemistry and Biophysics*, 2004, 430, p. 30-36.

COGDELL R. & FRANK H. How carotenoids function in photosynthetic bacteria. *Biochim. Biophys. Acta*, 1987, 895, p. 63-79.

COGDELL R.J., GILLBRO, T., ANDERSSON, P.O., LIU, R.S.H., and ASATO, A.E. Carotenoids as accessory light-harvesting pigments. *Pure Appl. Chem.*, 1994, 66, p. 1041-1046.

CROCE R. and VAN HAMERONGEN H. Light-harvesting and structural organization of Photosystem II: From individual complexes to thylakoid membrane. *J. Photochem. Photob. B.*, 2011, 104, p. 142-153.

CROCE, R., MOROSINOTTO, T., CASTELLETTI, S., BRETON, J. and BASSI, R. The Lhca antenna complexes of higher plants photosystem I. *Biochim. Biophys. Acta*, 2002, 1556, p. 29-40.

CUNNINGHAM, F.X., POGSON, B., SUN, Z.R., McDONALD, K.A., DELLA PENNA, D., and GANTT, E. Functional analysis of the beta and epsilon lycopene cyclase enzymes of Arabidopsis reveals a mechanism for control of cyclic carotenoid formation. *Plant Cell*, 1996, 8, p. 1613-1626.

CUNNINGHAM, F.X. and GANTT, E. Genes and enzymes of carotenoid biosynthesis in plants. *Annual review of plant physiology and plant molecular biology*, 1998, 49, p. 557-583.

DALE, J. Empirical relationships of the minor bands in the absorption spectra of polyenes. *Acta Chem. Scand.*, 1954, 8, p. 1235-1256.

DEKKER, J.P., and BOEKEMA, E.J. Supramolecular organization of thylakoid membrane proteins in green plants. *Biochim. Biophys. Acta*, 2005, 1706, p. 12-39.

DEMMIG, B., WINTER, K., KRÜGER, A., and CZYGAN, F.C. Photoinhibition and zeaxanthin formation in intact leaves. *Plant Physiol.*, 1987, 84, 218-224.

DEMMIG-ADAMS, B., WINTER, K., KRUGER, A., and CZYGAN, F.C. Zeaxanthin synthesis, energy-dissipation, and photoprotection of photosystem-II at chilling temperatures. *Plant Physiol.*, 1989, 90, p. 894-898.

DEMMIG-ADAMS, B. Carotenoids and photoprotection in plants: a role for the xanthophyll zeaxanthin. *Biochim. Biophys. Acta*, 1990, 1020, p. 1-24.

DEMMIG-ADAMS, B. and ADAMS, W.W. The role of xanthophyll cycle carotenoids in the protection of photosynthesis. *Trends in plant Science*, 1996, 1, p. 21-26.

DETTY, M.R., GIBSON, S.L., and WAGNER, S.J. Current Clinical and Preclinical Photosensitizers for Use in Photodynamic Therapy. *Journal of Medicinal Chemistry*, 2004; 47, p. 3897-3915.

DIRETTO, G., TAVAZZA, R., WELSCH, R., PIZZICHINI, D., MOURGUES, F., PAPACCHIOLI, V., BEYER, P., and GIULIANO, G. Metabolic engineering of potato tuber carotenoids through tuber-specific silencing of lycopene epsilon cyclase. *Plant Biology*, 2006, 6.

DREUW, A; FLEMING, G.R, and HEAD-GORDON, M. Role of electron-transfer quenching of chlorophyll fluorescence by carotenoids in non-photochemical quenching of green plants. *Biochem. Soc. Trans.*, 2005, 33, p. 858-862.

FARRÉ, G., SANAHUJA, G., NAQVI, S., BAI, C., CAPELL, T., ZHUA, C. and CHRISTOU, P. Travel advice on the road to carotenoids in plants. *Plant Science*, 2010, 179, p. 28-48.

FERREIRA, K.N., IVERSON, T.M., MAGHLAOU, K., and BARBER, J. Architecture of the photosynthetic oxygen-evolving centre. *Science*, 2004, 303, p. 1831-1838.

FOOTE C.S, Chang YC, Denny RW. Chemistry of singlet oxygen X. Carotenoid quenching parallels biological protection. *J. Am. Chem. Soc.*, 1970, 92, p. 5216-5218.

FOOTE, C. S. Photosensitized oxidation and singlet oxygen: consequences in biological systems. In: *Free radicals and biological systems*. New York, Academic Press, 1976, p. 85-133.

- FRANK, H.A, BAUTISTA, J.A., JOSUE, J., PENDON, Z., HILLER, R.G., SHARPLES, F.P., GOSZTOLA, D. and WASIELEWSKI, M.R. Effect of the solvent environment on the spectroscopic properties and dynamics of the lowest excited states of carotenoids. *Journal of Physical Chemistry B*, 2000, 104, p. 4569-4577.
- FRIGAARD, N.U., LARSEN, K.L., and COX, R.P. Spectrochromatography of photosynthetic pigments as a fingerprinting technique for microbial phototrophs. *FEMS Microbiology Ecology*, 1996, 20, p. 69-77.
- FUJIWARA, M., and TASUMI, M. Resonance Raman and infrared studies on axial coordination to chlorophylls-*a* and chlorophylls-*b* *in vitro*. *Journal of Physical Chemistry*, 1986, 90, p. 250-255.
- FUNK, C., SCHRODER, W.P., NAPIWOTZKI, A., TJUS, S.E., RENGER, G. and ANDERSSON, B. The PSII-S protein of higher plants-a new-type of pigment-binding protein. *Biochem.*, 1995, 34, p. 11131-11141.
- GALL, A., BERERA, R., ALEXANDRE, M.T.A, PASCAL, A.A., BORDES, L., MENDES-PINTO, M.M., ANDRIANAMBININTSOA,S., STOITCHKOVA, K.V., MARIN, A., VALKUNAS, L., HORTON, P., KENNIS, J.T.M., VAN GRONDELLE, R., RUBAN, A.V. and ROBERT, B. Molecular Adaptation of Photoprotection: Triplet States in Light-Harvesting Proteins. *Biophysical Journal*, 2011, 101, p. 934-942.
- GARAB, G., and MUSTÁRDY, L. Role of LHCII-containing macrodomains in the structure, function and dynamics of grana. *Australian journal of plant physiology*, 1999, 26, p. 649-658.
- GRADINARU, C.C., VAN STOKKUM, I.H.M., PASCAL, A.A., VAN GRONDELLE, R., and VAN AMERONGEN, H. Identifying the pathways of energy transfer between carotenoids and chlorophylls in LHCII and CP29. A multicolor, femtosecond pump-probe study. *Journal of physical chemistry B*, 2000, 104, p. 9330-9342.
- GREEN, B.R., and KUHLBRANDT, W. Sequence conservation of light-harvesting and stress-response proteins in relation to the three-dimensional molecular structure of LHCII. *Photosynt. Res.*, 1995, 44, p. 139-148.
- GROTH, G., and POHL, E. The structure of the chloroplast F1-ATPase at 3.2 Å resolution. *Journal of Biological Chemistry*, 2001, 13, p. 583-593.
- GUST, D., MOORE, T.A., MOORE, A.L., DEVADOSS, C., LIDDELL, P.A., HERMANT, R., NIEMAN, R.A., DEMANCHE, L.J., DEGRAZIANO, J.M., and GOUNI, I. Triplet and singlet energy transfer in carotene-porphyrin dyads: role of the linkage bonds. *J. Am. Chem. Soc.*, 1992, 114, p. 3590-3603.
- GUST, D., MOORE, T.A., and MOORE, A.L. Mimicking photosynthetic solar energy transduction. *Acc. Chem. Res.*, 2001, 34, p. 40-48.
- GUST, D., MOORE, T. A., and MOORE, A. L. Solar Fuels via Artificial Photosynthesis. *Acc. Chem. Res.*, 2009, 42, p. 1890-1898.
- GUST, D., MOORE, T.A., and Moore, A.L. Realizing artificial photosynthesis. *Faraday Discussions*, 2012, 155, p. 9-26.

HAKALA, M, TUOMINEN, I, KERÄNEN, M., TYYSTJÄRVI, T., and TYYSTJÄRVI, E. Evidence for the role of the oxygen-evolving manganese complex in photoinhibition of Photosystem II. *Biochim. Biophys. Acta*, 2005, 1706, p. 68-80.

HARRER, R., BASSI R., TESTI, M.G., and SCHAFER C. Nearest-neighbor analysis of a photosystem II complex from *Marchantia polymorpha* L. (liverwort), which contains reaction centre and antenna proteins. *Eur J Biochem.*, 1998, 255, p. 196-205.

HARRIMAN, A., and SAUVAGE, J.P. Strategy for constructing photosynthetic models: Porphyrin-containing modules assembled around transition metals. *Chem. Soc. Rev.*, 1996, 25, p. 45-&.

HEMLEY, R., and KOHLER, B. Electronic-structure of polyenes related to visual chromophore - simple-model for observed band shapes. *Biophys. J.*, 1977, 20, p. 377-382.

HERTLE, A.P., BLUNDER, T., WUNDER, T., PESARESI, P., PRIBIL, M., ARMBRUSTER, U., and LEISTER, D. PGRL1 is the elusive ferredoxin-plastoquinone reductase in photosynthetic cyclic electron flow. *Mol. Cell*, 49, 2013, p. 511-523.

HIRAYAMA, K.J. Absorption Spectra and Chemical Structure. II. Solvent Effect. *Am. Chem. Soc.*, 1955, 77, p. 379-381.

HOLT, N.E., ZIGMANTAS, D., VALKUNAS, L., LI, X.-P., NIYOGI, K.K., and FLEMIG, G.R. Carotenoid cation formation and the regulation of photosynthetic light-harvesting. *Science*, 2005, 307, p. 433-436.

HOLTEN, D, BOCIAN, D.F., and LINDSEY, J.S. Probing electronic communication in covalently linked multiporphyrin arrays. A guide to the rational design of molecular photonic devices. *Acc. Chem. Res.*, 2002, 35, p. 57-69.

HORTON, P., and HAGUE, A. Studies on the induction of chlorophyll fluorescence in isolated barley protoplasts. 4. Resolution of non-photochemical quenching. *Biochim. Biophys. Acta*, 1988, 932, p. 107-115.

HORTON, P., RUBAN, A.V., REES, D., PASCAL, A.A., NOCTOR, G.D., and YOUNG, A.J. Control of the light harvesting function of chloroplast membranes by aggregation of the LHCII chlorophyll protein complex. *FEBS Lett.*, 1991, 292, p. 1-4.

HORTON, P., and RUBAN, A.V. Regulation of photosystem II. *Photos. Res.*, 1992, 34, 375-385.

HORTON, P., RUBAN, A.V., and WALTERS, R.G. Regulation of light harvesting in green plants. *Ann. Rev. Plant Physiol. Plant Molec. Biol.*, 1996, 47, p. 655-684.

HORTON, P., RUBAN, A.V., and WENTWORTH, M. Allosteric regulation of light harvesting system pf photosystem II. *Phylos. Trans. Royal. Soc. London B-Biol. Sci.*, 2000, 355, p. 1361-1370.

HORTON, P., WENTWORTH, M., and RUBAN, A.V. Control of the light harvesting function of chloroplast membranes: the LHCII-aggregation model for non-photochemical quenching. *FEBS Lett.*, 2005, 579, p. 4201-4206.

HUMBECK, H., ROMER, S., and SENGER, H. Evidence for an essential role of carotenoids in the assembly of an active photosystem II. *Planta*, 1989, 179, p. 242-250.

ILIOAIA, C., JOHNSON, M. P., LIAO, P.-N., PASCAL, A. A., GRONDELLE, R. van, WALLA, P. J., RUBAN, A. V., and ROBERT, B. Photoprotection in Plants Involves a Change in Lutein 1 Binding Domain in the Major Light-harvesting Complex of Photosystem II. *J. Biol. Chem.*, 2011, 286, p. 27247-27254.

INOUE, S., EJIMA, K., IWAI, E., HAYASHI, H., APPEL, J., TYYSTJÄRVI, E., MURATA, N. and NISHIYAMA, Y. Protection by  $\alpha$ -Tocopherol of the Repair of Photosystem II During Photoinhibition in *Synechocystis* Sp. PCC 6803. *Biochim. Biophys. Acta*, 2011, p. 236-241.

JANSSON, S. The light-harvesting chlorophyll a/b binding proteins. *Biochimica et Biophysica Acta-Bioenergetics*, 1994, 1184, p. 1-19.

JENSEN, P.E., ROSGAARD, L., KNOETZEL, J., and SHELLER, H.V. Photosystem I activity is increased in the absence of the PSI-G subunit. *Journal of Biological Chemistry*, 2002, 277, p. 2798-2803.

JOHNSON, G.N. Reprint of: physiology of PSI cyclic electron transport in higher plants. *Biochim. Biophys. Acta*, 2011, 1807, p. 906-911.

JOLIOT, P and JOHNSON, G.N. Regulation of cyclic and linear electron flow in higher plants. *Proc. Natl. Acad. Sci. USA*, 2011, 108, p. 13317-13322.

JOSEFSEN L.B. and BOYLE R.W. Photodynamic Therapy and the Development of Metal-Based Photosensitisers. *Hindawi Publishing Corporation Metal-Based Drugs*, 2008, 24 p.

KOLLER, D. Light-driven leaf movements. *Plant Cell Environ.*, 1990, 13, p. 615-632.

KOTTING, C, and GERWERT, K Proteins in action monitored by time-resolved FTIR spectroscopy. *Chem. Phys. Chem*, 2005, 6, p. 881-888.

KOVÁCS, L., DAMKJAER, J., KEREÏCHE, S., ILIOAIA, C., RUBAN, A.V., BOEKEMA, E.J., JANSSON, S., and HORTON, P. Lack of the light-harvesting complex CP24 affects the structure and function of the grana membranes of higher plants chloroplasts. *Plant Cell*, 2006, 18, p. 3106-3120.

KOYAMA, Y TAKATSUKA, I ,NAKATA, M , and TASUMI, M. Raman and infrared-spectra of the all-*trans*, 7-*cis*, 9-*cis*, 13-*cis* and 15-*cis* isomers of beta-carotene - key bands distinguishing stretched or terminal-bent configurations from central-bent configurations. *Journal Of Raman Spectroscopy*, 1988, 19, p. 37-49.

KRINSKY, N. I. Function. *In Carotenoids*. O. Isler, G. Guttman, and U. Solms, editors. Birkhäuser, Basel, Switzerland, 1971, p. 669-716.

KUDOH, H. and SONOIKE, K. Irreversible damage to photosystem I by chilling in the light: cause of the degradation of chlorophyll after returning to normal growth temperature. *Planta* 2002, 215, p. 541-548.

KUKI, M., NAGAE, H., CODGELL, R.J., SHIMADA, K., and KOYAMA, Y. Solvent Effect on Spheroidene in Nonpolar and Polar Solutions and the Environment of Spheroidene in the Light-Harvesting Complexes of *Rhodobacter-Sphaeroides* 2.4.1 as Revealed by the Energy of the  $1A_g \rightarrow 1B_u$  Absorption and the Frequencies of the Vibronically Coupled C=C Stretching Raman Lines in the  $(1)A_g(-)$  and  $2(1)A_g(-)$  States. *Photochem. Photobiol.*, 1994, 59, p. 116-124.

KURISU, G., ZHANG, H., SMITH, J.L., and CRAMER, W.A. Structure of the cytochrome  $b_6/f$  complex of oxygenic photosynthesis: tuning the cavity. *Science*, 2003, 302, p. 614-621.

LEROSEN, A.L., and REID, E.D.J. An investigation of certain solvent effect in absorption spectra. *Chem. Phys.*, 1952, 20, p. 233-236.

LI, X.P., MULLER-MOULE, P., GILMORE, A.M., and NIYOGI, K.K. PsbS-dependent enhancement of feedback de-excitation protects photosystem II from photoinhibition. *Proc. Natl. Acad. Sci. USA*, 2002, 99, p. 15222-15227.

LI, Z., AHN, T.K., AVENSON, T.J., BALLOTTARI, M., CRUZ, J.A., KRAMER, D.M., BASSI, R., FLEMING, G., KEASLING, J.D., and NIYOGI, K.K. Lutein accumulation in the absence of zeaxanthin restores non-photochemical quenching in the *Arabidopsis thaliana* npq1 mutant. *Plant Cell*, 2009, 21, p. 1798-1812.

LIAO, P.N., HOLLEBOOM, C.P., WILK, L., KUHLBRANDT, W., and WALLA, J.P. Correlation of Car S1-Chl with Chl-Car S1 energy transfer supports the excitonic model in quenched light-harvesting complex II. *J. Phys. Chem. B*, 2010a, 114, p. 15650-15655.

LIAO, P.N., BODE, S., WILK, L., HAFI, P., and WALLA, P.J. Correlation of electronic carotenoid-chlorophyll interactions and fluorescence quenching with the aggregation of native LHCII and chlorophyll deficient mutants. *Chem. Phys.*, 2010b, 373, p. 50-55.

LIU, Z., YAN, H., WANG, K., KUANG, T., ZHANG, J., GUI, L., AN, X., and CHANG, W. Crystal structure of spinach major light-harvesting complex at 2.72 Å resolution. *Nature*, 2004, 428, p. 287-292.

LUNDE, C., JENSEN, P.E., HALDRUP, A., KNOETZEL, J., and SHELLER, H.V. The PSI-H subunit of photosystem I is essential for state transitions in plant photosynthesis. *Nature*, 2000, 408, p. 613-615.

LUTZ, M., SZPONARSKI, W., BERGER, G., ROBERT, B., and NEUMANN, J.M. The stereoisomerism of bacterial, reaction-center-bound carotenoids revisited: An electronic absorption, resonance Raman and  $^1\text{H-NMR}$  study. *Biochim. et Biophys. Acta- Bioenergetics*, 1987, 894, p. 423-433.

LUTZ, M., and Robert, B. In *Biological Applications of Raman Spectroscopy* (Spiro, T. G., Ed.), Wiley, New York, 1988, 111, Chapter 8.

MA, Y.Z., HOLT, N.E., LI, X.P., NIYOGI, K.K., and FLEMING, G.R. Evidence for direct carotenoid involvement in the regulation of light harvesting. *Proc. Natl. Acad. Sci. USA*, 2003, 100, p. 4377-4382.

MCCARTY, R.E., EVRON, Y., and JOHNSON, E.A. The chloroplast ATP synthase: A Rotary Enzyme? *Annu. Rev. Plant Physiol. Plant Mol. Biol.*, 2000, 51, p. 83-109.

MELIS, A. Photosystem-II damage and repair cycle in chloroplasts: what modulates the rate of photodamage in vivo? *Trends Plant Sci.*, 1999, 4, p. 130-135.

MOORE, A.L, GUST, D., and MOORE, T.A. Bio-inspired constructs for sustainable energy production and use. *Actual. Chim.*, 2007, p. 50-56.

- MOROSINOTTO, T., BARONIO, R., and BASSI, R. Dynamics of chromophore binding to Lhc proteins *in vivo* and *in vitro* during operation of the xanthophyll cycle. *J. Biol. Chem.*, 2002, 277, p. 36913-36920.
- MULLER, M.G., LAMBREV, P., REUS, M., WIENTJES, E., CROCE, R., and HOLZWARTH, A.R. Singlet energy dissipation in the photosystem II light-harvesting complex does not involve energy transfer to carotenoid. *Chem. Phys. Chem.*, 2010, 11, p. 1289-1296.
- MULLER, P., LI, X.P., and NIYOGI, K.K. Non-photochemical quenching. A response to excess light energy. *Plant Physiol.*, 2001, 125, p. 1558-1566.
- MURATA, N., TAKAHASHI, S., NISHIYAMA, Y., and ALLAKHVERDIEV, S.I. Photoinhibition of photosystem II under environmental stress. *Biochim. Biophys. Acta*, 2007, 1767, p. 414-421.
- NAVEKE, A., LAPOUGE, K., STURGIS, J.N., HARTWICH, G., SIMONIN, I., SCHEER, H. and ROBERT, B. Resonance Raman spectroscopy of metal-substituted bacteriochlorophylls: Characterization of Raman bands sensitive to bacteriochlorin conformation. *Journal of Raman Spectroscopy*, 1997, 28, p. 599-604.
- NISHIYAMA, Y., YAMAMOTO, H., ALLAKHVERDIEV, S.I., INABA, H., YOKOTA, A., and MURATA, N. Oxidative stress inhibits the repair of photodamage to the photosynthetic machinery. *EMBO J.*, 2001, 20, p. 5587-5594.
- NIYOGI, K.K., BJORKMAN, O., and GROSSMAN, A.R. The roles of specific xanthophylls in photoprotection. *Proc. Natl. Acad. Sci. USA.*, 1997, 94, p. 14162-14167.
- NIYOGI, K.K., GROSSMAN, A.R., BJÖRKMAN, O. Arabidopsis mutants define a central role for the xanthophyll cycle in the regulation of photosynthetic energy conversion. *Plant Cell*, 1998, 10, p. 1121-1134.
- NOJI, H., YASUDA, R., YOSHIDA, M., and KINOSITA, K. Direct observation of the rotation of F<sub>1</sub>-ATPase. *Nature*, 1997, 386, p. 299-302.
- OHAD, I., KYLE, D.J. and ARNTZEN, C.J. Membrane-protein damage and repair-removal and replacement of inactivated 32-kilodalton polypeptides in chloroplast membranes. *J. Cell. Biol.*, 1984, p. 481-485.
- OHNISHI, N., ALLAKHVERDIEV, S.I., TAKAHASHI, S., HIGASHI, S., WATANABE, M., NISHIYAMA, Y., and MURATA, N. Two-step mechanism of photodamage to Photosystem II: step 1 occurs at the oxygen-evolving complex and step 2 occurs at the photochemical reaction center. *Biochem.*, 2005, 44, p. 8494-8499.
- PAGANO, A., CINQUE, G., and BASSI, R. *In vitro* reconstitution of the recombinant photosystem II light-harvesting complex CP24 and its spectroscopic characterisation. *Journal of Biological Chemistry*, 1998, 273, p. 17154-17165.
- PALOZZA, P., and KRINSKY, N.I. Antioxidant effects of carotenoids *in vivo* and *in vitro* - an overview. *Methods Enzymol.*, 1992, 213, p. 403-420.
- PAN, X., LI, M., WAN, T., WANG, L., JIA, C., HOU, Z., ZHAO, X., JIPING, Z., and CHANG, W. Structural insights into energy regulation of light-harvesting complex CP29 from spinach. *Nature structural and molecular biology*, 2011, 18, p. 309-316.

- PAPAGIANNAKIS, E., KENNIS, J.M., VAN STOKKUM, I.M., COGDELL, R.J., and VAN GRONDELLE, R. An alternative carotenoid-to-bacteriochlorophyll energy transfer pathway in photosynthetic light harvesting. *Proc. Natl. Acad. Sci. USA*, 2002, 99, p. 6017-6022.
- PASCAL, A.A., CARON, L., ROUSSEAU, B., LAPOUGE, K., DUVAL, J.C., and ROBERT, B. Resonance Raman spectroscopy of a light-harvesting protein from the brown alga *Laminaria saccharina*. *Biochem.*, 1998, 37, p. 2450-2457.
- PASCAL, A.A., LIU, Z., BROESS, K., VAN OORT, B., VAN AMERONGEN, H., WANG, C., HORTON, P., ROBERT, B., CHANG, W. and RUBAN, A. Molecular basis of photoprotection and control of photosynthetic light-harvesting. *Nature*, 2005, 436, p. 134-137.
- PAULSEN, H. Pigment ligation to proteins of the photosynthetic apparatus in higher plants. *Physiol. Plantarum*, 1997, 100, p. 760-768.
- PETER, G.F., and THORNER, J.P. Biochemical composition and organization of higher-plant photosystem II light-harvesting pigment-proteins. *J. Biol. Chem.*, 1991, 266, p. 16745-16754.
- POLIVKA, T., ZIGMANTAS, D., SUNDSTRÖM, V., FORMAGGIO, E., CINQUE, G. and BASSI, R. Carotenoid S1 State in a Recombinant Light-Harvesting Complex of Photosystem II. *Biochem.*, 2002, 41, p. 439-450.
- POLIVKA, T., and SUNDSTROM, V. Ultrafast dynamics of carotenoid excited states - From solution to natural and artificial systems. *Chemical Reviews*, 2004, 104, p. 2021-2071.
- POWLES, S.B. Photoinhibition of photosynthesis induced by visible light. *Ann. Rev. Plant Physiol. Plant Mol. Biol.*, 1984, 35, p. 15-44.
- RAO, A.V., and RAO, L.G. Carotenoids and human health. *Pharmacological Research*, 2007, 55, p. 207-216.
- RENGE, I., and SILD, E. Absorption shifts in carotenoids-influence of index of refraction and submolecular electric fields. *J. Photochem. Photobiol. A-Chem.*, 2011, 218, p. 156-161.
- RICCI, M., BRADFORTH, S.E., JIMINEZ, R., and FLEMING, G.R. Internal conversion and energy transfer dynamics of spheroidene in solution and in the LH1 and LH2 light-harvesting complexes. *Chem. Phys. Lett.*, 1996, 259, p. 381-390.
- ROBERT, B. The electronic structure, stereochemistry and resonance Raman spectroscopy of carotenoids. In: *The photochemistry of Carotenoids. Advances in photosynthesis and respiration*, Frank HA, Young AJ, Britton G, Cogdell RJ (eds), Springer, Dordrecht, 1999, vol. 8, p. 189-201.
- RUBAN, A.V., REES, D., NOCTOR, G.D., YOUNG, A.J., and HORTON, P. Long wavelength chlorophyll species are associated with amplification of high energy state quenching in higher plants. *Biochim. Biophys. Acta*, 1991, 1059, p. 355-360.
- RUBAN, A.V. and HORTON, P. Mechanism of  $\Delta$ -pH-dependent dissipation of absorbed excitation energy by photosynthetic membranes. I. Spectroscopic analysis of isolated light-harvesting complexes. *Biochim. Biophys. Acta*, 1992, 1102, p. 30-38.

RUBAN, A.V., and HORTON, P. An investigation on the sustained component of non-photochemical quenching of chlorophyll fluorescence in isolated chloroplasts and leaves of spinach. *Plant Physiol.*, 1995, 108, 721-726.

RUBAN, A.V., HORTON, P., and ROBERT, B. Resonance Raman-spectroscopy of the photosystem-II light-harvesting complex of green plants -a comparison of trimeric and aggregated. *Biochemistry*, 1995, 34, p. 2333-2337.

RUBAN, A.V., LEE, P.J., WENTHWORTH, M., YOUNG, A.J., and HORTON, P. Determination of the stoichiometry and strength of binding of xanthophylls to the Photosystem II light-harvesting complexes. *J.Biol. Chem.*, 1999, 274, p. 10458-10465.

RUBAN, A.V., WENTHWORTH, M., YAKUSHEVSKA, A.E., ANDERSSON, J., LEE, P.J., KEEGSTR, W., DEKKER, J.P., BOEKEMA, E.J., JANSSEN, S., and HORTON, P. Plants lacking the main light-harvesting complex retain photosystem II macro-organisation. *Nature*, 2003, 421, p. 648-652.

RUBAN, A.V., BERERA, R., ILIOAIA, C., VAN STOKKUM, I., KENNIS, J., PASCAL, A., VAN AMERONGEN, H., ROBERT, B., HORTON, P., and VAN GRONDELLE, R. Identification of a mechanism of photoprotective energy dissipation in higher plants. *Nature*, 2007, 450, p. 575-U22.

RUBAN, A.V., and JOHNSON, M.P. Dynamics of higher plant photosystem cross-section associated with state transitions. *Photos. Res.*, 2009, 99, p. 173-183.

RUBAN, A.V., JOHNSON, M.P., and DUFFY, C.D.P. The photoprotective molecular switch in the photosystem II antenna. *Biochim. Biophys. Acta*, 2012, 1817, p. 167-181.

RUMEAU, D., PELTIER, G., and COURNAC, L. Chlororespiration and cyclic electron flow around PSI during photosynthesis and plant stress response. *Plant Cell And Environment*, 2007, 30, p. 1041-1051.

SANDONA, D., CROCE, R., PAGANO, A., CRIMI, M., and BASSI, R. Higher plant light harvesting proteins. Structure and function as revealed by mutation analysis of either protein or chromophores moieties. *Biochim. Biophys. Acta-Bioenergetics*, 1998, 1365, p. 207-214.

SENIGE, M.O. and SERGEEVA, N.N. Metamorphosis of Tetrapyrrole Macrocycles. *Chem. Int. Ed.*, 2006, 45, p.7492-7495.

SHELLER, H.V., and HALDRUP, A. Photoinhibition of photosystem I. *Planta*, 2005, 221, p. 5-8.

SIEBERT, F., MANTELE, W., and GERWERT, K. Fourier-transform infrared-spectroscopy applied to rhodopsin - the problem of the protonation state of the retinylidene schiff-base re-investigated. *European Journal Of Biochem.*, 1983, 136, p. 119-127.

SNODDERLY, D.M. Evidence for protection against age-related macular degeneration by carotenoids and antioxidant vitamins. *Am. J Clin Nutr.*, 1995, 62, p. 1448S-1461S.

STANDFUSS, J., VAN SCHELTINGA, A. C. T., LAMBORGHINI, M., and KÜHLBRANDT, W. Mechanisms of photoprotection and nonphotochemical quenching in pea light-harvesting complex at 2.5 Å resolution. *EMBO Journal*, 2005, 24, p. 919-928.

STEWART, D.H. and BRUDVIG, G.W. Cytochrome b559 of photosystem II. *Biochim. Biophys. Acta*, 1998, 1367, p. 63-87.

STRACHAN, J-P., O'SHEA, D.F., BALASUBRAMANIAN, T., and LINDSEY, J.L. Rational Synthesis of Meso-Substituted Chlorin Building Blocks. *J. Org. Chem.*, 2000, 65, p. 3160-3172.

TANIGUCHI, M., MASS, O., BOYLE, P.D., TANG, Q., DIERS, J.R., BOCIAN, D.F., HOLTEN, D., and LINDSEY, J.S. Structural studies of sparsely substituted synthetic chlorins and phorbines establish benchmarks for changes in the ligand core and framework of chlorophyll macrocycles. *Journal of Molecular Structure*, 2010, 979, p. 27-45.

TAVAN, P., and SCHULTEN, K. Electronic excitations in finite and infinite polyenes. *Phys. Rev. B.*, 1987, 36, p. 4337-4358.

TELFER, A., HE, W.Z., and BARBER, J. Spectral resolution of more than one chlorophyll electron donor in the isolated photosystem II reaction center complex. *Biochim. Biophys. Acta*, 1990, 1017, p. 143-151.

TRUSCOTT, T.G., LAND, E.J., and SYKES, A. In-Vitro Photochemistry of Biological Molecules-III. Absorption-Spectra, Lifetimes and Rates of Oxygen Quenching of Triplet-States of  $\beta$ -Carotene, Retinal and Related Polyenes. *Photochem. Photobiol.*, 1973, 17, p. 43-51.

TRUSCOTT, T.G. The photophysics and photochemistry of the carotenoids. *Journal Of Photochemistry And Photobiology B-Biology*, 1990, 6, p. 359-371.

UMENA, Y., KAWAKAMI, K., SHEN, J.-R., and KAMIYA, N. Crystal structure of oxygen-evolving photosystem II at a resolution of 1.9 Å. *Nature*, 2011, 473, p. 55-60.

VAN GRONDELLE, R., and NOVODEREZHKIN, V.I. Photosynthesis. Quantum design for a light trap. *Nature*, 2010, 463, p. 614-615.

VAN OORT, B. ALBERTS, M., DE BIANCHI, S., DALL'OSTO, L., BASSI, R., TRINKUNAS, G., CROCE, R., and VAN AMERONGEN, H. Effect of antenna-depletion in Photosystem II on excitation energy transfer in *Arabidopsis thaliana*. *Biophys. J.*, 2010, 98, p. 922-931.

VASS, I. Molecular mechanisms of photodamage in the Photosystem II complex. *Biochim. Biophys. Acta*, 2012, 1817, p. 209-217.

WALTER, M.H. and STRACK, D. Carotenoids and their cleavage products: Biosynthesis and functions. *Natural Product Reports*, 2011, 28, p. 663-692.

WALTERS, R.G., and HORTON, P. Resolution of components of non-photochemical chlorophyll fluorescence quenching in barley leaves. *Photos. Res.*, 1991, 27, p. 121-133.

WANG, P., NAKAMURA, R., KANEMATSU, Y., KOYAMA, Y., NAGAE, H., NISHIO, T., HASHIMOTO, H., and ZHANG, J.P. Low-lying singlet states of carotenoids having 8-13 conjugated double bonds as determined by electronic absorption spectroscopy. *Chem. Phys. Lett.*, 2005, 410, 108-114.

WASIELEWSKI, M.R. and KISPERS, L.D. Direct measurement of the lowest excited singlet-state lifetime of all-trans-beta-carotene and related carotenoids. *Chemical physics letters*, 1986, 128, p. 238-243.

WEISS, C. Electronic absorption spectra of chlorophylls. In: Dolphin D. (ed) *The porphyrins*, Academic press, New York, Vol. III, 1978, Physical Chemistry, part A, p. 211-213.

WENTHWORTH, M., RUBAN, A.V., and HORTON, P. Chlorophyll fluorescence quenching in isolated light harvesting complexes induced by zeaxanthin. *FEBS Lett.*, 2000, 471, p. 71-74.

WENTHWORTH, M., RUBAN, A.V., and HORTON, P. Kinetic analysis of nonphotochemical quenching of chlorophyll fluorescence. 2. Isolated light-harvesting complexes. *Biochem.*, 2001, 40, p. 9902-9908.

WIRTZ, A.C., VAN HEMERT, M.C., LUGTENBURG, J., FRANK, A.H., and GROENEN, E.J.J. Two stereoisomers of spheroidene in the *Rhodobacter sphaeroides* R26 reaction centre: A DFT analysis of resonance Raman spectra. *Biophys. J.*, 2007, 93, p. 981-991.

YAKUSHEVSKA, A.E., JENSEN, P.E., KEEGSTRAN, W., VAN ROON, H., SCHELLER, H.V., BOEKEMA, E.J., and DEKKER, J.P. Supermolecular organization of photosystem II and its associated light-harvesting antenna in *Arabidopsis thaliana*. *European Journal of Biochemistry*, 2001, 268, p. 6020-6028.

YAKUSHEVSKA, A.E., KEEGSTRAN, W., BOEKEMA, E.J., DEKKER, J.P., ANDERSSON, J., JANSSON, S., RUBAN, A.V., and HORTON, P. The structure of photosystem II in *Arabidopsis*: localization of the CP26 and CP29 antenna complexes. *Biochem.*, 2003, 42, p. 608-613.

YAMAMOTO, H.Y. Biochemistry and molecular biology of the xanthophyll cycle. In *Photochemistry of carotenoids. Advances in Photosynthesis*, 1999, 8, Kluwer. Dordrecht, p. 271-291.

YAN, H., ZHANG, P., WANG, C., LIU, Z., and CHANG, W. Two lutein molecules in LHCII have different conformations and functions: Insights into the molecular mechanism of thermal dissipation in plants. *Biochem. Biophysical Res. Commun.*, 2007, 355, p. 457-463

ZER, H., VINK, M., KEREN, N., DILLY-HARTWIG, H.G., PAULSEN, H., HERRMANN, R.G., ANDERSSON, B., and OHAD, I. Regulation of thylakoid protein phosphorylation at the substrate level: Reversible light-induced conformational changes expose the phosphorylation site of the light-harvesting complex II. *Proc. Natl. Acad. Sci. USA*, 1999, 96, p. 8277-8282.

ZHANG, J.P., FUJII, R., QIAN, P., INABA, T., MIZOGUCHI, T., KOYAMA, Y., ONAKA, K., WATANABE, Y., and NAGAE, H. Mechanism of the carotenoid-to-bacteriochlorophyll energy transfer via the S-1 state in the LH2 complexes from purple bacteria. *Journal Of Physical Chemistry B*, 2000, 104, p. 3683-3691.

ZOUNI, A., WITT, H.T., KERN, J., FROMME, P., KRAUSS, N., SAENGER, W., and ORTH, P. Crystal structure of photosystem II from *Synechococcus elongatus* at 3.8 Angstrom resolution. *Nature*, 2001, 409, p. 739-743.

**CHAPTER 2 MECHANISMS  
UNDERLYING CAROTENOID ABSORPTION IN  
OXYGENIC PHOTOSYNTHETIC PROTEINS<sup>1</sup>**



### Summary of the work

The electronic properties of carotenoid molecules underlie their multiple functions throughout biology, and tuning of these properties by their *in vivo* locus is of vital importance in a number of cases. This is exemplified by photosynthetic carotenoids, which perform both light-harvesting and photoprotective roles essential to the photosynthetic process.

Despite a large body of research performed in the last years, predicting the complete electronic structure of carotenoid molecules remains an extremely complex problem, particularly in anisotropic media such as proteins. Recently, the electronic properties of some carotenoids *in vitro* were addressed by the combined use of electronic absorption and resonance Raman spectroscopies (Mendes-Pinto *et al.*, 2013). It was found that linear carotenoids exhibit an excellent correlation between the  $S_0 \rightarrow S_2$  energy, the frequency of their  $\nu_1$  Raman band and their conjugation length. On the other hand, cyclic carotenoids in which the conjugation extends into the ring follow the same relationship between  $S_0 \rightarrow S_2$  and  $\nu_1$  frequency only. When plotted against their theoretical conjugation length, both these parameters show clear deviations from the correlation obtained with linear carotenoid molecules. It was concluded that carotenoids with conjugated end-cycles exhibit a shorter effective conjugation length than expected from their chemical structure, probably due to twisting of the end ring out of the plane.

In the following chapter, we go a step further and analyze two cases where identical cyclic carotenoid molecules are bound to the same protein, but nevertheless exhibit different absorption transitions. The reaction center of photosystem II binds two  $\beta$ -carotenes, one absorbing at 489 nm and the other one at 507 nm, while the major light-harvesting complex of photosystem II binds two lutein molecules, one absorbing at 495 nm and the other one at 510 nm.

In each case, identical molecular species in the same protein are seen to exhibit different electronic properties (most notably, shifted absorption peaks). We assess which molecular parameters are responsible for this *in vivo* tuning process, and attempt to assign it to specific molecular events imposed by their binding pockets.

<sup>1</sup>*This chapter is based on the following publication:*

MENDES-PINTO, M.M., GALZERANO, D., TELFER, A., PASCAL, A.A., ROBERT, B., and ILIOAIA C. *J. Biol. Chem.*, 2013, 288, 26, p. 18758-18765.

## 2.1 Introduction

Carotenoids are essential cofactors in the first steps of the photosynthetic process. They play a role as light-harvesters, complementing chlorophyll (Chl) absorption in the blue-green range of the spectrum (see *e.g.* Refs. 1–4). They also act as photoprotective molecules, through a number of different mechanisms. By quenching Chl triplet states ( $^3\text{Chl}$ ), they prevent the energy-transfer-mediated formation of singlet oxygen ( $^1\text{O}_2$ ), one of the most harmful reactive oxygen species (5).  $^3\text{Chl}$  species are inevitably formed, with a low but significant yield, during excitation energy transfer in light-harvesting proteins and/or after charge recombination in reaction centres (RCs; 6–8). Carotenoids can additionally quench any  $^1\text{O}_2$  that may nevertheless be formed. More recently it was shown that, in plants and cyanobacteria, carotenoids play an essential role in regulating the amount of excitation energy reaching the RC in high-light environments, thus preventing damage due to overexcitation of these proteins (9–11).

Carotenoids achieve these functions through their electronic properties, which arise from their linear conjugated polyene chain. They exhibit a fairly simple structure, built from the assembly of isoprenoid units (see figure 2.1), and a number of their electronic properties have been successfully predicted.

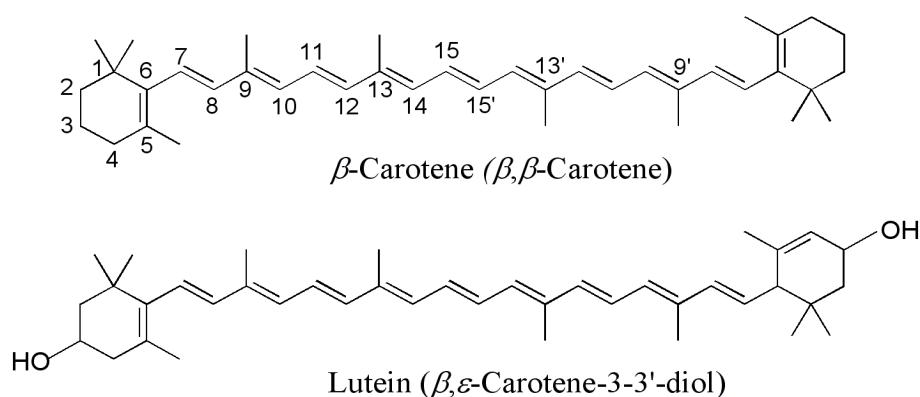


**Figure 2.1** Molecular structures of  $\beta$ -carotene and lutein

Their main absorption transition, which corresponds to a transition from the ground state to the second excited singlet state ( $S_0 \rightarrow S_2$ ), tightly depends on the number of conjugated carbon-carbon double bonds present in this chain (12–16), and on the refractive index of their local environment (17– 22). However, predicting the full electronic structure of carotenoid

molecules has turned out to be extremely complex. Despite the intense level of research on carotenoid properties over the last forty years, several new, low-energy excited states have been proposed for these molecules in the last decade alone (23, 24) and precise calculations of their electronic and vibrational properties still remain a challenge (25).

*In vivo*, protein binding sites provide a highly anisotropic environment to carotenoid molecules. In these conditions, it is extremely difficult to characterize the most important parameters which govern their electronic properties. However, determining these parameters would represent an important approach in our understanding of the role of the protein matrix in tuning the first steps of the photosynthetic process. Given that the role of carotenoids in other biological systems also generally involves their electronic properties (*e.g.* signaling functions, making specific use of their color), such an understanding should also prove more widely-applicable throughout carotenoid research.

The combined use of electronic absorption and resonance Raman (RR) spectroscopies may help in determining the molecular parameters underlying the tuning of carotenoid electronic transitions. In RR spectra, the frequency of the C=C stretching mode of these molecules (the  $\nu_1$  band) gives direct access to the structure of the alternated system of their electronic ground-state. As we recently showed (26), and as illustrated in figure 2.2, a different relationship is observed between the frequency of the  $\nu_1$  band and the position of the  $S_0 \rightarrow S_2$  transition, depending on the molecular mechanism tuning this transition. The frequency of the  $\nu_1$  band may thus yield direct indications on these mechanisms.

We have studied the absorption properties of  $\beta$ -carotene and lutein (figure 2.1) bound to two photosynthetic proteins isolated from photosystem II (PSII) - the RC and the major light-harvesting complex, LHCII, respectively. The PSII-RC binds two  $\beta$ -carotene molecules, which at low temperature have their main absorption transition at 489 and 507 nm (27–29), the former being perpendicular and the latter parallel to the membrane plane (27, 30, 31). These carotenoid molecules exhibit only limited singlet-singlet energy transfer to Chls, and essentially no quenching of Chl triplets, but are both able to transfer an electron to the oxidized primary electron donor, albeit with very low efficiency (27, 32–35). LHCII is assembled into a trimeric form in the photosynthetic membrane, with each monomer containing two lutein molecules whose binding sites are related by pseudosymmetry. Whilst in LHCII monomers these luteins both absorb at 495 nm, in LHCII trimers one of them (lut2) has its absorption shifted to 510 nm (lut1 absorption remains at 495 nm; 3, 36). It has been proposed that one of these two luteins (lut1) is involved in quenching Chl singlet excited

states during the pH-dependent phase of non-photochemical quenching (9), the central mechanism that regulates excitation transfer in PSII.

In this work, we determine the factors which underlie differences in the electronic properties of these carotenoid molecules. In addition, we attempt to relate these differences to the three-dimensional structures of these proteins, as determined by X-ray crystallographic studies (31, 37–39). We propose a mechanism by which their binding pockets may impose specific conformations on carotenoids to modulate their electronic structure, and thus tune their absorption spectra.

## 2.2 Experimental procedure

*Carotenoids and Solvents.*  $\beta$ -carotene ( $\beta,\beta$ -carotene synthetic type I, C-9750) was obtained from Sigma-Aldrich (St. Louis, MO, USA). Lutein ( $\beta,\epsilon$ -carotene-3,3'-diol) was isolated and purified as previously described (40). The molecular structure of these molecules is displayed in figure 2.1.

The solvents used in this study were all purchased from Sigma-Aldrich (St. Louis, MO, USA): tetrahydrofuran (THF), *n*-hexane, cyclohexane and acetonitrile (all absolute grade,  $\geq 99.5$  % GC); toluene, methanol and pyridine (anhydrous, 99.8 %); chloroform and carbon disulphide (CS<sub>2</sub>) (anhydrous,  $\geq 99$  %); diethylether ( $\geq 99.8$  % GC); and nitrobenzene ( $\geq 99.5$  % GC).

*Sample preparation.* LHCII complexes were prepared from *Spinacia oleracea* PSII-enriched particles by isoelectric focusing (IEF), followed by sucrose gradient centrifugation (41). These trimeric complexes contain two lutein molecules, one neoxanthin and only negligible amounts of violaxanthin per monomer (41). PSII-RCs with two bound  $\beta$ -carotenes were isolated following the method described in Telfer *et al.*, 2003 (35). Prior to use, LHCII trimers and PSII-RC were concentrated using Centricon 30 K and 100 K cut-off concentrating tubes, respectively, to a final optical density  $> 5$  OD at 675 nm.

*Spectroscopy.* Absorption spectra were collected using a Varian Cary E5 Double-beam scanning spectrophotometer. The S<sub>0</sub>→S<sub>2</sub> electronic transition of carotenoid molecules displays three vibrational sub-levels; the 0-0 sublevel (the red-most band) was used to determine the position of this transition. RR spectra were recorded with 90° signal collection using a two-stage monochromator (U1000, Jobin Yvon, Longjumeau, France) equipped with a front-illuminated, deep-depleted CCD detector (Jobin Yvon). Excitation wavelengths were provided by a 24 W Sabre laser (Coherent, Palo Alto, California); typically,  $< 20$  mW reached

the sample, and sample integrity was verified by following RR spectral evolution during the experiment. Measurements at low temperature (77 K) were performed using a nitrogen-flow cryostat (Air Liquide, Sassenage, France).

## 2.3 Results and discussion

### 2.3.1 Isolated $\beta$ -Carotene and Lutein

The position of the  $S_0 \rightarrow S_2$  transition of carotenoid molecules tightly depends on their molecular structure, and in particular on the length of the  $\pi$ -electron conjugated system. Increasing this length induces a progressive loss of the double bond character of the C=C bonds. This double bond character can be directly probed by RR spectroscopy, as it influences the frequency of the  $\nu_1$  Raman band. As a result, for a given solvent, a linear correlation between this frequency and the position of the  $S_0 \rightarrow S_2$  transition exists, when expressed as a function of the length of the carotenoid conjugated chain (figure 2.2, *black line*).

The frequency of the  $\nu_1$  Raman band for lutein and  $\beta$ -carotene does not correspond to that expected for Cars with 10 and 11 double bonds, respectively, while they nevertheless show the same relationship between  $\nu_1$  frequency and absorption position (figure 2.2 and Ref. 26). These cyclic carotenoids, when isolated in solvents, actually display effective conjugation lengths of 9.3 and 9.6, respectively. This result was attributed to rotation of the conjugated end-cycles out of the plane, such that the ring C=C's are only partially conjugated (26, 42). The position of the main absorption transition of carotenoid molecules also tightly depends on the properties of the solvent they are dissolved in, and particularly on its refractive index (17–22).

Again, there is a correlation between the position of the  $S_0 \rightarrow S_2$  absorption transition and the frequency of the  $\nu_1$  Raman band for a given carotenoid molecule, when expressed as a function of solvent polarizability. This correlation is plotted in figure 2.2 for  $\beta$ -carotene (*blue*) and lutein (*red*), and displays a different slope to that for different carotenoid in the same solvent (*black*), as already observed and discussed for several carotenoid molecules (26).

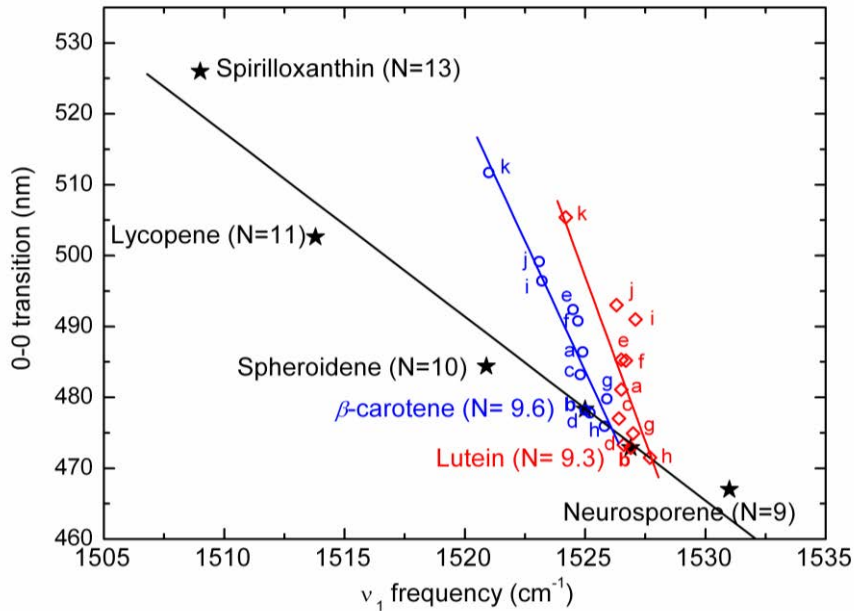


**Figure 2.2** Correlation between the  $S_0 \rightarrow S_2$  electronic transition and the frequency of the  $\nu_1$  Raman band for linear carotenoids with different conjugation length,  $N$  (performed in *n*-hexane; black line), compared to the same correlation for  $\beta$ -carotene (blue line) and lutein (red line) as a function of solvent polarizability. Solvents: *a*, tetrahydrofuran, *b*, *n*-hexane; *c*, cyclohexane; *d*, diethylether; *e*, toluene; *f*, chloroform; *g*, acetonitrile; *h*, methanol; *i*, pyridine; *j*, nitrobenzene, *k*,  $CS_2$ .

### 2.3.2 $\beta$ -Carotene in PSII Reaction Centres

At low temperature, PSII-RCs exhibit two main peaks in the carotenoid absorption region, at 489 and 507 nm (figure 2.3). Linear dichroism experiments showed that these peaks correspond to distinct Car molecules, with different orientations relative to the membrane plane (27) and, considering their position, they must be attributed to the 0-0 sub-level of the absorption transition of each molecule. Although the resolution between these peaks becomes much lower at room temperature, the overall position of the carotenoid absorption transition appears not to shift by more than a few nm between low temperature and room temperature (see figure 2.3). This is not specific to PSII and was already observed in other photosynthetic complexes. For instance, in light-harvesting complexes from purple bacteria it was shown that, in general, the absorption transitions of the bound carotenoid molecules are very poorly dependent on temperature (43).

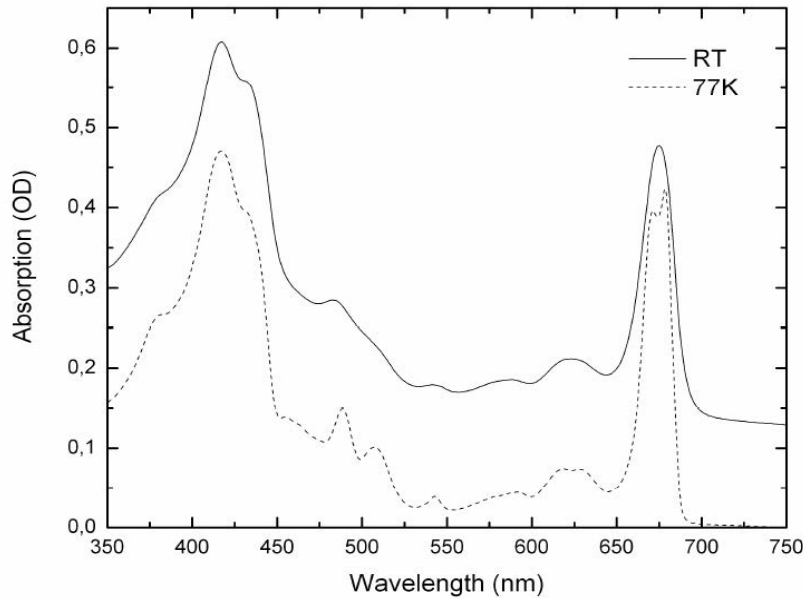


**Figure 2.3** Absorption spectra of PSII-RC particles at room temperature (RT; solid line) and 77 K (dashed line).

Figure 2.4A displays RR spectra of PSII-RCs obtained at room temperature with 514.5- and 488.0-nm excitation, chosen to be selective for the 507- and 489-nm-absorbing  $\beta$ -carotene, respectively. They contain four main groups of bands, denoted  $\nu_1$  to  $\nu_4$ , typical of carotenoid molecules. The  $\nu_1$  band around  $1520\text{ cm}^{-1}$  arises from stretching vibrations of C=C double bonds. As mentioned above, its frequency depends on the length of the  $\pi$ -electron conjugated chain and on the carotenoid conformation. The  $\nu_2$  band at  $1160\text{ cm}^{-1}$  arises from stretching vibrations of C-C single bonds coupled with CH in-plane bending modes. This region may be used as a fingerprint for the assignment of carotenoid configurations (*trans-cis*). The  $\nu_3$  band at  $\sim 1000\text{ cm}^{-1}$  arises from in-plane rocking vibrations of the methyl groups attached to the conjugated chain, coupled with in-plane bending modes of the adjacent C-Hs. Finally, the  $\nu_4$  band around  $960\text{ cm}^{-1}$  arises from C-H out-of-plane wagging motions coupled with C=C torsional modes (out-of-plane twists of the carbon backbone).

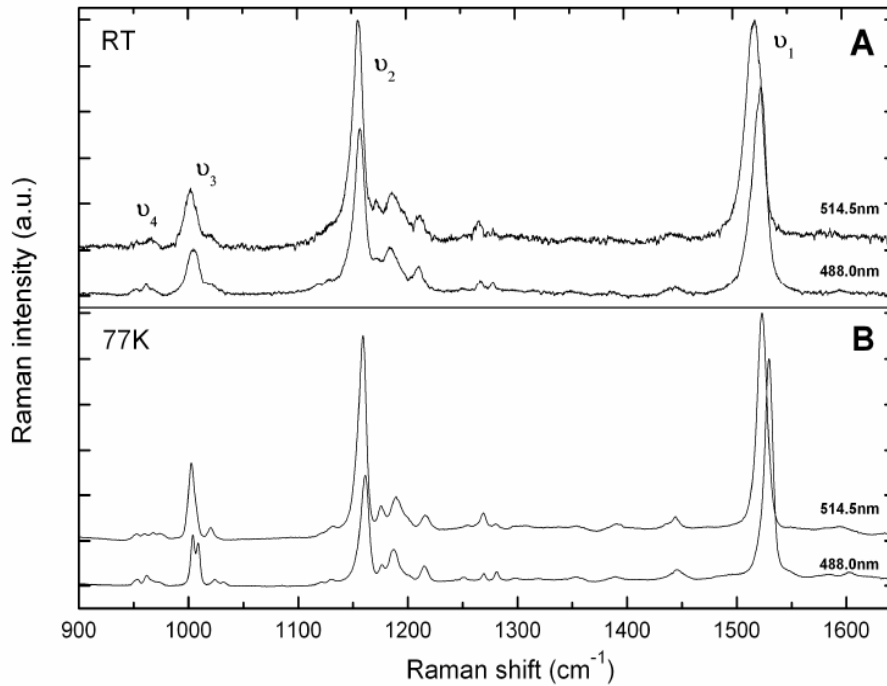


**Figure 2.4** RR spectra of PSII-RC recorded with 488.0- and 514- nm excitation at room temperature (RT; *A*) and 77 K (*B*).

When the conjugated system of the carotenoid is symmetrical and the molecule is planar, these out-of-plane modes will not be coupled with the electronic transition. As a result, these bands will not be resonance-enhanced upon excitation and will exhibit very low intensity in RR spectra. However, distortions around C-C single bonds will increase the coupling of these modes with the electronic transition, resulting in an increase in resonance enhancement, *i.e.*  $\nu_4$  gains intensity. Although both spectra are globally similar and typical for all-*trans*  $\beta$ -carotene, at 514.5 nm the  $\nu_1$  frequency is downshifted by  $6\text{ cm}^{-1}$  compared to 488.0 nm while  $\nu_3$  and  $\nu_4$  are both slightly narrower. These differences are also observed at 77 K (figure 2.4*B*; see also Ref. 35), indicating that the detailed structure of each  $\beta$ -carotene molecule is the same at both temperatures. It is worth noting that the increase at 488.0 nm in the width of  $\nu_3$  at RT is translated into a splitting of this band into two components at 77 K. In figure 2.5 we plot the  $\nu_1$  frequencies and absorption positions of the two  $\beta$ -carotenes from PSII-RCs at room temperature (*red triangles*), as compared with the frequencies and positions of different-length carotenoid molecules (*black line*) and of  $\beta$ -carotene in various solvents (*blue line*) taken from figure 2.2. The values obtained for the blue-absorbing carotene fit on the *blue slope*, suggesting that the position of this absorption transition is mainly governed by the local polarizability of its binding site. It may be noted that the binding site of this molecule exhibits a rather low local polarizability (equivalent to that found in chloroform,

*blue open symbol labeled f*, with a polarizability value,  $R_n$ , of 0.266). On the other hand, the difference in  $\nu_1$  frequency of the two  $\beta$ -carotene molecules accompanying the shift in their  $S_0 \rightarrow S_2$  transition (see *dashed red lines* in figure 2.5) is much too large to be accounted for by changes in the local polarizability of their protein binding sites. In this case, considering the difference in the position of their electronic transition, a change of  $\nu_1$  frequency of about  $2 \text{ cm}^{-1}$  should be expected, *i.e.* three times smaller than actually observed. The  $6 \text{ cm}^{-1}$  change seen here corresponds to a sizeable change of the apparent length of the conjugated chain, probably through perturbation of its alternated system. Such a change in the alternated system (observed upon increasing the length of the conjugated chain) would indeed up-shift the position of the Car absorption by about 17 nm, *i.e.* it is sufficient to explain the difference in absorption between the two PSII-RC-bound  $\beta$ -carotene molecules. Thus the *dashed line* connecting these two points is parallel to the *black line*, which relates Cars of different chain length in the same solvent (figure 2.5).

The same relationship between absorption position and  $\nu_1$  frequency is also shown for measurements of the PSII-RC at 77 K (figure 2.5, *inverted red triangles*). The *dashed line* between these two points exactly parallels that obtained at RT, but at the lower temperature there is a shift of about  $5 \text{ cm}^{-1}$  in the  $\nu_1$  frequency for both  $\beta$ -carotene molecules. Exactly the same shift for this Raman band, between room and low temperature, has recently been described in RR spectra of Cars in solution, and was explained by an intrinsic sensitivity of the Raman frequency to temperature (for details, see Ref. 44).

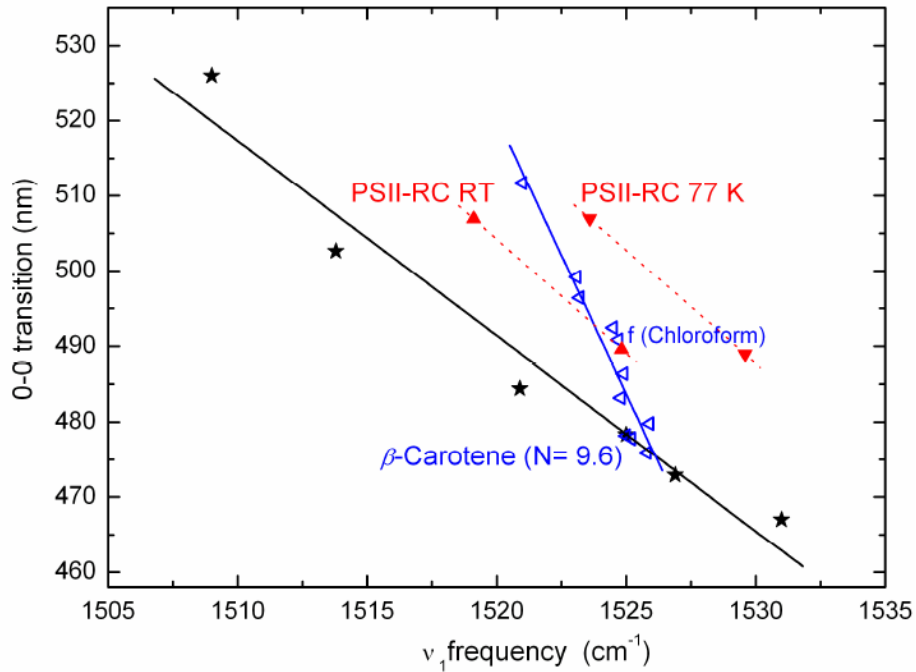


**Figure 2.5** Correlation between the  $S_0 \rightarrow S_2$  electronic transition and the frequency of the  $\nu_1$  Raman band for the two  $\beta$ -carotene molecules in PSII-RC at room temperature (RT; red triangles) and 77 K (red inverted triangles). For comparison, the relationship between carotenoids of different conjugation length in the same solvent (*n*-hexane) and the relationship expressed as a function of solvent polarizability for  $\beta$ -carotene are also shown (*c.f.* figure 2.2).

### 2.3.3 Lutein Molecules in LHCII

The absorption spectrum of LHCII trimers in the carotenoid region is rather complicated, as these complexes bind up to four carotenoid pigments per monomer, namely two luteins, one *9-cis* neoxanthin and usually one violaxanthin/zeaxanthin (present in negligible amounts in our sample). Indeed, the position of the individual absorption transitions could only be determined through second derivative analyses of absorption spectra obtained at 4 K (3). However, as in PSII, comparing the absorption spectra of LHCII at low temperature and room temperature suggests that the main band positions of the LHCII-bound carotenoid molecules are very poorly sensitive to temperature (figure 2.6).

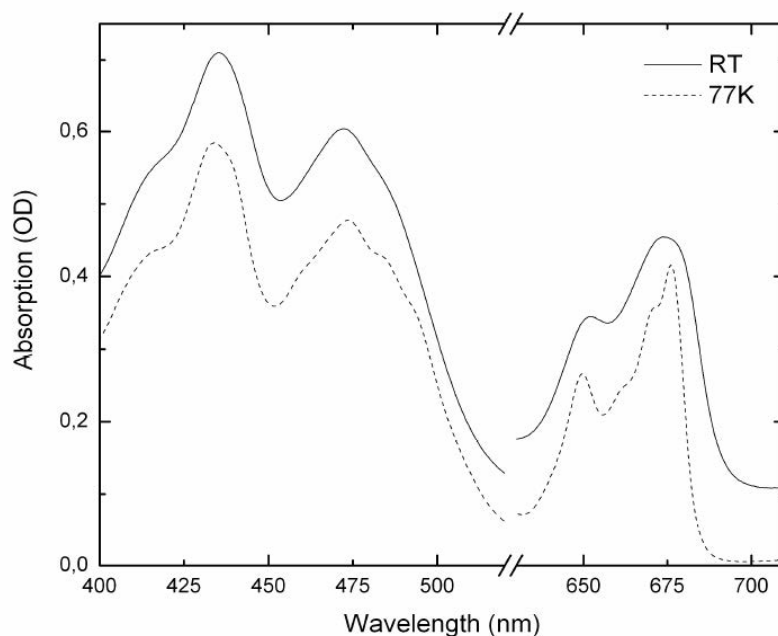


**Figure 2.6** Absorption spectra of LHCII trimers at room temperature (*RT*; *solid line*) and 77 K (*dashed line*).

RR spectra of the LHCII-bound luteins at 77 K are displayed in figure 2.7B. As extensively documented in the literature (3, 43, 44), at this temperature 496.5- and 514.5-nm excitations yield RR spectra dominated by contributions from lut1 (absorbing at 495 nm) and lut2 (absorbing at 510 nm), respectively. The frequency of the  $\nu_1$  band, which arises from the C=C stretching modes of lutein molecules, is observed at 1531 and 1527  $\text{cm}^{-1}$  for lut1 and lut2, respectively. In the  $\nu_3$  region (around 1000  $\text{cm}^{-1}$ ), lut1 (at 496.5 nm) exhibits two overlapping components of similar amplitude, at 1003 and 1007  $\text{cm}^{-1}$ . The same two bands are seen for lut2 (514.5 nm excitation), but the intensity of the higher frequency component is less than a third that of the lower frequency one. The  $\nu_4$  region exhibits higher intensity and structure for lut2 than for lut1 (514.5- and 496.5-nm excitation, respectively), indicating a higher degree of distortion for lut2 in its LHCII binding site (as previously concluded; 3, 45). At room temperature, the broadening of the Car electronic transitions must, at least in part, impair selective excitation of each Car. In room temperature spectra obtained using excitation at 514.5 nm (figure 2.7A, *upper trace*), the  $\nu_1$  is quite narrow (full-width at half maximum  $\sim 16 \text{ cm}^{-1}$ ) and the structure of the  $\nu_4$  region is very similar to that observed using the same excitation at 77 K. We may thus conclude that this wavelength still ensures selective excitation of the lut2 molecule at the higher temperature, and also that the distortion of this molecule, up to now only observed at low temperature, is also present in LHCII at RT. Thus this distortion does not result from temperature-induced reorganization of the binding site. In

this spectrum the position of the  $\nu_1$  band is at  $1522\text{ cm}^{-1}$ . As in PSII-RC, we thus observe a  $5\text{ cm}^{-1}$  shift between experiments conducted at 77 K and room temperature. In contrast, the spectrum at 496.5 nm exhibits significant broadening of  $\nu_1$  when the measurement is taken at room temperature (figure. 2.7A, lower trace; full width at half-maximum  $\sim 18\text{ cm}^{-1}$ ). The contributions of more than one carotenoid are thus present in this spectrum, due to a reduction in resonance selectivity as a result of broadening of the carotenoid absorption transitions at the higher temperature. Indeed, in the  $\nu_2$  region a small but significant increase in intensity is observed for the shoulder at  $\sim 1130\text{ cm}^{-1}$ . This is consistent with an increase in neoxanthin contributions to the spectrum, as bands on the low frequency side of  $\nu_2$  are quite typical for 9-*cis*-carotenoids. Contributions of lut1 thus cannot be selectively observed in RR spectra at room temperature. Indeed, this was found to be difficult even at 77 K, where a “pure” lut1 spectrum was only obtained after removing the Neo contribution by differential analysis (46).

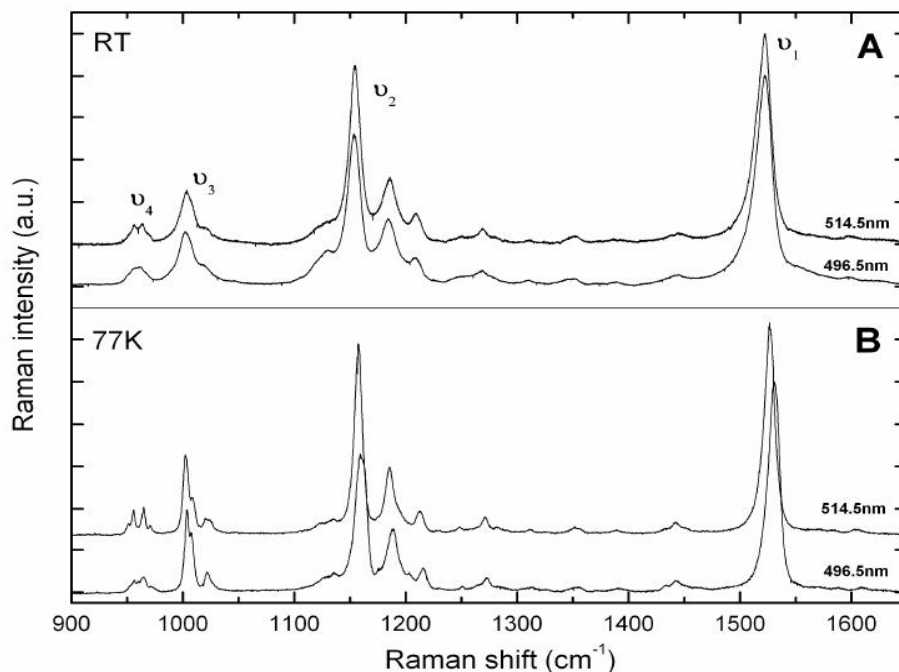


**Figure 2.7** RR spectra of LHCII trimers recorded with 496.5- and 514.5-nm excitation at room temperature (RT; A) and 77 K (B).

In figure 2.8, the absorption position and  $\nu_1$  frequency of luteins in LHCII are compared to those obtained for lutein in various solvents (*red line*) and with the frequencies and positions of different length carotenoid molecules (*black line*). A large shift is observed in  $\nu_1$  frequency between the two luteins at low temperature ( $4\text{ cm}^{-1}$ ; *blue inverted triangles*). As for  $\beta$ -carotene in PSII-RC, this shift, which reflects a change in the alternation of the conjugated C=C chain, is enough to account for the energy difference between their  $S_0 \rightarrow S_2$

absorption transitions. As in PSII-RC, the  $\nu_1$  frequency of lut2 at room temperature (the only one we could safely extract from the RR spectra) is shifted by about  $5 \text{ cm}^{-1}$  as compared to its low temperature value. By analogy, we can deduce the expected  $\nu_1$  frequency of lut1 at room temperature, by shifting its low temperature value by  $5 \text{ cm}^{-1}$ . The resulting value fits perfectly with the *in vitro* relationship between the lutein  $\nu_1$  frequency and the position of its  $S_0 \rightarrow S_2$  transition according to the polarizability of the solvent (figure 2.8, *red line*), tending to validate this approach. As in PSII-RC, we may conclude that the position of the electronic transition of this molecule is mainly governed by the local polarizability of its binding site. However, the deduced polarizability for this lutein is much higher than that calculated for the blue  $\beta$ -carotene in PSII-RC, as it corresponds to a value slightly higher than that for nitrobenzene (*j*, *red open symbol*; figure 2.8) with a refractive index,  $R_n$ , of 0.319.

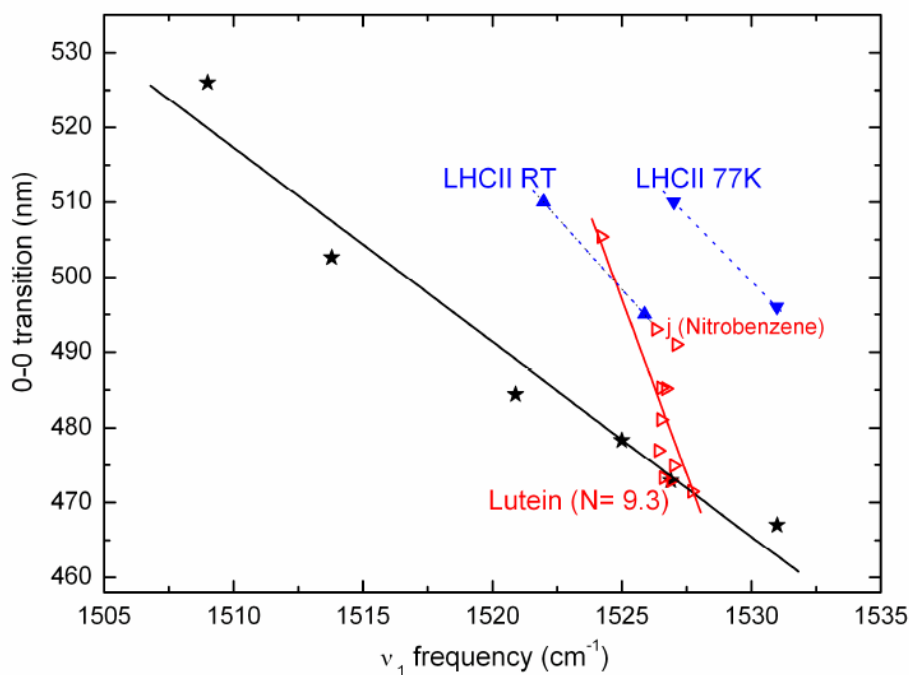


**Figure 2.8** Correlation between the  $S_0 \rightarrow S_2$  electronic transition and the frequency of the  $\nu_1$  Raman band for the two lutein molecules in LHCII trimers (*blue triangles*, room temperature, *RT*; *blue inverted triangles*, 77 K). For comparison, the relationship between carotenoids of different conjugation length in the same solvent (*n*-hexane) and the relationship expressed as a function of solvent polarizability for lutein are also shown (*c.f.* figure 2.2).

### 2.3.4 Mechanisms tuning carotenoid absorption in PSII-RC and LHCII

In both PSII-RC and LHCII, RR spectroscopy unambiguously shows that the position of the absorption transition of the blue-absorbing carotenoid molecule is mainly governed by the polarizability provided by the protein environment. Indeed, the position of this transition and the frequency of the  $\nu_1$  mode of these molecules strictly obey the correlation obtained for

both  $\beta$ -carotene and lutein according to solvent refractive index. The deduced average value of the environment polarizability of the blue-absorbing  $\beta$ -carotene in PSII-RC is lower than that of the blue absorbing lutein in LHCII. This is consistent with the environment deduced by analysis of X-ray crystallographic structures (30, 31, 37). In PSII-RCs, carotenoids are mainly surrounded by amino acids and are quite distant from other cofactors; they exhibit only low rates of energy transfer to the bound Chl molecules (27, 33, 34). On the other hand, the luteins in LHCII are in very close contact with the LHCII-bound Chl molecules, both at the levels of their end cycles and of the conjugated C=C chain (37). Some of these Chls, such as Chl *a* 603, are nearly in van der Waals contact with lut1 (closest distance 3.83 Å) and are likely to provide an environment of higher polarizability.

By contrast, it is quite clear that the energy shifts between the blue- and the red-absorbing carotenoid molecules in both studied complexes are not induced by a variation in polarizability of their binding sites. If so, the position of the absorption transition of these carotenoids and their  $\nu_1$  Raman frequency would obey a correlation similar to the *blue/red lines* in figure 2.2, whereas it is clear that they deviate from these lines (see figures 2.5 and 2.8). Again, this conclusion is consistent with the description of the environment of these molecules provided by the crystallographic structures of the two pigment-protein complexes: the blue and red luteins in LHCII, as well as the blue and red  $\beta$ -carotene molecules in PSII-RC, are embedded in quite similar protein environments, which are unlikely to display large changes in average polarizability (indeed in LHCII, the two binding pockets are related by the local 2-fold symmetry of the complex). Instead, the absorption transition of these molecules and the frequency of their  $\nu_1$  Raman band behave as if the conjugated chain of the carotenoid molecules was increased by nearly one C=C double bond at constant polarizability (figures 2.5 and 2.8). Note that for both red-absorbing Cars, the main  $\nu_2$  band is also seen to shift to lower frequency in parallel with the downshift in  $\nu_1$  (figures 2.4 and 2.7); this is exactly as expected for an increase in conjugation length (see *e.g.* 47). Thus the apparent length of the conjugated chain of the red-absorbing lutein and  $\beta$ -carotene in LHCII and PSII-RC (at room temperature) become 10 and 10.2, respectively (figures 2.5 and 2.8). The external parameters susceptible to induce such changes are not documented in the literature and, again, there is no dramatic change in the environment of these pigments which could be at the origin of such a change. It was shown that the luteins of LHCII and the  $\beta$ -carotenes in PSII-RC experience different distortions at low temperature (3, 35) and we show in this work that these distortions also exist at room temperature. However, small distortions around C-C bonds are expected to

have little influence on the structure of the C=C conjugated chain and, while in LHCII the red-absorbing lutein is distorted (48), in PSII it is the blue-absorbing carotenoid which exhibits the larger distortion (35).

However, lutein and  $\beta$ -carotene both exhibit shorter conjugation length in solvents than expected from their chemical structure (9.3 and 9.6, respectively; 26). This was explained in terms of out-of-plane rotations of the conjugated end-cycles, resulting in a loss of conjugation. In the crystal structure of  $\beta$ -carotene, the  $\beta$ -ionone rings are indeed twisted out of the conjugated plane (dihedral angles  $\sim 42^\circ$ ; 49). Although no solution structure currently exists for either carotenoid, DFT simulations performed on  $\beta$ -carotene predict dihedral angles for the end-cycles of  $\sim 47^\circ$  (42, 50, 51; see figure 2.9), and this has been calculated to shorten the conjugation length by the exact amount predicted from the Raman  $\nu_1$  position (42). Bringing one of these end-cycles back into the plane of the C=C conjugated chain should accordingly result in a net increase of the effective conjugation length of these molecules of about 0.6 - 0.7, exactly as observed here for the red-absorbing lutein and  $\beta$ -carotene in LHCII and PSII-RC. We thus propose that these proteins are able to tune the absorption of their red-absorbing carotenoid via the rotation of conjugated end-cycles towards the conjugated plane of the molecule, this rotation being imposed by their binding pocket through steric hindrance. As lutein only has one conjugated end-cycle it must be this  $\beta$ -ring that is implicated in LHCII, while for  $\beta$ -carotene in PSII-RC this rotation may involve one or both end-cycles.

The initial crystallographic structure of LHCII led to the conclusion that the lutein end-rings were all in a conformation perpendicular to the C=C chain (37), a conformation which would induce a further shortening of the C=C chain of the lutein molecules. This is at variance with the present vibrational analysis of these pigments, and with the position of their electronic transitions. However, a more recent analysis led to the conclusion that these molecules display different conformations, with lut2 being more distorted than lut1 (39), fully in agreement with our previous conclusions (3). The progressive distortion of lut2 occurring from C9 to C13, as observed in the latter analysis, twists one of the end-rings to orient it parallel to residue TRP46,  $\sim 3.4 \text{ \AA}$  away, to optimize van der Waals interactions with it (see figure 2.9E; note, however, that this figure was drawn using the earlier structure). As a result, this ring is brought back into the plane of the C=C chain, assuming this ring contains the (partially) conjugated C=C bond (*i.e.* that it is the  $\beta$ -ring) then it would become more conjugated as a result of this distortion, entirely consistent with our proposed mechanism. It would also explain why the red-shift of lut2 absorption only occurs when this molecule is

distorted; in LHCII monomers, where the lut2 conformation is relaxed, its absorption transition coincides with that of lut1 (495 nm; 3).

Similarly, in the most recent crystallographic structure of photosystem II, a clear difference appears between the cycle geometries of the two  $\beta$ -carotenes bound to the PSII reaction center (31). This is illustrated in figure 2.9, *A-D*, where the four end-rings are compared to that of the DFT-calculated in vitro structure (42). Both cycles of the (blue-absorbing)  $\beta$ -carotene perpendicular to the membrane plane (Bcr645 in Protein Data Bank structure 3ARC) make a large angle with the conjugated C=C chain (dihedral angles  $59^\circ$  and  $68^\circ$ ; Figure 2.9, *C* and *D*). This is quite different for the (red-absorbing)  $\beta$ -carotene parallel to the membrane (Bcr651), where one of the cycles makes a dihedral angle of only  $12^\circ$  with the plane of the C=C chain, as seen in figure. 2.9*A*. Once again this twisting back into the plane allows the end-ring to lie more or less parallel to an overlapping aromatic residue, this time PHE113 of the PsbD polypeptide ( $\sim 3.9$  Å away; figure 2.9*A*). Note that the second end-ring, while lying out of the plane, also makes a smaller angle than those measured for the blue-absorbing carotenoid ( $48^\circ$ ; figure 2.9*B*). These structural differences are perfectly in line with the conclusions of this study, and would account for the difference in conjugation length measured by Raman between these two molecules.

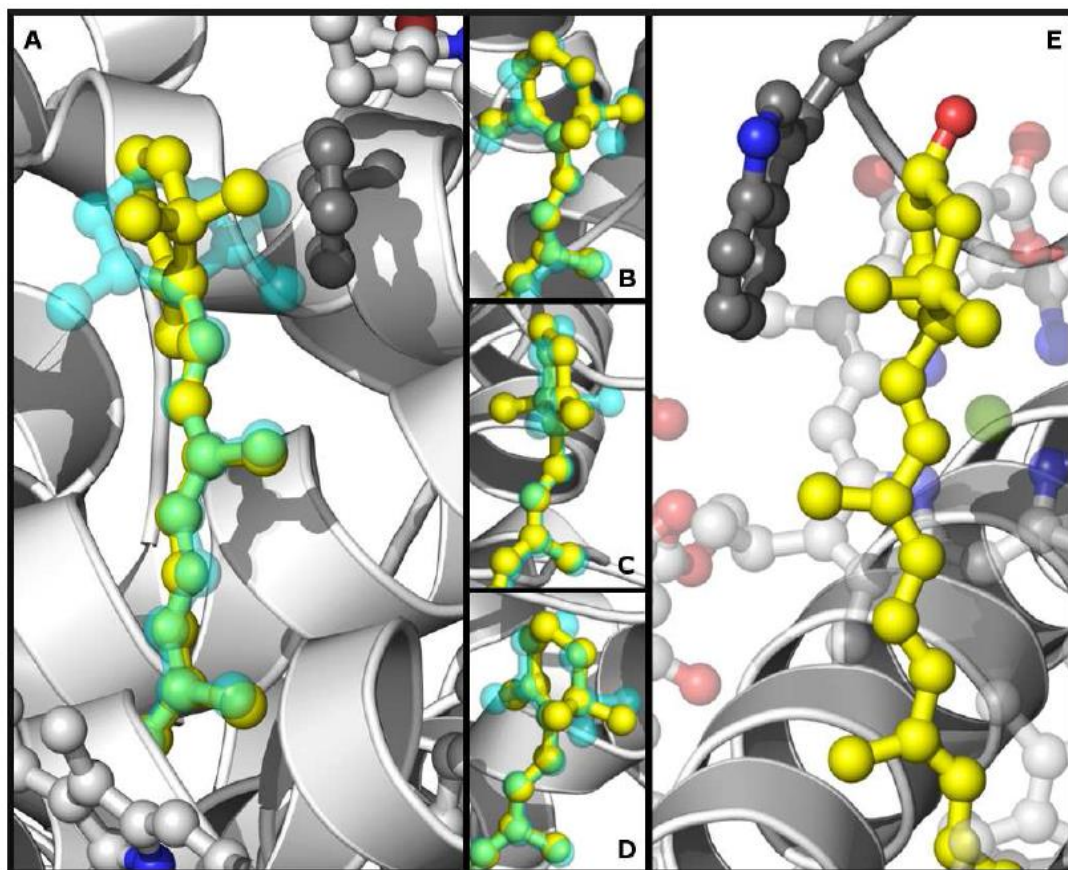


**Figure 2.9** Structural details of the carotenoid end rings in PSII-RC and LHCII, drawn using PyMOL from Protein Data Bank entries 3ARC and 1RWT, respectively. Ball-and-stick representations colored by atom except for carbons are shown for: protein-bound carotenoids (carbons in *yellow*); aromatic residues discussed in the text (*gray*); and other cofactors present (*white*). For PSII-RC, the DFT-calculated  $\beta$ -carotene structure (42; *cyan*) has been fitted to Bcr651 (*A* and *B*) and Bcr645 (*C* and *D*). For LHCII, the latest structure containing the twist in lut2 is not yet available; in the structure shown here (*E*), whereas the ring orientation relative to TRP46 is correct, the position of carbon atoms immediately preceding the ring (C7–9) is not.

It is worth noting that, in the RR spectra of the red-absorbing  $\beta$ -carotene bound to PSII, only a single, narrow contribution is seen in the  $\nu_3$  region, whereas for the blue-absorbing  $\beta$ -carotene  $\nu_3$  is relatively broad at room temperature and even splits into two components at 77 K (figure 2.4). Although this tendency is not so clear for LHCII, it is nevertheless seen; the red-absorbing lutein exhibits one major component with a satellite at higher frequency, while this higher-frequency component is more prominent for the blue-absorbing lutein (figure 2.7).  $\nu_3$  arises from in-plane rocking vibrations of the methyl groups attached to the conjugated chain, coupled with in-plane bending modes of the adjacent C-Hs. In Raman spectra of fucoxanthin the  $\nu_3$  band is similarly composed of two components, which was attributed to differences in the methyl nearest neighbors in the chemical structure of the carotenoid (46). Along the same lines, the splitting of this band observed in the blue-absorbing carotenoid may reflect the out-of-plane rotation of the end cycles, as this rotation is

likely to perturb the rocking frequency of the neighboring methyl group. It is striking that in lutein, where only one rocking mode should be concerned, the intensity of the additional component is weaker than in  $\beta$ -carotene (where potentially two methyl groups may be concerned). In solvents, where it was concluded that the end cycles are at least partially out of the plane, the  $\nu_3$  is also observed to be broader in Raman spectra at room temperature (26). The structure of this band could thus be a direct indication of the conformation of the end cycles in both  $\beta$ -carotene and lutein, representing a probe for this mechanism of conjugation-length modulation.

Finally, it is striking that Nature has generally used carotenoids with conjugated end cycles in oxygenic photosynthesis. Our results show that by playing on the conformation of these cycles, the position of the absorption transitions of these cyclic carotenoid molecules may be tuned by up to 15 nm/ring. Note that for a carotenoid without end-rings it would be highly unfavorable, energetically, to rotate the ends such that a conjugated C=C became (partially) unconjugated. This is not the case when conjugated end-rings are present; steric factors have already determined that these rings are poised in a partially conjugated conformation. It may be that this property explains the recruitment of carotenoid molecules with conjugated end cycles in the photosynthetic process, allowing for an optimization of the excitation energy cascade in these complex light transducing structures.

## References

1. COGDELL, B. J., GILLBRO, T., ANDERSSON, P. O., LIU, R. S. H., and ASATO, A. E. Carotenoids as accessory light-harvesting pigments. *Pure and Applied Chemistry*, 1994, 66, p. 1041-1046.
2. HORTON, P., RUBAN, A. V., and WALTERS, R. G. Regulation of light harvesting in green plants, *Annu. Rev. Plant Physiol. Plant Molec. Biol.*, 1996, 47, p. 655-684.
3. RUBAN, A., PASCAL, A., and ROBERT, B. Xanthophylls of the major photosynthetic light-harvesting complex of plants: identification, conformation and dynamics. *FEBS Letters*, 2000, 477, p. 181-185.
4. POLÍVKA, T., and FRANK, H. A. Molecular Factors Controlling Photosynthetic Light Harvesting by Carotenoids. *Acc. Chem. Res.*, 2010, 43, p. 1125-1134.
5. FOOTE, C. S. CHAPTER 3. Photosensitized Oxidation and Singlet Oxygen: Consequences in Biological Systems. *In Free Radicals in Biology* (William Pryor, Ed.), 1976, p. 85-133, (Academic Press).
6. BRITTON, G., LIAAEN-JENSEN, S., and PFANDER, H. *Carotenoids*, Springer, 2008.
7. TRUSCOTT, T., LAND, E., and SYKES, A. *In-Vitro* Photochemistry of Biological Molecules-III. Absorption-Spectra, Lifetimes and Rates of Oxygen Quenching of Triplet-States of  $\beta$ -Carotene, Retinal and Related Polyenes. *Photochem. Photobiol.*, 1973, 17, p. 43-51.
8. NIYOGI, K. K., BJÖRKMAN, O., and GROSSMAN, A. R. The roles of specific xanthophylls in photoprotection. *Proc. Natl. Acad. Sci. USA*, 1997, 94, p.14162-14167.
9. RUBAN, A., BERERA, R., ILIOAIA, C., VAN STOKKUM, I., KENNIS, J., PASCAL, A., VAN AMERONGEN, H., ROBERT, B., HORTON, P., and VAN GRONDELLE, R. Identification of a mechanism of photoprotective energy dissipation in higher plants. *Nature*, 2007, 450, p. 575-U22.
10. AHN, T. K., AVENSON, T. J., BALLOTTARI, M., CHENG, Y.-C., NIYOGI, K. K., BASSI, R., and FLEMING, G. R. Architecture of a Charge-Transfer State Regulating Light Harvesting in a Plant Antenna Protein. *Science*, 2008, 320, p. 794-797.
11. WILSON, A., PUNGINELLI, C., GALL, A., BONETTI, C., ALEXANDRE, M., ROUTABOUL, J.-M., KERFELD, C. A., VAN GRONDELLE, R., ROBERT, B., KENNIS, J. T. M., and KIRILOVSKY, D. A photoactive carotenoid protein acting as light intensity sensor. *Proc. Natl. Acad. Sci. USA*, 2008, 105, p.12075-12080.
12. ARAKI, G., and MURAI, T. Molecular Structure and Absorption Spectra of Carotenoids, *Progress of Theoretical Physics*, 1952, 8, p. 639-654.
13. SUZUKI, H., and MIZUHASHI, S.  $\pi$ -Electronic Structure and Absorption Spectra of Carotenoids. *J. Phys. Soc. Jpn.*, 1964, 19, p. 724-738.

14. DALE, J. Empirical Relationships of the Minor Bands in the Absorption Spectra of Polyenes. *Acta Chemica Scandinavica*, 1954, 8, p. 1235-1256.
15. HEMLEY, R., and KOHLER, B. E. Electronic structure of polyenes related to the visual chromophore. A simple model for the observed band shapes. *Biophysical Journal*, 1977, 20, p. 377-382.
16. CHRISTENSEN, R. L., BARNEY, E. A., BROENE, R. D., GALINATO, M. G. I., and FRANK, H. A. Linear polyenes: models for the spectroscopy and photophysics of carotenoids. *Archives of Biochemistry and Biophysics*, 2004, 430, p. 30-36.
17. LERSEN, A. L., and REID, C. E. An Investigation of Certain Solvent Effect in Absorption Spectra. *J. Chem. Phys.*, 1952, 20, p. 233-236.
18. HIRAYAMA, K. Absorption Spectra and Chemical Structure. II. Solvent Effect, *J. Am. Chem. Soc.*, 1955, 77, p. 379-381.
19. ANDERSSON, P., GILLBRO, T., FERGUSON, L., and COGDELL, R. Absorption Spectral Shifts of Carotenoids Related to Medium Polarizability. *Photochem. Photobiol.*, 1991, 54, p. 353-360.
20. KUKI, M., NAGAE, H., COGDELL, R., SHIMADA, K., and KOYAMA, Y. Solvent Effect on Spheroidene in Nonpolar and Polar Solutions and the Environment of Spheroidene in the Light-Harvesting Complexes of Rhodobacter-Sphaeroides 2.4.1 as Revealed by the Energy of the  $1A_g \rightarrow 1B_u$  Absorption and the Frequencies of the Vibronically Coupled C=C Stretching Raman Lines in the  $(1)A_g(-)$  and  $2(1)A_g(-)$  States. *Photochem. Photobiol.*, 1994, 59, p. 116-124.
21. CHEN, Z., LEE, C., LENZER, T., and OUM, K. Solvent effects on the  $S_0(1)A_g(-) \rightarrow S_0(1)B_u(+)$  transition of beta-carotene, echinenone, canthaxanthin, and astaxanthin in supercritical CO<sub>2</sub> and CF<sub>3</sub>H, *J. Phys. Chem. A*, 2006, 110, p. 11291-11297.
22. RENGE, I., and SILD, E. Absorption shifts in carotenoids-influence of index of refraction and submolecular electric fields. *J. Photochem. Photobiol. A-Chem.*, 2011, 218, p. 156-161.
23. PAPAGIANNAKIS, E., KENNIS, J. T. M., STOKKUM, I. H. M. van, COGDELL, R. J., and GRONDELLE, R. van. An alternative carotenoid-to-bacteriochlorophyll energy transfer pathway in photosynthetic light harvesting. *Proc. Natl. Acad. Sci. USA*, 2002, 99, p. 6017-6022.
24. WANG, P., NAKAMURA, R., KANEMATSU, Y., KOYAMA, Y., NAGAE, H., NISHIO, T., HASHIMOTO, H., and ZHANG, J.-P. Low-lying singlet states of carotenoids having 8-13 conjugated double bonds as determined by electronic absorption spectroscopy. *Chemical Physics Letters*, 2005, 410, p. 108-114.
25. WIRTZ, A. C., VAN HEMERT, M. C., LUGTENBURG, J., FRANK, H. A., and GROENEN, E. J. J. Two stereoisomers of spheroidene in the Rhodobacter sphaeroides R26 reaction centre: A DFT analysis of resonance raman spectra. *Biophys. J.*, 2007, 93, p. 981-991.
26. MENDES-PINTO, M. M., SANSIAUME, E., HASHIMOTO, H., PASCAL, A. A., GALL, A., and ROBERT, B. Electronic Absorption and Ground State Structure of Carotenoid Molecules. *J. Phys. Chem. B*, 2013, 117, p. 11015-11021.

27. VAN DORSSSEN, R. J., BRETON, J., PLIJTER, J. J., SATOH, K., VANGORKOM, H. J., and AMESZ, J. Spectroscopic Properties of the Reaction Centre and of the 47kda Chlorophyll Protein of Photosystem- II. *Biochim. Biophys. Acta*, 1987, 893, p. 267-274.
28. KWA, S., NEWELL, W., VAN GRONDELLE, R., and DEKKER, J. The Reaction Centre of Photosystem-II Studied with Polarized Fluorescence Spectroscopy. *Biochim. Biophys. Acta*, 1992, 1099, p. 193-202.
29. TOMO, T., MIMURO, M., IWAKI, M., KOBAYASHI, M., ITOH, S., and SATOH, K. Topology of pigments in the isolated Photosystem II reaction centre studied by selective extraction. *Biochim. Biophys. Acta- Bioenerg.*, 1997, 1321, p. 21-30.
30. LOLL, B., KERN, J., SAENGER, W., ZOUNI, A., and BIESIADKA, J. Towards complete cofactor arrangement in the 3.0 Å resolution structure of photosystem II. *Nature*, 2005, 438, p.1040-1044.
31. UMENA, Y., KAWAKAMI, K., SHEN, J.-R., and KAMIYA, N. Crystal structure of oxygen-evolving photosystem II at a resolution of 1.9 Å. *Nature*, 2011, 473, p. 55-60.
32. TAKAHASHI, Y., HANSSON, Ö., MATHIS, P., and SATOH, K. Primary radical pair in the Photosystem II reaction centre. *Biochim. Biophys. Acta - Bioenergetics*, 1987, 893, p. 49-59.
33. DURRANT, J. R., GIORGI, L. B., BARBER, J., KLUG, D. R., and PORTER, G. Characterisation of triplet states in isolated Photosystem II reaction centres: Oxygen quenching as a mechanism for photodamage. *Biochim. Biophys. Acta - Bioenergetics*, 1990, 1017, p. 167-175.
34. MIMURO, M., TOMO, T., NISHIMURA, Y., YAMAZAKI, I., and SATOH, K. Identification of a photochemically inactive pheophytin molecule in the spinach D1-D2-cyt b559 complex. *Biochim. Biophys. Acta (BBA) – Bioenergetics*, 1995, 1232, p. 81-88.
35. TELFER, A., FROLOV, D., BARBER, J., ROBERT, B., and PASCAL, A. Oxidation of the two beta-carotene molecules in the photosystem II reaction centre. *Biochemistry*, 2003, 42 p. 1008-1015.
36. CAFFARRI, S., CROCE, R., BRETON, J., and BASSI, R. The Major Antenna Complex of Photosystem II Has a Xanthophyll Binding Site Not Involved in Light Harvesting. *J. Biol. Chem.*, 2001, 276, p. 35924-35933.
37. LIU, Z., YAN, H., WANG, K., KUANG, T., ZHANG, J., GUI, L., AN, X., and CHANG, W. Crystal structure of spinach major light-harvesting complex at 2.72 Å resolution. *Nature*, 2004, 428, p. 287-292.
38. STANDFUSS, J., VAN SCHELTINGA, A. C. T., LAMBORGHINI, M., and KÜHLBRANDT, W. Mechanisms of photoprotection and nonphotochemical quenching in pea light-harvesting complex at 2.5 Å resolution. *EMBO J.*, 2005, 24, p. 919-928.
39. YAN, H., ZHANG, P., WANG, C., LIU, Z., and CHANG, W. Two lutein molecules in LHCII have different conformations and functions: Insights into the molecular mechanism of thermal dissipation in plants. *Biochemical and biophysical research communications*, 2007, 355, p. 457-463.

40. PHILLIP, D., RUBAN, A. V., HORTON, P., ASATO, A., and YOUNG, A. J. Quenching of chlorophyll fluorescence in the major light-harvesting complex of photosystem II: a systematic study of the effect of carotenoid structure. *Proc. Natl. Acad. Sci. USA*, 1996, 93, p. 1492-1497.
41. RUBAN, A. V., LEE, P. J., WENTWORTH, M., YOUNG, A. J., and HORTON, P. Determination of the stoichiometry and strength of binding of xanthophylls to the photosystem II light harvesting complexes. *J. Biol. Chem.*, 1999, 274, p. 10458-10465.
42. LIU, W., WANG, Z., ZHENG, Z., JIANG, L., YANG, Y., ZHAO, L., and SU, W. Density Functional Theoretical Analysis of the Molecular Structural Effects on Raman Spectra of  $\beta$ -Carotene and Lycopene. *Chinese J. Chem.*, 2012, 30, p. 2573-2580.
43. GALL, A., and ROBERT, B. Characterization of the different peripheral light-harvesting complexes from high- and low-light grown cells from *Rhodospseudomonas palustris*. *Biochemistry*, 1999, 38, p. 5185-5190.
44. ANDREEVA, A., APOSTOLOVA, I., and VELITCHKOVA, M. Temperature dependence of resonance Raman spectra of carotenoids. *Spectrochimica Acta Part A: Molecular and Biomolecular Spectroscopy*, 2011, 78, p. 1261-1265.
45. ROBERT, B., HORTON, P., PASCAL, A., and RUBAN, A. Insights into the molecular dynamics of plant light-harvesting proteins in vivo. *Trends Plant Sci.*, 2004, 9, p. 385-390.
46. ILIOAIA, C., JOHNSON, M. P., LIAO, P.-N., PASCAL, A. A., GRONDELLE, R. van, WALLA, P. J., RUBAN, A. V., and ROBERT, B. Photoprotection in Plants Involves a Change in Lutein 1 Binding Domain in the Major Light-harvesting Complex of Photosystem II. *J. Biol. Chem.*, 2011, 286, p. 27247-27254.
47. MERLIN, J. C. Resonance Raman spectroscopy of carotenoids and carotenoid-containing systems. *Pure and Applied Chemistry*, 1985, 57, p. 785-792.
48. RUBAN, A., PASCAL, A., ROBERT, B., and HORTON, P. Configuration and dynamics of xanthophylls in light-harvesting antennae of higher plants - Spectroscopic analysis of isolated light-harvesting complex of photosystem II and thylakoid membranes. *J. Biol. Chem.*, 2001, 276, p. 24862-24870.
49. SENGE, M., HOPE, H., and SMITH, K. Structure and Conformation of Photosynthetic Pigments and Related Compounds 3. Crystal Structure of  $\beta$ -Carotene, *Z.Naturforsch.(C)*, 1992, 47, p. 474-476.
50. GOLIBRZUCH, K., EHLERS, F., SCHOLZ, M., OSWALD, R., LENZER, T., OUM, K., KIM, H., and KOO, S. Ultrafast excited state dynamics and spectroscopy of 13,13'-diphenyl- $\beta$ -carotene. *Phys. Chem. Chem. Phys.*, 2011, 13, p. 6340-6351.
51. CEREZO, J., ZÚÑIGA, J., BASTIDA, A., REQUENA, A., CERÓN-CARRASCO, J. P., and ERIKSSON, L. A. Antioxidant Properties of  $\beta$ -Carotene Isomers and Their Role in Photosystems: Insights from Ab Initio Simulations. *J. Phys. Chem. A*, 2012, 116, p. 3498-3506.

**CHAPTER 3 EFFECT OF CONSTITUTIVE  
EXPRESSION OF BACTERIAL PHYTOENE  
DESATURASE CRTI ON PHOTOSYNTHETIC  
ELECTRON TRANSPORT IN *ARABIDOPSIS  
THALIANA*<sup>1</sup>**



### Summary of the work

In the past years, many efforts have been made in order to genetically modifying the biosynthetic carotenoid pathways in the multitude of photosynthetic organisms, with a special focus on plants. The aim is generally the alteration of the carotenoid levels produced in all or part of the organism tissues. An important example is represented by the so called “Golden Rice” project (Schaub *et al.*, 2005), where two genes, phytoene synthase (PSY) and the bacterial carotene desaturase (CRTI) have been inserted into the rice genome by genetic engineering, to restart the carotenoid biosynthetic pathway leading to the production and accumulation of  $\beta$ -carotene in the grains, the edible part. Both genes are naturally involved in carotene biosynthesis, but while PSY needs to be supplemented, the need for the CrtI transgene in Golden Rice is presumably due to insufficient activity of the phytoene desaturase and/or zeta-carotene desaturase enzyme in endosperm. The difference here is that in the mutants the reconstructed pathway is not subject to downregulation, as usually happens in the grain. At a later stage, the effect of CRTI expression was also investigated in leaves of transgenic rice and *Arabidopsis thaliana*. The main finding was that the carotenoid pattern changed, showing a decrease in lutein concentration, while that of the  $\beta$ -carotene-derived xanthophylls increased.

In the present work we further characterize the *Arabidopsis thaliana* mutant lines to investigate the consequences of alteration of the carotenoid composition at the photosynthetic and photoprotective levels.

<sup>1</sup>*This chapter is based on the following publication:*

GALZERANO, D., FEILKE, K., SCHAUB, P., BEYER, P. and KRIEGER-LISZKAY, A.  
*Biochim. Biophys. Acta*, 2014, 1837, 3, p. 345-353.

### 3.1 Introduction

When plants are exposed to light intensities exceeding the intensity needed to saturate photosynthetic electron transport, light-induced damage of the photosystems occurs [1,2]. The reaction centre of photosystem II (PSII) is particularly susceptible to photoinhibition. Light-induced damage is caused by excessive production of reactive oxygen species such as singlet oxygen, superoxide, hydrogen peroxide and hydroxyl radicals [3,4]. Plants have developed several protective mechanisms to avoid photoinhibitory damage. These include short-term processes that modulate the structure and function of antenna complexes, comprising non-photochemical quenching (NPQ) of chlorophyll fluorescence, alternative electron transport pathways and movement of chloroplasts or even leaves away from intense light [5,6]. There are three components of NPQ: the qE type which depends on the reversible conversion of violaxanthin to zeaxanthin in the so-called xanthophyll cycle and on the protonation of the protein PsbS; state transitions (qT) and photoinhibition (qI) [7]. Changes in the xanthophyll content affect qE quenching as has been shown for a number of Arabidopsis mutants [8, 9]. For instance, Arabidopsis mutants that lack lutein (*lut2*) exhibit a partial defect in qE while mutants with elevated lutein content show a larger qE [8,9]. Lutein has also been shown to be involved in the dissipation of excess light energy as heat in the light harvesting complex of photosystem II, LHCII [10].

Mutations and the constitutive overexpression of genes coding for carotenoid biosynthetic enzymes can affect the carotenoid composition in leaves. In lutein-deficient mutants *lut1* and *lut2* and in the neoxanthin and violaxanthin-deficient mutant *aba1*, the total carotenoid content remained unchanged and the xanthophylls reduced in amount were replaced by others [8]. Moreover, the *lut2* mutant exhibited alterations in PSII antenna size and had a reduced stability of the LHCII [11]. Constitutively expressing the bacterial phytoene desaturase CRTI in addition to the endogenous carotene desaturation pathway in rice and Arabidopsis resulted in a decrease in lutein, while the  $\beta$ -carotene-derived xanthophylls increased [12]. The mRNA levels of intrinsic carotenogenic enzymes remained unaffected in these plants [12]. In potato plants, the constitutive overexpression of CRTI and/or of the bacterial lycopene cyclase CRTY interfered negatively with leaf carotenogenesis also showing signs of chlorosis [13].

There is a functional connection between carotenoid biosynthesis and the reduction state of the photosynthetic electron transport chain since quinones are involved in plant-type phytoene desaturation [14,15]. In chloroplasts, the redox state of the plastoquinone pool is modulated by linear electron transport, by cyclic electron transport and by chlororespiration. It has been demonstrated that carotenoid biosynthesis is affected in mutants of the plastid terminal oxidase (PTOX) which oxidizes plastoquinol and transfers electrons to oxygen [16-18]. Furthermore, a tomato mutant deficient in the plastid NAD(P)H dehydrogenase (NDH) complex catalyzing non-photochemical electron fluxes to plastoquinone accumulated less carotenoids and had yellow-orange fruits [19]. In contrast, the bacterial CRTI which is inhomologous to plant-type desaturases, is an oxidase not involving quinones in the reaction mechanism [20].

*Crti*-overexpressing *Arabidopsis* lines differing in expression levels were obtained in previous work [12]. Among these, the plants with the highest level of CRTI showed an approximately 50% decrease in lutein content compared to the wt [12], partially compensated by  $\beta$ -carotene derived xanthophylls.

We used these plants to investigate in greater detail whether firstly, the alteration of the carotenoid composition increased their susceptibility to light and secondly, whether the redox state of the electron transport chain was altered. To investigate these two aspects, we followed non-photochemical quenching of chlorophyll fluorescence and photoinhibition of PSII by measuring the loss of variable fluorescence in leaves of wt and CRTI expressing lines in the presence or absence of the protein synthesis inhibitor lincomycin. Furthermore, we measured P700 oxidation and the light-induced generation of  $^1\text{O}_2$  and of  $\text{H}_2\text{O}_2$ -derived hydroxyl radicals by spin trapping EPR spectroscopy. We demonstrate that the expression of CRTI increases the level of PTOX, promotes the generation of reactive oxygen species in chloroplasts and inhibits cyclic electron flow. Since the plant-type carotene desaturation pathway is present in these plants in parallel to CRTI and the former, but not the latter is dependent on PTOX at varying degrees, it is conceivable that the insertion of CRTI can indirectly through CRTI/PDS competition affect the reduction state of the plastoquinone pool. In this scenario, plastoquinones have dual functions in that they are integral constituents of photosynthetic electron transport besides being electron acceptors of the endogenous PDS (but not of the overexpressed CRTI).

### 3.2 Materials and Methods

*Arabidopsis thaliana* (ecotype Columbia) plants were grown for 6-8 weeks in soil under short day conditions (8 h white light,  $120 \mu\text{mol quanta m}^{-2}\text{s}^{-1}$ ,  $21^\circ\text{C}/16 \text{ h dark}$ ,  $18^\circ\text{C}$ ). We used two transgenic *Arabidopsis* lines expressing *crtI* under 35S promoter control as described in Schaub et al. [12]: the high expressing lines 2 (11) and 4 (14) were used in the present study. For measurements on single leaves, we used plants from the same age and selected for the measurements leaves from the same age.

#### *Extraction of thylakoid membranes and proteins from A. thaliana*

*Thylakoid membrane preparation.* For thylakoid preparations, we used complete rosettes from 5 plants for each preparation. Leaves were ground in 0.33 M sorbitol, 60 mM KCl, 10 mM EDTA, 1 mM  $\text{MgCl}_2$ , 25 mM Mes pH 6.1. After centrifugation, the pellet was first washed with 0.33 M sorbitol, 60 mM KCl, 10 mM EDTA, 1 mM  $\text{MgCl}_2$ , 25 mM HEPES pH 6.7, then resuspended in 5 mM  $\text{MgCl}_2$ , 20 mM  $\text{KPO}_4$  pH 7.6 to break all intact chloroplast. After centrifugation, the pellet was resuspended in 0.3 M sucrose, 5 mM  $\text{MgCl}_2$ , 20 mM  $\text{KPO}_4$  pH 7.6 (measurement buffer) so as to have a final concentration of  $1 \text{ mg Chl ml}^{-1}$  of thylakoids. All centrifugations were performed at  $3,000 \text{ g}$  for 3 min at  $4^\circ\text{C}$ .

*Protein extraction.* Leaves were ground in liquid nitrogen before homogenization in lysis buffer. The lysis buffer contained 100 mM Tris-HCl pH 6.8, 4% SDS, 20 mM EDTA, protease inhibitor cocktail (Sigma-Aldrich, St-Louis, Missouri, United States). Samples were then centrifuged for 15 min,  $10,000 \text{ g}$  at  $4^\circ\text{C}$  to remove the cell debris and the supernatants were recovered.

*Pigment analysis.* For each analysis, 10 leaves of the same age from 5 different plants were collected, lyophilized and ground to a fine powder using a stone mill (MM200, Retsch, Germany) at 30 Hz for 1 min. 5-10 mg of leaf sample were extracted with 2 ml Tris-buffered acetone (10 vol% 100 mM Tris) by sonication. After centrifugation for 5 min at  $3000 \times \text{g}$  the supernatant was transferred to a new tube and the remaining pellet re-extracted twice with 2 ml acetone, each. The combined extracts were mixed with 2 ml PE:DE (2:1, v,v) and partitioned twice against a 1% (w/v) sodium chloride solution. The combined organic phases were dried and dissolved in 100  $\mu\text{l}$  chloroform out of which five  $\mu\text{l}$  were subjected to quantitative analysis using a (Shimadzu Prominence UPLC system with a YMC C30 150 x

2.1 reversed-phase column (YMC Europe GmbH, Germany). The gradient system employed A: MeOH/tert-butylmethylether (TBME)/water 30:1:10 (v/v/v) and B: MeOH/TBME 1:1 (v/v). The gradient started at 100% A, followed by a linear gradient to 0% A within 20 min at a flow-rate of 0.5 ml min<sup>-1</sup>. An isocratic segment run for 4 min at 0% A, completed the run.

For quantitative analyses, 5 µg VIS682A (QCR Solutions, USA) were added to each sample as an internal standard prior to extraction. All peaks were normalized relative to the internal VIS682A standard to correct for extraction and injection variability. A β-carotene calibration curve, run separately, was used to calculate carotenoid amounts. All carotenoid peaks were integrated at their individual λ<sub>max</sub> and underwent a second normalization to correct for their individual molar extinction coefficients relative to β-carotene (=1), using violaxanthin (1.01), lutein-epoxyd (0.96), antheraxanthin (1.01), lutein (1.09), chlorophyll *a* (1.48) and chlorophyll *b* (1.00). Carotenoids were identified by their retention times and absorption spectra, monitored using a photodiode array detector (Shimadzu Prominence UPLC system, München, Germany).

*O<sub>2</sub> measurements.* Measurements of O<sub>2</sub> production and consumption were performed in a Liquid-Phase Oxygen Electrode Chamber (Hansatech Instruments, Norfolk, England). Total electron transport activity was measured as O<sub>2</sub> evolution using thylakoids (10 µg Chl/ml) in the presence of 1 mM K<sub>3</sub>[Fe(CN)<sub>6</sub>], PSII activity was measured in the presence of 1 mM 2,6-dichloro-1,4-benzoquinone and 0.5 mM K<sub>3</sub>[Fe(CN)<sub>6</sub>]. PSI activity was measured in the presence of 10 µM DCMU, 5 mM ascorbate, 30 µM 2,6-dichlorophenol-indophenol and 500 µM methylviologen. All activities were measured in the presence of 5 µM nigericin as uncoupler.

*Chlorophyll fluorescence.* Room temperature chlorophyll fluorescence was measured using a pulse-amplitude modulation fluorometer (DUAL-PAM, Walz, Effeltrich, Germany). As actinic light, red light at 635 nm was used. The intensity of the measuring light was sufficiently low (integral intensity about 9 µmol quanta m<sup>-2</sup> s<sup>-1</sup>, frequency of modulated light) to prevent the stable reduction of plastoquinone. Saturating flashes (1 s) were given to probe the maximum fluorescence level. The maximum quantum yield of PSII, Fv/Fm, was assayed by calculating the ratio of the variable fluorescence, Fv, to maximal fluorescence, Fm, in the dark-adapted state. Photochemical (qP) and non-photochemical quenching (NPQ) was assayed during 5 min of actinic light (660 µmol quanta m<sup>-2</sup>s<sup>-1</sup>), followed by a recovery period of 3 min. NPQ was defined as (Fm-Fm')/(Fm-Fo') with Fm' being the maximal fluorescence

in the actinic light and qP as  $(F_m' - F)/(F_m - F_o')$ . Plants were taken from the growth chamber during the light period and dark-adapted for 10 min prior to the measurement to allow most of the reversible quenching to relax.

The  $F_o'$  rise in the dark was measured after illumination with actinic red light ( $I = 825 \mu\text{mol quanta m}^{-2}\text{s}^{-1}$ ). After 10 min actinic light, the measuring light was set on and the actinic light was switched off.

*Photoinhibition.* Photoinhibition of PSII was carried out on detached leaves at  $1000 \mu\text{mol quanta m}^{-2} \text{s}^{-1}$ . To block chloroplast-encoded protein synthesis, detached leaves were vacuum-infiltrated with lincomycin ( $1 \text{ g l}^{-1}$ ) and floating on the lincomycin solution for 3 h in dim light prior to the photoinhibitory treatment. During the photoinhibition treatment leaves were kept hydrated on wet filter paper. As a measure of PSII activity  $F_v/F_m$  was determined.

*Thermoluminescence.* Thermoluminescence was measured on leaf segments taken from plants dark-adapted for 5 min with a home-built apparatus. Thermoluminescence was excited with single turnover flashes at  $1^\circ\text{C}$  spaced with a 1 s dark interval. Samples were heated at a rate of  $20^\circ\text{C}/\text{min}$  to  $70^\circ\text{C}$ , and the light emission was recorded. Graphical and numerical data analyses were performed according to Ducruet and Miranda [21].

*P<sub>700</sub> measurements.* The redox state of the  $P_{700}$  was monitored by following changes in absorbance of 15 min at 830 nm using a DUAL-PAM. Leaves attached to the plants were used. The plants were kept in the light in the growth chamber so that the enzymes Calvin-Benson cycle were activated and were dark-adapted for 15 min prior to the measurements. To probe the maximum extent of  $P_{700}$  oxidation leaves were illuminated with far-red light ( $190 \mu\text{mol quanta m}^{-2}\text{s}^{-1}$ , highest light intensity provided by the DUAL-PAM). At each intensity of actinic light, the increase in absorption was followed until a constant level was reached.

Kinetics of  $P_{700}$  oxidation were probed by far-red illumination. For this assay, plants were dark-adapted for 10 min, then preilluminated for 3 min with red light ( $I=600 \mu\text{mol quanta m}^{-2}\text{s}^{-1}$ ). After this pre-illumination the  $P_{700}$  measurement was started using the following illumination protocol: 10 s dark, 5 s actinic red light ( $I=600 \mu\text{mol quanta m}^{-2}\text{s}^{-1}$ ), 2 s dark, 17 s far-red light (highest intensity of the DUAL-PAM). Only the first seconds after onset of far-red light are shown in figure 3.11. The amplitudes of the signals were normalised to the signal size of wt.

*Room-Temperature EPR Measurements.* Spin-trapping assays with 4-pyridyl-1-oxide-*N*-*tert*-butylnitron (4-POBN) (Sigma-Aldrich) to detect the formation of hydroxyl radicals were carried out using thylakoid membranes at a concentration of 10  $\mu\text{g Chl ml}^{-1}$ . Samples were illuminated for 2 min with red light (RG 630) ( $500 \mu\text{mol quanta m}^{-2} \text{s}^{-1}$ ) in the presence of 50 mM 4-POBN, 4% ethanol, 50  $\mu\text{M Fe-EDTA}$ , and buffer (20 mM phosphate buffer, pH 7.5, 5 mM  $\text{MgCl}_2$ , 0.3 M sorbitol). When required, 10  $\mu\text{M}$  octyl gallate was added prior to the illumination.

To detect singlet oxygen, samples ( $10 \mu\text{g Chl ml}^{-1}$ ) were illuminated for 2 min with red light (RG 630) ( $1000 \mu\text{mol quanta m}^{-2} \text{s}^{-1}$ ) in the presence of 100 mM of the spin probe 2,2,6,6-tetramethyl-4-piperidone hydrochloride (TEMPD).

EPR spectra were recorded at room temperature in a standard quartz flat cell using an ESP-300 X-band spectrometer (Bruker, Rheinstetten, Germany). The following parameters were used: microwave frequency 9.73 GHz, modulation frequency 100 kHz, modulation amplitude: 1 G, microwave power: 63 milliwatt in TEMPD assays, or 6.3 milliwatt in 4-POBN assays, receiver gain:  $2 \times 10^4$ , time constant: 40.96 ms; number of scans: 4.

*Immunoblots.* 5  $\mu\text{g Chl}$  from leaf extracts were used for analysis by SDS-PAGE (12% acrylamide) and immunoblotting. Proteins were blotted onto nitrocellulose filters. Labelling of the membranes with anti-PTOX (generous gift from Marcel Kuntz, Grenoble), anti-PsbP, anti-PsbO (both Agrisera, Vännäs, Sweden) or anti-NDH-H (generous gift from Dominique Rumeau, CEA Cadarache) was carried out at room temperature in 1x TBS (50 mM Tris-HCl pH 7.6, 150 mM NaCl), 0.1% Tween 20 and 5% non-fat milk powder. After washing, bound antibodies were revealed with a peroxidase-linked secondary anti-rabbit antibody (Agrisera, Vännäs, Sweden) and visualized by enhanced chemiluminescence.

### 3.3 Results

#### 3.3.1 Light sensitivity of CRTI expressing lines

We investigated the light sensitivity of Arabidopsis lines which expressed the bacterial phytoene desaturase (CRTI) constitutively in addition to their endogenous plant desaturases. We used two high CRTI expressing lines (named hereafter CRTI-lines, see Materials) which showed the strongest relative reduction in their lutein proportion [12]. These lines showed growth retardation (figure 3.1; fresh weight wt:  $100 \pm 23\%$ ; line 11:  $77 \pm 21\%$ ; line 14:  $48 \pm 9\%$ ;  $n=22$ ) when grown under short day conditions (8 h light/16 h dark), and the leaves were paler.



**Figure 3.1** Phenotypes of *Arabidopsis thaliana* wild type (wt), CRTI-lines 11 and 14 after 7 weeks grown on soil.

Pigment analysis (figure 3.2) showed that the total carotenoid content in leaves from the CRTI-lines decreased from 2.38  $\mu\text{g}/\text{mg}$  dry mass to 2.05  $\mu\text{g}/\text{mg}$  dry mass in the CRTI-lines. The CRTI-lines contained about 50% less lutein as has been published previously [12]. A part of the missing lutein was replaced by violaxanthin and antheraxanthin. The  $\beta$ -carotene content remained unchanged. In addition to these changes in the carotenoid composition, the chlorophyll content was slightly decreased. Chl *b* decreased by 9-10% in both CRTI-lines, Chl *a* by 10-14% in line 11 and 14, respectively. Changes in the carotenoid composition did not lead to changes in activity of the main complexes of the photosynthetic electron transport chain measured in the presence of an uncoupler. In isolated thylakoid membranes from wt and the two CRTI-lines the total electron transport activity was  $97 \pm 7 \mu\text{mol O}_2 \text{ mg chl}^{-1}\text{h}^{-1}$ , the PS II activity was  $108 \pm 5 \mu\text{mol O}_2 \text{ mg chl}^{-1}\text{h}^{-1}$  and the PSI activity was  $345 \pm 7 \mu\text{mol O}_2 \text{ mg chl}^{-1}\text{h}^{-1}$ . These values show that the ratio of PSII:PSI was unaltered in the CRTI-lines.

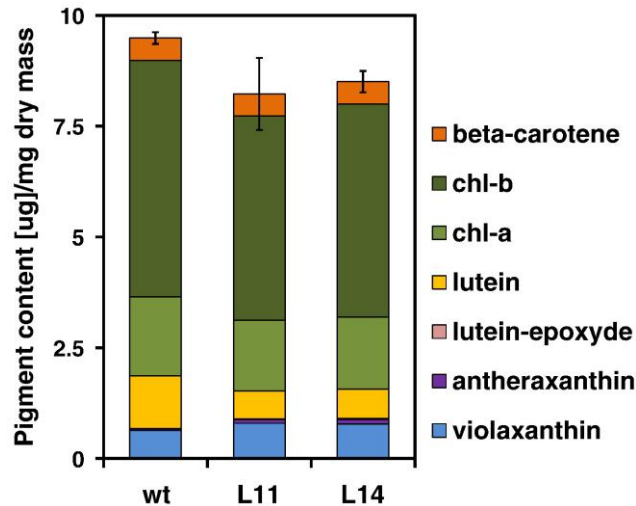


**Figure 3.2** Chlorophyll and carotenoid content of mature leaves from wt (filled squares) and CRTI-lines 11(circles) and 14 (triangles). Curves for each line were displaced horizontally. The maximum value of NPQ was the same in wt, line 11 and 14. Each bar represents a pool of extracts made from mature leaves from five different plants. The mean of three measurements are shown ( $n = 3 \pm SE$ ).

However, measurements of chlorophyll fluorescence showed that the quantum efficiency of PSII was slightly lowered in the two CRTI-lines (table 3.1). This may be taken as an indication for a more light-sensitive PSII. When leaves were exposed to high light ( $1000 \mu\text{mol quanta m}^{-2}\text{s}^{-1}$ ) for 1 h in the presence of lincomycin to inhibit synthesis of the D1 protein, leaves from the CRTI-lines showed a higher loss of Fv/Fm than wt (table 3.1).

sample	Fv/Fm before high light	Fv/Fm after high light
wt	$0.83 \pm 0.01$	$0.66 \pm 0.02$
Line 11	$0.78 \pm 0.03$	$0.57 \pm 0.02$
Line 14	$0.77 \pm 0.04$	$0.51 \pm 0.03$

**Table 0.1** Photoinhibition of PSII in leaves from wild-type and the CRTI-lines 11 and 14. Leaves subjected to high light illumination ( $I=1000 \mu\text{mol quanta m}^{-2}\text{s}^{-1}$ ) for 1 h. The maximum quantum yield of PSII (Fv/Fm) was determined before and after the high light exposure. Prior to the measurements, leaves had been infiltrated with lincomycin and were dark-adapted for 10 min before measuring fluorescence. Error bars represent SE (7 independent experiments). After 1 h high light treatment, Fv/Fm values of the CRTI-lines are significantly different to wt ( $P<0.01$ ).

A higher susceptibility to light may be caused by alteration in the antenna, of NPQ and of the yield of  $^1\text{O}_2$  generation or by alterations in the photosynthetic electron transport chain. To investigate whether the lower lutein content of the antenna influences the ability of the plants to dissipate excess energy by non-photochemical quenching, chlorophyll fluorescence curves were analyzed in more detail. As shown in figure 3.3, the CRTI-lines showed a slower induction of NPQ than wt while the total extent of NPQ and also the photochemical quenching (qP) (not shown) were not affected.

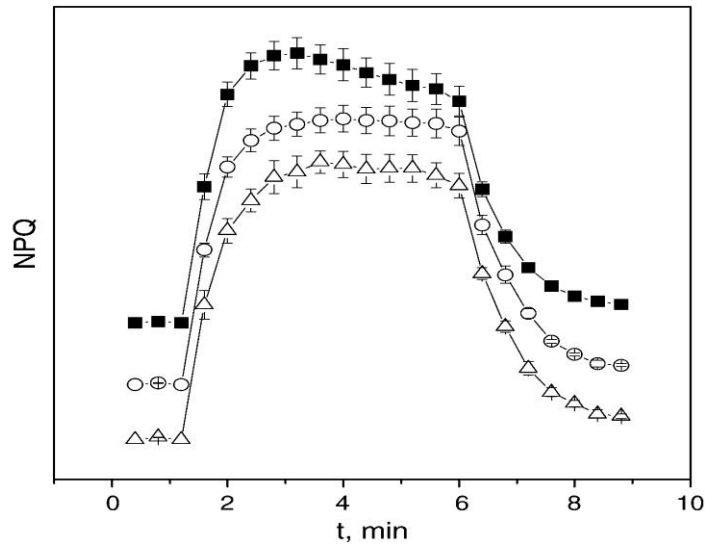


**Figure 3.3** Non-photochemical (NPQ) and photochemical (qP) quenching in wt (filled squares), CRTI-lines 11 (circles) and 14 (triangles). Dark-adapted leaves were illuminated with red light ( $I = 660 \mu\text{mol quanta m}^{-2} \text{s}^{-1}$ ) and chlorophyll fluorescence was measured on leaves still attached to the plant. Individual plants were measured ( $n = 3 \pm \text{SE}$ ).

A change in NPQ is supposed to lead to a higher yield of  $^1\text{O}_2$  generation as has been shown for the *npq4* mutant [22]. The generation of the  $^1\text{O}_2$  during 2 min of illumination was followed by spin trapping EPR spectroscopy in thylakoid membranes from the the CRTI-lines and wt. Figure 3.4 shows typical EPR spectra of the spin adduct TEMPDO which results from the reaction of 2,2,6,6-tetramethyl-4-piperidone hydrochloride (TEMPD) with  $^1\text{O}_2$  [23]. Illumination of thylakoid membranes of wt and the two CRTI-lines gave approximately the same signal size. This shows that although the carotenoid composition of the thylakoid membranes was altered [12], the yield of light-induced  $^1\text{O}_2$  generation remained unchanged. Thus, the higher susceptibility to photoinhibition cannot be explained by a higher yield of  $^1\text{O}_2$  formation. Moreover no substantial alterations in the antenna composition (LHCII monomers and trimers) were observed when PSII-enriched membrane fractions of wt and the CRTI-lines were compared (Supplementary information; figure S1). It has to be noted that although at 77K the ratio between the fluorescence emission at 730 nm (reflecting PSI) and the fluorescence emission at 685 nm and 695 nm (reflecting PSII) was unchanged between wt and the CRTI-lines, there was a change in the relative intensity of the fluorescence emitted at 685 nm and that at 695 nm in the CRTI-lines (Supplementary Information; figure S2). This may indicate that the coupling of the LHCII is slightly perturbed in the CRTI-lines leading to stronger emission of fluorescence from CP47 at 695 nm [24] for unknown reasons.

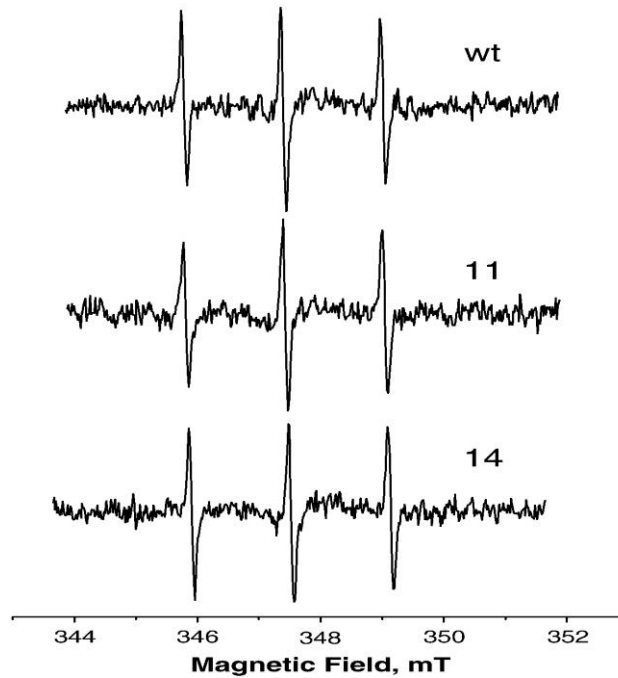


**Figure 3.4** Generation of  $^1\text{O}_2$  in isolated thylakoids from wild-type and CRTI-lines 11 and 14. Samples were illuminated in the presence of 100 mM TEMPD for 2 min with  $1000 \mu\text{mol quanta m}^{-2} \text{s}^{-1}$  red light, filtered by RG 630. Typical EPR spectra are shown.

### 3.3.2 Generation of $\text{H}_2\text{O}_2$ -derived hydroxyl radicals in the CRTI-lines

Next we investigated whether other ROS may be responsible for the observed phenotype in the insertion lines. Superoxide ( $\text{O}_2^{\bullet-}$ ), hydrogen peroxide ( $\text{H}_2\text{O}_2$ ) and hydroxyl radicals ( $\text{HO}^\bullet$ ) can be generated by the reduction of  $\text{O}_2$  in photosynthetic electron transfer in a number of different reactions:  $\text{O}_2$  can act as terminal acceptor in the so-called Mehler reaction at the acceptor side of PSI [25], it can be reduced by plastosemiquinones in the membrane [26], it can be reduced at the acceptor side of PSII [27] and it is the electron acceptor of the plastid terminal oxidase (PTOX) which uses plastoquinol as electron donor. During photosynthetic electron transport the reduction of  $\text{O}_2$  to  $\text{O}_2^{\bullet-}$  may occur under conditions of limited electron acceptor availability other than  $\text{O}_2$ . Two molecules of  $\text{O}_2^{\bullet-}$  dismutate, either spontaneously or catalyzed by superoxide dismutase, to  $\text{H}_2\text{O}_2$  and  $\text{O}_2$ . In the presence of reduced transition metal ions such as  $\text{Fe}^{2+}$ ,  $\text{H}_2\text{O}_2$  gives rise to the hydroxyl radical ( $\text{HO}^\bullet$ ) supported by the reduction of  $\text{Fe}^{3+}$  by  $\text{O}_2^{\bullet-}$  (Haber-Weiss reaction). We investigated the light-induced formation of  $\text{O}_2^{\bullet-}/\text{H}_2\text{O}_2$  by EPR spectroscopy using ethanol/4-POBN as spin trap. FeEDTA was added as catalyst of the Haber-Weiss reaction. Performing 4-POBN spin trapping in the presence of ethanol is a general procedure to indirectly prove the formation of  $\text{HO}^\bullet$  through the detection of the secondary 4-POBN/ $\alpha$ -hydroxyethyl spin adduct. Whereas little or no signal was observed when samples were maintained in the dark in the presence of

ethanol/4-POBN, illumination of thylakoids resulted in strong EPR signals giving sextets of lines ( $a_N = 15.61$  G;  $a_{HB} = 2.55$  G) characteristic of the 4-POBN/ $\alpha$ -hydroxyethyl aminoxy radical (figure 3.5). In the absence of FeEDTA, no EPR signal was detected, showing that the detected radical originates from  $O_2^{\bullet-}/H_2O_2$ . CRTI-lines produced a signal which was approximately 50% larger than the signal obtained from wt thylakoids after 5 min illumination with  $500 \mu\text{mol quanta m}^{-2}\text{s}^{-1}$  white light (table 3.2). Addition of DCMU, an inhibitor that binds to the  $Q_B$ -binding pocket in PSII thereby blocking linear electron transport, almost completely inhibited spin adduct formation. This shows that ROS were generated by photosynthetic electron transfer reactions beyond PSII. In the presence of DNP-INT, an inhibitor of the cytochrome  $b_6f$  complex, about 80% of the EPR signal was lost in the wt and about 60% in the CRTI-lines, showing that the main site of ROS generation is localized at the acceptor side of PSI. However, still a significant amount of ROS was detected when the electron transport was blocked at the level of the cytochrome  $b_6f$  complex. This site of ROS production was more important in the CRTI-lines than in the wt. Superoxide may be generated by reduced plastoquinone, especially when it is in its semi-reduced form ( $PQH^{\bullet-}$ ) or by the action of PTOX. It has been shown that the overexpression of PTOX in tobacco leads to  $O_2^{\bullet-}$  generation [28]. In addition, it has been reported recently that a tobacco line that expresses PTOX from *Chlamydomonas reinhardtii* suffers from photoinhibition [29].

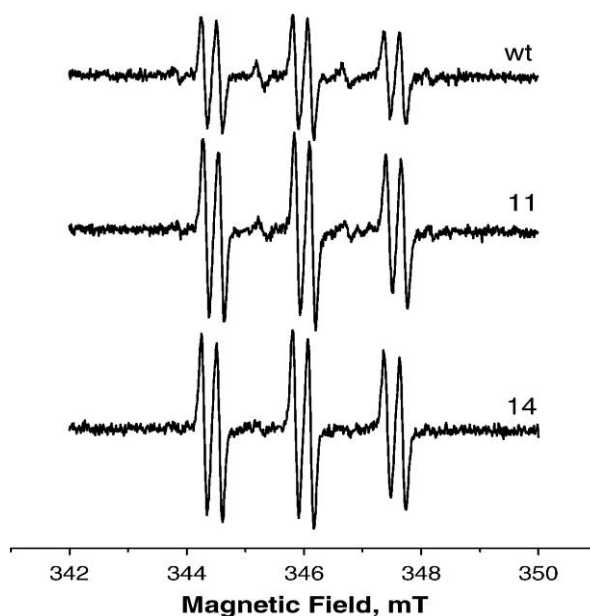


**Figure 3.5** Light-induced hydroxyl radical formation in thylakoids from wt and the CRTI-lines 11 and 14. Generation of hydrogen peroxide-derived hydroxyl radicals was measured by indirect spin trapping with 4-POBN/ethanol. Representative EPR spectra of the 4-POBN/ $\alpha$ -hydroxyethyl adduct are shown. Samples were illuminated for 5 min with white light ( $500 \mu\text{mol quanta m}^{-2}\text{s}^{-1}$ ).

To test whether ROS generation is stimulated in the CRTI-lines, octyl gallate, a specific inhibitor of PTOX, was added to the samples. As shown in Figure 3.6, the formation of the EPR signal was largely suppressed by octyl gallate. The effect of octyl gallate was larger in the transgenic lines than in the wt (Table 3.2). Immunoblots show that the PTOX content was increased in the insertion lines compared to wt while the amount of the NDH complex showed no significant change (Figure 3.7).

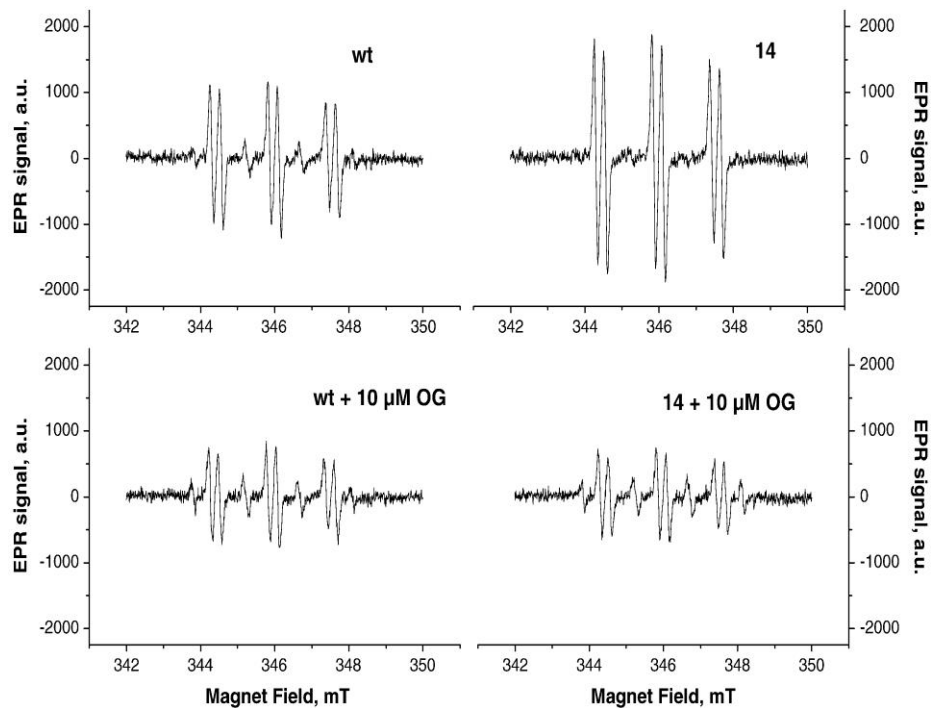


**Figure 3.6** Light-induced hydroxyl radical formation in thylakoids from wt and line 14 in the presence and absence of 10  $\mu\text{M}$  octylgallate (OG). Generation of hydrogen peroxide-derived hydrogen hydroxyl radicals was measured by indirect spin trapping with 4-POBN/ethanol. Typical EPR spectra of the 4-POBN/ $\alpha$ -hydroxyethyl adduct are shown. Samples were illuminated for 5 min with white light ( $500 \mu\text{mol quanta m}^{-2} \text{s}^{-1}$ ).

Sample	EPR signal size (norm.)
wt	1
11	1.48 ± 0.08
14	1.50 ± 0.05
wt + DCMU	< 0.03
11 + DCMU	< 0.03
14 + DCMU	< 0.03
wt + DNP-INT	0.20 ± 0.06
11 + DNP-INT	0.37 ± 0.04
14 + DNP-INT	0.42 ± 0.05
wt + OG	0.73 ± 0.07
11 + OG	0.61 ± 0.05
14 + OG	0.59 ± 0.05
wt + DNP-INT + OG	0.07 ± 0.02
11 + DNP-INT + OG	0.06 ± 0.02
14 + DNP-INT + OG	0.05 ± 0.02

**Table 3.2** Hydroxyl radical production in isolated thylakoids from wild-type, line 11 and line 14. Thylakoids were illuminated for 5 min with white light ( $500 \mu\text{mol quanta m}^{-2} \text{s}^{-1}$ ) in the presence of the spin trap 4-POBN, ethanol and FeEDTA. When indicated, 10  $\mu\text{M}$  DCMU, 100  $\mu\text{M}$  DNP-INT and/or 10  $\mu\text{M}$  octyl gallate (OG) were added prior to the illumination. In the absence of inhibitors, the double integral of the total signal obtained with each type of sample was normalized to the wt. The signal sizes in the presence of the inhibitors were normalized to the corresponding signal sizes in the absence of the inhibitors. SE is given, n = 8 independent experiments of different thylakoid preparations from three different growth sets.

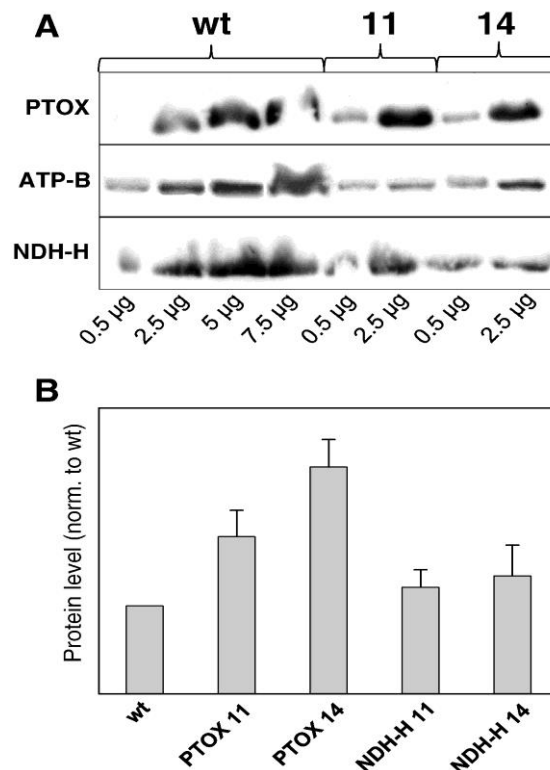


**Figure 3.7** PTOX content in wt and the CRTI-lines 11 and 14. Protein composition of the protein extracts from leaves was analyzed by SDS-PAGE and immunoblotting with antisera against PTOX, the  $\beta$ -subunit of ATP-synthase and NDH-H. Leaf extracts were used. **A:** a typical immunoblot; **B:** Density of the bands recognized by anti-PTOX and anti-NDH-H in lines 11 and 14 were normalized to the density measured in wt (mean  $\pm$  SE). In case of PTOX 6 immunoblots and in case of NDH-H 4 immunoblots, each with proteins from different preparations, were used for the statistical analysis. Gels were loaded based on chlorophyll content.

### 3.3.3 Reduction state of the plastoquinone pool in CRTI-lines

An increase in PTOX abundance can be interpreted as a response of the system to maintain the PQ pool in a more oxidized state. One possibility to measure the reduction state of the PQ pool is to follow the transient increase of the chlorophyll fluorescence level after a short period of illumination of the leaves with actinic light. In the light, NADP<sup>+</sup> is reduced and immediately after offset of the light, electrons are fed via the NDH complex into the PQ pool [30]. The chlorophyll fluorescence level increases because the plastoquinol is in equilibrium with the plastoquinone molecules at the acceptor side of PSII. An increase of  $F_0'$  indicates the reduction of the primary quinone acceptor  $Q_A$  by the highly reduced plastoquinone pool. The rise of  $F_0'$  after illumination with actinic light was followed to test for an enhanced PTOX activity in the CRTI-lines. Figure 3.8 shows that, in the absence of the PTOX inhibitor octyl gallate, the  $F_0'$  rise was clearly visible in the wt, while it was much lower in the CRTI-line 14 and completely suppressed in line 11. The  $F_0'$  rise was restored in both CRTI-lines by the addition of octyl gallate. This shows that, after exposure to actinic light, the PQ pool is more oxidized in the dark in the CRTI-lines compared to wt. Infiltration of the leaves with octyl gallate had no effect on the  $F_v/F_m$  values (data not shown). The  $F_0'$  rise after illumination shows qualitatively the re-reduction of the PQ pool via the NDH complex or via a different metabolic route.

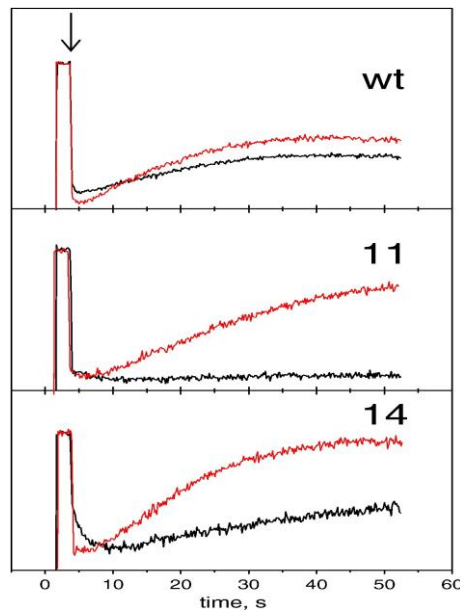


**Figure 3.8**  $F_0'$  rise after illumination with actinic light in leaves from wt and the CRTI-lines 11 and 14. Leaves were vacuum-infiltrated with water (black line) or with 50  $\mu\text{M}$  octyl gallate (red line) and dark-adapted on damped tissue paper for 3 h. Then they were illuminated with red actinic light ( $I = 825 \mu\text{mol quanta m}^{-2} \text{s}^{-1}$ ) for 10 min. After 10 min, the measuring light was set on, the actinic light was switched off (arrow) and the  $F_0'$  rise was followed. Typical traces, each from an individual leaf, are shown.

We performed as a second test thermoluminescence measurements to probe the reduction of the plastoquinone pool in the dark and to demonstrate further that the PTOX activity was higher in the two CRTI-lines than in the wt. As shown in figure 3.9, leaves of the CRTI-lines showed a very different profile of the luminescence emission after three single turnover flashes than the wild-type. The thermoluminescence curve of wt could be fitted by two bands, the first with a temperature maximum between 25-30°C, characteristic of the B-band ( $S_{2/3}Q_B^-$  recombination, with  $S_{2/3}$  being oxidation states of the Mn cluster and  $Q_B$  being the secondary quinone electron acceptor of PSII) [31], and the second band with a temperature maximum at about 45°C, the so-called afterglow band (AG-band) [32]. The afterglow band is detected in samples in which cyclic electron flow is active [33], so that the PQ pool becomes reduced in the dark. The intensity of the AG-band relative to the B-band is highest after the third excitation flash [34]. While the AG-band was clearly visible in the wt, it was suppressed in the two CRTI-lines (figure 3.9) indicating that the increased level and activity of PTOX does not allow the accumulation of  $PQH_2$  in the dark.

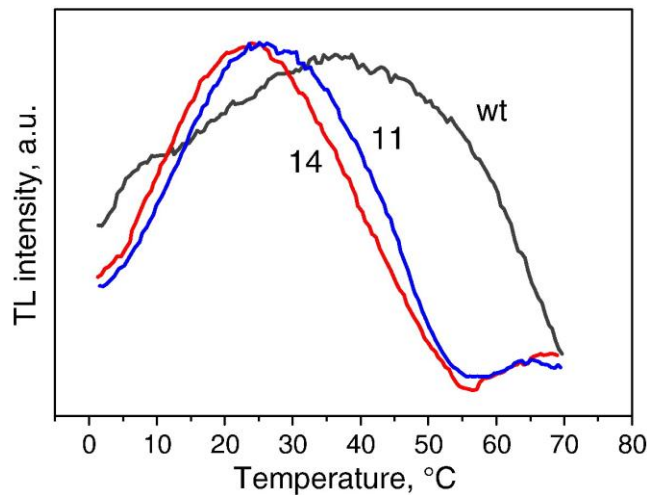


**Figure 3.9** Thermoluminescence measurements of dark-adapted leaves. Black line: wild-type; blue: CRTI line 11; red: CRTI line 14. Samples were excited by three single turnover flashes spaced with 1 s interval.

### 3.3.4 Cyclic electron flow in the CRTI-lines

Since the lack of the AG-band in the CRTI-lines indicates a low re-reduction of the PQ pool in the dark and since this is interpreted to reflect the activity of the cyclic electron flow in the light [33], we tested the activity of cyclic electron flow in the CRTI-lines compared to wt. Cyclic electron flow operates via two different routes, one involving a plastoquinone reductase which is homologous to the mitochondrial complex I, the so-called NDH complex, and the other via a putative ferredoxin-quinone reductase, feeding electrons

directly into the cytochrome  $b_6f$  complex, the so-called PGRL1/PGR5-dependent pathway [35] (for a recent review see Johnson, [36]). Cyclic electron flow may be affected in the insertion lines because PTOX may compete with the cytochrome  $b_6f$  complex for the substrate PQH<sub>2</sub>.

Figures 3.10 and 3.11 show absorption measurements of leaves at 830 nm which are indicative for the oxidation state of P<sub>700</sub>. In figure 3.10, the maximum signal of P<sub>700</sub><sup>+</sup> was probed for each leaf with far-red light which preferentially excites PSI. The far red illumination was followed by illumination with increasing intensities of actinic red light and the maximum level of P<sub>700</sub><sup>+</sup> formation was plotted for each light intensity. As shown in Figure 3.10, the extent of P<sub>700</sub> oxidation in the wild-type was slightly lower at a given light intensity than in the CRTI-lines 11 and 14. Even at the highest light intensity, the signal of P<sub>700</sub><sup>+</sup> was lower than the value obtained with far-red light. The difference between the wt and the CRTI-lines was small but significant. This indicates active cyclic electron flow to take place in wt leaves in contrast to leaves from the CRTI-lines. A lower extent of P<sub>700</sub> formation at high light intensities may alternatively be explained by charge recombination events taking place in the reaction centre of PSI from wt and not in those from the CRTI-lines. To support our hypothesis that the lower extent of P<sub>700</sub> oxidation was caused by cyclic electron flow, we followed the kinetics of P<sub>700</sub> oxidation by far-red light in wt and the CRTI-lines (Figure 3.11). This method shows the activity of cyclic flow upon short illumination times and not during steady state conditions. In the CRTI-lines, the oxidation of P<sub>700</sub> by far-red illumination was faster than in the wt, further demonstrating that fewer electrons were available for reducing P<sub>700</sub><sup>+</sup> and that thus cyclic flow was suppressed in these lines.

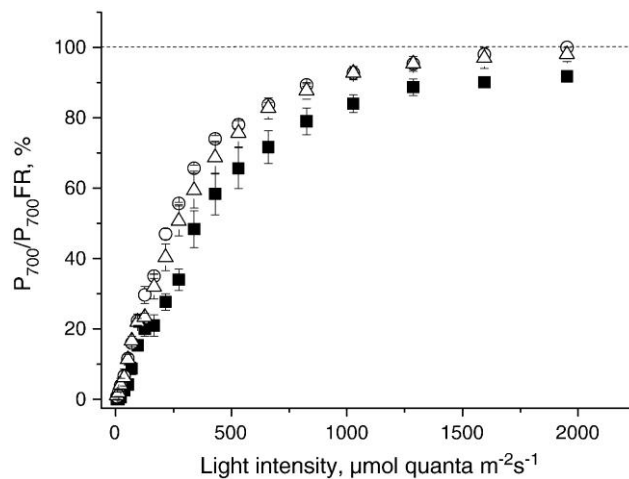


**Figure 3.10** Dependence of PSI oxidation on the intensity of actinic light. Leaves from wt (filled squares), CRTI line 11 (circles) and CRTI line 14 (triangles) were illuminated at 120  $\mu\text{mol quanta m}^{-2} \text{s}^{-1}$  for at least 1 h and then dark-adapted for 15 min prior to the measurements. Leaves were first illuminated with far red light (FR) to obtain the maximum signal corresponding to P<sub>700</sub><sup>+</sup> formation (n = 4–6  $\pm$  SE).

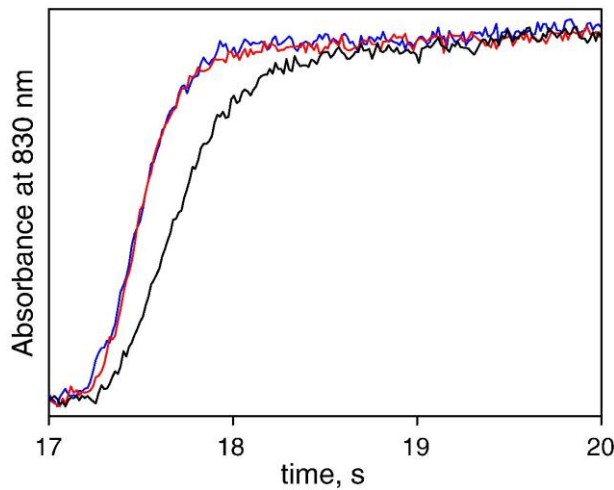


**Figure 3.11** PSI oxidation was probed by far-red illumination in wt and CRTI-lines 11 and 14. Plants were dark-adapted for 10 min, then preilluminated for 3 min with red light ( $I = 600 \mu\text{mol quanta m}^{-2} \text{s}^{-1}$ ). After the preillumination the  $P_{700}$  measurement with the DUAL-PAM was started using the following illumination protocol: 10 s dark, 5 s actinic red light ( $I = 600 \mu\text{mol quanta m}^{-2} \text{s}^{-1}$ ), 2 s dark, 17 s far-red light (highest intensity of the DUAL-PAM). Only the first seconds after onset of far-red light are shown. The amplitudes of the signals were normalized to the signal size of the wild-type. Black: wt, blue: line 11, red: line 14. Typical traces are shown.

### 3.4 Discussion

Here we show that the constitutive expression of the bacterial carotene desaturase CRTI in addition to the endogenous desaturases leads to a higher susceptibility of PSII to photodamage (table 3.1) and to an increased level and activity of PTOX (figures 3.6-9). The increase in PTOX activity causes a higher yield of  $\text{O}_2^{\bullet-}/\text{H}_2\text{O}_2$  formation (figures 3.5 and 3.6; table 3.2). In contrast to these results, PTOX has been proposed previously to act as a safety valve keeping the PQ pool oxidized and avoiding thereby photooxidative damage [37]. Especially under harsh environmental conditions like in alpine plants [38,39], plants exposed to extreme temperatures [40, 41] or to high salinity [42], the PTOX protein level is increased and PTOX seems to play an important role in allowing the plant to adapt to the stress condition. However, in model plants like *Arabidopsis* and Tobacco grown under standard conditions, the role of PTOX is less clear. Overexpression of PTOX in *Arabidopsis* did not improve the susceptibility of the plants against photoinhibition [43] or even triggered photoinhibition in tobacco [28,29].

The question arises whether the increase in  $\text{O}_2^{\bullet-}/\text{H}_2\text{O}_2$  generation as shown here and in tobacco overexpressing PTOX [28] or the suppression of cyclic electron flow (figures 3.10 and 3.11) is responsible for increased photodamage. As shown in table 3.2, most of  $\text{O}_2^{\bullet-}/\text{H}_2\text{O}_2$  are generated at acceptor side of PSI in the Mehler reaction since the cytochrome  $b_6f$

inhibitor DNP-INT inhibits approximately 60% of the ROS formation in the CRTI-lines. We attribute the proportion that is still detectable in the presence of DNP-INT to the action of PTOX since the PTOX inhibitor octyl gallate has a stronger effect on the CRTI-lines than on wt (figure 3.6; table 3.2). At present, we cannot decide whether PTOX itself produces reactive oxygen species as a side product of the reduction of oxygen or whether reactive oxygen species are produced by the semiplastoquinone  $PQH^{\bullet-}$  or, *in vivo*, by a higher activity of the Mehler reaction. The difference in the signal size between the signals obtained in the absence and in the presence of octyl gallate corresponds to about  $3 \mu\text{mol H}_2\text{O}_2 \text{ mg Chl}^{-1}\text{h}^{-1}$ . It is questionable whether this amount is sufficient for triggering photoinhibition of PSII. As shown in figures 3.10 and 3.11, cyclic electron flow is suppressed in the CRTI-lines. Cyclic electron flow protects against photodamage of PSI since it keeps its acceptor side oxidized [1,44-46]. Furthermore, it participates also in the photoprotection of PSII by 1) contributing to the generation of the proton gradient across the thylakoid membrane and thereby to NPQ and by 2) limiting the  $\text{O}_2^{\bullet-}$  generation at the acceptor side of PSI.  $\text{O}_2^{\bullet-}$  generated at PSI has been shown to damage PSII [4]. Since the amount of  $^1\text{O}_2$  produced is not increased in the CRTI-lines, we suggest that the higher photodamage is caused by both, the suppression of the cyclic flow and the increased  $\text{O}_2^{\bullet-}/\text{H}_2\text{O}_2$  level.

Arabidopsis mutants that lack PTOX show a variegated phenotype and were called *immutans* (*im*) with the white plastids accumulating phytoene in leaf sectors [16,17,47,48]. Mutants of cyclic electron flow defective in the activity of NDH complex or/and lacking PGR5, a thylakoid protein involved in cyclic electron transport, rescued *im* variegation [49]. This indicates that the redox state of the PQ pool has to be very well controlled to allow optimal photosynthetic electron transport activities *in vivo*. A too reduced PQ pool as in the case of *im* with functional cyclic flow renders leaves more susceptible to photoinhibition. It has been shown recently using the *ghost* mutant in tomato which lacks PTOX that PTOX modulates the balance between linear and cyclic flow rather than acting as a safety valve [50]. These authors suggest that the concerted action of the NDH complex and PTOX is important to set the redox poise in the thylakoid membrane. In the CRTI-lines, the amount of PTOX is increased while the amount of the NDH complex is unchanged. The PQ pool is held so oxidized that less electron donors for cyclic flow are available, a condition which facilitates photoinhibition. It is unknown whether PTOX oxidizes plastoquinol independent of the  $\text{PQH}_2$  localization in the thylakoid membrane or whether it oxidizes  $\text{PQH}_2$  in well-defined regions of the membrane. PTOX has been shown to be localized in the stroma lamellae [51] and may

therefore preferentially oxidize PQH<sub>2</sub> implicated in cyclic electron flow. In analogy to the supercomplex found in state 2 in *Chlamydomonas* [52], a tight coupling between cytochrome b6f complex and PSI may also be required in higher plants for cyclic electron flow to operate.

It still remains to be clarified why the constitutive expression of CRTI exerts such profound effects on PTOX levels and activity and consequently on plastoquinone redox-homeostasis. It is conceivable that two pathways of carotene desaturation, the endogenous pathway via PDS and the added pathway via CRTI, are in competition. CRTI is, in fact, active in chloroplasts as has been shown several times including this work: norflurazon treatment blocking PDS allows carotenoids to form through CRTI (see Supplementary Information; figure S3). Pigment analysis showed that the pigment composition in the CRTI-line 14 was not altered by norflurazon. Assuming that the PDS route is kept less “busy” by the additional catalysis of CRTI, is likely that all the measured consequences need to be traced back to the mechanistic differences existing between the two, which will be better investigated in the final chapter (parag. 5.3).

In conclusion, our study on *Arabidopsis* plants that constitutively express CRTI provides evidence that the PTOX level is crucial for the balance between the different pathways of photosynthetic electron flow –linear, cyclic, Mehler reaction. The increase in the amount and activity of PTOX leads to a perturbation of the redox state of the photosynthetic electron transport chain and seems to be responsible for the increased susceptibility to light while the plants seem to cope well with the alteration in the carotenoid composition as seen by the small effects on maximum NPQ and the unchanged level of <sup>1</sup>O<sub>2</sub> generation.

## Supplementary information

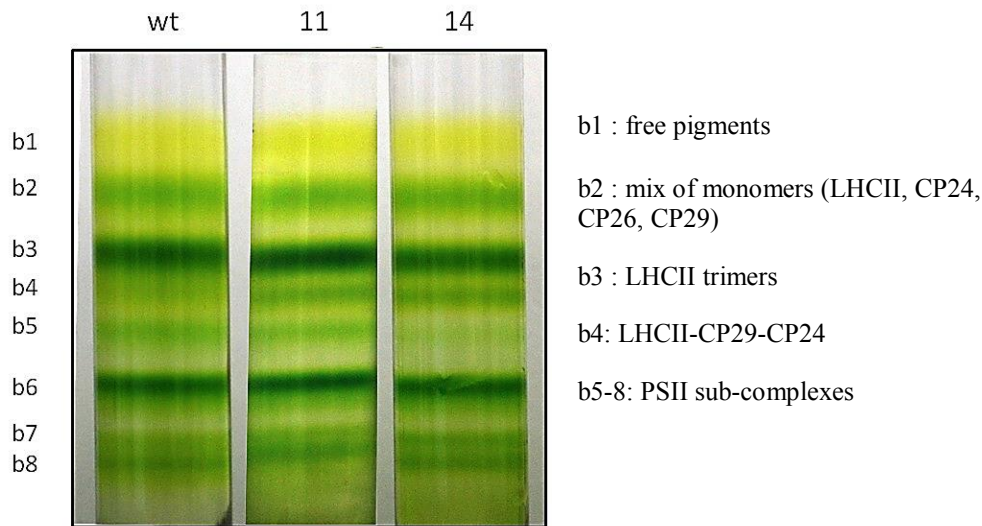


**Figure S 1** Protein complexes of PSII-enriched membrane fragments from wt, 11 and 14. Sucrose density gradient profiles of solubilized PSII particles from wt, 11 and 14. Band assignment is based on the absorption spectra of the single bands according to P. Dainese, R. Bassi, *J. Biol. Chem.* 266, (1991), p. 8136–8142.

Preparation of PSII-enriched membrane fragments (PSII particles) was carried according to Berthold *et al.* (*FEBS Lett.* 134 (1981); p. 231-234) with few modifications. Thylakoid membranes were left on ice in the dark without stirring for 45 min to promote membrane stacking before dilution with half the volume of 7.5 % (v/v) Triton X-100 in stacking medium to give a final detergent concentration of 2.5 %. The sample was left in the dark on ice for 1 h and given occasional gentle inversion to help membrane digestion. The samples were centrifuged at 30.000 g, 4C for 30 min. The pellet was resuspended in 2 mM EDTA (pH 7.5) and again centrifuged for 30 min at 30,000 g. The final pellet was resuspended in 10 mM HEPES, pH 7.5 to a final chl concentration of 1 mg ml<sup>-1</sup>.

*Fractionation of PSII particles by sucrose gradient.* PSII particles were solubilized for 30 min on ice with dodecyl- $\alpha$ -D-maltoside, 10 mM HEPES, pH 7.5. The final detergent concentration of 0.6% with 1 mg Chl ml<sup>-1</sup>. Solubilized samples were then fractionated by ultracentrifugation in a 0.1–1 M sucrose gradient containing 0.06%  $\alpha$ -DM, 10 mM HEPES pH 7.5. The centrifugation was carried out for 16 h at 263,000 g, 4C.

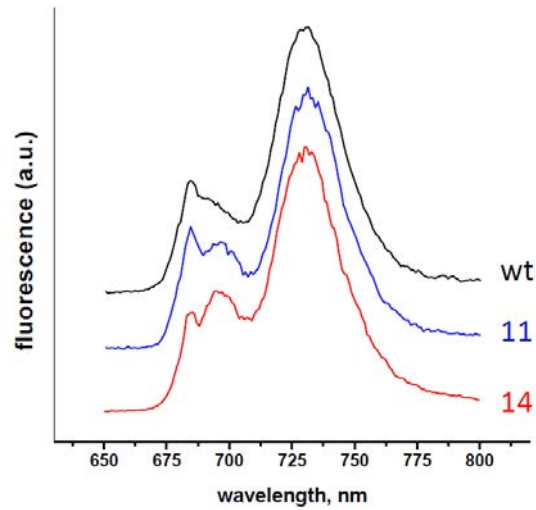


**Figure S 2** 77K fluorescence emission spectra of thylakoids membranes from wt, and the CrtI insertion lines 11 and 14. Fluorescence was excited at 435 nm, slit width for emission monochromator: 2.5 nm. The samples contained 5  $\mu\text{g Chl}^{-1}$ .

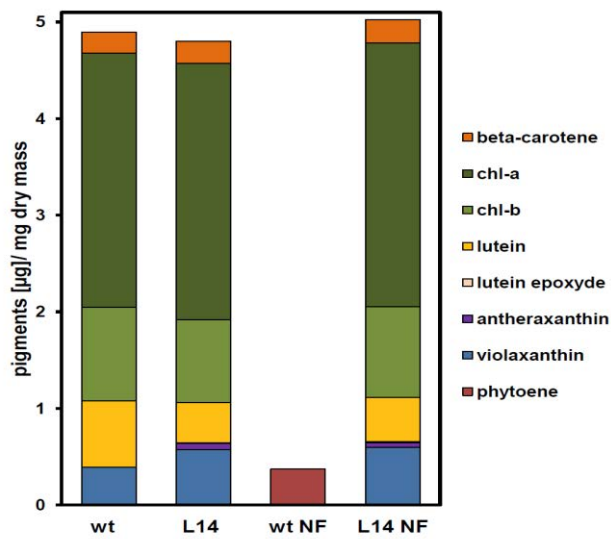


**Figure S 3** Pigment analysis from 7 days old Arabidopsis plantlets grown in the absence (control) or in the presence (NF) of 1  $\mu\text{M}$  norflurazon.

## References

- [1] SONOIKE, K. Photoinhibition of photosystem I. *Physiol. Plant.*, 2011, 142, p. 56-64.
- [2] VASS, I. Molecular mechanisms of photodamage in the Photosystem II complex, *Biochim. Biophys. Acta*, 2012, 1817, p. 209-217.
- [3] KRIEGER-LIZSKAY A., FUFUZAN, C., and TREBST, A. Singlet oxygen production in photosystem II and related protection mechanism. *Photosynth. Res.*, 2008, 98, p. 551-564.
- [4] KRIEGER-LISZKAY, A., KÓS, P.B., and HIDEG, E. Superoxide anion radicals generated by methylviologen in photosystem I damage photosystem II. *Physiol. Plant.*, 2011, 142, p. 17-25.
- [5] BAKER, N.R., HARBINSON, J., and KRAMER, D.M. Determining the limitations and regulation of photosynthetic energy transduction in leaves. *Plant Cell Environ.*, 2007, 30, p. 1107-1125.
- [6] ROCHAIX, J.D. Regulation of photosynthetic electron transport. *Biochim. Biophys. Acta*, 2011, 807, p. 375-383.
- [7] MÜLLER, P., LI, X.P., and NIYOGI, K.K. Non-photochemical quenching, A response to excess light energy. *Plant Physiol.*, 2001, 125, p. 1558-1566.
- [8] POGSON, B.J., NIYOGI, K.K., BJÖRKMAN, O., and DELLAPENNA, D. Altered xanthophyll compositions adversely affect chlorophyll accumulation and non-photochemical quenching in Arabidopsis mutants. *Proc Natl Acad Sci USA*, 1998, 95, p. 13324-13329.
- [9] POGSON, B.J., and RISSLER, H.M. Genetic manipulation of carotenoid biosynthesis and photoprotection. *Philos. Trans. R. Soc. Lond. B. Biol. Sci.*, 2000, 355, p. 1395-1403.
- [10] ILIOAIA, C., JOHNSON, M.P., LIAO, P.N. PASCAL, A.A., VAN GRONDELLE, R., WALLA, P.J., RUBAN, A.V., and ROBERT, B. Photoprotection in plants involves a change in lutein 1 binding domain in the major light-harvesting complex of photosystem II, *J. Biol. Chem.*, 2011, 286, p. 27247-27254.
- [11] LOKSTEIN, H., TIAN, L., POLLE, J. E., and DELLAPENNA, D. Xanthophyll biosynthetic mutants of Arabidopsis thaliana: altered nonphotochemical quenching of chlorophyll fluorescence is due to changes in Photosystem II antenna size and stability, *Biochim. Biophys. Acta*, 2002, 1553, p. 309-319.
- [12] SCHAUB, P., AL-BABILI, S., DRAKE, R., and BEYER, P. Why is golden rice golden (yellow) instead of red? *Plant Physiol.*, 2005, 138, p. 441-450.

- [13] DIRETTO, G., AL-BABILI, S.R., TAVAZZA, P., PAPACCHIOLI, V., BEYER, P. and G. GIULIANO. Metabolic Engineering of Potato Carotenoid Content through Tuber-Specific Overexpression of a Bacterial Mini-Pathway. *PLoS One*, 2007, 2, e350.
- [14] MAYER, M.P., BEYER, P., and KLEINIG, H. Quinone compounds are able to replace molecular oxygen as terminal electron acceptor in phytoene desaturation in chromoplasts of *Narcissus pseudonarcissus* L. *Eur. J. Biochem.*, 1990, 191, p. 359-363.
- [15] NORRIS, S.R., BARRETTE, T.R., and DELLAPENNA, D. Genetic dissection of carotenoid synthesis in *Arabidopsis* defines plastoquinone as an essential component of phytoene desaturation. *Plant Cell*, 1995, 7, p. 2139–2149.
- [16] CAROL, P., STEVENSON, D., BISANZ, C., BREITENBACH, J., SANDMANN, G., MACHE, R., COUPLAND, C., and KUNTZ, M. Mutations in the *Arabidopsis* gene IMMUTANS cause a variegated phenotype by inactivating a chloroplast terminal oxidase associated with phytoene desaturation. *Plant Cell*, 1999, 11, p. 57-68.
- [17] WU, D., WRIGHT, D.A., WETZEL, C., VOYTAS, D.F., RODERMEL, S. The IMMUTANS variegation locus of *Arabidopsis* defines a mitochondrial alternative oxidase homolog that functions during early chloroplast biogenesis. *Plant Cell*, 1999, 11, p. 43-55.
- [18] JOSSE, E.M., SIMKIN, A.J., GAFFÉ, J., LABOURÉ, A.M., KUNTZ, M., Carol, P. A plastid terminal oxidase associated with carotenoid desaturation during chromoplast differentiation. *Plant Physiol.*, 2000, 123, p. 1427-1436.
- [19] NASHILEVITZ, S., MELAMED-BESSUDO, C., IZKOVICH, Y., ROGACHEV, I., S., OSORIO, ITKIN, M., ADATO, A., PANKRATOV, I., HIRSCHBERG, J., FERNIE, A.R., WOLF, S., USADEL, B., LEVY, A.A., RUMEAU, D., and AHARONI, A. An orange ripening mutant links plastid NAD(P)H dehydrogenase complex activity to central and specialized metabolism during tomato fruit maturation. *Plant Cell*, 2010, 22, p. 1977-1997.
- [20] SCHAUB, P., YU, Q., GEMMECKER, S., POUSSIN-COURMONTAGNE, P., MAILLIOT, J., MCEWEN, A.G., GHISLA, S., AL-BABILI, S., CAVARELLI, J. and BEYER, P. On the structure and function of the phytoene desaturase CRTI from *Pantoea ananatis*, a membrane-peripheral and FAD-dependent oxidase/isomerase. *PLoS One*, 2012, 7, e39550.
- [21] DUCRUET, J.M., and MIRANDA, T. Graphical and numerical analysis of thermoluminescence and fluorescence  $F_0$  emission in photosynthetic material. *Photosynth. Res.*, 1992, 33, p. 15-27.
- [22] ROACH, T. and KRIEGER-LISZKAY, A. The role of the PsbS protein in the protection of photosystems I and II against high light in *Arabidopsis thaliana*. *Biochim. Biophys. Acta*, 2012, 1817, p. 2158-2165.
- [23] HIDEG, E., DEÁK, Z., HAKALA-YATKIN, M., KARONEN, M., RUTHERFORD, A.W., TYYSTJÄRVI, E., VASS, I., and KRIEGER-LISZKAY, A. Pure forms of the

- singlet oxygen sensors TEMP and TEMPD do not inhibit Photosystem II. *Biochim. Biophys. Acta*, 2011, 1807, p. 1658-1661.
- [24] ANDRIZHIYEVSKAYA, E.G., CHOJNICKA, A., BAUTISTA, J.A., DINER, B.A., VAN GRONDELLE, R., and DEKKER, J. P. Origin of the F685 and F695 fluorescence in photosystem II. *Photosynth. Res.*, 2005, 84, p. 173-180.
- [25] ASADA, K., KISO, K., and YOSHIKAWA, K. Univalent reduction of molecular oxygen by spinach chloroplasts on illumination. *J. Biol. Chem.*, 1974, 249, p. 2175-2181.
- [26] MUBARAKSHINA, M.M., and IVANOV, B.N. The production and scavenging of reactive oxygen species in the plastoquinone pool of chloroplast thylakoid membranes. *Physiol. Plant.*, 2010, 140, p. 103-110.
- [27] POSPÍŠIL, P. Molecular mechanisms of production and scavenging of reactive oxygen species by photosystem II. *Biochim. Biophys. Acta*, 2012, 1817, p. 218-231.
- [28] HEYNO, E., GROSS, C.M., LAUREAU, C., CULCASI, M., PIETRI, S., and KRIEGER-LISZKAY, A. Plastid alternative oxidase (PTOX) promotes oxidative stress when overexpressed in tobacco. *J. Biol. Chem.*, 2009, 284, p. 31174-31180.
- [29] AHMAD, N., MICHOUX, F., and NIXON, P.J. Investigating the production of foreign membrane proteins in tobacco chloroplasts: expression of an algal plastid terminal oxidase. *PLoS One*, 2012, 7, e41722.
- [30] RUMEAU, D., BÉCUWE-LINKA, N., BEYLY, A., LOUWAGIE M, GARIN J, and PELTIER G. New subunits NDH-M, -N, and -O, encoded by nuclear genes, are essential for plastid Ndh complex functioning in higher plants. *Plant Cell*, 2005, 17, p. 219-232.
- [31] RUTHERFORD, A.W., CROFTS, A.R., and INOUE, Y. Thermoluminescence as a probe of photosystem II photochemistry-the origin of the flash-induced glow peaks. *Biochim. Biophys. Acta*, 1982, 682, p. 457-465.
- [32] DUCRUET, J.M. Pitfalls, artefacts and open questions in chlorophyll thermoluminescence of leaves or algal cells. *Photosynth. Res.*, 2013, 115, p. 89-99.
- [33] PEEVA, V.N., TÓTH, S.Z., CORNIC, G., and DUCRUET, J.M. Thermoluminescence and P700 redox kinetics as complementary tools to investigate the cyclic/chlororespiratory electron pathways in stress conditions in barley leaves. *Physiol. Plant.*, 144, 2012, p. 83-97.
- [34] KRIEGER, A., BOLTE, S., DIETZ, K. J., and DUCRUET, J. M. Thermoluminescence studies on the facultative CAM plant *Mesembryanthemum crystallinum*. *Planta*, 1998, 205, p. 587-594.
- [35] HERTLE, A.P., BLUNDER, T., WUNDER, T., PESARESI, P., PRIBIL, M., ARMBRUSTER, U., and LEISTER, D. PGRL1 is the elusive ferredoxin-plastoquinone reductase in photosynthetic cyclic electron flow. *Mol. Cell*, 2013, 49, p. 511-523.

- [36] JOHNSON, G.N. Reprint of: physiology of PSI cyclic electron transport in higher plants, *Biochim. Biophys. Acta*, 2011, 1807, p. 906-911.
- [37] RUMEAU, D., PELTIER, G., and L. COURNAC. Chlororespiration and cyclic electron flow around PSI during photosynthesis and plant stress response. *Plant Cell Environ.*, 2007, 30, p. 1041-1051.
- [38] STREB, P., JOSSE, E-M., GALLOUËT, E., BAPTIST, F., KUNTZ, M., CORNIC, G. Evidence for alternative electron sinks to photosynthetic carbon assimilation in the high mountain plant species *Ranunculus glacialis*. *Plant Cell Environ.*, 2005, 28, p. 1123-1135.
- [39] C., LAUREAU, DE PAEPE, R., LATOUCHE, G., MORENO-CHACÓN, M., FINAZZI, G., KUNTZ, M., CORNIC, G., STREB, P. Plastid terminal oxidase (PTOX) has the potential to act as a safety valve for excess excitation energy in the alpine plant species *Ranunculus glacialis* L. *Plant Cell Environ.* (2013) (in press) doi: 10.1111/pce.12059.
- [40] QUILES, M.J. Stimulation of chlororespiration by heat and high light intensity in oat plants. *Plant Cell Environ.*, 2006, 29, p. 1463-1470.
- [41] SAVITCH, L.V., IVANOV, A.G., KROL, M., SPROTT, D.P., ÖQUIST, G., and HUNER, N.P.A. Regulation of energy partitioning and alternative electron transport pathways during cold acclimation of lodgepole pine is oxygen dependent. *Plant Cell Physiol.*, 2010, 51, p. 1555-1570.
- [42] STEPIEN, P., and JOHNSON, G.N. Contrasting responses of photosynthesis to salt stress in the glycophyte *Arabidopsis* and the halophyte *Thellungiella*: role of the plastid terminal oxidase as an alternative electron sink. *Plant Physiol.*, 2009, 149, p. 1154-1165.
- [43] ROSSO, D., IVANOV, A.G., FU, A., GEISLER-LEE, J., HENDRICKSON, L., GEISLER, M., STEWART, G., KROL, M., HURRY, V., RODERMEL, S.R., MAXWELL, D.P., and HÜNER, N.P. IMMUTANS does not act as a stress-induced safety valve in the protection of the photosynthetic apparatus of *Arabidopsis* during steady-state photosynthesis. *Plant Physiol.*, 2006, 142, p. 574-585.
- [44] MUNEKAGE, Y., HOJO, M., MEURER, J., ENDO, T., TASAKA, M., SHIKANAI, T. PGR5 is involved in cyclic electron flow around photosystem I and is essential for photoprotection in *Arabidopsis*. *Cell*, 2002, 110, p. 361-371.
- [45] MUNEKAGE, Y.N., GENTY, B., and PELTIER, G. Effect of PGR5 impairment on photosynthesis and growth in *Arabidopsis thaliana*. *Plant Cell Physiol.*, 2008, 49, p. 1688-1698.
- [46] JOLIOT, P., and JOHNSON, G.N. Regulation of cyclic and linear electron flow in higher plants. *Proc. Natl. Acad. Sci. U.S.A.*, 2011, 108, p. 13317-13322.
- [47] WETZEL, C.M., JIANG, C.Z., MEEHAN, L.J., VOYTAS, D.F., RODERMEL, S.R. Nuclear-organelle interactions: the immutans variegation mutant of *Arabidopsis* is plastid autonomous and impaired in carotenoid biosynthesis. *Plant J.*, 1994, 6, p. 161-175.

- [48] FOUOREE, A., PUTARJUNAN, A., KAMBAKAM, S., NOLAN, T., FUSSELL, J., POGORELKO, G., and RODERMEL, S. The mechanism of variegation in *Immutans* provides insights into chloroplast biogenesis. *Front. Plant. Sci.*, 2012, 3, p. 1-10.
- [49] OKEGAWA, Y., KOBAYASHI, Y., and SHIKANAI, T. Physiological links among alternative electron transport pathways that reduce and oxidize plastoquinone in *Arabidopsis*. *Plant J.*, 2010, 63, p. 458-468.
- [50] TROUILLARD, M., SHAHBAZI, M., MOYET, L., RAPPAPORT, F., JOLIOT, P., KUNTZ, M., and FINAZZI, G. Kinetic properties and physiological role of the plastoquinone terminal oxidase (PTOX) in a vascular plant. *Biochim. Biophys. Acta*, 2012, 1817, p. 2140-2148.
- [51] LENNON, A.M., PROMMEENATE, P., and NIXON, P.J. Location, expression and orientation of the putative chlororespiratory enzymes, Ndh and IMMUTANS, in higher-plant plastids. *Planta*, 2003, 218, p. 254-260.
- [52] IWAI, M., TAKIZAWA, K., TOKUTSU, R., OKAMURO, A., TAKAHASHI, Y., and J. MINAGAWA. Isolation of the elusive supercomplex that drives cyclic electron flow in photosynthesis. *Nature*, 2010, 464, p. 1210-1213.



**CHAPTER 4 CAROTENOTETRAPYRROLE DYADS  
MIMIC PHOTOSYNTHETIC TRIPLET-TRIPLET  
ENERGY TRANSFER<sup>1</sup>**



### Summary of the work

As already mentioned, advances in chemical synthesis have made possible to synthesize biomimetic systems made up of a small number of chromophores (dyads or triads) arranged in a well-defined three-dimensional structure. These constructs are now capable of reproducing a number of features of their natural counterparts such as fluorescence quenching of the chlorophyll-like molecule, singlet-singlet and triplet-triplet energy transfer (see *e.g.* Gust *et al.*, 1992; Berera *et al.*, 2006; 2007) thanks to a precise engineering of the interactions between the components.

Carotenoids naturally present in photosynthetic pigment-binding proteins rapidly quench chlorophyll triplets by triplet-triplet energy transfer. This generates low-energy carotenoid triplet states which cannot sensitize singlet oxygen production and which decay to the ground state within a few  $\mu\text{s}$  by a non-radiative process. In anoxygenic organisms such as purple bacteria, the triplet-triplet transfer is in the tens of nanoseconds range, while in plants, where the chances to sensitize oxygen singlet from chlorophyll triplet are much higher, it is ultrafast (the chlorophyll triplet state is actually quenched faster than it is formed). It was recently suggested that the mechanisms underlying the triplet transfer to the carotenoid are fundamentally different in these two classes of organisms. To address this question, we studied triplet energy transfer from a porphyrin moiety to a linked carotenoid in a series of synthetic carotenoporphyrin and carotenophthalocyanine molecule. In these dyads, the cascade of events after photon absorption is the following (Gust *et al.*, 1992; Berera *et al.*, 2006):



where *Car* is for carotenoid, *P* is for porphyrin or phthalocyanine, *isc* and *tt* are intersystem crossing and triplet-triplet transfer respectively. The triplet-triplet energy transfer rate depends on the nature of the linkage between the carotene and the tetrapyrrole.

In this work the mechanisms of triplet-triplet energy transfer of two different dyads have been investigated by transient absorption, resonance Raman and step-scan time resolved FTIR spectroscopies. Our aim was to better characterize the dynamic and the

spectroscopic features of the triplets states in a carotenophthalocyanine and a carotenoporphyrin dyad in which the carotenoid and the tetrapyrrole are differently linked generating a dyad with highly or loosely coupled components, respectively.

<sup>1</sup>*This chapter is based on the following work:*

GALZERANO, D., WONGCARTER, K., MOORE, A.L., ALEXANDRE, M., KENNIS, J., MÉNDEZ-HERNÁNDEZ, D., MUJICA, V., PILLAI, S., LIDDELL, P.A., KODIS, G., GUST, D., VAN GRONDELLE, R., LEIBL, W., MOORE, T.A., and ROBERT, B. *To be submitted*

## 4.1 Introduction

During the first steps of the photosynthetic process, the absorption of photons by antenna pigment-protein complexes and the subsequent transfer of the excitation energy to the reaction centers are both intimately linked with the potential production of dangerous oxidative species. Although its yield is low, production of (bacterio)chlorophyll ((B)Chl) triplet excited states by intersystem crossing from (B)Chls excited singlet states is a major source of singlet oxygen in photosynthetic organisms, one of the most dangerous chemical species for living organisms (Foote, 1976). In photosynthetic pigment-protein complexes, this sensitization reaction is precluded by transfer of the triplet excited state from (B)Chls to carotenoid molecules, which feature a triplet state energy below that of singlet oxygen. This quenching reaction reduces the lifetime of the (B)Chl triplet state by many orders of magnitudes (Monger *et al.*, 1976; Mathis *et al.*, 1979).

In the light-harvesting (LH) proteins from most (anoxygenic) purple bacteria, the triplet-triplet (T-T) transfer from BChl to carotenoid molecules has a characteristic lifetime in the nanosecond range (Angerhofer *et al.*, 1995; Bittl *et al.*, 2001). By contrast, in light-harvesting complexes (LHC) from oxygenic organisms, we recently showed that this transfer is ultrafast, the chlorophyll triplet state decaying faster than it is formed (Gall *et al.*, 2011). The mechanisms underlying this ultrafast T-T energy transfer, which was proposed to represent an adaptation of oxygenic photosynthetic organisms to their oxygen-rich environment, are not yet fully understood. Some relevant observations are that when ultrafast T-T energy transfer occurs between chlorophyll and carotenoid molecules, the presence of the triplet state on the carotenoid has an usually strong influence on the chlorophyll  $Q_y$  electronic transition, and the decay of this perturbation decays with the carotenoid lifetime (Van der Vos *et al.*, 1991; Angerhofer *et al.*, 1995; Peterman *et al.*, 1995). Moreover, the carotenoid triplet state exhibits an abnormal resonance Raman signature, suggesting a partial loss of its typical triplet state character. Finally, when time-resolved infrared absorption experiments were performed on these complexes, clear chlorophyll contributions are observed to decay in parallel with the decay of the carotenoid triplet state. From these observations, it was tentatively proposed that the triplet state could be delocalized over the carotenoid/chlorophyll couple, and thereby shared between these molecules (Gall *et al.*, 2011). Understanding in detail the relationship between photoprotective T-T energy transfer mechanisms and the exposure of the photosynthetic

organism to oxygen is essential in order to extend those mechanisms to reengineered photosynthetic systems where the production of oxygen and therefore the steady state level of oxygen in the membranes would be much higher than current levels.

Over the last three decades, a large numbers of carotenoid/tetrapyrrole synthetic dyads have been designed and synthesized, in which the absorption of a photon is followed by the formation of a triplet state by intersystem crossing at the level of the tetrapyrrole, and subsequent transfer of the tetrapyrrole triplet energy to the carotenoid (Bensasson et al., 1981; Moore et al., 1984; Gust et al., 1985; Gust and Moore, 1991). In these dyads, depending on their precise chemical properties and on the way the tetrapyrrole and the carotenoid molecules are linked, the T-T energy transfer kinetics range from tens of microseconds to the sub-nanosecond range in which the actual T-T energy transfer rate was not determined because intersystem crossing in the tetrapyrrole is the rate limiting step (Bensasson et al., 1981; Moore et al., 1984; Liddell et al., 1986). In this work, we have studied both slow and fast T-T energy transfer in two dyads using a combination of vibrational and transient absorption spectroscopic methods and have found they mimic the dynamics and spectroscopic signatures characteristic of the natural systems.

## 4.2 Methods

*Synthesis.* The synthesis of the carotenophthalocyanine **1** and the phthalocyanine **3** model have been reported previously (Berera et al., 2006). The carotenopurpurin ester **2** and purpurin model **4** were synthesized starting with 5,15-bis(3,5-dimethoxyphenyl)-10-(methyl-3-propenoate)-2,8,12,18-tetrabutyl-3,7,13,17-tetramethylporphyrin, following a published procedure (Gunter & Robinson, 1990). This porphyrin was cyclized to form the purpurin macrocycle, and the purpurin model **4**, before the methyl-ester was hydrolyzed to the carboxylic acid for coupling to a carotenoid benzyl alcohol. The esterification reaction of the purpurin acid and the 7'-apo-7-(4-hydroxymethylphenyl)- $\beta$ -carotene took place via a triazine adduct. The synthesis of the apocarotenoid was based on procedures previously published (Gust et al., 1992).

*Absorption Spectroscopy.* Steady-state absorption spectra were measured on a Shimadzu UV-3101PC UV-vis-NIR spectrometer. The nanosecond-millisecond transient absorption measurements were made with excitation from an optical parametric oscillator driven by the third harmonic of a Nd:YAG laser (Ekspla NT342B). The pulse width was

~4–5 ns, and the repetition rate was 10 Hz. The detection portion of the spectrometer (Proteus) was manufactured by Ultrafast Systems. The instrument response function was ca. 5 ns.

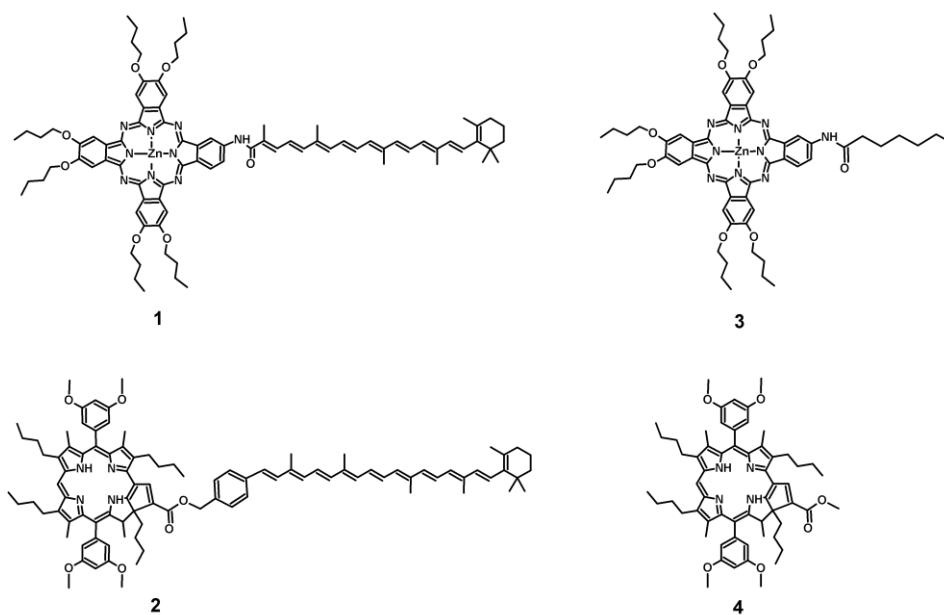
The transient absorption data analysis was carried out using ASUFIT developed in a MATLAB environment (Mathworks Inc.). Evolution-associated-difference spectra (EADS) were obtained by global analysis of the transient absorption data using a kinetic model consisting of sequentially interconverting species, e.g.  $1 \rightarrow 2 \rightarrow 3 \rightarrow \dots$ , where the arrows indicate successive mono-exponential decays with increasing time constants, which can be regarded as the lifetimes of each species. Associated with each species is a lifetime and a difference spectrum. Each EADS corresponds in general to a mixture of states and does not portray the spectrum of a pure state or species. This procedure enables us to describe the evolution of the transient states of the system. The global analysis procedure described here has been extensively reviewed (van Stokkum et al., 2004). Random errors associated with the reported lifetimes obtained from transient absorption measurements were typically  $\leq 5\%$ .

*Resonance Raman.* Resonance Raman spectra were obtained using excitations provided by a 24 W Sabre laser (Coherent, Palo Alto, California), and recorded at room temperature with  $90^\circ$  signal collection using a two stage monochromator (U1000, Jobin Yvon, Longjumeau, France), equipped with a front-illuminated, deep-depleted CCD detector (Jobin Yvon, Longjumeau, France). Low temperature (77K) resonance Raman spectra were recorded using a Helium flow cryostat (Air Liquide, Sassenage, France). Resonance Raman spectra of the ground and triplet state of the carotenoid moiety of the dyads were recorded as extensively described in (Gall et al., 2011).

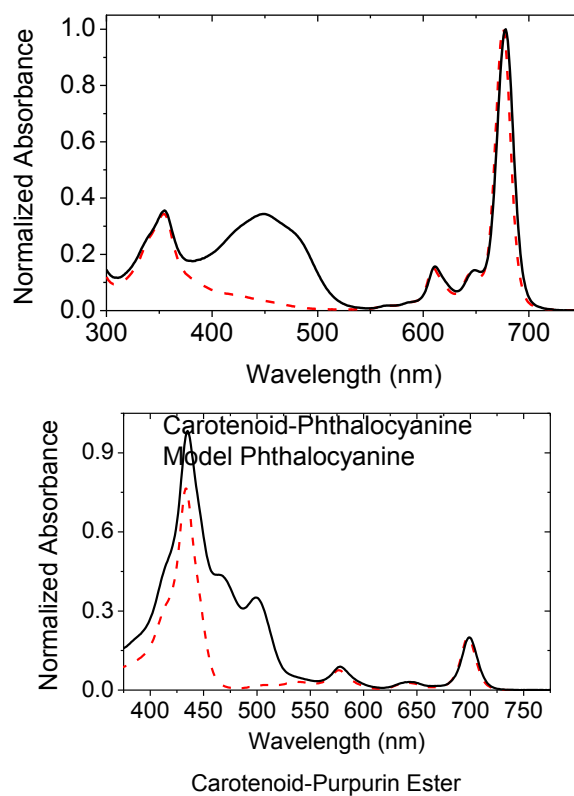
*FTIR.* FTIR difference spectra were recorded at room temperature using a step-scan FTIR spectrometer (Vertex 80V). A global infrared (IR) source and a fast pre-amplified photovoltaic MCT detector (16 MHz, KV 100, Kolmar Technologies) were used. The IR light impinging on the sample was sent through  $1850\text{ cm}^{-1}$  and  $4000\text{ cm}^{-1}$  low-pass filters. The detector signal was recorded with an external digitizer (MI3120; Spectrum, Grosshansdorf, Germany; 10 MS/s, 12 bit) or with the internal digitizer (96 kHz, 24 bit A/D converter). A 10 Hz Nd: YAG laser (5 ns, 100 mJ at 355 nm, Surelite Continuum, Santa Clara, CA) was used to pump an optical parametric oscillator (Surelite Continuum), producing tunable visible light from 400–700 nm, with pulse duration of 5–7 ns. This light

was attenuated to  $\sim 2 \text{ mJ/cm}^2$  (for all excitation wavelengths), weakly focused to a spot of 5 mm in diameter and overlapped with the IR probe beam. The temporal resolution for this set up is 12.5  $\mu\text{s}$  with the internal digitizer and 100 ns with the external digitizer. All the measurements were performed at 10 °C by using a Harrick thermo regulated liquid cell. FTIR difference spectra averaged over 100 ns were too noisy to extract the temporal evolution of the signal. However, averaging these spectra over the 3 first microseconds led to FTIR difference spectra remarkably similar to those recorded at lower time resolution.

*Computational Calculations.* Using Gaussian 09 (Frisch et al., 2009), density functional theory (DFT) calculations were performed at the B3LYP/6-31G(d) level of theory in order to optimize the ground state of the carotenoid dyads (Hehre et al.; 1972;.Becke et al., 1993) All calculations were done in the gas phase.

**A**

**Figure 4.1 A:** Molecular structure of carotenophthalocyanine dyad (1) and model phthalocyanine (3), carotenopurpurin dyad (2) and model purpurin (4).

**B**

**B:** Room temperature electronic absorptions in purpurin model carotenophthalocyanine, dyad 1, (solid line), model phthalocyanine 3 (dash line) on the top and carotenopurpurin, dyad 2, (solid line), model purpurin 4 (dash line) on the bottom.

### 4.3 Results

#### *Carotenophthalocyanine, dyad 1*

In dyad **1**, where a carotenoid having 9 conjugated double bonds is linked to a phthalocyanine by an amide bond (see figure 4.1), excitation of the phthalocyanine at 680 nm is followed by intersystem crossing over the 500 ps phthalocyanine singlet lifetime to yield the phthalocyanine triplet state, which immediately decays by T-T energy transfer to the linked carotenoid (Berera *et al.*, 2007). The phthalocyanine triplet spectrum was not observed as an intermediate between the decay of the phthalocyanine singlet and the rise of the carotenoid triplet and therefore the dynamics of the triplet transfer process were not determined. Based on the detection limits and our experience with this system, we estimate that the T-T energy transfer is at least 10-times faster than the 500 ps lifetime of the phthalocyanine singlet state. The lifetime of 7.3  $\mu\text{s}$  (figure 4.2, second EADS) is assigned to a species closely resembling the carotenoid triplet. The position of the  $T_1/T_n$  transition, deduced from these time-resolved experiments, peaks at about 510 nm and the carotenoid ground-state bleach is centered at around 440 nm (Peterman *et al.*, 1995; Christensen, 1999) (figure 4.2). The population of the carotenoid triplet state (or carotenoid triplet-based state, *vide infra*) is associated with a perturbation of the phthalocyanine Q transitions as shown by the noticeable bleaching located at 610 and 680 nm (7.3  $\mu\text{s}$  EADS). This bleaching decays with the same 7.3  $\mu\text{s}$  time constant as the carotenoid triplet excited state. The third non-decaying EADS corresponds to the decay of triplet excited state of small amount of free, unattached phthalocyanine impurity or decomposition product. Global analysis also reveals a 1.1  $\mu\text{s}$  EADS, showing the similar spectra features at 440 nm and 515 nm, and a slightly larger perturbation of the phthalocyanine Q transitions. This EADS is likely to be associated with some kind of a relaxation of the carotenoid triplet-based excited state in the dyad.

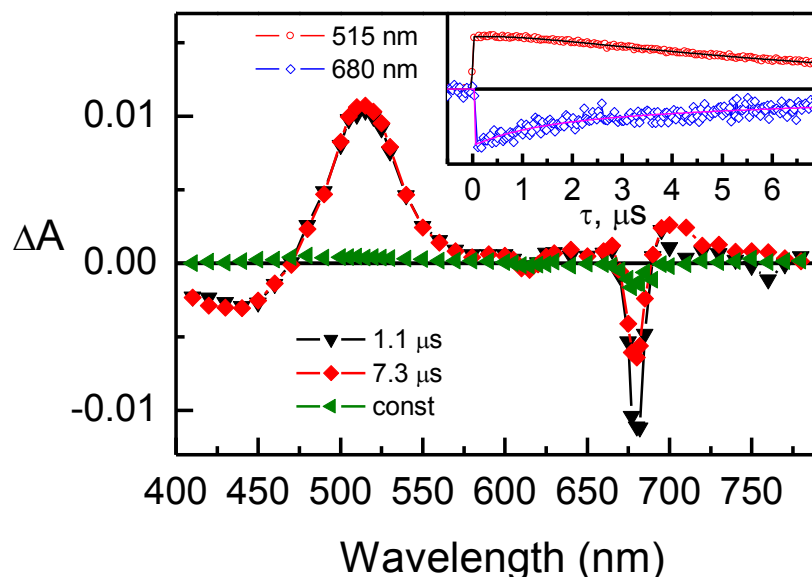


**Figure 4.2** Evolution-associated-difference spectra (EADS) for the carotenophthalocyanine, dyad **1**, with excitation at 680 nm in argon bubbled (30 min) *me*-THF solution. Inset shows kinetics at 515 and 680 nm with solid lines as fits.

Resonance Raman spectra of this dyad dissolved in THF were performed with various excitation conditions, ranging from 457 nm to 528 nm. Figure 4.3A displays resonance Raman spectra obtained with 501 and 514 nm excitations. As these excitation lines match the position of the  $S_0/S_2$  electronic transition of the carotenoid in the dyad, they are expected to enhance the contribution of this part of the molecule only. These spectra actually contain the four groups of bands typical from carotenoid molecules. The  $\nu_1$ , observed at  $1531\text{ cm}^{-1}$  arises from the C=C stretching modes, the  $\nu_2$ , at  $1160\text{ cm}^{-1}$ , which arises from a combination of C-C stretching modes and in-plane C-bending modes, the  $\nu_3$  at about  $1000\text{ cm}^{-1}$  from in-plane rocking vibrations of the methyl groups attached to the conjugated chain and the weak  $\nu_4$  band, at about  $950\text{ cm}^{-1}$ , from C-H out-of-plane wagging motions coupled with C=C torsional modes. The frequency of  $\nu_1$  and the structure of  $\nu_2$  (*i.e.* the number of spectral components observed in that region) are exquisitely sensitive to the carotenoid configuration (Koyama *et al.*, 1988). Both these bands indicate that the carotenoid in the dyad is in *all-trans* configuration. Of course, as carotenoid *cis* isomers do not absorb exactly at the same position as the *all-trans*, these particular conditions of resonance may favor the *all-trans* carotene. However, as the same conclusion may be drawn at every excitation used (namely 457, 476, 488, 496, 501, 514 and 528 nm, data not shown), we safely conclude that the carotene configuration in this dyad is *all-trans* only. These spectra do not change upon dyad illumination at 77K or at room temperature (data not shown), indicating that no light-induced *cis-trans* isomerization occurs, although the carotenoid triplet state is populated at the end of the excitation energy decay cascade.

With increasing laser power, using an excitation at 514 nm, located close to the  $T_1/T_n$  transition of the carotene, a number of small bands appear in the spectrum (figure 4.3B). As discussed extensively by Gall *et al.* (2011), the observed power dependence of the appearance of these features is consistent with progressive, dynamic accumulation of a transient state, and the bands observed at higher laser intensity are characteristic of the resonance Raman spectra of carotenoid molecules in their triplet states (Hashimoto and Koyama, 1988; Hashimoto *et al.*, 1991; Ohashi *et al.*, 1996; Mukai-Kuroda *et al.*, 2002; Rondonuwu *et al.*, 2004). Figure 4.3B, right, displays the  $\nu_1$  region of the resonance Raman spectra obtained with a 514.5 nm excitation at low and high power, together with the computed difference. The  $\nu_1$  frequency of the dyad carotenoid triplet is at  $1515\text{ cm}^{-1}$ , i.e.,  $16\text{ cm}^{-1}$  downshifted as compared to that of the carotenoid ground state (located at  $1531\text{ cm}^{-1}$ ). As discussed in Gall and coworkers (2011), the build-up of a ‘normal’ triplet state of a carotenoid induces a  $24\text{ cm}^{-1}$  downshift of that band, due to the transition of one electron from the bonding highest occupied molecular orbital (HOMO) to an antibonding orbital. The build-up of the carotenoid triplet state in this dyad thus induces a smaller downshift of this mode.

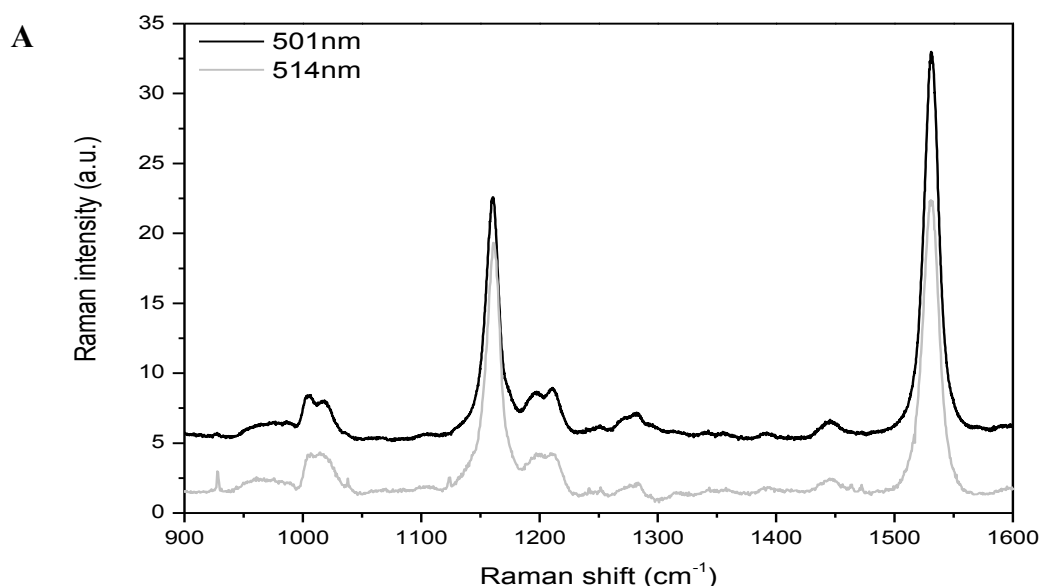
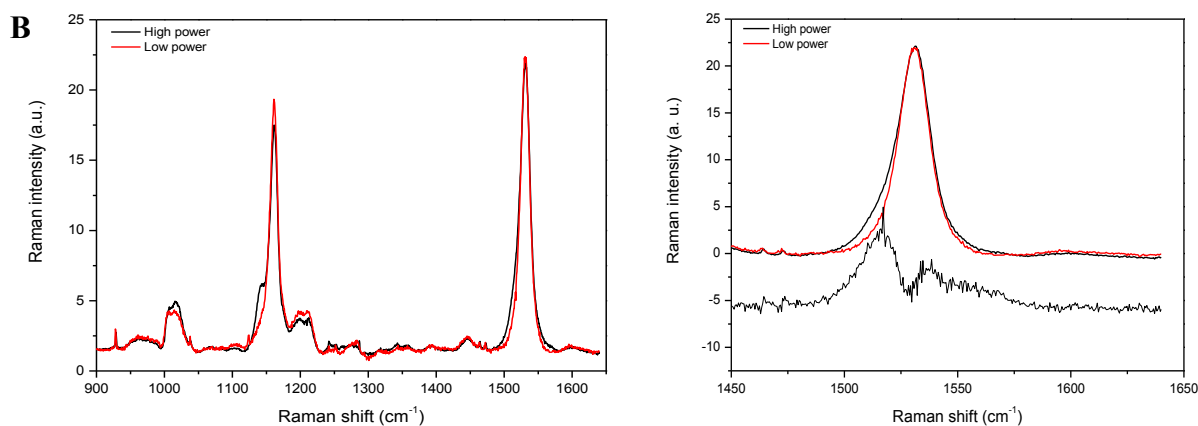


**Figure 4.3 A:** Resonance Raman spectra of the carotenophthalocyanine, dyad **1**, in THF excited at 501 and at 514 nm.



**B:** Resonance Raman spectra of the carotenophthalocyanine, dyad **1**, in THF obtained with 514 nm excitation, at low and high laser power (see text). Left: full spectra (900-1600  $\text{cm}^{-1}$ ). Right: high frequency region (1450-1650  $\text{cm}^{-1}$ ) with computed spectral difference on the bottom.

In order to better characterize the carotenoid triplet state in the carotenophthalocyanine dyad, we recorded the FTIR difference spectrum [triplet – ground state] of the dyad and of the phthalocyanine model in THF obtained 12  $\mu\text{s}$  after excitation by a 670 nm flash (figure 4.4). Due to the ultrafast T-T energy transfer time, at 12  $\mu\text{s}$  the triplet state should be located on carotenoid moiety. The difference FTIR spectrum obtained for the dyad is obviously similar – but not identical – to that of model phthalocyanine, indicating that the phthalocyanine makes a major contribution to these spectra. We note that the major differences between the spectrum of the dyad and the spectrum of the model phthalocyanine are an intense positive signal at 1475  $\text{cm}^{-1}$  and a negative signal at 1455  $\text{cm}^{-1}$ , accompanied by positive features at 1410, 1355, and 1274  $\text{cm}^{-1}$ . These five features (although not exactly at the same frequencies) are found in the FTIR difference spectra of carotenoids bound to purple bacteria LH2 (Galzerano *et al.*, in preparation). The same experiment was performed with a 100 ns time resolution (data not shown). The average of the spectra collected in the first 3  $\mu\text{s}$  after the flash, even though quite noisy, show the same features of the spectra obtained with the 12  $\mu\text{s}$  time resolution, indicating that the latter can be satisfactorily representative of the dynamics occurring in the first microseconds after the laser flash.

As discussed below, we tentatively interpret the similarities between the spectra of the dyad and the model phthalocyanine as an indication of contributions of the phthalocyanine electronic structure to the triplet carotenoid moiety of the dyad. This finding is in contrast to the case of dyad **2** presented below

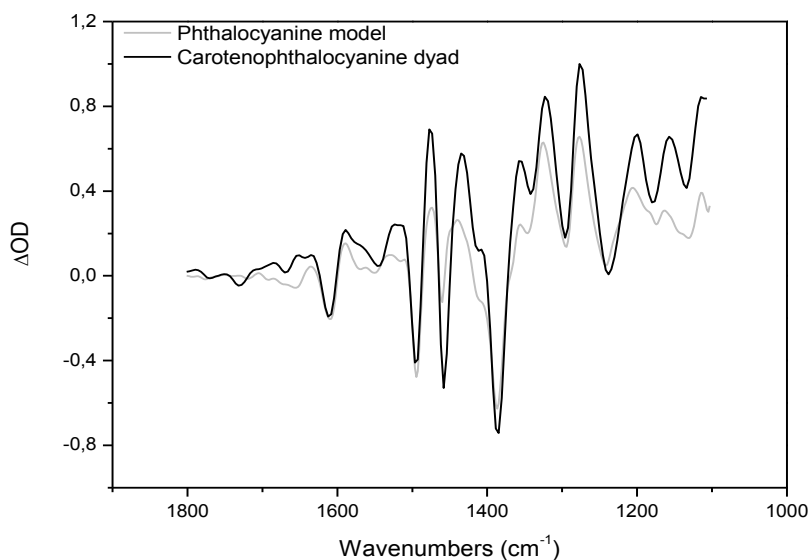


**Figure 4.4** Time-resolved FTIR absorption measurements performed on the phthalocyanine model **3**, compared to the carotenophthalocyanine, dyad **1**, in THF obtained with excitation at 670 nm.

### *Carotenopurpurin, dyad 2*

Dyad **2** comprises a purpurin linked by a methyl ester to a 10 double bond phenyl apocarotenoid (figure 4.1). For this dyad, dissolved in methyl-THF, excitation by a laser flash at 578 or 699 nm populates the purpurin singlet excited state (see absorption spectrum, figure 1B), which undergoes intersystem crossing followed by T-T energy transfer to yield the carotenoid triplet state (figure 4.5). The 42 ns EADS has the characteristic shape of the purpurin triplet excited state, with Soret and  $Q_y$  bleaching around 435 and 700 nm, respectively. With a 42 ns time constant the purpurin triplet spectrum is transformed into the carotenoid triplet spectrum, which shows an intense induced absorption around 530 nm and broad ground state bleaching around 460 nm, and decays in 5.8  $\mu$ s. There are two other minor EADS required for a satisfactory fit of the data. The non-decaying one can be associated with the decay of triplet excited state of a very small amount of free (unattached) purpurin and the 1  $\mu$ s EADS is possibly due to relaxation of the carotenoid triplet excited state and/or slower T-T energy transfer between purpurin and carotenoid in some minor dyad population. In the case of dyad **2**, the triplet state of the carotenoid moiety does not significantly perturb the purpurin electronic absorption spectrum, as shown by minimal  $Q_y$  bleaching signal in the 5.8  $\mu$ s EADS.

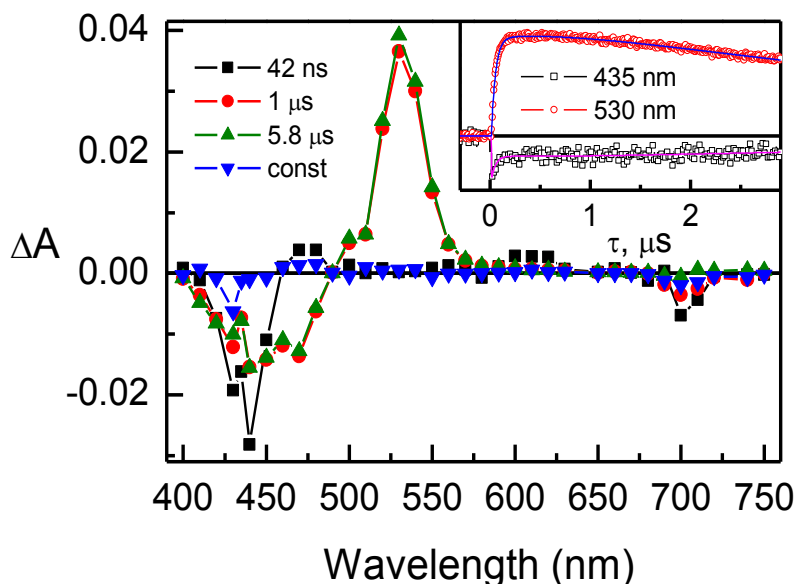


**Figure 4.5** Evolution-associated-difference spectra (EADS) for the carotenopurpurin, dyad **2**, with excitation at 699 nm in argon bubbled (30 min) me-THF solution. Inset shows kinetics at 435 and 530 nm with solid lines as fits.

Resonance Raman spectra of this dyad dissolved in THF were performed with various excitation conditions, ranging from 457 nm to 528 nm. Figure 4.6A displays, as an example, a resonance Raman spectra of this dyad obtained with a 528 nm excitation at low laser power. As was the case for dyad **1**, the resulting resonance Raman spectra of the carotenoid indicated an *all-trans* configuration, which pertains even after extensive illumination of the dyad at 77K or room temperature.

With increasing laser power, using excitation at 528 nm, located close to the  $T_1/T_n$  transition of the carotenoid, a number of small bands appear in the spectrum (figure 4.6A). Figure 4.6B displays the  $\nu_1$  region of resonance Raman spectra obtained at this excitation at low and high power. The  $\nu_1$  frequency of the carotenoid triplet (figure 4.6B), which appears at high power, is centered at about  $1500\text{ cm}^{-1}$  *i.e.* downshifted by  $24\text{ cm}^{-1}$  as compared to that of the carotenoid ground state (located at  $1524\text{ cm}^{-1}$ ). This value is very similar to that observed upon the build-up of an unperturbed triplet state of isolated  $\beta$ -carotene in THF (Hashimoto *et al.*, 1991).

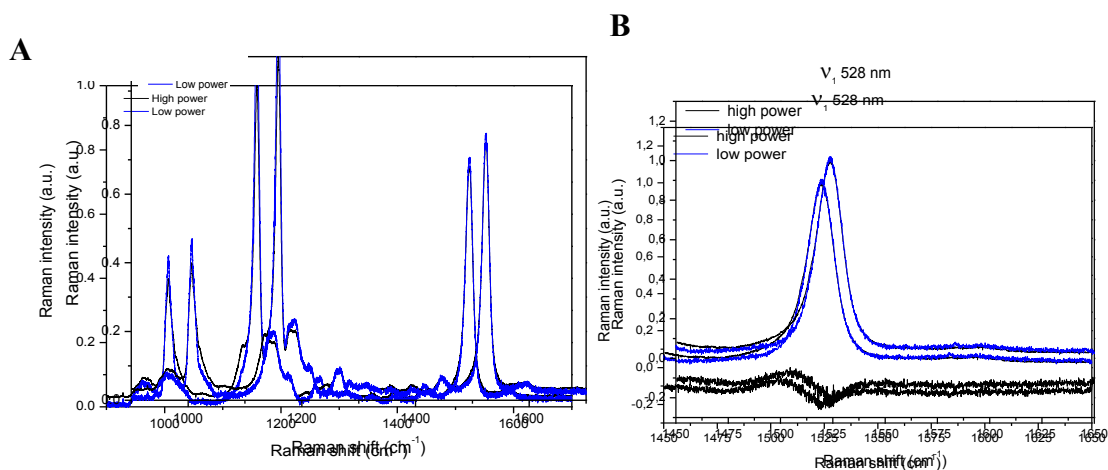


**Figure 4.6** Resonance Raman spectra of carotenopurpurin, dyad **2**, in THF excited at 528 nm. **A**: Full spectrum (900-1700  $\text{cm}^{-1}$ ). **B**: High frequency region (1450-1600  $\text{cm}^{-1}$ ) with computed spectral difference on the bottom.

The FTIR difference spectrum of the carotenopurpurin dyad in THF was recorded 12  $\mu\text{s}$  after a 435 nm flash, exciting the purpurin Soret transition. On this timescale the triplet state should be essentially 100% located on the carotenoid moiety. Figure 4.7 presents the FTIR difference spectrum obtained for dyad **2** and model purpurin **4** in THF. The difference FTIR spectrum of dyad **2** is qualitatively different from that of the model purpurin; it reveals major features not present in the model purpurin. Outside of an intense carbonyl signal, located at 1663 (-)/1630 (+), some of the main contributions are located at 1455 (-), 1420 (+), 1349 (+) and 1260 (-)  $\text{cm}^{-1}$  and are reasonably consistent with what is observed in the FTIR difference spectra of carotenoid bound to purple bacteria LH2 (Galzerano *et al.*, paper in preparation).

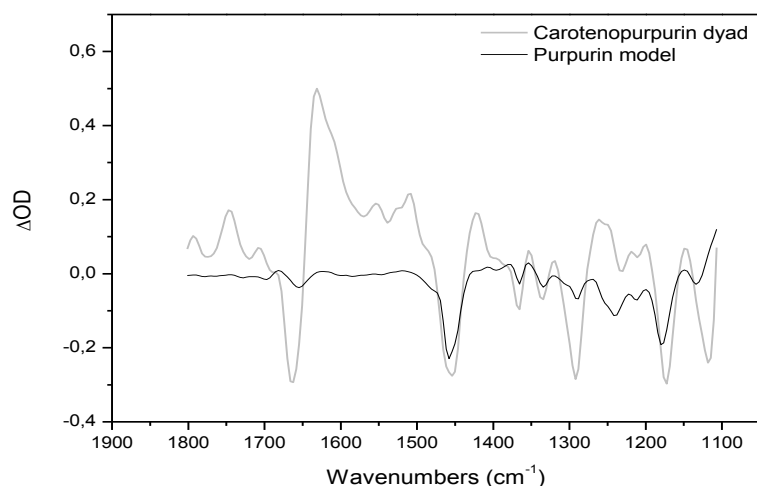


**Figure 4.7** Time-resolved FTIR absorption measurements in THF performed on the purpurin model **4**, compared to carotenopurpurin, dyad **2**, obtained with excitation at 435 nm.

## 4.4 Discussion

### *Transient Absorption Spectroscopy*

Cartenopurpurin, dyad **2**, is a new artificial photosynthetic dyad designed to have weaker electronic coupling between the chromophores than in the case of carotenophthalocyanine dyad **1**. The coupling is a function of the linkage between the carotenoid and the tetrapyrroles, the purpurin and phthalocyanine. In the carotenopurpurin, a methylene ester was used to link pigments resulting in a dyad with very weak through bond coupling and slow T-T energy transfer (Bensasson *et al.*, 1981). In carotenophthalocyanine, an amide linkage was used, which greatly increases the coupling yielding much faster triplet transfer lifetimes (Gust *et al.*, 1992).

From the absorption spectra (figure 4.1B) there are similarities between the tetrapyrroles: their Soret electronic transition is located in the blue region, their Q bands in the red/NIR, and there is minimal overlap between these transitions and the carotenoid absorption bands. In carotenopurpurin **2** the carotenoid with 10 C=C absorbs at maximally at 467 nm, which is at longer wavelength than that of carotenophthalocyanine **1** which has 9 C=C and maximally absorbs at 448 nm.

In the case of carotenophthalocyanine **1** efficient and fast singlet energy transfer and intersystem crossing limited triplet energy transfer was observed (Berera *et al.*, 2006). The carotene triplet lifetime was found to be 7.3  $\mu$ s. The same intersystem-crossing-limited triplet energy transfer phenomenon occurs in the LHCII of green plants (Peterman *et al.*, 1995; Gall *et al.*, 2011). In addition, the Q band bleach of the phthalocyanine that occurs during the lifetime of the dyad **1** carotenoid triplet state imitates the chlorophyll Q band bleach observed during the carotenoid triplet lifetime in LHCII (Peterman *et al.*, 1995). Thus, with respect to these spectroscopic features, dyad **1**, mimics the behavior of LHCII. In the case of dyad **2** the purpurin triplet state decay is accompanied by the rise of the carotene triplet species. The triplet energy transfer lifetime is 42 ns. Unlike dyad **1** there is a minimal purpurin Q band bleach at around 700 nm observed during the lifetime of the carotenoid triplet state. Taken together, these features indicate weaker coupling between the chromophores, which is consistent with previous observations in dyads using this linkage (Gust *et al.*, 1985; 1992). The behavior of dyad **2** mimics that observed in LH2 of many purple photosynthetic bacteria where the T-T energy transfer is slower (nanosecond time scale) and the triplet carotenoid has very limited influence on the Q band from BChl (Angerhofer *et al.*, 1995).

**Resonance Raman**

Using power-resolved experiments similar to those used in the natural systems (Gall et al., 2011), we were able to accumulate carotenoid triplet states in both dyads and to measure the corresponding resonance Raman spectra. The typical  $\nu_1$  transition for an unperturbed carotenoid is downshifted  $25\text{ cm}^{-1}$  due to the lower C=C bond order resulting from a change in excited state electronic structure (Hashimoto et al., 1991). As discussed below, the features of both the  $\nu_1$  shift and the IR difference spectra are interpreted as indicators of the electronic coupling between the chromophores. In this view, the coupling arises from charge transfer (CT) interactions in which the electron in the carotenoid-based LUMO (an antibonding orbital) is shared with the nearby tetrapyrrole. As the electron is shared, the antibonding character is reduced, which increases the C=C bond order resulting a smaller  $\nu_1$  shift in the Raman triplet spectra. Therefore, the  $\nu_1$  shift is inversely proportional to the electronic coupling between the chromophores.

The resonance Raman spectrum of the carotenoid-based triplet state in the carotenophthalocyanine **1** (figure 4.3B) shows that  $\nu_1$  undergoes only a  $16\text{ cm}^{-1}$  downshift, which is much less than that observed for unperturbed carotenoids (Hashimoto et al., 1991). Thus, in dyad **1** the electronic coupling is strong and, as measured by the shift in  $\nu_1$ , mimics quantitatively that found in LHCII. In both cases T-T energy transfer is very fast. For dyad **2**, the  $\nu_1$  frequency downshift is  $24\text{ cm}^{-1}$  (figure 4.6) which is similar to that expected for unperturbed  $\beta$ -carotene ( $\Delta\nu_1 -25\text{ cm}^{-1}$ ) (Hashimoto et al., 1991) and matches the frequency shift found in LH2 proteins (Gall et al., 2011). Thus, in dyad **2** the electronic coupling is much less, and it quantitatively mimics that found in LH2. In both dyad **2** and LH2, T-T transfer is relatively slow.

We note that the natural system relies on Van der Waals contact between the carotenoid and tetrapyrrole for the orbital overlap necessary for coupling, whereas in dyad **1** the coupling is provided by the amide bond and the much weaker coupling found in dyad **2** is provided by the methylene ester linkage (Gust et al., 1992).

DFT calculations of dyad **1** in the ground state show LUMO orbital amplitudes over both the carotenoid and phthalocyanine (figure 4.8A). As a first approximation, it can be expected that in such systems the excited state, either singlet or triplet, in which the LUMO is singly occupied will be delocalized between both the carotenoid moiety and the attached tetrapyrrole. In contrast, DFT calculations of dyad **2** show orbital amplitude exclusively on the carotenoid moiety in both the HOMO and LUMO (figure 4.8B). Thus, the singlet or

triplet excited state of this system would be expected to be localized on the carotenoid moiety, and not significantly influenced by the attached tetrapyrrole.

### ***FTIR***

Qualitatively, the IR difference spectra report the change in the bond orders making up the normal modes that accompany the change in electronic structure from ground state in which the HOMO is doubly occupied to the triplet state in which the HOMO and LUMO are singly occupied. Predicting the quantitative changes in the IR spectrum is beyond the scope of this report. We interpret common features in the IR difference spectrum between the model tetrapyrrole and the dyad as an indication of triplet electronic structure characteristic of the tetrapyrrole but found when the dyad is nominally in the carotenoid-based lowest triplet state. In other words, the greater the similarity of the IR difference spectra, the more the electronic structure of the tetrapyrrole has triplet character. We propose CT interactions in which the tetrapyrrole LUMO is partially occupied by an electron from the carotenoid as the mechanism for delocalizing the triplet over the two chromophores.

FTIR time-dependent spectroscopic measurements were made 12  $\mu\text{s}$  after exciting the phthalocyanine moiety of carotenophthalocyanine dyad **1** at 670 nm. Based on the information obtained from the transient absorption measurements, T-T energy transfer is very fast and the triplet of the carotenoid decays in 7.3  $\mu\text{s}$ . Thus at 12  $\mu\text{s}$  when the FTIR spectra were measured, the dominant state is the carotenoid-based triplet. The minor contribution of the free phthalocyanine, which was observed in transient absorption spectroscopy (figure 4.2), is considered too small to contribute significantly to the FTIR difference spectrum. Comparing the dyad **1** FTIR difference spectrum (figure 4.4) with that of the model phthalocyanine, vibrational signals and intensities occurring at 1610, 1500, 1390, 1260, and 1240  $\text{cm}^{-1}$  are found in both samples and provide evidence that the phthalocyanine electronic structure in dyad **1** has characteristics in common with those of the model phthalocyanine. We interpret this similarity as an indication of the partial presence of an electron in the LUMO of dyad **1** even though the dyad lowest triplet state is nominally the carotenoid triplet. DFT calculations (figure 4.8A) further support this interpretation by indicating that the LUMO orbital amplitudes are spread over the carotenoid and phthalocyanine components.

Similar IR difference results have been reported in oxygenic photosynthetic complexes. In these complexes, namely peridinin-chlorophyll protein (PCP) and LHCII, where the T-T energy transfer between chlorophyll and carotenoid molecules is sub-nanosecond, FTIR difference spectra in the microsecond timescale also yielded mainly signals arising from chlorophyll molecules (Alexandre et al., 2007; Gall et al., 2011). Thus this is an additional evidence of the fact that dyad **1** mimics the fast T-T energy transfer and the IR difference spectrum “fingerprint” of electronic coupling found in LHCII and PCP, both oxygenic photosynthetic proteins.

The triplet state of carotenopurpurin dyad **2** was populated by T-T energy transfer from the excited purpurin with a 42 ns time constant. Therefore, 12  $\mu$ s after the excitation laser pulse the excited state must reside on the carotenoid molecule. As shown in figure 7, in this case the differences between the purpurin model difference spectrum and the dyad difference spectrum are qualitatively obvious. For example, the features at 1790, 1660, 1625  $\text{cm}^{-1}$  were not observed in the purpurin model difference spectrum but are seen in dyad **2**. Thus the vibrational transitions observed in dyad **2** indicate a purpurin electronic structure that has little in common with the triplet electronic structure of the purpurin model. This would be expected if the electronic structure of the two chromophores is not extensively shared or delocalized in the triplet state. This can be explained by the weak coupling provided by the methylene ester linkage between the two chromophores, which effectively isolates the LUMO wavefunction on the carotenoid. Indeed, DFT calculations predict that the LUMO is localized on the carotenoid moiety (figure 4.8B).

The behavior of dyad **2** is reminiscent of that found in LH2 proteins from purple bacteria in which the IR difference spectrum of LH2 is very different from that of the (BChl) (; Galzerano et al., paper in preparation).

Dyads **1** and **2** thus demonstrate that by controlling the coupling, artificial photosynthetic systems can be designed to mimic their natural counterparts.

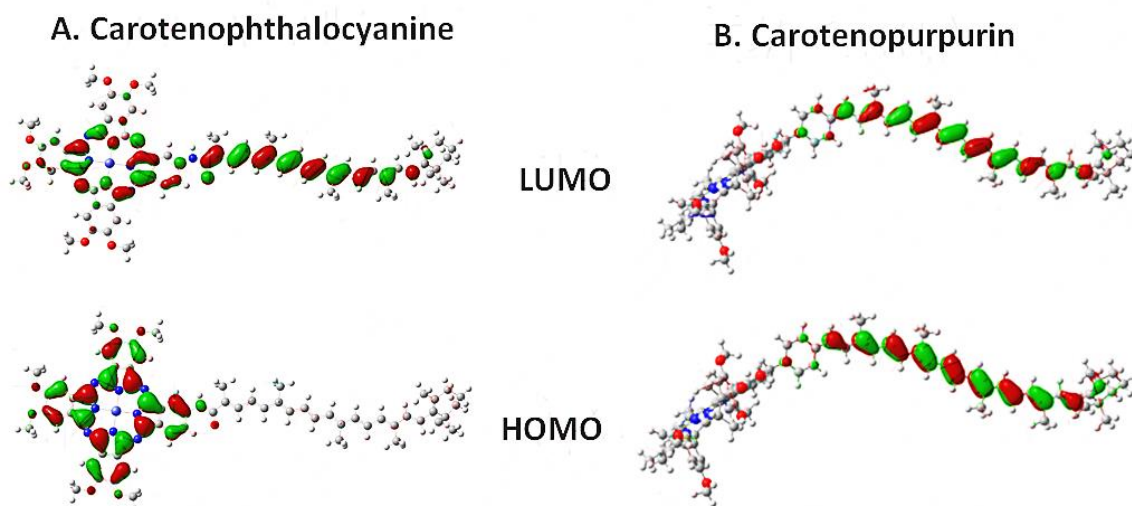


**Figure 4.8** Orbital diagrams of the carotenophthalocyanine, dyad **1**, (A) and the carotenopurpurin, dyad **2** (B) calculated using DFT (B3LYP/6-31G(d)).

## Conclusions

In dyad **1** both FTIR difference spectra and Raman shifts indicate a triplet electronic structure shared between the carotenoid and tetrapyrrole moieties. This coupling gives rise to ultrafast T-T energy transfer. Similar results were found in pigment-protein complexes from oxygen evolving photosynthetic organisms. We postulate that a shared electronic structure is essential for protection from singlet oxygen sensitization in photosynthetic membranes in oxygenic organisms. In the carotenopurpurin, dyad **2**, in which the linkage provides less electronic coupling, T-T energy transfer is slower and there is much less spectroscopic evidence of a delocalized triplet state. This mimics the behavior of the BChl and carotenoids in the LH2 complexes of anaerobic photosynthetic bacteria in which the exposure to oxygen is intermittent and much lower.

Altogether, our experiments indicate a remarkable similarity between the electronic structure required for the coupling necessary for ultrafast T-T energy transfer in photosynthetic proteins and in synthetic dyads. These results are encouraging for artificial systems because efficient water oxidation will expose membranes to high levels of oxygen production and this work demonstrates that nature's mechanism for protection can be provided in artificial photosynthetic constructs.

Additionally, the artificial systems of the present study clearly outline the evolutionary advantage that aerobic systems developed using well-coupled chromophores for fast T-T energy transfer to effectively dissipate the triplet of chlorophylls to prevent the sensitization of singlet oxygen, while the anaerobic organisms have a milder and possibly more ancient version of this protection mechanism.

## References

- ALEXANDRE, M T. A., LÜHRS, D C, VAN STOKKUM, I H. M., HILLER, R, GROOT, M-L, J T. M. KENNIS AND VAN GRONDELLE, R. Triplet State Dynamics in Peridinin-Chlorophyll-a-Protein: A New Pathway of Photoprotection in LHCS? *Biophysical Journal*, 2007, 93, p. 2118-2128.
- ANGERHOFER, A., BORNHAUSER, F., GALL, A., and COGDELL, R.J. Optical and optically detected magnetic-resonance investigation on purple photosynthetic bacterial antenna complexes. *Chemical physics*, 1995, 194, p. 259-274.
- BECKE, A. D. Density-functional thermochemistry. III. The role of exact exchange. *J. Chem. Phys.*, 1993, 98, p. 5648-5653.
- BENSASSON, R.V., LAND, A.J., MOORE, A.L., CROUCH, R.L., DIRKS, G., MOORE, T.A., and GUST, D. Mimicry of antenna and photo-protective carotenoid functions by a synthetic carotenoporphyrin. *Nature*, 1981, 290, p. 329-332.
- BERERA R., HERRERO, C., VAN STOKKUM, I.H.M., VENGRIS,M., KODIS, G., PALACIOS, R.E., VAN AMERONGEN, H., VAN GRONDELLE, R., GUST,D., MOORE, T.A., MOORE, A. L., and KENNIS, J.T.M. A simple artificial light-harvesting dyad as a model for excess energy dissipation in oxygenic photosynthesis. *Proc. Natl. Acad. Sci. USA*, 2006, 103, p. 5343-5348.
- BERERA, R., VAN STOKKUM, I. H. M., KODIS, G., KERISTEAD, A. E., PILLAI S., HERRERO C., PALACIOS, R. E., VENGRIS M., VAN GRONDELLE, R., GUST, D., MOORE, T. A., MOORE, A. L., KENNIS, J. T. M. Energy Transfer, Excited-State Deactivation, and Exciplex Formation in Artificial Caroteno-Phthalocyanine Light-Harvesting Antennas. *J. Phys. Chem. B*, 2007, 111, p. 6868-6877.
- BITTL, R., SCHLODDER, E., GEISENHEIMER, I., LUBITZ, W., and COGDELL, R.J. Transient EPR and absorption studies of carotenoid triplet formation in purple bacterial antenna complexes. *Journal Of Physical Chemistry B*, 2001, 105, p. 5525-5535.
- CHRISTENSEN, R. L. The electronic states of carotenoids. *In Advances in Photosynthesis*. H. A. Frank, A. J. Young, G. Britton, and R. J. Cogdell, editors. Kluwer Academic, Dordrecht, The Netherlands, 1999), p. 137-157.
- FOOTE, C. S. CHAPTER 3. Photosensitized Oxidation and Singlet Oxygen: Consequences in Biological Systems Free radicals and biological systems. *Academic Press*: New York, 1976.
- GALL, A., BERERA, R., ALEXANDRE, M.T.A, PASCAL, A.A., BORDES, L., MENDES-PINTO, M.M., ANDRIANAMBININTSOA,S., STOITCHKOVA, K.V., MARIN, A., VALKUNAS, L., HORTON, P., KENNIS, J.T.M., VAN GRONDELLE, R., RUBAN, A.V. and ROBERT, B. Molecular Adaptation of Photoprotection: Triplet States in Light-Harvesting Proteins. *Biophysical Journal*, 2011, 101, p. 934-942.

GUNTER, M.J. and ROBINSON, B.C. Purpurins bearing functionality at the 6,16-meso-positions - synthesis from 5,15-disubstituted meso-[beta-(methoxycarbonyl)vinyl]porphyrins. *Aust. J. Chem.*, 1990, 43, p. 1839-1860.

GUST, D., and MOORE, T.A. Mimicking photosynthetic electron and energy transfer-Advances in photochemistry, 1991 (book)

GUST, D., MOORE, T. A., MOORE A. L. and LIDDELL, P. A. Synthesis of Carotenoporphyrin Models for Photosynthetic Energy and Electron Transfer. *Methods in Enzymology*, 1992, 213, p. 87-100.

GUST, D., MOORE, T.A., BENSASSON, R.V., MATHIS, P., LAND, E.J., CHACHATY, C., MOORE, A.L., LIDDELL, P.A., NEMETH, G.A. Stereodynamics of intramolecular triplet energy-transfer in carotenoporphyrins. *J. Am. Chem. Soc.*, 1985, 107, p. 3631-3640.

HASHIMOTO, H., and KOYAMA, Y. Time-resolved resonance Raman-spectroscopy of triplet  $\beta$ -carotene produced from all-trans, 7-cis, 9-cis, 13-cis, and 15-cis isomers and high-pressure liquid-chromatography analyses of photoisomerization via the triplet-state. *J. Phys. Chem.*, 1988, 92, p. 2101-2108.

HASHIMOTO, H., KOYAMA, Y, HIRATA, Y, and MATAGA, N. S1 and T1 species of  $\beta$ -carotene generated by direct photoexcitation from the all-trans, 9-cis, 13-cis, and 15-cis isomers as revealed by picosecond transient absorption and transient Raman spectroscopies. *J. Phys. Chem.*, 1991, 95, p. 3072-3076.

HEHRE, W. J., DITCHFIELD, R., and POPLE, J. A. Self-Consistent Molecular-Orbital Methods. IX. An Extended Gaussian-Type Basis for Molecular-Orbital Studies of Organic Molecules. *J. Chem. Phys.*, 1971, 54, p. 724-728.

KOYAMA, Y., TAKATSUKA, I., NAKATA, M., and TASUMI, M. Raman and infrared-spectra of the all-trans, 7-cis, 9-cis, 13-cis and 15-cis isomers of beta-carotene - key bands distinguishing stretched or terminal-bent configuration from central-bent configurations. *Journal of Raman spectroscopy*, 1988, 19, p. 37-49.

LIDDELL, P.A., BARRETT, D., MAKINGS, L.R., PESSIKI, P.J., GUST, D., MOORE, T.A. Charge separation and energy transfer in carotenopyropheophorbide-quinone triads. *J. Am. Chem. Soc.*, 1986, 108, p. 5350-5352.

M.J Frisch, GW Trucks, HB Schlegel, GE Scuseria, MA Robb, et al. *Revision A.02; Gaussian, Inc.*, Wallingford, CT, 2009.

MATHIS, P., BUTLER, W.L., and SATOH, K. Carotenoid Triplet State and Chlorophyll fluorescence quenching in chloroplasts and subchloroplast particles. *Photochem. Photobiol.*, 1979, 30, p. 603-614.

MONGER, T.G, COGDELL, R.J, and PARSON, W.W. Triplet-states of bacteriochlorophyll and carotenoids in chromatophores of photosynthetic bacteria. *Biochim. Biophys. Acta*, 1976, 449, p. 136-153.

MOORE, T.A., DEVENS, G., MATHIS, P., MIALOCQ, J-C., CHACHATY, C., BENSASSON, R.V., LANDPARALLEL, E.J., DOIZI, D., LIDDELL, P.A., LEHMAN,

W.R., NEMETH, G.A., and MOORE, A.L. Photodriven charge separation in a carotenoporphyrin–quinone triad. *Nature*, 1984, 307, p. 630-632.

MUKAI-KURODA, Y., FUJII, R., KO-CHI, N, SASHIMA, T, and KOYAMA, Y. Changes in molecular structure upon triplet excitation of all-trans-spheroidene in n-hexane solution and 15-*cis*-spheroidene bound to the photo-reaction center from Rhodobacter sphaeroides as revealed by resonance-Raman spectroscopy and normal-coordinate analysis. *J. Phys. Chem. A.*, 2002, 106, p. 3566-3579.

OHASHI, N., KOCHI, N., KUKI, M, SHIMAMURA, T, COGDELL, RJ, and KOYAMA, Y. The structures of S-0 spheroidene in the light-harvesting (LH2) complex and S-0 and T-1 spheroidene in the reaction center of Rhodobacter sphaeroides 2.4.1 as revealed by Raman spectroscopy. *Biospectroscopy*, 1996, 2, p. 59-69.

PETERMAN, E. J. G., DUKKER, F. M., VAN GRONDELLE, R., and VAN AMERONGEN, H. Chlorophyll *a* and carotenoid triplet states in light-harvesting complex II of higher plants. *Biophys. J.*, 1995, 69, p. 2670-2678.

RONDONUWU, F. S., TAGUCHI, T., FUJII, R, YOKOYAMA, K, KOYAMA, Y., and WATANABE, Y. The energies and kinetics of triplet carotenoids in the LH2 antenna complexes as determined by phosphorescence spectroscopy. *Chem. Phys. Lett.*, 2004, 384, p. 364-371.

VAN DER VOS, R., D. CARBONERA, and A. J. HOFF. Microwave and optical spectroscopy of carotenoid triplets in light-harvesting complex LHC II of spinach by absorbance-detected magnetic resonance. *Appl. Magn. Res.*, 1991, 2, p.179-202.

VAN STOKKUM, I. H. M., LARSEN, D. S., and VAN GRONDELLE, R. Global target analysis of time-resolved spectra. *Biochim. Biophys. Acta-Bioenergetics*, 2004, 1658, p. 82-104.



**CHAPTER 5 EFFECT OF THE ISOMERIC FORMS OF  
DODECYL-MALTOSE DETERGENT ON LHCII  
SPECTROSCOPIC PROPERTIES**



**Summary of the work**

Studying membrane proteins represents a major challenge in protein biochemistry, with one of the major difficulties being the fact of working outside the natural lipid environment. *In vitro* studies rely on the successful solubilization or reconstitution of membrane proteins, by a careful selection of solubilizing detergents and mixed lipid/detergent systems. The importance of detergents as tools for the study of membrane proteins cannot be thus underestimated. Some membrane proteins are soluble only in a single detergent species that fulfils specific solubilization requirements.

In this work the two isomeric forms of *n*-dodecyl-D-maltoside detergent are used to solubilise the major plant light harvesting complex, LHCII. We show here that the two isomers have a different effect on the spectroscopic properties of this protein, influencing in particular the properties of the bound pigments. At this stage, we are not able to formally explain the results, but just to propose hypotheses which would satisfactorily explain the observed differences between LHCII solubilized in one or the other isomer of dodecyl-maltoside. The following chapter describes in more details a series of possible explanation for the obtained results.

## 5.1 Introduction

Photosynthetic membrane proteins are naturally embedded in a mosaic lipid bilayer, which is a complex, heterogeneous and dynamic environment. Like all the membrane proteins, they possess a hydrophobic surface in contact with the alkyl chains of the lipids, and a polar surface in contact with the aqueous phases on both sides of the membrane or with the polar headgroups of the lipids. The use of many standard biophysical techniques to determine structure and function such as NMR, X-ray crystallography, circular dichroism, ligand-binding studies, classical kinetic characterization and the identification of structure–function relationships require the protein to be extracted from its native membrane and studied in a detergent or lipid environment *in vitro*. In order to solubilize, to isolate and to characterize membrane proteins one has to use detergents, amphiphilic molecules which forms micelles above a certain concentration (CMC). Detergents solubilize membrane proteins by creating a mimic of the natural lipid bilayer environment normally inhabited by the protein: the micelles take up the membrane proteins and cover the hydrophobic surface with their alkyl chains in a belt-like manner while the polar head groups of the detergents face the aqueous environment. Usually detergent micelles, mixed lipid/detergent micelles and bicelles, as well as liposomes are used for the reconstitution and crystallization of membrane proteins (for a review see Seddon *et al.*, 2004).

Among the different classes of detergents, non-ionic detergents with an alkyl chain longer than 8, are generally considered to be mild and relatively non-denaturing, as they break lipid–lipid interactions and lipid–protein interactions rather than protein–protein interactions. This allows many membrane proteins to be solubilized in non-ionic detergents without affecting the protein’s structural features, such that it can be isolated in its biologically active form. Dodecylmaltoside (DM) belongs to this class of detergents and it has been extensively and successfully used for solubilisation and extraction of photosynthetic membrane proteins, like light harvesting complexes (LHCs), photosystems I (PSI) and photosystem II (PSII) leading in some cases to the determination of their crystal structures (Standfuss *et al.*, 2005; Amunts *et al.*, 2007; Umena *et al.*, 2011). DM is a glucoside-based surfactant with a bulky hydrophilic head group composed of two sugar rings (maltoside) and a non-charged alkyl glycoside chain (C12). Two isomers of this molecule exist, differing only in the configuration of the alkyl chain around the anomeric center of the carbohydrate head group, axial in  $\alpha$ -DM and equatorial in  $\beta$ -DM. Some of their features are summarized and compared in figure 5.1.

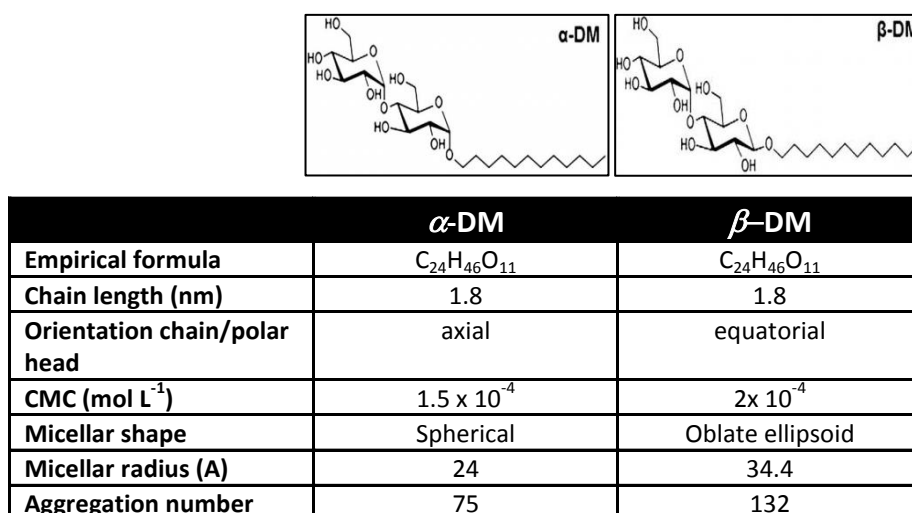


**Figure 5.1** Structural formula of *n*-dodecyl- $\alpha$ -D-maltoside ( $\alpha$ -DM) and *n*-dodecyl- $\beta$ -D-maltoside ( $\beta$ -DM) and chemical properties of the two isomers

$\beta$ -DM has been extensively used for isolating LHCII, the main light-harvesting protein from higher plants, and a very large number of biophysical studies of this protein –including the determination of its atomic structure- relies on  $\beta$ -DM. LHCII is naturally present as a trimer of subunits, each one binding no less than 14 chlorophylls and four carotenoid molecules. These chromophores allow highly selective techniques such as resonance Raman to be used to characterise their structure of, and the interactions they assume. It was in particular shown that the structure of this protein was exquisitely sensitive to its environment, as aggregating LHCII by removing the detergent was shown to alter the binding sites of its bound carotenoid 9-*cis*-neoxanthin and lutein (Horton *et al.*, 2005), as well as that of at least one chlorophyll *b*. As these structural changes were accompanied by a dramatic decrease of the fluorescence yield of this protein, these experiments were at the basis on the so-called ‘molecular switch’ model for LHCII, which proposes that this protein exists in at least two conformations, one in which it harvests efficiently the solar photons and transfers them with high yield to the reaction centers, and one in which it efficiently quenches the excitation energy, thus providing to the plants a way of regulating the energy fluxes in the photosynthetic membrane.

However, in the recent years, by using the  $\alpha$ -isomer of DM, which is generally perceived to be milder than  $\beta$ -DM, it became possible to solubilize plant thylakoid membranes in a single step treatment, and to obtain a range of macrocomplexes of PSI and PSII (Caffarri *et al.*, 2009). It thus seems that this  $\alpha$ -isomer better preserves the integrity even

of the largest pigment–protein supercomplexes embedded into the thylakoids membranes, and is more able to extract these complexes from the membrane in a reasonably stable form than  $\beta$ -DM (Pagliano *et al.*, 2012). Studying the influence of these macrocomplexes on the plastic structure of LHCII emerges as a particularly interesting task, however, the influence of  $\alpha$ -DM on the LHCII structure has not yet been fully characterised. It was shown, in 2007, that the circular dichroism properties of LHCII depend on whether the protein has been isolated using  $\alpha$ - or  $\beta$ -DM, suggesting that the nature of the detergent used during isolation could indeed play a role on the structural and spectroscopic properties of LHCII (Georgakopoulou *et al.*, 2007). In this work we have studied, using in particular resonance Raman, LHCII isolated using each of the isomeric forms of dodecyl-maltoside detergents.

## 5.2 Material and methods

### *Sample preparation*

*Arabidopsis* LHCIIb was isolated on one hand as previously described in Ruban *et al.* (1994), during which both solubilisation of the thylakoid membrane and sample isolation is performed using dodecyl- $\beta$ -D-maltoside. In parallel, the same proteins, from wild-type *Arabidopsis* and the *npq2* mutant were isolated according to the method described in Caffarri *et al.* (2001), where dodecyl- $\alpha$ -D-maltoside was used rather than dodecyl- $\beta$ -D-maltoside, at a final concentration of 0.03% w/v. LHCII was desalted in a PD10 desalting column (GE Healthcare) in a buffer containing 20 mM HEPES (pH 7.8) and 0.03% (w/v) *n*-dodecyl  $\alpha/\beta$ -D-maltoside. Quenched LHCII was prepared by removal of detergent using bio absorbent beads (Biorad).

### *Raman spectroscopy*

Low temperature (77 K) resonance Raman spectra were obtained in a helium flow cryostat (Air Liquide) using a Jobin-Yvon U1000 Raman spectrophotometer equipped with a liquid nitrogen-cooled charge-coupled device detector (Spectrum One, Jobin-Yvon). Excitation was provided by a Coherent Argon laser (Innova 100; 488.0 nm) and a Liconix helium-cadmium laser (441.6 nm). The choice of these wavelengths was determined by the absorption maxima of the xanthophylls derived from low temperature absorption spectra, as described previously by Ruban *et al.* (2000).

### 5.3 Results

#### *Composition of the samples*

Figure 5.2 displays the absorption spectra of LHCIIb from *Arabidopsis* WT, isolated using  $\alpha$ -DM or  $\beta$ -DM, as well as a difference computed between these two spectra. A clear increase in the absorption is observed in the carotenoid region, displaying the three characteristic bands from a carotenoid molecule, as well as in the Chl *b* region, peaking at 651 nm in  $\alpha$ - compared to  $\beta$ -DM. This result is consistent with previous observations (Ruban *et al.*, 1999) from which it was concluded that the carotenoid from the violaxanthin cycle (violaxanthin and zeaxanthin) were more easily lost during isolation procedures using  $\beta$ -DM. Figure 5.2 shows the effect of adding  $\beta$ -DM on absorption spectra of LHCIIb isolated using  $\alpha$ -DM. Presence of  $\beta$ -DM has a clear effect on the Chl *b* transition at 641 nm, however nearly no absorption change is observed in the carotenoid region.

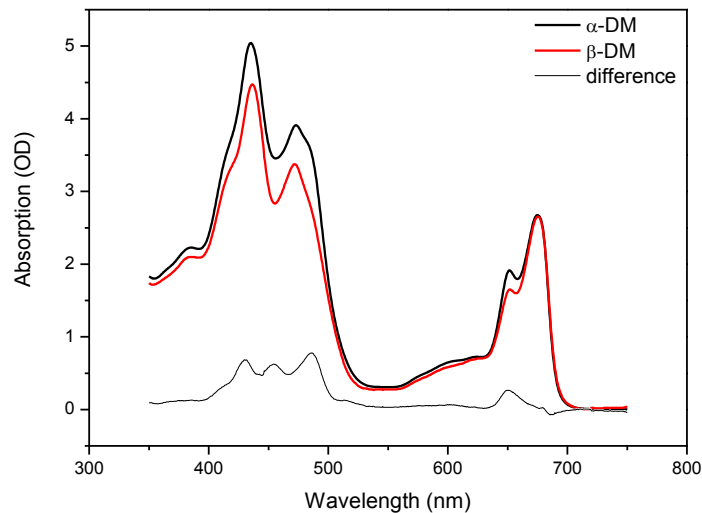


**Figure 5.2** Absorption spectra of LHCII trimers in  $\alpha$ -DM or  $\beta$ -DM and difference between the two samples.

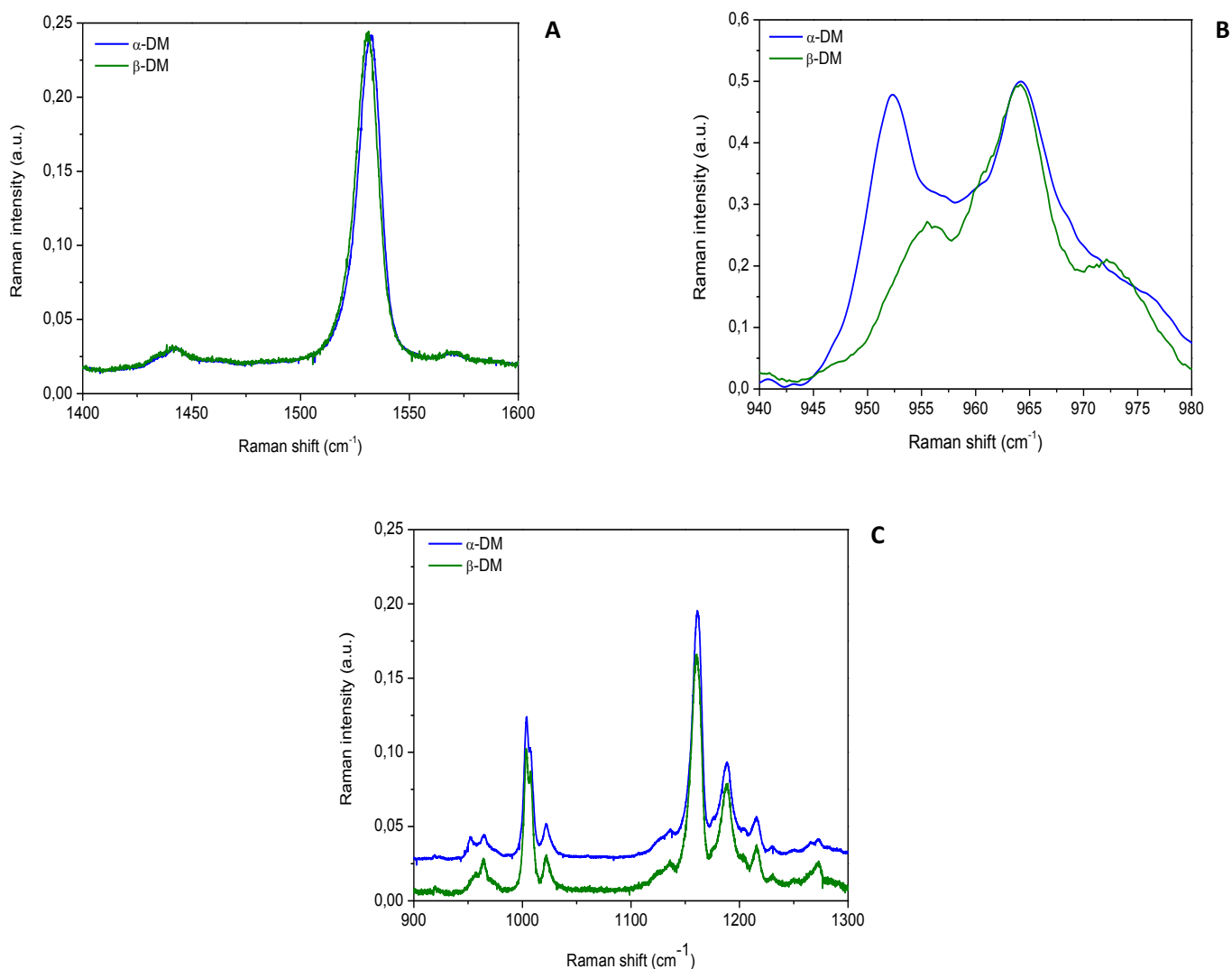
#### *Raman spectroscopy*

Resonance Raman spectroscopy, when applied to proteins containing many chromophores like LHCII, yields very selective information about the chromophores conformation and intermolecular interactions. In resonance Raman, the signal is enhanced when the excitation wavelength matches the absorption of the chromophores. It was well

documented that the resonance Raman signal of chlorophyll *b* molecules is enhanced when the excitation is at 441 nm, *i.e.* close to the maximum of the Soret transition of these molecules. Carotenoid molecules are very powerful resonance Raman scatterers, and, even though their resonance signal may be observed with any excitation wavelength, it is the most intense when Raman excitation lies in the blue green range. On LHCII, it was shown that, depending on the precise position of the excitation wavelength, resonance Raman spectra containing mainly contributions from each of the bound carotenoid molecules could be observed (Ruban *et al.*, 2000).

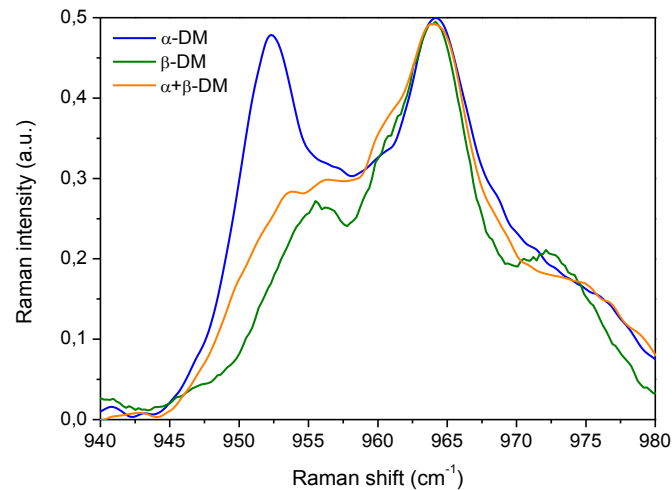
Carotenoid resonance Raman signal is composed of four main groups of bands, termed  $\nu_1$  to  $\nu_4$ . The  $\nu_1$  arises from the stretching modes of the C=C bonds, and gives direct access to the structure of the conjugated chain of the molecule (Mendes Pinto *et al.*, 2013). The  $\nu_2$  involves the stretching modes of the C-C bonds, among other modes, and its structure (*i.e.* the number of satellites present in this region) gives information on the configuration of the carotenoid. The  $\nu_4$  arises from the C-H out-of-plane wagging modes. These modes are not active in resonance Raman when the molecule is planar. In case of distortions of the backbone structure, induced by rotation around C-C bonds, result in increase in coupling of certain C-H and C-CH<sub>3</sub> wagging modes with the electronic transition, and the band arising from these modes increase. Parallel analysis of the  $\nu_1$  and  $\nu_2$  on resonance Raman spectra of LHCIIb isolated in  $\beta$ -DM led to the conclusion that neoxanthin was best observed at 488 nm excitation wavelength (where a clear *9-cis* satellite is observed, and where the  $\nu_1$  exhibits the highest frequency, indicating contributions of a shorter carotenoid molecule). This conclusion was recently confirmed by the study of LHCIIb isolated from the *npq2* mutant from *Arabidopsis*, which are unable to synthesize neoxanthin (Iliaia *et al.*, 2011): in the spectra of these complexes, dramatic changes are observed as compared to the WT, in particular in the  $\nu_4$  region, at this excitation wavelength.

Figure 5.3 shows the comparison of resonance Raman spectra of LHCIIb at 488 nm excitation wavelength isolated with one or the other detergent isomer. In panel 3a, where only the  $\nu_1$  region is displayed, it is clear that this band is not observed at the same frequency in both samples, indicating that the contribution of the different carotenoid of the complex to the resonance Raman spectra is not the same. Changes are even more dramatic in the  $\nu_4$  region, where the pattern of distortion observed, revealed by the intensity of the bands present in that region, is completely different (panel 5.3b). It is worth noting however, that the  $\nu_2$  region is very similar in both these samples, indicating that neoxanthin still contributes to the resonance Raman spectra in that region in similar proportion (panel 5.3c).



**Figure 5.3** Resonance Raman spectra of LHCII trimers at 488 excitation wavelength. A)  $\nu_1$  spectral region (1400-1600 cm<sup>-1</sup>); B)  $\nu_4$  spectral region (940-980 cm<sup>-1</sup>); C) spectral region including  $\nu_1$  and  $\nu_2$  bands (900-1300 cm<sup>-1</sup>).

To test whether this effect was due to detergent, and solely detergent,  $\beta$ -DM was added to the LHCIIb isolated in the presence of  $\alpha$ -DM. From figure 5.4, it clearly appears that addition of this detergent is enough to modify the resonance Raman spectra, dragging their properties towards what is observed for LHCIIb isolated in  $\beta$ -DM. This result indicates that the nature of the detergent used for isolating LHCIIb has a clear effect on the structural/electronic properties of this complex.



**Figure 5.4**  $\nu_4$  band Raman band spectra of LHCII trimers in  $\alpha$ -DM,  $\beta$ -DM (from figure 5.3B) and of trimers in  $\alpha$ -DM with the addition of  $\beta$ -DM. The excitation wavelength is 488 nm.

Resonance Raman spectra may change either because the structure of the scattering molecules changes or, in a mixture of molecules, because changes in the electronic transitions affect the resonance of one component which then would contribute more or less to the spectra of the ensemble. In order to understand the changes observed in the  $\nu_4$  region, we analysed the resonance Raman spectra obtained from LHCIIb isolated from the *npq2* mutant in  $\alpha$ -DM from *Arabidopsis*, which does not contain neoxanthin. In this mutant, the bands characteristic from *9-cis* configuration in the  $\nu_2$  region disappear, however, there is nearly no influence on the  $\nu_4$  band compared to the LHCIIb wt isolated in the same detergent (figure 5.5). This is at odd of what was observed for LHCIIb isolated in  $\beta$ -DM. For these complexes, the *npq2* mutation has a large effect on the  $\nu_4$  components. This indicates that the neoxanthin does not contribute to this region in our excitation conditions.

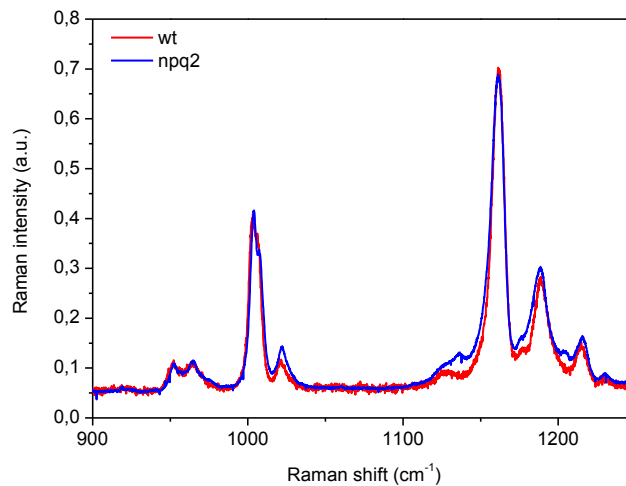


**Figure 5.5** Resonance Raman spectra of LHCII trimers in  $\alpha$ -DM from wild type (wt) and npq2 mutants (npq2) at 488 nm excitation wavelength. The spectral region shown here includes  $\nu_1$ ,  $\nu_2$  and  $\nu_3$  bands.

Using resonance Raman, it was shown that aggregation of the LHCIIb complexes induces a large change in the neoxanthin conformation, revealed by a change of the  $\nu_4$  structure (Robert *et al.*, 2004) We have performed aggregation of the LHCIIb purified in  $\alpha$ -DM, which results, as previously described, in a progressive quenching of the excitation. It is striking that the fingerprint of the neoxanthin change, which usually accompanies the appearance of quenching, is not present in the resonance Raman spectra of the aggregate  $\alpha$ -DM-purified LHCII, suggesting the absence of neoxanthin contribution in this spectral range (figure 5.6). A small change occurs upon aggregation of these complexes, which is clearly reminiscent of what was observed in LHCIIb isolated from the *np2* mutant of *Arabidopsis*, and which was attributed to a slight conformational change of the lutein 1 molecule (Iliaia *et al.*, 2011). Altogether, these experiments show that the *resonance* conditions of the pigments in LHCII isolated in  $\alpha$ -DM are slightly different from those observed for LHCIIb isolated in  $\beta$ -DM. Again, adding  $\beta$ -DM to the LHCIIb isolated in  $\alpha$ -DM induces a change in the resonance Raman spectra, dragging them towards a pattern looking as that obtained from LHCII isolated in  $\beta$ -DM. The effects we see here are thus clearly induced by the detergent.

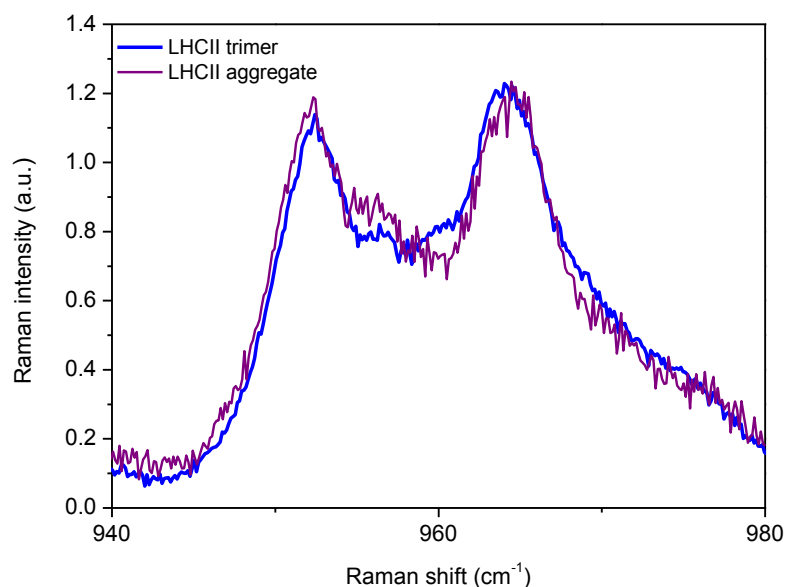


**Figure 5.6** Comparison of  $\nu_4$  band between LHCII trimers and aggregates in  $\alpha$ -DM at 488 nm excitation wavelength.

When exciting the complexes at 441.6 nm, in resonance conditions where the contributions of Chl *b* are enhanced, also clear differences are observed between LHCIIb isolated in  $\alpha$  and  $\beta$ -DM (figure 5.7). These differences mainly concern the carbonyl stretching region of the resonance Raman spectra, in the higher frequency range (1620-1720  $\text{cm}^{-1}$ ). In this region there is the contribution of the C=O stretching modes of the formyl and keto groups of Chl *b*, the frequency of which is exquisitely sensitive to the interaction state of these groupings. The 1620  $\text{cm}^{-1}$  band, arising from very strongly H-bonded formyl groups, is much more intense in LHCIIb isolated in  $\alpha$ -DM. This suggests that either these molecules are more strongly resonating in these complexes, or that additional Chls *b* are H-bonded in these complexes. Addition of  $\beta$ -DM again partially restores the pattern observed in  $\beta$ -DM-isolated complexes.

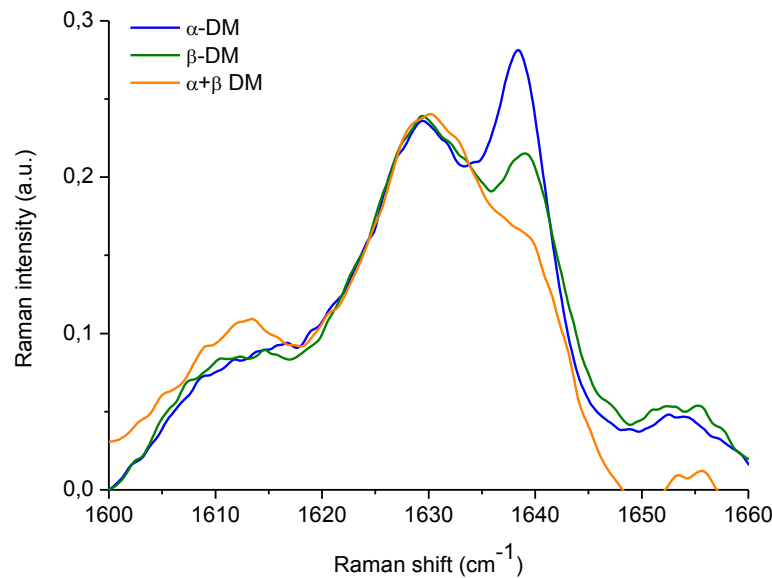


**Figure 5.7** Resonance Raman spectra of LHCII trimers in  $\alpha/\beta$ -DM or  $\alpha$ -DM with the addition of  $\beta$ -DM. The excitation wavelength is 441 nm; the spectral region (1600-1660  $\text{cm}^{-1}$ ) contains the contribution from the carbonyl groups.

## 5.4 Discussion

### *Origin of the resonance Raman changes observed in LHCIIb*

Resonance Raman has been at the origin of the so-called ‘molecular switch’ model, which explains the regulations in whole photosynthetic membrane by a change in the LHCIIb conformation. It is thus of the utmost interest to understand the variations of the Raman signal according to the detergent used for isolating LHCIIb.  $\alpha$ -DM has been progressively used as it retains a higher number of pigments in the LHCIIb complex. The results we obtain here could result from the difference in the pigment content between the different preparations (as suggested from figure 2). However, improvements of the isolation of LHCIIb with  $\beta$ -DM leads to about the same stoichiometries, and these changes have never been observed in any complex purified with this detergent. Moreover, the fact that adding  $\beta$ -DM to LHCIIb purified in  $\alpha$ -DM is by itself able to wipe out the differences observed in resonance Raman between the two samples clearly indicate that they do not arise from differences in stoichiometry.

We are thus left with the conclusion that, when using  $\alpha$ -DM, the LHCIIb complex is present in a different conformation, which alters the resonance Raman spectra of the bound pigments. Purification in  $\alpha$ -DM of the LHCII results firstly in an increase of the contributions of Chl *b* with a strongly H-bonded formyl group, which may be induced either by a change of the Chl *b* interactions in the complex, or by a change in the Chl *b* resonance. This is accompanied by a full disappearance of the neoxanthin contribution to the  $\nu_4$  band with 488

nm excitation, while the *9-cis* fingerprint band is still present in the  $\nu_2$ . Only two possible explanations may explain the latter phenomenon: i) the neoxanthin is locked in a fully planar configuration in the presence of  $\alpha$ -DM, which would decrease its contribution to the  $\nu_4$  band. However, even in solvent, most carotenoids display a small, but significant intensity in that spectral area and carotenoid with 0 intensity  $\nu_4$  band have never been observed. Accordingly, if the neoxanthin participates to the  $\nu_4$  band, even if planar, its absence should alter this band. ii) due to the nature of the detergent used, the electronic spectra of the different pigments are slightly altered, which then would result in changes in the resonance Raman contributions. In complex, interacting, systems of pigments, very complex phenomena may occur in resonance Raman spectroscopy. It was shown, for instance, as soon as in 1988 that the resonance conditions of bacteriochlorophyll in WT and R26 reaction centers were very different, although these proteins just differ by their content in carotenoid (Robert and Lutz, 1988). As the relative intensities of the different carotenoid bands tightly depend on the position of the excitation relative to their absorption transition, it could be imagined that neoxanthin is mainly excited in a 0-2 like resonance, which would enhance primarily its  $\nu_2$  band. Equivalent steep changes in resonance have already been observed (but not published) by Frolov *et al.*, in bacterial reaction centers.

As a support of such a complex explanation, the CD spectra (figure 5.8; gently provided by Pengqi Xu from Amsterdam University) of LHCIIb isolated in  $\alpha$ -dodecyl-maltoside are deeply perturbed by the addition of  $\beta$ -DM. This suggests that the interactions between pigments in this complex system are indeed detergent-sensitive.

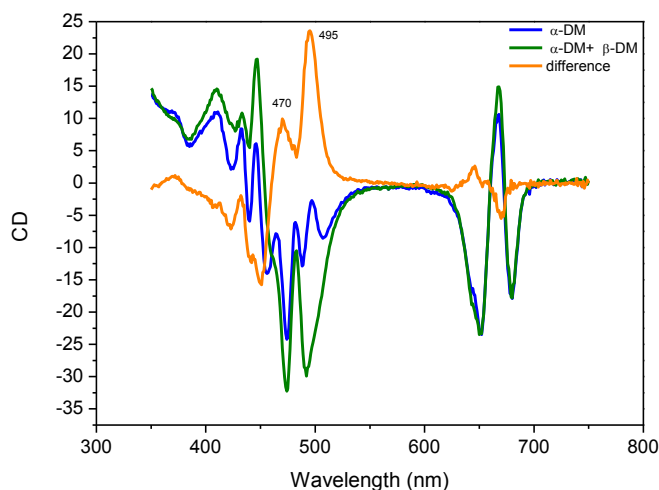


**Figure 5.8** CD spectra of LHCII trimers in  $\alpha$ -DM compared to the trimers in  $\alpha$ -DM with the addition of  $\beta$ -DM.

### ***Consequences for the NPQ models in the literature***

The dissipative state of LHCII was associated with a protein conformational change, evidenced by resonance Raman spectroscopy, during which, in particular the LHCII-bound carotenoid neoxanthin changes configuration (Ruban *et al.*, 1995; Pascal *et al.*, 2005; Iliaia *et al.*, 2011). Similar conformational changes were observed *in vivo*, associated with the rapid response of plant to high light intensities (Ruban *et al.*, 2007). The switching ability of LHCII between fluorescing and dissipative states was thus proposed to be at the origin of the regulation of the amount of excitation energy in the thylakoid membrane (Ruban *et al.*, 2007). However, in this work, we find that changes in the concerned spectral regions can be induced by detergent without appearance of dissipation. This indicates that LHCIIb has actually a plastic structure, which may be sensitive to external interactions. While the changes observed upon aggregation or *in vivo* strongly suggests that the conformational change of LHCII plays a role in the excitation energy quenching, our experiments question what was observed in LHCII crystals (Liu *et al.*, 2004; Pascal *et al.*, 2005). Indeed, although crystals were produced from  $\beta$ -dodecylmaltoside purified LHCIIb, the spectral changes observed between solution and crystal could actually arise from slight changes in pigment interactions. Although little likely, such an explanation would dissociate the quenched state observed in crystals from the apparent conformational change observed in resonance Raman of crystals.

### ***Molecular Origins of the Observed Signals***

In this work we are left with clear uncertainty about the molecular mechanisms which underlie the observed differences between LHCIIb isolated in  $\alpha$  and  $\beta$ -DM. Changing the detergent used during purification procedure could eventually either induce specific binding of the detergent molecules to the LHCIIb, or on the contrary maintain lipids and/or chromophores to a specific location, eventually related with that they have in the photosynthetic membrane (see *e.g.* Le Maire *et al.*, 2000) Both these effects could have an influence on the electronic absorption properties of the complexes, on their apparent stoichiometries, or on the way the pigments are bound to the apoprotein. In the present state of our knowledge, and in particular in the absence of electronic studies of LHCIIb in crystals, we cannot disentangle to different parameters which play a role in this phenomenon. A precise study has now to be made, comparing the different ways of purifying the LHCIIb, to understand precisely the origin of what we observe. At the same, time, such a study may prove to be important, as the slight tuning of the LHCIIb may be important to understand its quenching abilities.

## References

- AMUNTS, A., DRORY, O., and NELSON, N. The structure of a plant photosystem I supercomplex at 3.4 Å resolution. *Nature*, 2007, 447, p. 58-63.
- CAFFARRI, S., CROCE, R., BRETON, J., and BASSI, R. The Major Antenna Complex of Photosystem II Has a Xanthophyll Binding Site Not Involved in Light Harvesting. *The Journal of Biological Chemistry*, 2001, 276, p. 35924-35933.
- CAFFARRI, S., KOURİL, R., KEREÏCHE, S., BOEKEMA, E.J. and CROCE, R. Functional architecture of higher plant photosystem II supercomplexes. *The EMBO Journal*, 2009, 28, p. 3052-3063.
- DUPUY, C., AUVRAY, X., PETIPAS, C., RICO-LATTES, I., and LATTES, A. Anomeric effects on the structure of micelles of alkyl maltosides in water. *Langmuir*, 1997, 13, p. 3965-3967.
- ESHAGHI, S., ANDERSSON, B. and BARBER, J. Isolation of a highly active PSII-LHCII supercomplex from thylakoid membranes by a direct method. *FEBS Lett.*, 1999, 446 (1999), p. 23-26.
- GEORGAKOPOULOU, S., VAN DER ZWAN, Z; BASSI, R., VAN GRONDELLE, R., VAN AMERONGEN, H. and CROCE, R. Understanding the Changes in the Circular Dichroism of Light Harvesting Complex II upon Varying Its Pigment Composition and Organization. *Biochemistry*, 2007, 46, p. 4745-4754.
- HORTON, P., WENTWORTH, M., and RUBAN, A.V. Control of the light harvesting function of chloroplast membranes: the LHCII-aggregation model for non-photochemical quenching. *FEBS Lett.*, 2005, 579, p. 4201-4206.
- ILIOAIA, C., JOHNSON, M. P., LIAO, P.-N., PASCAL, A. A., GRONDELLE, R. van, WALLA, P. J., RUBAN, A. V., and ROBERT, B. Photoprotection in Plants Involves a Change in Lutein 1 Binding Domain in the Major Light-harvesting Complex of Photosystem II. *J. Biol. Chem.*, 2011, 286, p. 27247-27254.
- LE MAIRE, M., P. CHAMPEIL, P., and J.V. MbLLER, J.V. Interaction of membrane proteins and lipids with solubilizing detergents, . *Biochim. Biophys. Acta*, 2000, 1508, p. 86-111.
- LIU, Z., YAN, H., WANG, K., KUANG, T., ZHANG, J., GUI, L., AN, X., and CHANG, W. Crystal structure of spinach major light-harvesting complex at 2.72 Å resolution. *Nature*, 2004, 428, p. 287-292.
- MENDES-PINTO, M. M., SANSIAUME, E., HASHIMOTO, H., PASCAL, A. A., GALL, A., and ROBERT, B. Electronic Absorption and Ground State Structure of Carotenoid Molecules. *J. Phys. Chem. B*, 2013, 117, p. 11015-11021.
- PAGLIANO, C., BARERA, S., CHIMIRRI, F., SARACCO, G., and BARBER, J. Comparison of the  $\alpha$  and  $\beta$  isomeric forms of the detergent n-dodecyl-D-maltoside for solubilizing photosynthetic complexes from pea thylakoid membranes. *Biochim. Biophys. Acta*, 2012, 1817, p. 1506-1515.

PASCAL, A.A., LIU, Z., BROESS, K., VAN OORT, B., VAN AMERONGEN, H., WANG, C., HORTON, P., ROBERT, B., CHANG, W. and RUBAN, A. Molecular basis of photoprotection and control of photosynthetic light-harvesting. *Nature*, 2005, 436, p. 134-137.

ROBERT, B., and LUTZ, M. Proteic events following charge separation in the bacterial reaction center - Resonance Raman-spectroscopy. *Biochemistry*, 1988, 27, p. 5108-5114

ROBERT, B., HORTON, P., PASCAL, A.A., and RUBAN, A.V. Insights into the molecular dynamics of the plant light harvesting proteins in vivo. *Trends Plant Sci.*, 2004, 9, p. 385-390.

RUBAN, A.V., YOUNG, A.J., PASCAL, A.A., and HORTON, P. The effects of illumination on the xanthophyll composition of the photosystem II light harvesting complexes of spinach thylakoid membranes. *Plant Physiology*, 1994, 34, p. 227-234. RUBAN, A.V., HORTON, P., and ROBERT, B. Resonance Raman-spectroscopy of the photosystem-II light-harvesting complex of green plants -a comparison of trimeric and aggregated. *Biochemistry*, 1995, 34, p. 2333-2337.

RUBAN, A.V., LEE, P.J., WENTHWORTH, M., YOUNG, A.J., and HORTON, P. Determination of the stoichiometry and strength of binding of xanthophylls to the Photosystem II light-harvesting complexes. *J.Biol. Chem.*, 1999, 274, p. 10458-10465. CD measurements

RUBAN, A.V., PASCAL, A.A., and ROBERT, B. Xanthophylls of the major photosynthetic light-harvesting complex of plants: identification, conformation and dynamics. *FEBS Lett.*, 2000, 477, 181-185.

RUBAN, A.V., BERERA, R., ILIOAIA, C., VAN STOKKUM, I., KENNIS, J., PASCAL, A., VAN AMERONGEN, H., ROBERT, B., HORTON, P., and VAN GRONDELLE, R. Identification of a mechanism of photoprotective energy dissipation in higher plants. *Nature*, 2007, 450, p. 575–U22.

SEDDON, A.M., CURNOW, P., and BOOTH, P.J. Membrane proteins, lipids and detergents: not just a soap opera. *Biochim. Biophys. Acta*, 2004, 1666, p. 105-117.

STANDFUSS, J., TERWISSCHA VAN SCHELTINGA, A.C., LAMBORGHINI, M., and KÜHLBRANDT, W. Mechanisms of photoprotection and nonphotochemical quenching in pea light harvesting complex at 2.5 Å resolution. *EMBO J.*, 2005, 24, p. 919-928.

UMENA, Y., KAWAKAMI, K., SHEN, J.R., and KAMIYA, N. Crystal structure of oxygen evolving photosystem II at a resolution of 1.9 Å. *Nature*, 2011, 473, p. 55-60.

VAN AKEN, T., FOXALL-VAN AKEN, S., CASTLEMAN, S., and FERGUSON-MILLER, S. Alkyk glycoside detergents—synthesis and applications to the study of membrane proteins, *Methods Enzymol.*, 1986, 125, p. 27- 35.



**CHAPTER 6 GENERAL DISCUSSION AND FUTURE  
PERSPECTIVE**



## 6.1 Introduction

Photosynthesis is a highly regulated process and the organization of its machinery is highly sophisticated. The fluctuation of sunlight intensity at the earth's surface as a function of the diurnal nature of solar radiation and of the season and weather conditions made necessary the evolution of an apparatus able to respond to all the variations and to keep the photosynthetic yield close to the maximum.

The photosynthetic membrane contains a set of well-arranged pigment-binding membrane proteins. The bound pigments, namely chlorophyll and carotenoid molecules, are responsible for the absorption and transfer of light energy and for the protection of the apparatus in high light condition.

Carotenoid molecules play an essential role in both absorbing light in a spectral range where chlorophylls poorly or not absorb and in photoprotection. Biological functions of carotenoids involving interaction with light, such as photosynthesis, are determined by the electronic properties of the conjugated polyene chain that is characteristic of carotenoid molecules. Understanding how these properties are tuned, is essential for understanding the mechanisms underlying carotenoid functions, and is a major challenge for carotenoid research. In this thesis four major studies have been performed in order to study how:

- carotenoid absorption properties can be tuned *in vivo* in carotenoid-binding proteins;
- the alteration of the genes involved in the biosynthetic pathway of carotenoids can have a pleiotropic effect on the photosynthetic organisms;
- artificial constructs are able to reproduce the photoprotective mechanism of triplet-triplet energy transfer between chromophores by mimicking the photosynthetic proteins;
- the structural flexibility of the major light harvesting complex can be probed by modifying its surrounding environment.

## 6.2 Tuning of carotenoid absorption properties

Tuning of the electronic properties of carotenoid molecules by their *in vivo* locus is of vital importance in a number of cases (Britton *et al.*, 2008)). On our study we have chosen two specific cases, the two  $\beta$ -carotene molecules in photosystem II reaction centers and the two luteins in the major photosystem II light-harvesting complex, to investigate how such a tuning may occur. The PSII-RC binds two  $\beta$ -carotene molecules, which have their main

absorption transition at 489 and 507 nm the former being perpendicular and the latter parallel to the membrane plane. LHCII is present as a trimer in the photosynthetic membrane, with each monomer containing two lutein molecules forming a cross-brace. While in LHCII monomers these luteins both absorb at 495 nm, in LHCII trimers the absorption of one of them (lut2) shifts to 510 nm. The lut1 absorption remains at 495 nm. Thus, in each case, identical molecular species in the same protein are seen to exhibit different electronic properties (most notably, shifted absorption peaks).

Resonance Raman spectroscopy can discriminate between the different effects underlying the shifts in the  $S_0 \rightarrow S_2$  transition of carotenoid molecules (Mendes-Pinto et al., 2013). In particular, polarizability effects and changes in the effective conjugation length of these molecules can easily be distinguished due to the different correlations between the frequency of the  $\nu_1$  Raman band and the position of the carotenoid absorption electronic transition. A combined Raman/absorption study of these carotenoids may help in discriminating between polarizability effects and changes in the effective conjugation length due, for instance, to changes in the conformation of end cycles induced by steric hindrance.

In our case we show that the binding protein environment influences the carotenoid properties in a different way: the PSII b-carotene absorbing at 487 nm and the LHCII lutein absorbing at 495 nm are mainly influenced by the local polarizability of their binding pocket. This observation fits with the structural information on the binding site and it is also analogous to three different carotenoids bound to three LH proteins. The relationship between the  $\nu_1$  frequency and the position of the  $S_0 \rightarrow S_2$  transition for these three LH-bound carotenoids follows the correlation seen when varying the polarizability of the solvent and so the average polarizability of the protein binding pocket is enough by itself to explain the shift in carotenoid  $S_0 \rightarrow S_2$  transition upon binding to their light-harvesting protein host (Mendes-Pinto et al., 2013). By contrast, the 507 nm  $\beta$ -carotene and the 510 nm absorbing lutein are influenced by the structure of their binding site: local steric hindrances are in this case inducing a coplanarization of the beta- ring with the polyene chain. Both  $\beta$ -carotene and lutein are cyclic carotenoid and contain two and one rings at their extremities, respectively. In solution, lutein and  $\beta$ -carotene both exhibit shorter conjugation length in solvents than expected from their chemical structure. This was explained in terms of out-of-plane rotations of the conjugated end-cycles, resulting in a loss of conjugation (Mendes-Pinto et al., 2013)

Bringing one of these end-cycles back into the plane of the C=C conjugated chain should accordingly result in a net increase of the effective conjugation length of these

molecules, exactly as observed here for the red-absorbing lutein and  $\beta$ -carotene in LHCII and PSII-RC. We thus propose that these proteins are able to tune the absorption of their red-absorbing carotenoid (by up to 15 nm per conjugated ring) via the rotation of conjugated end-cycles towards the conjugated plane of the molecule, this rotation being imposed by their binding pocket through steric hindrance.

By combining these results with structural data we propose that in both LHCII and PSII-RC, steric hindrance from a nearby aromatic residue forces an end-ring of the red-absorbing carotenoid back towards the conjugated plane of the molecule. This presents the possibility of testing our conclusions by site-directed mutagenesis; replacing this residue with a smaller, non-aromatic one (*e.g.* Ala) should allow the carotenoid end-ring to take up its relaxed conformation. As a result its conjugation length, absorption position and Raman  $\nu_1$  frequency would all be similar to that of the blue-absorbing carotenoid and *in vitro* and in general, the mutations will lead to severe changes in the spectroscopic characteristics of the antenna complex. We are currently designing mutagenesis experiments to carry out this work in photosystem II of the cyanobacterium *Synechocystis* sp. PCC6803. Note that, in the absence of well-established isolation protocols for cyanobacterial PSII-RC, the analysis will have to be performed on core preparations of photosystem II, containing around 50 pigment cofactors including more than 10  $\beta$ -carotenes. Extracting the absorption and Raman signatures of two individual carotenoids from this large population, while substantially more difficult, should nevertheless be possible.

### 6.3 Regulation of the photosynthetic electron flow in *Arabidopsis thaliana*

Carotenoid biosynthesis is regulated throughout the life cycle of a plant with dynamic changes in response to developmental requirements and external environmental stimuli. There are key regulatory nodes in the network that control the flux of metabolites into the pathway and alter flux through it. Modification of this pathway can affect the photosynthetic organism at different and multiple levels.

In rice and *Arabidopsis thaliana*, expressing the bacterial phytoene desaturase (CRTI) in addition to the endogenous enzymes of the phytoene desaturation reactions (PDS) resulted in a change in the carotenoid pattern, showing a decrease in lutein, while the  $\beta$ -carotene-derived xanthophylls increased (Schaub *et al.*, 2005).

We decided to further study the effect of the constitutive expression of CRTI in *Arabidopsis thaliana* mutant lines, in particular to investigate whether the alteration of the carotenoid

composition increased their susceptibility to light and secondly, whether the redox state of the electron transport chain was altered. Mutants showed an increased susceptibility of leaves to light-induced damage. It turns out that changes in the photosynthetic electron transport chain rather than alterations of the carotenoid composition in the antenna were responsible for the increased photoinhibition. When illuminated a much higher level of superoxide/hydrogen peroxide was generated in thylakoid membranes from the CRTI expressing lines than in wild-type, while the level of singlet oxygen generation remained unchanged. The increase in reactive oxygen species was related to the activity of plastid terminal oxidase (PTOX) since their generation was inhibited by the PTOX-inhibitor octyl gallate, and since the protein level of PTOX was increased in the CRTI-expressing lines. Furthermore, cyclic electron flow was suppressed in these lines. These results suggest that PTOX competes efficiently with cyclic electron flow for plastoquinol in the CRTI-expressing lines and that it plays a crucial role in the control of the reduction state of the plastoquinone pool. This would once more weaken the hypothesis of PTOX having a major role in photoprotection or at least wouldn't always be the case, possibly depending on species and/or stress conditions. Indeed it seems more and more evident that by playing a major role in the control of the stromal redox poise, PTOX is also capable of modulating the balance between linear and cyclic electron flow around PSI (Trouillard et al 2012).

The question raising now is: which are the differences existing between PDS and CRTI which could explain why the constitutive expression of CRTI exerts such effects on PTOX levels and activity and consequently on plastoquinone redox-homeostasis?

CRTI is a bacterial phytoene desaturase that is distinct from the cyanobacterial/plant carotene desaturation system. With the exception of the FAD-binding domain, CRTI shares no sequence homology with plant desaturases. Mechanistically, CRTI is an oxidase that transfers the electrons from phytoene directly to oxygen, forming water (Schaub et al., 2012) In contrast, all evidence accumulated so far indicates that the PDS-mediated plant-type desaturation interact with oxygen only indirectly, through PTOX, using plastoquinone as an intermediate electron carrier (Mayer et al., 1990; Norris et al. 1995). Therefore, CRTI by itself is not a cause for any major Q/QH<sub>2</sub> imbalance. CRTI does not produce radicals (Schaub et al., 2012), so it cannot be responsible of the elevated ROS found in the mutant lines. It is likely that, a reduced PDS involvement may affect the redox state of quinones directly (and much more profoundly than ever anticipated) leading to redox-dependent retrograde signaling

and the upregulation of PTOX levels and maybe, the transcriptional activation of other genes. Work has been initiated to clarify this issue.

Additionally, there is a second property in which the two systems differ. CRTI catalyzes the introduction of all four double bonds needed to form all-*trans* lycopene in one step through all-*trans* configured (predominantly enzyme-bound) intermediates (Schaub et al., 2012; figure 6.1). In contrast, PDS requires a second desaturase,  $\zeta$ -carotene desaturase (ZDS) and two *cis-trans* isomerases, namely  $\zeta$ -carotene isomerase (Z-ISO) and carotene isomerase (CRTISO) to carry out a desaturation pathway that is characterized by poly-*cis* configured intermediates (see Cazzonelli 2011 for a review), finally producing all-*trans* lycopene, like CRTI. In other words, expressing CRTI is expected to lower the rate of poly-*cis* carotene intermediate formation. The function of these plant-specific poly-*cis* carotene intermediates is not understood at present, however, evidence is accumulating that they are the source of regulatory molecules capable in modifying gene expression (Kachanovsky et al., 2012). Work is in progress to identify this conceivable causal association.

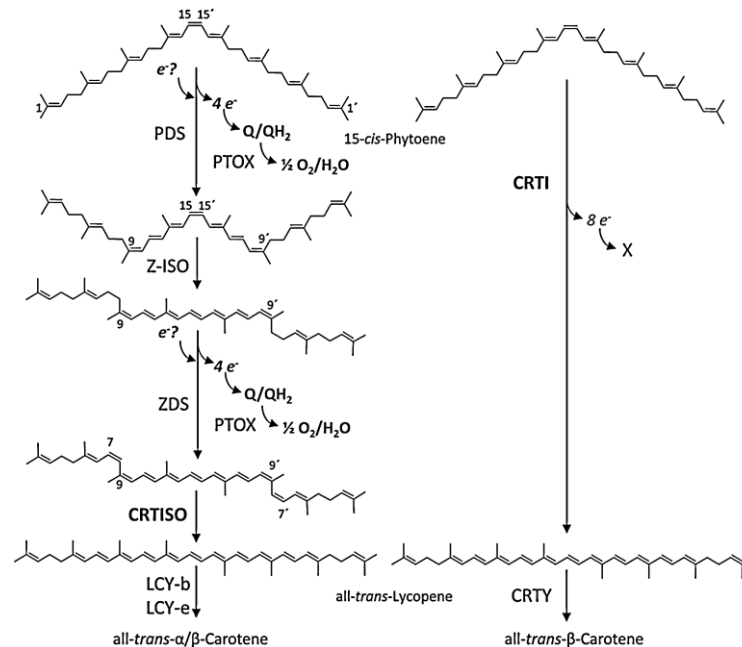


**Figure 6.1 Phytoene desaturation** Left, the plant/cyanobacterial system consisting of the two desaturases, phytoene desaturase (PDS) and  $\zeta$ -carotene desaturase (ZDS). The pathway involves specific poly-*cis*-intermediates and results in the formation of 7,9,9'7'-tetra-*cis*-lycopene (= polycopene). *Cis-trans* isomerases act at the 9,15,9'-tri-*cis*- $\zeta$ -carotene (Z-ISO) and polycopene (CRTISO) stage, the latter forming all-*trans*-lycopene, the substrate for lycopene cyclases (LCY). The electron acceptors identified so far for PDS (assumed here to be the same for the related ZDS) are plastoquinone and the plastoquinone:oxygen oxidoreductase PTOX. Right, CRTI-mediated phytoene desaturation encompassing all four desaturation steps and one *cis-trans* isomerization step to form all-*trans*-lycopene (Schaub et al., 2012).

## 6.4 Reengineering photosynthesis: artificial antenna system

Artificial photosynthesis is based on the use of the fundamental science underlying photosynthetic energy conversion to design synthetic systems for converting light into stored chemical energy. This approach aims to provide a solution for the production and storage of energy efficiently and in forms useful to humans.

Artificial photosynthetic systems need to be equipped with antenna systems which have to achieve both a strong absorption throughout the visible and rapid, efficient energy transfer among the chromophores. Understanding the photophysics and the photochemistry of these systems and the underlying factors governing them can provide valuable information to the understanding of the behavior of the far more complicated natural systems.

Chapter 4 shows an example of such artificial constructs (dyads) and illustrates how we can make an use of the knowledge about the electronic energy transfer mechanisms we already possess. In particular, two artificial photosynthetic dyads were studied and their triplet-triplet (T-T) energy transfer rates and spectroscopic features of their triplet states compared to those of natural systems. In the carotenophthalocynaine dyad (dyad 1) an ultrafast T-T energy transfer between the two chromophores occurs, while in the carotenopurpurin dyad (dyad 2) the T-T energy transfer between the two less coupled chromophores is in the order of 42 ns. In dyad 1, in addition to the carotenoid ground state bleach signal and  $T_1/T_n$  induced absorbance, the carotenoid triplet spectra presents a bleaching in the Q transitions of phthalocyanine which decay in  $7.3\mu\text{s}$ , the typical lifetime of the carotenoid triplet. In dyad 2, the carotenoid triplet spectrum shows little influence on the purpurin Q transitions. Resonance Raman and time-resolved FTIR show that in dyad 1, the carotenoid triplet state is not solely located on the carotenoid moiety but that it is shared across a larger conjugated system, like already observed in pigment-binding proteins from oxygenic photosynthetic organisms, while in dyad 2 the triplet seems to be mainly localized on the carotenoid moiety, a situation resembling the one of LH2 from anoxygenic photosynthetic bacteria.

The two artificial photosynthetic dyads here investigated thus share functional similarities with light-harvesting proteins of plants and purple bacteria, respectively, considering the triplet-triplet energy transfer mechanisms. These results demonstrate the need for a coupled chlorophyll and carotenoid triplet state for performing ultrafast triplet-triplet transfer, a process likely to be required in oxygen-rich environments.

Concerning the last point, some considerations can be done. In our current aerobic environment on earth, carotenoids are required to provide protection against the destructive effect of  $^1\text{O}_2$ , which is formed as a consequence of chlorophyll triplet formation. Indeed, all chlorophyll-containing pigment-protein complexes also contain carotenoid. However in the photosynthetic bacteria that inhabit environments which are strictly anaerobic, there is no problem if chlorophyll triplets are formed. The question is thus why does this latter system possess carotenoid evolved to be in van der Waals distance with chlorophyll? The closeness of the carotenoid to chlorophyll suggests that their light-harvesting role was very important and it is possible that as an aerobic environment developed their potential as photo-protectants was exploited to the full. In anaerobic bacteria, the mechanism of triplet-triplet was thus quite rudimentary as they didn't really need to counteract with oxygenic potential damages. With the atmosphere becoming rich in  $\text{O}_2$  and the developing of an oxygenic photosynthesis, a more sophisticated apparatus evolved and the role of carotenoid became crucial not only for light harvesting but for protecting the photosynthetic apparatus in dangerous conditions. Artificial constructs are able to reproduce this situation and can be thus useful for instance to obtain insights into the factors that govern the partition between light capture and photoprotection and how eventually it is possible to switch from one mechanism to the other by playing with the architecture of these artificial antenna systems.

Dyads represent the simplest way of mimicking tetrapyrrole-carotenoid interaction but many examples show that by playing with the architecture of these synthetic constructs, phenomena like photoinduced electron transfer and proton coupled electron transfer as is observed in photosynthetic water oxidation or electron transfer versus energy transfer can be reproduced and studied (Gust *et al.*, 2012). Additional experiments on dyads with a different linkage and/or orientation of chromophores have been planned for the next future.

## 6.5 Dynamic and flexibility of LHCII

The structural flexibility of the light-harvesting proteins allows control over the transfer of excitation energy to particular quenching species, associates of chlorophyll or chlorophyll and xanthophyll. The recent elucidation of the three dimensional structure of LHCII has revealed the possible molecular mechanisms by which this may occur (Liu *et al.*, 2004). The preliminary results presented and discussed in chapter 5, show how the experimental conditions used for the extraction and purification of membrane proteins (LHCII in our specific case) need to be accurate and reproducible between different laboratories. At the

same time they confirm the importance of maintaining the intactness and the functionality of these proteins when we remove them from their natural environment.

At this point a valuable strategy would be to investigate LHCII in a membrane-like by using the same experimental procedure. Preliminary results have been recently obtained in our laboratory by measuring the Raman spectra of two kinds of samples:

1) LHCII trimer complexes assembled into lipid nanodiscs consisting of a bilayer lipid matrix surrounded by a membrane scaffold protein (MSP) which reproduce a lipid environment devoid from detergent interactions (Pandit A. *et al.*, 2011);

2) LHCII in liposomes (sample from Dr. Helmut Kirchhoff; unpublished data). The results are still under interpretation but they will certainly add a significant contribution to clarify the role of the environment surrounding LHCII complexes.

Moreover, the speculations about LHCII protein dynamics could be extended on the same principles to other proteins of the Lhcb family and we could for instance apply the same analysis to the minor complexes. Recently the crystal structure of CP29, one of the minor antenna complexes, has been resolved at 2.80 Å of resolution (Pan *et al.*, 2011) and preliminary results show that the protein in solution is not quenched, while its crystalline form show a reduction of the chlorophyll fluorescence. Once again we observe a certain flexibility in the protein when we compare its soluble form to its crystalline form.

An additional important point to make is that *in vivo* LHCII is surrounded by other proteins of the photosynthetic apparatus, forming complexes of different size and composition. However, how the higher order architectures of biological macromolecules finely tune the functional structure of their constituting proteins is still largely unknown. High resolution electron microscopy and image analysis of wild-type and genetically altered plants are showing how these structures are organized within the intact membrane (Yakushevskaya *et al.*, 2003; Ruban *et al.*, 2003) and new spectroscopic approaches to the investigation of intact systems revealed some details of how such mechanisms operate (Robert *et al.*, 2004; Ruban *et al.*, 2007). We could thus investigate if and how, the association of LHCII to these macrocomplexes could potentially drive its structure in between its different conformations.

It has been already suggested that *in vivo* the structure of LHCII stabilized by protein-protein interactions is close to a transition point which could facilitate the regulatory response of higher plants to harmful intense light environments (Holleboom *et al.*, 2013). Obviously, the membrane architecture could also have an important role in modulating the structure/function of the embedded protein (Kirchhoff, 2013).

## 6.6 Conclusions

The study of functions of the carotenoid molecules involving interaction with light requires a multidisciplinary and multilevel approach. This thesis shows how a combination of spectroscopic and biochemical techniques contribute to highlight and describe the chemophysical properties that make carotenoids having such an essential role in photosynthesis. This work also show that affecting the carotenoid photosynthetic pathway can have consequences on the regulation of the photosynthetic electron flow which follow the absorption of light by the antenna system. Moreover the analysis performed here demonstrate how in order to obtain a complete picture we need precise details about how the structure, the dynamicity and the complex protein assemblies of light harvesting proteins modulate the properties of the bound carotenoid(s).

## References

- BRITTON, G., LIAAEN-JENSEN, S., and PFANDER, H. *Carotenoids*, Springer, 2008
- CAZZONELLI, C.I. Carotenoids in nature: insights from plants and beyond. *Funct. Plant Biol.*, 2011, 38, p. 833-847.
- HOLLEBOOM, C.P., YOO, S., LIAO, P.N., COMPTON, I., HAASE, W., KIRCHHOFF, H. and WALLA, P.J. Carotenoid–Chlorophyll Coupling and Fluorescence Quenching Correlate with Protein Packing Density in Grana-Thylakoids. *J. Phys. Chem. B*, 2013, 117, p. 11022-11030.
- KACHANOVSKY, D.E., FILLER, S., ISAACSON, T., and HIRSCHBERG, J. Epistasis in tomato color mutations involves regulation of phytoene synthase 1 expression by *cis*-carotenoids. *Proc. Natl. Acad. Sci. USA*, 2012, 109, p. 19021-19026.
- KIRCHHOFF, H. Architectural switches in plant thylakoid membranes. *Photosynth. Res.*, 2013, 116, 481-487.
- LIU, Z., YAN, H., WANG, K., KUANG, T., ZHANG, J., GUI, L., AN, X., and CHANG, W. Crystal structure of spinach major light-harvesting complex at 2.72 Å resolution. *Nature*, 2004, 428, p. 287-292.
- MAYER, M.P., BEYER, P., and KLEINIG, H. Quinone compounds are able to replace molecular oxygen as terminal electron acceptor in phytoene desaturation in chromoplasts of *Narcissus pseudonarcissus* L. *Eur. J. Biochem.*, 1990, 191, p. 359-363.
- MENDES-PINTO, M. M., SANSIAUME, E., HASHIMOTO, H., PASCAL, A. A., GALL, A., and ROBERT, B. Electronic Absorption and Ground State Structure of Carotenoid Molecules. *J. Phys. Chem. B*, 2013, 117, p. 11015-11021.
- NORRIS, S.R., BARRETTE, T.R., and DELLAPENNA, D. Genetic dissection of carotenoid synthesis in *Arabidopsis* defines plastoquinone as an essential component of phytoene desaturation. *Plant Cell*, 1995, 7, p. 2139–2149.
- PAN, X., LI, M, WAN, T., WANG, L., JIA, C., HOU, Z., ZHAO, X., JIPING, Z., and CHANG, W. Structural insights into energy regulation of light-harvesting complex CP29 from spinach. *Nature structural and molecular biology*, 2011, 18, p. 309-316.
- PANDIT, A., SHIRZAD-WASEI, N., WLODARCZYK, L.M., VAN ROON, H., BOEKEMA, E.J., DEKKER J.P., and DE GRIP, W.J. Assembly of the major light-harvesting complex II in lipid nanodiscs. *Biophys J.*, 2011, 101, p. 2507-2515.
- ROBERT, B., HORTON, P., PASCAL, A., and RUBAN, A. Insights into the molecular dynamics of plant light-harvesting proteins in vivo. *Trends Plant Sci.*, 2004, 9, p. 385-390.
- RUBAN, A.V., WENTWORTH, M., YAKUSHEVSKA, A.E., ANDERSSON, J., LEE, P.J., KEEGSTR, W., DEKKER, J.P., BOEKEMA, E.J., JANSSON, S., and HORTON, P. Plants

lacking the main light-harvesting complex retain photosystem II macro-organisation. *Nature*, 2003, 421, p. 648-652.

RUBAN, A.V., BERERA, R., ILIOAIA, C., VAN STOKKUM, I., KENNIS, J., PASCAL, A., VAN AMERONGEN, H., ROBERT, B., HORTON, P., and VAN GRONDELLE, R. Identification of a mechanism of photoprotective energy dissipation in higher plants. *Nature*, 2007, 450, p. 575–U22.

SCHAUB, P., YU, Q., GEMMECKER, S., POUSSIN-COURMONTAGNE, P., MAILLIOT, J., MCEWEN, A.G., GHISLA, S., AL-BABILI, S., CAVARELLI, J., and BEYER, P. On the structure and function of the phytoene desaturase CRTI from *Pantoea ananatis*, a membrane-peripheral and FAD-dependent oxidase/isomerase. *PLoS One*, 2012, 7, e39550.

TROUILLARD, M., SHAHBAZI, M., MOYET, L., RAPPAPORT, F., JOLIOT, P., KUNTZ, M., and FINAZZI, G. Kinetic properties and physiological role of the plastoquinone terminal oxidase (PTOX) in a vascular plant. *Biochim. Biophys. Acta*, 2012, 1817, p. 2140-2148.

YAKUSHEVSKA, A.E., KEEGSTRA, W., BOEKEMA, E.J., DEKKER, J.P., ANDERSSON, J., JANSSON, S., RUBAN, A.V., and HORTON, P. The structure of photosystem II in *Arabidopsis*: localization of the CP26 and CP29 antenna complexes. *Biochem.*, 2003, 42, p.608-613.



## **Étude des propriétés électroniques des caroténoïdes dans la photosynthèse naturelle et artificielle**

Les caroténoïdes jouent un rôle essentiel dans les premiers événements photosynthétiques. Ils absorbent la lumière et transfèrent l'énergie résultante en excitation aux molécules voisines, le respect de la succession des étapes photosynthétiques. En plus de l'absorption de la lumière, les caroténoïdes protègent l'appareil photosynthétique du stress photo-oxydatif survenant en condition de lumière intense, évitant les éventuels dommages. Les propriétés électroniques des caroténoïdes sont à la base de leurs mécanismes d'action et dans ce travail de recherche une combinaison de techniques biochimiques et spectroscopiques est utilisée pour examiner plus loin ces mécanismes avec un accent mis sur le rôle photoprotecteur joué par des caroténoïdes. Les d'échantillons analysés représentent différents niveaux d'organisation des protéines collectrices de lumière contenant ces pigments. Dans cette travail de thèse quatre études principales ont été réalisées pour comprendre comment: les propriétés d'absorption des caroténoïdes lutéine et  $\beta$ -carotène près les plantes peuvent être réglées *in vivo* par le site de liaison à leur protéines, le majeur complexe de capture de la lumière (LHCII) et le photosystème II (PSII) respectivement; l'altération des gènes de la voie biosynthétique des caroténoïdes peut indirectement provoquer une altération du transport d'électrons dans l'organisme photosynthétique; des molécules artificielles sont capable d'imiter le mécanisme photoprotecteur de transfert d'énergie entre les états de triplet des chromophores en mimant les protéines de l'appareil photosynthétique; la flexibilité structurelle de l'LHCII peut être explorée en modifiant son environnement.

**Mots clés :** photosynthèse ; photoprotection ; caroténoïdes ; transport d'électrons ; dyades ; LHCII.

### **Studying the electronic properties of carotenoids in natural and artificial photosynthesis**

Carotenoids play an essential role in the first steps of photosynthesis. They absorb light and they transfer the resulting excitation energy to the neighboring molecules, guaranteeing the correct order of the photosynthetic events. Additionally, carotenoids are able to protect the photosynthetic apparatus from the oxidative stress occurring in high light condition. Biological functions of carotenoids involving interaction with light, such as photosynthesis, are determined by the electronic properties of the conjugated polyene chain that is characteristic of carotenoid molecules. Understanding how these properties are tuned, is essential for understanding the mechanisms underlying carotenoid functions. Here we show that, by using a combination of different spectroscopic and biochemical approaches, these characteristics can be assessed in different kind of samples having the carotenoid molecules as common denominator. In this thesis four major studied have been performed in order to study how: the absorption properties of the two  $\beta$ -carotenes molecules in PSII-RC and those of the two luteins in LHCII are tuned *in vivo* by their protein binding site; the alteration of the genes involved in the biosynthetic pathway of carotenoids has a pleiotropic effect on the photosynthetic organisms; artificial constructs are able to reproduce the photoprotective mechanism of triplet-triplet energy transfer between chromophores by mimicking the naturally occurring photosynthetic proteins; the structural flexibility of the major light harvesting complex can be probed by modifying its surrounding environment.

**Key words:** photosynthesis; photoprotection; carotenoids; electron transport; dyads; LHCII.

